Selenium and Iodine Sorption and Fixation on Calcareous Soils from Somalia

By

Ibrahim Rashid Ali Haji

BSc Agricultural and Environmental Sciences; MSc.

Thesis submitted to the University of Nottingham for the degree of Doctor of Philosophy

June 2020

Dedication

This PhD research Thesis is dedicated to my parents

Acknowledgement

I would like to thank my supervisors Scott Young and Liz Bailey for their long journey supervision of my thesis, I acknowledge all their patience, constructive comments and support. I would like to acknowledge the financial sponsorship I received from the IDB.

I also acknowledge all the help and support I had from all my colleagues and officemates at department of agriculture and environmental sciences. Special thanks go to Emma Hooley and John Corrie for their help and administrative support. I would like to thank Laura Holt and Saul Vazquez Reina for their guidance and technical support. I really appreciate the logistical support from the administrative and technical staff during the field survey. I would like to acknowledge the help I had from the North lab, especial thanks go to Darren Hepworth for his help during the design of the co-precipitation experiments. I want to thank Abdul Mossa for his valuable help and contributions during thesis compilation.

I also would like to acknowledge the collaborations from the Somali Agricultural Technical Group (SATG) and WARDI Relief and Development Initiatives during the field work and sample collections.

Table of Contents

Dedication i

Acknowledgement ii

Glossary of Terms, Abbreviations, and Acronyms xx

Abstract xxv

1. Literature review 1

1.1. Background 1

1.1.1. Geography and climate 1

1.1.2. Water resources 2

1.1.3. Geology and soils 3

1.1.4. Agriculture 3

1.1.5. Nutritional status of the Somali population 4

1.2. Selenium 5

1.2.1. Importance in human health 5

1.2.2. Dietary selenium intake 6

1.2.3. Sources of selenium in agriculture 7

1.2.4. Chemistry of selenium 8

1.2.5. Uptake by plants 15

1.3. Iodine 16

1.3.1. Importance of iodine in human health 17

1.3.2. Dietary iodine 18

1.3.3. Sources of iodine in agriculture 18

1.3.4. Chemistry of iodine in soil 21

1.3.5. Uptake by plants 24

1.4. Objectives and outline of the thesis 25

2. General materials and methods 28
2.1 Introduction 28
2.2 Sample Collection 28
2.2.1. Water 28
2.2.2. Soil 29
2.2.3. Plant Sampling 31
2.3 Sample characterization 31
2.3.1. Water Samples 31
2.3.2. Soil Samples 31
2.3.3. Plant Samples 34
2.4 Analytical Methods 35
2.4.1. Ion Chromatography 35
2.4.2. Dissolved Carbon Analysis, ... 35
2.4.3. Total Carbon and Nitrogen Analysis 35
2.4.4. Total Organic Carbon Analysis 35
2.4.5. Total Elemental Analysis 36
2.4.6. Speciation Analysis 38
2.4.7. Preparation of working stock solutions 38
2.4.8. Sample preservations 39
2.4.9. Determination of isotopically exchangeable I and Se 39
2.5 Statistical analysis 42
3. Selenium and iodine in drinking and irrigation water of south Somalia 43
3.1. Introduction 43
3.2. Materials and methods 46
3.2.1. Study area 46

3.2.2. Field sampling 46
3.2.3. Sample processing 47
3.2.4. Water characterization 47
3.2.5. Iodine determination 48
3.2.6. Selenium determination 49
3.2.7. Multi-elemental analysis 49
3.2.8. Hydrogeochemical characterization 49
3.3. Results and discussion 50
3.3.1. General properties of the surface and groundwater samples 50
3.3.2. Comparisons between major anions of the different water types 55
3.3.3. Iodine 60
3.3.4. Selenium 67
Conclusion 74
4. Selenium and iodine in agricultural soils of South Somalia 75
4.1. Introduction 75
4.2. Materials and methods 77
4.2.1. Study areas 77
4.2.2. Soil sampling 79
4.2.3. Soil characterization 79
4.2.4. Selenium and iodine fractionation 79
4.2.5. Speciation of inorganic Se and iodine 79
4.2.6. Chemical analysis 79
4.3. Results and discussion 80
4.3.1. Soil characteristics 80
4.3.2. Multi-elemental analysis 81

4.3.3. Selenium 86
4.3.4. Iodine 102
4.4. Summary, discussion and conclusions 112
Assessment of the validity of the TMAH extraction method 116
5. Selenium and iodine in crop plants and their corresponding soils 120
5.1 Introduction 120
5.2 Materials and methods 123
5.3 Results and discussion 124
5.3.1 Soil characteristics 124
5.3.2 Iodine, Se and Zn concentration in the grain samples 125
5.3.3 Fractionation and speciation 127
5.3.4 Correlations 131
5.3.5 Estimated dietary intakes 133
5.4 Conclusion and discussion 136
6. Selenium adsorption and fixation on calcareous and gypsiferous minerals 139
6.1 Introduction 139
6.2 Materials and methods 142
6.2.1 Materials, chemicals and standards 142
6.2.2 Characterization of the calcite, gypsum and soils 142
6.2.3 Sorption Experiments 142
6.2.4 Determination of Isotopically Exchangeable Se 143
6.2.5 Desorption Experiments 143
6.2.6 Speciation 144
6.2.7 EXAFS Sample Preparation 144
6.2.8 EXAFS Data Collection and Analysis 145

6.2.9 Modelling and calculations 145
6.3 Results and Discussion 146
6.3.3 Characterization of the soils and mineral phases 146
6.3.4 Pre-Equilibration Time 147
6.3.5 Selenium Sorption on Calcite 148
6.3.6 Selenium adsorption onto calcite under environmentally relevant conditions 154
6.3.7 Isotopic Exchangeability of Se adsorbed on calcite. 159
6.3.8 Effect of the CO_2/air bubbling on Se coprecipitation 163
6.3.9 Selenium Sorption on Gypsum 165
6.3.10 Isotopic Exchangeability of Se adsorbed on Gypsum 167
6.3.11 EXAFS study of Adsorbed Selenium 167
6.4 Conclusions 172
7. Iodine fixation on calcite and gypsum minerals 173
7.1. Introduction 173
7.2. Materials and methods 176
7.2.1. Materials, chemicals and standards 176
7.2.2. Characterization of the calcite and gypsum 176
7.2.3. Sorption experiments 176
7.2.4. Background electrolyte 177
7.2.5. Solid phase pre-equilibration 177
7.2.6. Desorption experiments 177
7.2.7. Isotopically exchangeable iodine 177
7.2.8. Effect of the CO_2 partial pressure fluctuation 178
7.2.9. Speciation 178
7.2.10. Modelling and calculations 178

7.3. Results and Discussion 180
7.3.1. Range finding sorption experiment 180
7.3.2. Sorption under realistic environmental conditions 183
7.3.3. Comparison between ^{127}I and ^{129}I adsorption 185
7.3.4. $^{127}IO_3^-$ desorption 185
7.3.5. Iodate fixation into pure calcium carbonate minerals 186
7.3.6. Speciation of iodine in iodate-calcite adsorption experiments 188
7.3.7. Effect of the CO_2/air bubbling on iodate co-precipitation 188
7.3.8. Adsorption and fixation of iodate on gypsum 189
7.4. Conclusions 192
8. General Discussion and Conclusions 193
Overview 193
8.1. Water survey 194
8.2. Soil survey 197
8.3. Crops survey: Demonstration plots 204
8.4. Batch adsorption experiments 204
8.5. Future work 205
References 206
Appendices 229
Appendix B: Aqua regia data 229
Appendix C : Pearson correlation coefficients (chapter 4, soils) 231
Appendix D: Comparison between HNO_3 and TMAH preservation 235
Appendix E: Notes on XRD phase identification 236
Appendix F: Photographs from the field survey and laboratory experiments: 255

Table of figure

Figure 2.1. Sampling points of drinking and irrigation water in south Somalia during the field survey conducted in 2016/2017. Samples comprised both groundwater and surface water samples. The surface water samples were collected from the Shabelle River; the river was sampled from three points in each major city, i.e. entry, mid and end points. The R package was used to produce the map. 29
Figure 2.2. Map showing the locations of sampling of the agricultural soils in south Somalia during the field survey conducted in 2016/2017 (n=12). In each district two samples were collected i.e. both rainfed and irrigation systems. Each sample is made up from five sub-samples. The R package was used to produce this map. 30
Figure 3.1. The soil and water sampling locations in southern Somalia. 48
Figure 3.2. The frequency distribution of the pH of groundwater and surface water. The assessment of the compatibility of distributions for fitting was made using the Anderson–Darling (A–D) test for a significance level of $\alpha = 0.05$. 51
Figure 3.3. Piper diagram describing the hydro-geochemical properties of (A) Shabelle river water samples; (B) groundwater from Shabelle riverine areas and Bay region. 52
Figure 3.4. Box and whisker plot of measured chloride concentration in groundwater and surface water samples collected in a survey in Somalia, the dashed reference line is the maximum permissible limit in drinking water (WHO). 55
Figure 3.5. Relationship between total anions (Cl, SO_4-S and NO_3-N) and the electrical conductivity (EC) of the surface water and groundwater samples collected from south Somalia. 56
Figure 3.6. Scatter plot showing the correlation between Cl and major cations: a) Na; b) Ca and c) Mg present in the surface and groundwater systems of the study area. 57
Figure 3.7. Scatter plot of a) cations (including Ca and Mg) versus anions (Cl and SO_4); b) The scatter plots of Ca versus SO_4 in groundwater and the Shabelle river, Somalia. 58
Figure 3.8. Measured sulphate concentrations in groundwater and surface water samples collected from south Somalia; the dashed line represents the maximum permissible limit in drinking water (WHO). 59

Figure 3.9. Nitrate-nitrogen concentration in groundwater and surface water samples collected in a survey in Somalia, the dashed reference line (10 mg L^{-1} of NO_3-N) is the maximum permissible limit in drinking water according to the US Environmental Protection Agency (EPA)..... 60
Figure 3.10. Box and whisker plot for total iodine concentration in groundwater and surface water samples in south Somalia; the Box and whisker plot data is classified by water type. The recommended daily intake (RDI) is 150 µg day^{-1} (WHO, 2006). 61
Figure 3.11. Correlation between total iodine concentration of the water samples and the distance from the Indian Ocean coastline, these are mean values of the groundwater from four districts. 62
Figure 3.12. Box and whisker plot for total Se concentrations in surface water and groundwater samples of south Somalia. The data is classified by water type. 68
Figure 4.1. Major nutrients (Ca_{Tot}, K_{Tot}, Mg_{Tot}) of the soil root zone as determined by ICP analysis after HF digestion. Each bar represents the mean and corresponding standard error; n = 12; each value of the 12 is the mean of 3 replications. Rainfed (white), irrigated (grey); the soil codes are described in Table 4.1. 84
Figure 4.2. Minor plant nutrients (Cu_{Tot}, Co_{Tot}, Zn_{Tot}) of the soil root zone as determined by ICP analysis after HF digestion. Each bar represents the mean and corresponding standard error; n = 12; each value of the 12 is the mean of 3 replicates. Rainfed (white), irrigated (grey); the soil codes are described in Table 4.1. 84
Figure 4.3. Potentially toxic elements (Cd_{Tot}, Pb_{Tot}, As_{Tot} and Ni_{Tot}) of the soil root zone as determined by ICP analysis after HF digestion. Each bar represents the mean and corresponding standard error; n = 12; each value of the 12 is the mean of 3 replicates. Rainfed (white), irrigated (grey); the soil codes are described in Table 4.1. 85
Figure 4.4. Structural elements (Al_{Tot}, Fe_{Tot} and Mn_{Tot}) of the soil root zone as determined by ICP analysis after HF digestion. Each bar represents the mean and corresponding standard error; n = 12; each value of the 12 is the mean of 3 replicates. Rainfed (white), irrigated (grey); the soil codes are described in Table 4.1. 85
Figure 4.5. Total Se concentrations (Se_{Tot}) in Somali agricultural soils as determined by ICP analysis after HF digestion. Each bar represents the mean and corresponding standard error; n = 12; each value of the 12 is the mean of 3 replicates. Rainfed (white), irrigated (grey); the soil codes are described in Table 4.1. 87

Figure 4.6. Relationship between loss on ignition (representing soil organic matter content) and total selenium (Se_{Tot}) in agricultural soil samples from south Somalia. 88
Figure 4.7. Histogram illustrating distribution of total selenium concentration in agricultural soil samples from south Somalia. The assessment of the compatibility of fitted distributions was made using the Anderson–Darling (A–D) test for the significance level of $\alpha = 0.05$. 88
Figure 4.8. Histogram illustrating the distribution of soluble Se (Se_{Sol}) concentration in agricultural soil samples from south Somalia. The assessment of the compatibility of fitted distributions was made using the Anderson–Darling (A–D) test for the significance level of $\alpha = 0.05$. 91
Figure 4.9. Scatterplot showing relationship between soluble selenium speciation a) selenate; b) selenite, and c) organic-Se and total soluble selenium (Se_{Sol}; $\mu g\ kg^{-1}$) in agricultural soil samples of south Somalia. 92
Figure 4.10. Correlation between Se in water samples (Se_{water}) and the soluble soil Se fraction (Se_{Sol}). Values of Sewater are averages for each region whereas soil data are the averages for both rainfed and irrigated soils; the circle, triangle, diamond, square and asterisk represent averages for Belet weyn, Bulo Burte, Jowhar, Balad and Afgoi respectively. Green colour represents rainfed sites and grey colour for irrigated sites. 93
Figure 4.11. Normality test of the distribution of the adsorbed Se (Se_{Ads}) concentration in agricultural soil samples from south Somalia. Assessment of the compatibility of fitted distributions was made using the Anderson–Darling (A–D) test for a significance level of $\alpha = 0.05$. 95
Figure 4.12. Normality test of the distribution of the organically bound Se (Se_{TMAH}) concentration in agricultural soil samples from south Somalia. The assessment of the compatibility of fitted distributions was made using the Anderson–Darling (A–D) test for the significance level of $\alpha = 0.05$..... 96
Figure 4.13. Scatter plot illustrating the relationship between the Se_{TMAH} (%) and total soil organic carbon (TOC; %)..... 97
Figure 4.14. Scatter plot illustrating the relationship between the Se_{TMAH} (%) and total soil inorganic carbon (TIC; %). 97
Figure 4.15. Histogram illustrating distribution of recalcitrant soil Se ($Se_{Residue}$) in agricultural soil samples from south Somalia. The assessment of the compatibility of fitted distributions was made using the Anderson–Darling (A–D) test for the significance level of $\alpha = 0.05$. 98

Figure 4.16. Scatter plot illustrating the relationship between soil organic carbon (TOC; %) and the ratio of Se_{TMAH}: $Se_{Residue}$. 99
Figure 4.17. Scatter plot illustrating the relationship between soil organic carbon (TIC; %) and the ratio of Se_{TMAH}: $Se_{Residue}$. 100
Figure 4.18. The mean concentration (µg kg^{-1}) of soluble, adsorbed, organically bound and total selenium measured in triplicate (± the standard error) is summarized for ease of comparison between these fractions. Data is produced after the sequential extraction for the soil samples and were determined by ICPMS (codes in Table 4.1). 101
Figure 4.19. Total iodine concentration (I_{Tot}; mg kg^{-1}) in Somali agricultural soils as determined by ICP analysis after the sequential extraction. Each bar represents the mean and corresponding standard error; n = 12; each value of the 12 is the mean of 3 replicates. Rainfed (white), irrigated (grey); the soil codes are described in Table 4.1. The dashed line is the world geometric mean. 103
Figure 4.20. Histogram illustrating distribution of total iodine (I_{Tot}) concentration in agricultural soil samples from south Somalia. The assessment of the compatibility of fitted distributions was made using the Anderson–Darling (A–D) test for the significance level of $\alpha = 0.05$. 104
Figure 4.21. Histogram illustrating distribution of the soluble iodine (I_{Sol}) concentration in the agricultural soil samples from south Somalia. The assessment of the compatibility of fitted distributions was made using the Anderson–Darling (A–D) test for the significance level of $\alpha = 0.05$..... 105
Figure 4.22. Relationship between total soluble iodine in the soil (^{127}Isol) and total iodine (^{127}Iwater) in surface water and groundwater samples. 106
Figure 4.23. Histogram illustrating distribution of the adsorbed iodine (I_{Ads}) concentration in the agricultural soil samples from south Somalia. The assessment of the compatibility of fitted distributions was made using the Anderson–Darling (A–D) test for the significance level of $\alpha = 0.05$..... 108
Figure 4.24. Normality test of the distribution of the organically bound iodine (I_{TMAH}) concentration in agricultural soil samples from south Somalia. The assessment of the compatibility of fitted distributions was made using the Anderson–Darling (A–D) test for the significance level of $\alpha = 0.05$. 110

Figure 4.25. The mean concentration (µg kg^{-1}) of soluble, adsorbed, organically bound and total iodine measured in triplicate ± the standard error is summarized for ease of comparison between these fractions. Data was produced after ICP-MS analysis of the sequentially extracted soil samples. (codes in Table 4.1)..... 111
Figure 5.1. Phosphate-extractable selenite (Se^{IV}_{Ads}; µg kg^{-1}) as a function of the total phosphate extractable selenium (Se_{Ads}; µg kg^{-1}) for all soils collected from the demonstration plots in lower Shabelle, Somalia (n=9)..... 132
Figure 6.1. Changes in (a) pH and (b) dissolved Ca concentration in calcite suspensions; each measurement is an average of ten replicates. Systems were at ambient conditions with no pCO_2 control. 148
Figure 6.2. Selenite adsorption on calcite as a function of solid: solution ratio. Initial Se concentration was 1 mg L^{-1}..... 149
Figure 6.3. Selenite (a) and selenate (b) adsorption on calcite at initial concentrations in the range 1 to 5 mg L^{-1} using a 0.01 M Ca $(NO_3)_2$ background electrolyte. 150
Figure 6.4. K_d values as a function of contact time for adsorption of selenite on calcite, a) 1 mg L^{-1}; b) 2 mg L^{-1}; c) 3 mg L^{-1}; d) 4 mg L^{-1} and e) 5 mg L^{-1}; dashed line is the average K_d value... 151
Figure 6.5. Selenite adsorption isotherm over a three-week period for initial concentrations in the range 0.025 – 1 mg L^{-1} and contact times of 1, 3, 7, 14 and 21 days. The background electrolyte was 0.01 M Ca $(NO_3)_2$. 152
Figure 6.6. Change in the pH of the suspensions as a function of initial selenite concentration and contact time..... 152
Figure 6.7. K_d values as a function of contact time; values are calculated from the experimental data presented in Figure 6; a) 0.025 mg L-1; b) 0.01 mg L^{-1}; c) 0.3 mg L^{-1}; d) 0.7 mg L^{-1} and e) 1 mg L^{-1}..... 153
Figure 6.8. Selenite desorption isotherms following 21 days adsorption. Initial selenite concentrations were in the range 0.025 – 1 mg L^{-1}. The background electrolyte was 0.01 M Ca $(NO_3)_2$. 153
Figure 6.9. Langmuir and Freundlich modelling for the adsorption of selenite on calcite. Initial selenite concentrations were in the range 0.025 – 1.0 mg L^{-1}. The background electrolyte was 0.01 M Ca $(NO_3)_2$. 154

Figure 6.10. Selenite (a) and selenate (b) adsorption isotherms of environmentally realistic Se concentration 0.005 – 0.05 mg L^{-1} at contact times of 1, 3, 7, 14 and 21 days. The background electrolyte was 0.01 M Ca $(NO_3)_2$. 155
Figure 6.11. Comparison of selenite and selenate adsorption isotherms on calcite after 21 days contact time. Initial Se concentrations were 0.005 – 0.05 mg L^{-1}. The background electrolyte was 0.01 M Ca $(NO_3)_2$. 156
Figure 6.12. Change in (a) adsorbed Se (%) and (b) K_d as a function of contact time for Se concentrations of a) 5 µg L^{-1}, b) 10 µg L^{-1}, c) 15 µg L^{-1}, d) 25 µg L^{-1}, e) 50 µg L^{-1}. 157
Figure 6.13. Selenite (a) and selenate (b) desorption isotherms following 21 days adsorption. Initial selenite concentrations were in the range 0.005 – 0.050 mg L^{-1}. The background electrolyte was 0.01 M Ca $(NO_3)_2$. 158
Figure 6.14. Test of the effect of ^{77}Se spike isotopic mixing time for a calcite suspension equilibrated with multi-isotopic Se for (a) 14 days and (b) 21 days. 160
Figure 6.15. Labile adsorbed selenite plotted as a function of the total adsorbed for initial Se concentrations of (a) 0.025 – 1 mg L^{-1} and (b) 0.005 – 0.050 mg L^{-1}. Isotopic exchangeability was measured at three contact times after allowing 24-hour equilibration of the ^{77}Se spike. The dashed line is the 1:1 line. 161
Figure 6.16. Labile amount of Se (%) plotted as a function of contact time (days) for initial Se concentrations of (a) 0.025 – 1 mg L^{-1} and (b) 0.005 – 0.050 mg L^{-1}. 162
Figure 6.17. Comparison between labile adsorbed and total adsorbed selenite and selenate after 21 days reaction with calcite. 163
Figure 6.18. pH recorded under three experimental set ups; i) continuous CO_2 bubbling, ii) fluctuation between CO_2 & air, and iii) continuous air bubbling. 164
Figure 6.19. Dissolved Ca under three experimental set ups; i) continuous CO_2 bubbling, ii) fluctuation between CO_2 & air, and iii) continuous air bubbling. 164
Figure 6.20. Comparison of Se adsorption in systems with i) continuous CO_2 bubbling, ii) fluctuation between CO_2 & air, and iii) continuous air bubbling, as a function of time (days). 165
Figure 6.21. Comparison between the different Se species adsorbed on gypsum in range finding batch experiment; initial concentration 0.005 – 5 mg L^{-1}. 166
Figure 6.22. Selenite sorption on gypsum under lower Se concentration 25 µg L^{-1} – 1000 µg L^{-1}. 166

Figure 6.23. Labile adsorbed selenite plotted as a function of the total adsorbed for initial Se concentrations of (a) 0.025 – 1 mg L^{-1}. Isotopic exchangeability was measured after allowing 24-hour equilibration of the ^{77}Se spike. The dashed line is the 1:1 line. 167
Figure 6.24. Adjusted k^3 weighted EXAFS spectra of raw data (solid lines) and model fit (circles). 169
Figure 6.25. Fourier transform magnitude (k^2X (k)) of the EXAFS spectra for Se $^{(IV)}$ and Se $^{(VI)}$ incorporated into calcite, gypsum and soil samples. Solid lines correspond to raw data and circles to model fits. The FT magnitude is adjusted to stack the plots..... 170
Figure 7.1. Pilot iodate sorption experiment (Pre-equilibration: 3 weeks; subsamples were collected for two contact times 1 and 7 days; initial concentrations (0.005 – 5 mg L^{-1})..... 180
Figure 7.2. Pilot iodide sorption experiment (Pre-equilibration: 3 weeks; subsamples were collected for two contact times 1 and 7 days; initial concentrations (0.005 – 5 mg L^{-1})..... 181
Figure 7.3. Comparison between iodate and iodide sorption experiment (Pre-equilibration: 3 weeks; subsamples were collected for two contact times 1 and 7 days; initial concentrations (0.005 – 5 mg L^{-1}). 181
Figure 7.4. Iodate sorption as a function of six contact times; initial concentrations (5 g L^{-1} – 5 mg L^{-1}). (a) Adsorbed amounts (mg kg^{-1}); (b) Adsorbed amounts (%). 182
Figure 7.5. Iodate adsorption isotherm over a three-week equilibration period. The initial concentration was 0.025 – 1 mg L^{-1}; contact times were 1, 3, 7, 14 and 21 days; the background electrolyte was 0.01 M Ca $(NO_3)_2$. 183
Figure 7.6. Iodate adsorption isotherm on calcite described by the Freundlich adsorption model (K_d = 25; n = 0.64). Adsorption was for a period of 21 days, followed by three desorption events at 24-hour intervals. 184
Figure 7.7. Comparison of the adsorption strength (Freundlich K_d) on calcite of ^{127}I and ^{129}I isotopes, added as iodate, as a function of time (21 days). 185
Figure 7.8. Iodate desorption isotherm following a three-week initial adsorption equilibration period; the initial concentrations were relatively low (0.025 – 1 mg L^{-1}); desorption commenced after 21 days adsorption; the background solution was 0.01 M Ca $(NO_3)_2$. 186
Figure 7.9. Labile adsorbed iodate-I ($IO_3^-{}_{E, Ads}$) on calcite plotted as a function of the total adsorbed iodate-I. Equilibration was for 7, 14 and 21 days. 187

Figure 7.10. Labile iodate as a percentage of the total adsorbed iodate (%) plotted as a function of the contact time (days); 4 initial IO_3^- concentrations were used (100, 300, 700 and 1000 µg L^{-1}). 187
Figure 7.11. Comparison of iodate adsorption under continuous suspension aeration with CO_2 (4%) and air and under a fluctuating (CO_2-air) regime as a function of time (days). 189
Figure 7.12. Adsorption–desorption of iodine (in the iodate form) by gypsum; a) adsorption; b) desorption..... 190
Figure 7.13. Labile adsorbed iodate plotted as a function of the total adsorbed; the initial I concentrations of 0.025 – 1 mg L^{-1}. 191
Figure 8.1. Dietary selenium availability (a) and risk of inadequacy (b) in Africa 194
Figure 8.2. Correlations between Se_{TMAH} and soil properties: (a) Mg_{Tot}, (b) Ca_{Tot} and (c) soil pH; Note that Fig 8.2 c is compiled from several datasets. 201
Figure 8.3. The percentage of Se_{TMAH} as a function of soil $CaCO_3$ content (%)..... 202
Figure 8.4. Relationship between residual soil Se (%) and the corresponding soil $CaCO_3$ content (%) in the soils of the study area (n=12). 202

Table of Tables

Table 3.1. The main physico-chemical properties of the groundwater samples from South Somalia. Data are means ± standard deviation for each measured parameter. 53
Table 3.2. The main physico-chemical properties of the surface water samples from South Somalia. Data are means ± standard deviation for each measured parameter. 54
Table 3.3. Measured total iodine concentration and speciation (^{127}I; µg L^{-1}) in groundwater samples, south Somalia. Data are means ± standard deviation; "minimum", first quartile (Q1), median, third quartile (Q3), and "maximum". 65
Table 3.4. Measured total iodine concentration and speciation (^{127}I; µg L^{-1}) in Shabelle river water samples, south Somalia. Data are means ± standard deviation; "minimum", first quartile (Q1), median, third quartile (Q3), and "maximum". 66
Table 3.5. Measured total selenium concentration and speciation (^{78}Se; µg L^{-1}) in groundwater samples from south Somalia. Data are means ± standard deviation; "minimum", first quartile (Q1), median, third quartile (Q3), and "maximum". 70
Table 3.6. Measured total selenium concentration and speciation (^{78}Se; µg L^{-1}) in Shabelle river water samples, south Somalia. Data are means ± standard deviation; "minimum", first quartile (Q1), median, third quartile (Q3), and "maximum". 71
Table 3.7. Total Se addition from groundwater and surface water samples. Calculation of the added Se (g ha^{-1} $season^{-1}$) is based on the median Se concentrations (µg L^{-1}) in the water samples. 72
Table 3.8. Factors influencing total concentrations of selenium, iodine and their speciation in the Shabelle river water and groundwater samples from south Somalia. 73
Table 4.1. General characteristics of the twelve study soils (mean and coefficient of variation, or CV). Triplicate technical replications are used except for the pH measurements where duplicate measurement is used. Total concentrations of Zn (Zn_{Tot}), Se (Se_{Tot}) and I (I_{TMAH}) are in units of mg kg^{-1}). 81
Table 4.2. Validation of the HF digestion method. Triplicate samples of certified reference material (NIST SRM 2711a Montana II Soil) were HF digested and analyzed by ICP-MS. 83
Table 4.3. Comparison between the total Se concentrations (mg kg^{-1}) of rainfed and irrigated soils; a T-test was used to test for differences between the two land uses. 89

Table 4.4. Speciation of selenium in the soluble fraction (Se_{Sol}) and proportion of organic and inorganic Se in Se_{Sol}. Concentrations are given in µg kg^{-1}; proportions are expressed as percentages. Data are means ± standard deviation for each measured parameter. 90
Table 4.5. Speciation of selenium in the adsorbed fraction and proportions of organic and inorganic Se. Concentrations are given in µg kg^{-1}; proportions are expressed as percentages. Data are means ± standard deviation for each measured parameter..... 94
Table 4.6. Selenium concentration (µg kg^{-1}) of the Somali Agricultural soil samples after a three-step sequential extraction. The operationally defined fractions include soluble Se, exchangeable Se, organic matter-bound Se, and the residual Se fraction. N=12; a is (rainfed soils) and b (irrigated soils). 101
Table 4.7. Speciation of iodine in the soluble fraction (I_{Sol}) and proportion of organic and inorganic I in I_{Sol}. Concentrations are given in µg kg^{-1}; proportions are expressed as percentages. Data are means ± standard deviation for each measured parameter. 107
Table 4.8. Speciation of iodine in the soluble fraction (I_{Ads}) and proportion of organic and inorganic I in I_{Ads}. Concentrations are given in µg kg^{-1}; proportions are expressed as percentages. Data are means ± standard deviation for each measured parameter. 109
Table 4.9. Iodine content (µg kg^{-1}) of the Somali Agricultural soil samples after a three-step sequential extraction. The operationally defined fractions are soluble I, exchangeable I, organic matter-bound I and the residual I fraction. N=12; a is (rainfed soils) and b (irrigated soils). 111
Table 5.1. Physico-chemical characteristics of the experimental soils collected from demonstration plots in lower Shabelle, Somalia (mean ± SD, n = 9 plots). 126
Table 5.2. Grain total selenium (Se), Iodine (I) and Zinc (Zn) concentrations in maize, mung bean and cow pea grown in demonstration plots in lower Shabelle, Somalia (mean ± SD, n = 9 plots). 127
Table 5.3. The chemical forms of iodine (I^- and IO_3^-) in the soils corresponding to the crop samples. Speciation is performed in both the operationally defined soluble and adsorbed fraction (mean ± SD, n = 9 plots). 128
Table 5.4. The chemical forms of selenium ($Se^{(vi)}$ and $Se^{(iv)}$) in the soils corresponding to the crop samples. Speciation was performed in both the operationally defined soluble and adsorbed fractions (mean ± SD, n = 9 plots). 129

Table 5.5. Iodine and selenium concentration (µg kg^{-1}) of the soils from the demonstration plots in lower Shabelle, Somalia (mean ± SD, n = 9 plots) after a three-step sequential extraction. The operationally defined fractions are soluble I, exchangeable I, organic matter-bound I and the residual Se fraction. 130
Table 5.6. Estimated dietary intakes for selected nutrient element; (Ca, K, Mg, Zn, Fe, Cu and Mn) from maize. Calculations are based on measured maize elemental compositions (ICP analysis; mg kg^{-1}) integrated with the mean per capita consumption of maize (kg $capita^{-1}$ $year^{-1}$) from two east African countries (Ethiopia and Kenya). 135
Table 5.7. Estimated dietary intakes for selected nutrient element; (Mo, Cr, Ni, Se and I) from maize. Calculations are based on measured maize elemental compositions (ICP analysis; µg kg^{-1}) integrated with the mean per capita consumption of maize (kg $capita^{-1}$ $year^{-1}$) in two east African countries (Ethiopia and Kenya). 136
Table 6.1. Summary of conditions for the batch experiments, the solid phase is either 1 g of calcite or gypsum..... 143
Table 6.2. General characteristics of the experimental soils (n=2). Values are arithmetic mean of triplicate measurements ± the standard error. 146
Table 6.3. The adsorption-desorption distribution coefficients (K_d) of $Se^{(IV)}$ into calcite. Values are arithmetic mean of duplicate measurements ± the standard error..... 159
Table 6.4. EXAFS fitting parameters derived for $Se^{(VI)}$ and $Se^{(IV)}$ sorption on calcite, gypsum, and calcareous and gypsiferous soils. 168
Table 7.1. Summary of the batch experimental conditions, the solid phase (*) is either calcite or gypsum..... 176
Table 7.2. Iodate ($^{127}IO_3^-$) speciation during the batch adsorption experiment. Each value is the mean of duplicate experiments. 188

Glossary of Terms, Abbreviations, and Acronyms

^{127}I: Iodine 127 isotope

^{129}I: Iodine 129 isotope

^{77}Se: Selenium 77 isotope

^{78}Se: Selenium 78 isotope

ABIC: Agri-Business Incubation Centre

AFM: Atomic force microscopy

ANOVA: Analysis of variance

BGS: British Geological Survey

$CaCO_3$: Calcium carbonate

$CaSO_4.2H_2O$: Gypsum

CEC: Cation exchange capacity

CV: Coefficient of variation

CVD: Cardiovascular disease

DAP: Diammonium phosphate

DIC: Dissolved inorganic carbon

DOC: Dissolved organic carbon

DW: Dry weight

EAR: Estimated Average Requirement

EC: Electrical conductivity

EDTA: Ethylenediaminetetraacetic acid

EXAFS: Extended X-ray absorption fine structure

FA: Fulvic acids

FAO: Food and Agriculture Organization

FBS: Food Balance Sheets

FSNAU: Food Security and Nutrition Analysis Unit

GDP: Gross Domestic Product (GDP)

GPS: Global Positioning System

GW: Groundwater

HA: Humic acids

HDI: Human Development Index

HI: Hysteresis index

HPLC: High-performance liquid chromatography

HPLC-ICP-MS: High-performance liquid chromatography and inductively coupled plasma mass spectrometry.

HS: Humic substances

I: Iodine

$I_{Ads(I^-)}$: Adsorbed iodide

$I_{Ads(IO_3^-)}$: Adsorbed iodate

I_{Ads}: Adsorbed iodine

ICCIDD: International Council for Control of Iodine Deficiency Disorders

ICP-MS: Inductively coupled plasma mass spectrometry

IDD: Iodine deficiency disorders

IED: Iodine excessive disorders

$I_{Sol(I^-)}$: Soluble iodide

$I_{Sol(IO_3^-)}$: Soluble iodate

I_{Sol}: Soluble iodine

ITCZ: inter-Tropical Convergence Zone

I_{TMAH}: Organically bound iodine

I_{Tot}: Total soil iodine

K_d: Solid ⇌ liquid partition coefficient

LOI: Loss on ignition

LRNI: Lower Reference Nutrient Intake

MDF: Mass discrimination factor

MQ: MilliQ

NDIR: Non-dispersive infrared detector

NPK: Nitrogen, phosphorus, and potassium

OM: Organic matter

PES: Polyethersulfone Membranes

RDA: Recommended daily allowances

RNI: Reference nutrient intake

S_A: Pseudo total sulphur (aqua regia extractable)

SATG: Somali Agriculture Technical Group

SD: Standard Deviation

SE: Standard error

Se: Selenium

Se_{Ads}: Total Adsorbed selenium

SEM: Scanning electron microscope

SEP: Sequential extraction procedure

$Se_{Residue}$: Residual selenium (recalcitrant)

$Se_{Sol(IV)}$: Soluble selenite

$Se_{Sol(VI)}$: Soluble selenate

Se_{Sol}: Total Soluble selenium

Se_{TMAH}: Organically bound selenium

Se_{Tot}: Total selenium

SOM: Soil organic matter

SPSS: Statistical Package for Social Sciences

SSA: Sub-Saharan Africa

SW: Surface water

SWALIM: Somalia Water and Land Information Management

TIC: Total inorganic carbon

TMAH: Tetramethylammonium hydroxide

TN: Total Nitrogen

TOC: Total organic carbon

UIC: Urinary iodine concentration

UNDP: United Nations Development Programme

UNICEF: United Nations Children's Fund

US EPA: United States Environmental Protection Agency

USGS: United States Geological Survey

WEAP: Water Evaluation And Planning System

WHO: World Health Organization

XAFS: X-ray absorption fine structure

XANES: X-ray absorption near edge structure

XRF: X-ray fluorescence

Abstract

Knowledge of the geochemical behaviour of selenium (Se) and iodine (I) in the calcareous and gypsiferous soils of Somalia is critical to a better understanding of their implications for human health. In particular, it is important to understand the effects of soil-type and sources of drinking water and irrigation water on Se and I provision to the human diet. Though dietary Se inadequacy is widespread in Africa (22%), no data is available for Somalia yet. Thus, this study aimed to understand and describe, for the first time, the soil-plant-water Se status and trace the causes of excess iodine reported in Somalia using a geo-nutrition approach. In addition, the study aimed to investigate the effect of soil properties on total Se and I concentrations, speciation and extractability in Somali agricultural soils. Samples of topsoil (n=12, 15 cm depth) were collected from rainfed and irrigated fields in Somalia and analysed for several trace elements (TEs) including Se and I. In addition, crops, which included maize (*Zea mays* L.), cowpea (*Vigna unguiculata* L.) and mung bean (*Vigna radiata* L.), and samples of their corresponding soils were collected from several farms (n=9). The Se and I concentrations of the surface water and groundwater samples were also measured. The results showed that Se deficiency is more likely to be prevalent in Somalia based on the Se status of agricultural soils (mean: 400 μg kg^{-1}), crops (Cow pea: 158 μg kg^{-1}; Mung bean: 41.7 μg kg^{-1}; and maize: 16.7 μg kg^{-1}), surface water (0.595 μg L^{-1}) and groundwater (3.63 μg L^{-1}). The total I concentration in groundwater (median: 990 μg L^{-1}) is consistent with the high urinary iodine contents reported in literature, revealing that drinking water was a greater source of excess iodine than iodised salt. Only the labile fractions of trace elements within the soil's rooting zone have the potential to be taken up by plants. Therefore much of the current study focussed on assessing the reactive forms of both Se and I in Somali soils and investigating the speciation of both elements. A three-step sequential extraction scheme was employed for the soil Se and I fractionation adapted to distinguish the operationally defined "soluble", "adsorbed", "organically bound" and recalcitrant fractions. The sequential extraction procedures applied to Somali agricultural soils demonstrated the presence of a large non-extractable Se pool, especially in carbonate-rich soils. Thus, the calcareous soil minerals (i.e. calcite and gypsum) are hypothesised to influence the dynamics of the Se and I species. This hypothesis is supported by the correlation between the residual Se and the $CaCO_3$ content of the soils. Therefore, the field survey was augmented by batch trials that examined the following: i) the interaction between Se species and calcareous minerals; ii) the interaction between I species and

these pure phases. The adsorption-desorption and fixation of Se and I on calcite/gypsum was investigated in a series of batch adsorption experiments covering a wide range of initial concentration ranges (5 µg L^{-1} – 5 mg L^{-1}), species (selenite, selenate and iodate) and contact times (from 1 to 21 days). Selenium sorption results revealed that the degree of Se sorption is dependent on the Se species and the solid phase. Selenium adsorption on gypsum (mean K_d value 4.60) was lower than that of calcite (mean K_d value 30). Both minerals showed greater affinities for selenite when compared to selenate. Adsorption of freshly added I (e.g. in irrigation water or rainfall) on calcite occurred rapidly (< 24 hours) with no evidence of consistent time-dependent sorption. However, desorption hysteresis for both Se and I was seen. In addition, stable isotopic Se (^{77}Se) and radioactive iodine (^{129}I) techniques were applied, using isotopic exchange principles, to determine the 'labile' pool of Se and I. Results from the batch adsorption and isotopic dilution experiments were supported by an EXAFS study aimed at understanding the Se bonding mechanisms on calcite, gypsum and calcareous soils. The EXAFS results indicated that selenite forms inner-sphere complexes on these minerals.

The data obtained from the field samples can be used as a predictive model for Se and I availabilities in crops grown in Somali calcareous soils. The batch sorption/desorption and isotopic dilution data is useful to model the dynamics and mobilisation of Se and I in carbonate-rich environments. Selenium mobilisation in these calcareous soils would improve uptake by plants and consequently improve animal and human health.

1. Literature review

1.1. Background

1.1.1. Geography and climate

The study presented in this thesis was primarily conducted in the agricultural areas of South Somalia. Somalia is located in the easternmost part of Africa (commonly known as the Horn of Africa) covering a total area of 637,657 km^2. It is bounded with three countries and two water bodies: the Gulf of Aden is on the north and the Indian Ocean on the east; Ethiopia and Kenya are on the west and Djibouti is to the northwest. Somalia officially consists of eighteen administrative regions. Mogadishu (at a latitude of 2° 2' N and longitude of 45° 20' E) is the capital city and administrative centre of the country. The most fertile land is found in the Juba and Shabelle Riverine areas in southern Somalia, between 41°53' and 46°09' east of the Prime Meridian; and between 0°16' south of the Equator and 5°04' north of the Equator (Venema & Vargas, 2007). Somalia is among thirteen countries crossed by the Equator (at 0° latitude). According to Venema and Vargas (2007) the climate varies from arid and dry semi-arid in the north-eastern and central regions to moist semi-arid in the northwest and south. There are four distinct seasons in the climatic year in Somalia, namely: the *Gu*, the main rainy season (April – June); the *Dayr*, is the second rainy season (October – December); the *Jilaal*, is a dry season (December- March); and the second dry season is the *Hagaa* (July – September). The annual rainfall in Somalia varies from 100 to 600 mm per year. The lowest annual rainfall (<100 mm a year) is in the northeast areas, followed by the central plateaus (200 to 300 mm); rainfall is greater in the southwest and northwest (500 to 600 mm a year). The mean daily maximum temperatures are 30 to 40 °C, whereas the mean daily minimum temperatures are 15 to 30 °C; both high temperatures (>45 °C) and very low temperatures below freezing point have been recorded in the northern region. The land is 600 m above sea level and is mainly flat except the mountainous coastal zone in the north and the valleys of the riverine zone in the south; the *Surud Cad* Mountain near Ceerigaabo (Erigavo) is the highest elevation in the country at about 2,408 m. The flatness of the land is important as it allows nomads and their herds greater freedom of movement. About 60% of the population practice a mobile way of life although this varies from 'highly nomadic' to 'agro-pastoralist'. Agriculture occupies about 70% of the total land area. Land under cereal production is 280,637 ha, representing only 0.4% of the total land area, although up to 13% of the land is suitable for cultivation. The forested area is 62,862 km^2 (10% of the total land) and 60% of the land area is categorized as pasturelands

(Hadden, 2007). The population in Somalia is estimated to be 15,442,905 and the population density is 63.77 per square mile (United Nations Population Division, 2019). These are only estimated figures, the last accurate census was made in 1975 when the population was 3.3 million (Fitzgerald, 2002). Population estimations are very difficult in Somalia because of the nomadic lifestyle, where settlements depend mainly on rainfall and the availability of natural pastures. The population is mainly clustered in villages near the rivers and also along the coast in the old trading centres including Kismaayo, Baraawe, Marca, Mogadishu, Berbera and Bosaaso.

1.1.2. Water resources

Somalia's main water resources are rivers, seasonal wadis, groundwater and precipitation which reaches up to 600 mm in some parts of the country, there are no natural lakes in the country. Somalia has two perennial transboundary international rivers, the *Jubba* and *Shabelle*, both originate from the Ethiopian highlands an enter Somalia through the Luuq and Belet-Weyne runoff stations respectively. These two rivers are very significant in southern Somalia as they are the main fresh water sources that sustain the livelihoods and economy of these areas. The Shabelle river's total length is 1,820 km, in Somalia the *Shabelle* river is about 1,100 km long and 82 m wide, with an area of about 90,000 km^2; the *Jubba* on the other hand is about 800 km long and 122.5 metres wide and its area is about 98,000 km^2 (Van den Bossche and Bernacsek, 1991). The water volume of these two rivers is variable and is dependent on precipitation; the *Jubba* carries more water than the *Shabelle*. Recently Sebhat (2015) used WEAP, a 'water evaluation and planning' model to assess water use and demands along the *Jubba* and *Shabelle* Rivers, he found that the long-term mean annual flow volume at entering points from Ethiopia to Somalia were 5,638 and 3,499 million $m^3\ yr^{-1}$ in the *Jubba* and *Shabelle* Rivers, respectively. The current estimated annual water use rates for irrigation are 11,428 $m^3\ ha^{-1}$ and 11,829 $m^3\ ha^{-1}$, respectively (Sebhat, 2015). In the northern part of Somalia there are no rivers, instead there are several deep valleys; the *Dharoor* and *Nugaal* are examples of seasonal *wadis* that form during the rainstorm.

In addition, groundwater resources are a major water source for the majority of the Somali population, providing fresh water for domestic use, livestock consumption and for small scale irrigation. The groundwater in Somalia is accessed mainly through boreholes, shallow wells and springs; the boreholes are more important than other sources because they provide a strategic year-round water supply when other sources dry up. The water in boreholes can be reached at a depth

in the range of 90 to 250 m, though it can be deeper, reaching up to 400 m in some locations; shallow wells on the other hand are < 20 m deep (FAO SWALIM, 2020).

1.1.3. Geology and soils

The geology of Somalia consists mainly of sedimentary formations, mostly young limestone and sandstone formations (BGS, 2020). These sediments are mainly Quaternary, Tertiary and Mesozoic in age. Three main Mesozoic sediments are recognized (i) Jurassic largely sandstone or limestone; (ii) Cretaceous undifferentiated; (iii) Upper Cretaceous. The tertiary sediments were formed during Palaeocene/Eocene or Oligocene/Miocene time. The remainder of the area is covered by unconsolidated Quaternary deposits, Quaternary volcanic and Precambrian-Cambrian basement (BGS, 2020). In southern Somalia where this study was conducted two main sedimentary basins can be distinguished, the NE–SW trending Mesozoic-Tertiary Somali coastal basin, and the NNE–SSW Mesozoic Luuq-Mandera basin. The two basins are detached by the Bur region where the Proterozoic-Early Paleozoic Metamorphic basement of southern Somalia outcrops (Carmignani et al., 2002). Data regarding Somali soils are scarce, the surveys conducted by Venema and Vargas (2007) provide a detailed background about the soils of riverine zones and the northwest zones.

1.1.4. Agriculture

The Somali economy largely depends on the Agricultural sector; livestock being more important than crop production. There are three types of agricultural practices in Somalia: (i) nomadic pastoralism, (ii) subsistence farming and (iii) market-oriented farming (Encyclopedia Britanica, 2020). In *nomadic pastoralism* goats, sheep, camels, and cattle are raised; livestock exports are the largest traded product in Somalia. In *subsistence farming,* practiced by small farmers, there are two approaches: (i) rain-fed farming in the south and northwest and (ii) irrigated farming along the rivers. In the rain-fed system sorghum, a crop known for its suitability in dry areas is grown, whereas in the irrigated farming system maize, sesame, cowpeas, vegetables and fruits are produced. *Market-oriented farming* consists of medium and large-scale irrigated plantations along the lower Jubba and Shabelle rivers.

According to Elmi (1991), the livestock sector accounted for more than 40% of the gross domestic product in 1988. It was also reported that a large proportion of the population were employed in this sector. Although agriculture is practiced in more than half of the country, local production is

not sufficient to meet the needs of the population; according to recent reports the cereal harvest only meets 40-50 % of the national cereal requirements (FAO, 2018). This deficit dictates the need for imported food to cater for the deficits (Gavin et al., 2019). Agricultural production is severely affected by recurrent droughts as it is heavily dependent on rainfall, and there is also substantial disruption to production as a result of the civil war. Currently Somalia is among the poorest countries, with the fifth lowest gross domestic product (GDP) per capita (c. $500) in the world (UNICEF, 2015).

1.1.5. Nutritional status of the Somali population

Globally, more than 800 million people are undernourished and over one third suffer from lack of essential vitamins and minerals in their food (Kumssa et al., 2015). People in Sub-Saharan Africa have the highest level of food insecurity in the world. According to the Food and Agriculture Organization of the United Nations (FAO) food security was defined to be a state in which "all people, at all times, have physical and economic access to sufficient safe and nutritious food to meet their dietary needs and preferences for a healthy and active life (Pinstrup-Andersen, 2009). In this context, there are food insecurities among Somali populations. The nutritional status of the Somali population is affected by the civil war, recurrent droughts and famine. After the collapse of the Siad Barre's regime in 1991, Somalia experienced poverty and the state of food insecurity was nearly in a constant state, most notably are the two officially declared famines of 1992 and 2011(Gavin et al., 2019). Somalia is one of the least developed countries; according to the United Nations Development Programme (UNDP)'s Human Development Index (HDI), Somalia is among the five least developed countries in the world (UNICEF, 2015). Moreover, according to FAO the country ranks the second last in terms of the proportion of undernourished members of the total population (FAO, 2003). High global acute malnutrition rates (15–20%) are also reported in Somalia. In order to understand the nutritional status of the Somali population, a significant understanding of each of the elements that contribute to the Somali food supply is required. The Somali diet is mainly composed from cereal crops (30 to 50%); maize and sorghum being the only meaningful elements of Somalia's domestic cereal production; the production of these crops dramatically declined after the civil war (Gavin et al., 2019). Although, a recent research Gavin et al., (2019) have shown that the country can potentially increase cereal production by the implementation of simple agricultural best management practices, however the country relies on cereal imports and aid due to production deficit. Therefore, understanding the dietary intakes of

macronutrients/micronutrients in Somalia necessitate knowledge regarding the chemical constituents of not only the local foods, but also the composition of the imported cereals and aid. In Somalia, there is lack of studies that measure the chemical constituents of the local diets. The available literature on micronutrient malnutrition in Somalia have shown that micronutrient deficiencies are widespread; especially iron deficiency, vitamin A deficiency; in addition, excessive iodine intake in Somalia was unexpectedly found (Kassim et al., 2010; Kassim et al., 2014), however, these studies did not consider Se or I geochemistry

1.2. Selenium

1.2.1. Importance in human health

Selenium (Se) is essential for human and animal health in trace amounts, but it is toxic in excess. In the past, Se was considered to be a toxic element until Schwarz and Foltz (1957) recognized its essentiality for mammals in the late 1950s; the researchers reported that Se could replace vitamin E in the diets of rats for the prevention of vascular, muscular, and hepatic lesions. The awareness of Se's significance to human health then increased after the landmark trial of Clark et al. (1996) that indicated an inverse relationship between Se status and the risk of cancer. Selenium is necessary for humans because it plays a key role in a number of metabolic processes, including antioxidant systems, thyroid hormone metabolism, immune system functions, and fertility. To date, approximately 25 genes that express essential selenoproteins have been identified; Se also forms a vital constituent of the biologically important enzyme glutathione peroxidase (Fairweather-Tait et al., 2011; Hurst et al., 2010; Rayman, 2005, 2008). Despite the benefits, both deficient and excessive intake of Se have adverse health effects.

Deficiency of Se in humans is common; approximately one billion people (15% of the world's population) suffer from an inadequate intake of Se (Combs, 2001). Selenium deficiency is associated with Keshan disease (cardiomyopathy) and Kashin-Beck disease (an osteoarthritis disorder) in some parts in China. The affected areas demonstrated low dietary Se intakes and were characterized by a high dependence on subsistence farming (Fordyce, 2005). Moreover, low Se status has been associated with cardiovascular disease (CVD), pancreatitis, asthma, inflammatory response syndrome, immune system functioning, response to viral infection, female and male fertility, and thyroid functioning (Rayman, 2000, 2002). Se toxicity is far less widespread than Se deficiency, and only a few cases of human exposure to high levels of Se have been observed in

several populations in seleniferous areas (Fordyce, 2005). For example, selenosis was reported in Enshi, China and was associated with high dietary intakes of Se. The Se-rich local food supplies, grown in soils containing nearly 8 mg kg^{-1} resulted in the highest Se concentration reported in local corn (6.3 mg kg^{-1}; see (Combs, 2001).

1.2.2. Dietary selenium intake

Globally, it is estimated that about 1 billion of the population have low dietary Se intake (White & Broadley, 2009). Dietary Se studies have been undertaken in many countries worldwide, and Se deficiency has been found in both underdeveloped and developed countries. Selenium has a fairly narrow margin between dietary deficiency (40 μg day^{-1}) and toxicity (400 μg day^{-1}; see Fordyce, 2013), and the UK reference nutrient intake (RNI) values for Se are 75 and 60 μg day^{-1} for adult males and females, respectively.

Per capita supply of dietary Se can be estimated by integrating the Food Balance Sheets (FBSs) of the Food and Agriculture Organization (FAO) and food composition tables for Se (Joy et al., 2014). Joy et al. (2014) estimated the per capita supply of dietary Se for 46 African countries. They reported that the average Se supply in Africa was 71 μg $person^{-1}$ d^{-1} but that supplies were highly variable with very high and very low Se supplies in Ghana and Djibouti, respectively. They presented variations within the continent and found that the southern and mid parts of Africa tended to have lower Se supplies. In sub-Saharan Africa, micronutrient deficiencies are widespread; for example, in eastern Africa alone, the estimated Se deficiency risk was 52% (Joy et al., 2014). The overall risk of inadequate Se intake in Africa is 22% (230 million people). In general, the Se intake depends on the food type available and the Se status of the location in which crops are produced.

Selenium concentrations in food crops are highly variable as a result of the variation in underlying geology and soil conditions; relatedly, human intake of Se also varies greatly between countries and regions. The likely estimated dietary intakes range from 3 to 7,000 μg day^{-1}, reflecting the variation in the Se concentrations in foods (Combs, 2001; Rayman, 2008). Selenium deficiencies in human populations are correlated to deficiencies in the soil. For example, the soil-type influences humans' Se status and contributes to widespread Se deficiency in Malawi. Higher Se intakes are found in villages with calcareous soil because of the greater bioavailability compared to the majority of (acidic) soils in Malawi (Hurst et al., 2013). Dietary selenium intake varies

between Europe and the USA: the range was estimated as 7–4,990 μg day^{-1} and mean values of 40 μg day^{-1} in Europe compared to an average of 93 μg day^{-1} for women and 134 μg day^{-1} for men in the USA (Rayman, 2012).

1.2.3. Sources of selenium in agriculture

1.2.3.1. Parent material

Geology can be used to some extent to predict the chemical characteristics of soils, including the presence of Se. A link between the Se concentrations in soil and the parent material has been reported (Fordyce, 2013; Fordyce, 2007). Generally, soils derived from sandstones and limestone materials have lower Se concentrations compared to those formed from finer grained sedimentary rocks, including clays and shales (Fordyce, 2013). The average Se concentrations vary between rock types: ultramafic igneous (0.05 mg kg^{-1}); basaltic igneous (0.05 mg kg^{-1}); granitic igneous (0.05 mg kg^{-1}); shales and clay (0.06 mg kg^{-1}); deep-sea clay (0.17 mg kg^{-1}); lime stone (0.08 mg kg^{-1}) and sandstones (0.05 mg kg^{-1}; (Sparks, 2003). Intrusive igneous rocks tend to have a lower Se concentration than that found in extrusive rocks such as basalt and ash (Saha et al., 2017). It has been reported that soils formed from Jurassic siltstones and sandstones have low a Se content, while high Se concentrations are found in clay rich sedimentary rocks such as mudstones and shales (Mayland et al., 1989; Saha et al., 2017; Statwick & Sher, 2017).

1.2.3.2. Precipitation

Selenium wet deposition contributes to the distribution of Se in soils; in China, the East Asian summer monsoon has been linked with the trace elements levels, including Se (Sun et al., 2016). In southeast China, high Se input (200–400 μg m^{-2} yr^{-1}) occurred from wet deposition (Sun et al., 2016). Similarly, in Norway the soil Se concentration has risen in high precipitation areas from 0.2 to 1.4 mg kg^{-1} (Wu and Låg, 1988). Rainfall samples collected from several locations in the USA and Denmark have indicated selenium concentrations of 0.02–0.37 μg L^{-1} (Risher, 2011).

1.2.3.3. Irrigation water

Since the Se concentrations of most soils is generally low (mean is 0.4mg kg^{-1} ; Fordyce, 2013), its addition through irrigation water can be an important tool in the long-term Se biofortification

of agricultural systems. The natural addition of Se in the form of selenate into the soil-plant system through irrigation water at sites in Punjab was reported; the irrigation-induced Se concentration was high, ranging from 2.6 to 5.2 kg ha^{-1}(Eiche et al., 2019). Similar Se enrichments in soils irrigated with Se rich groundwater were also reported (Bajaj et al., 2011). In addition, the sequential extraction of these soils revealed that the Se bioavailability in these soils was also high, reaching up to 50%. Selenium additions reached 881 g ha^{-1} y^{-1} as a result of irrigating with high Se groundwater that had 2.5–69.5 μg L^{-1} (Dhillon and Dhillon, 2014).

1.2.3.4. Incidental input from fertilizer

Selenium is found naturally in some phosphorites, phosphate fertilizers, and coal; therefore, incidental Se addition may occur from these sources through the application of phosphate fertilizer that contains trace amounts of Se (Combs & Combs, 1986).

1.2.3.5. Biofortification inputs

Selenium biofortification of food crops can be achieved in the long-term (genetic biofortification) and in the short-term through agronomic biofortification (Broadley et al., 2006). Agronomic biofortification of Se using foliar application can increase the Se contents in grain, fruit, and storage roots (Lyons, 2018). Although the application of both selenate or selenite has been reported, the agronomic biofortification of food crops has indicated the efficacy of Se biofortification in the selenate form (Boldrin et al., 2013; Broadley et al., 2006; Li et al., 2018; Lyons, 2018; Mao et al., 2014; Ros et al., 2016). Other studies such as the recent review of (Ros et al., 2016) have demonstrated that selenate was 33 times more efficient than selenite. Selenium can also be combined with nitrogen-phosphorus-potassium (NPK) fertilization; for example, a study in Malawi indicated that the Se content of grain increased by 21 μg kg^{-1} for each gram of Se applied as NPK + Se (Chilimba et al., 2012).

1.2.4. Chemistry of selenium

Selenium is a naturally occurring metalloid element in the oxygen group. It has an atomic number of 34, an atomic mass of approximately 79, and six natural isotopes, namely ^{74}Se (0.87%), ^{76}Se (9.02%), ^{77}Se (7.58%), ^{78}Se (23.52%), ^{80}Se (49.82%), and ^{82}Se (9.19%). It is a chalcophile element,

and it replaces sulphur (S) in many sulphide minerals. Like S, Se can exist in four oxidation states, namely the oxidation states of -2 (selenide Se^{2-}), 0 (elemental selenium), +4 (selenite SeO_3^{2-}) and +6 (selenate SeO_4^{2-}(Martens, 2003).

1.2.4.1. Factors affecting adsorption in soils

Selenium can be strongly retained by surface reaction with soil constituents. In the soil selenate is highly soluble but selenite is strongly adsorbed onto surfaces such as iron oxide surfaces, clay minerals, soil organic matter and soil carbonates (Aurelio et al., 2010). The magnitude of this sorption is influenced by the soil properties such as the pH and redox potential, Se speciation, and biological assimilation and transformation (Etteieb et al., 2019). The following subsections describe the soil factors that control Se retention in soils.

- **Effect of pH and Redox Potential**

The soil pH affects both selenium speciation and the electrostatic charge on organic and mineral surfaces and, thereby, partly controls Se affinity for adsorption surfaces. Typically, under high pH conditions selenite anion adsorption onto clays and metal (i.e., Fe, Al, Mn) oxides is favoured as compared with selenate (Mayland et al., 1991). Highest sorption was reported between pH 3 and 5 for all clay minerals, and a decline was observed above neutral pH (Hamdy & Gissel-Nielsen, 1977). Goldberg and Glaubig (1988) offered an excellent overview of selenium adsorption on calcareous and clay minerals under various pH conditions. They highlighted the importance of pH on the sorption on kaolinite, montmorillonite, and calcite in calcareous soils. They found that sorption increased between pH 6–8, the maximum sorption occurred between 8 and 9, and decreased above pH 9. Frost and Griffin (1977) studied the effect of pH on Se adsorption by the clay minerals kaolinite and montmorillonite, and they suggested that the sorption is strongly dependent on solution pH and that the adsorption was greater with montmorillonite. In general, an increase in the pH is associated with a less positive surface charge, which therefore causes a decrease in the adsorption strength (Lounsbury et al., 2016).

The redox potential, which is the electrochemical potential or electron availability of a system, plays a pivotal role in all inorganic and organic chemical reactions (Hillel and Hatfield, 2005). The redox potential has been used by geochemists and soil scientists to describe the oxidation-reduction status of environmental systems such as soils, sediments, and water (DeLaune & Reddy, 2005). Redox potential (Eh) and pH diagrams can be used to describe the solubility and speciation of Se

in the environment. Elrashidi et al. (1987) studied the chemical equilibria of Se in soils, and they reported that under high (positive) redox potentials, selenate is the major species in the soil solution while selenite is the predominant Se species under medium redox conditions. Selenides (Se^{2-}) and elemental Se (Se^{0}) are dominant at low redox conditions. In general, selenate (Se^{VI}) is favoured under oxidizing alkaline conditions while selenite (Se^{IV}) is favoured under reducing environments (Etteieb et al., 2019).

- **Soil organic matter (humus)**

Selenium is commonly associated with organic matter in soils (Gustafsson and Johnsson, 1994). Gustafsson and Johnsson (1994) described the mechanism of the interaction between selenium and humic substances in soils and aquatic systems of forests by applying labelled and unlabelled selenite to these ecosystems. They confirmed that there is rapid selenium retention by the surface horizons of forest soils, and they suggested that the mechanism is mediated by microorganisms by reducing Se to low valence states to facilitate its incorporation into low-molecular-weight humus fractions. Selenium association with organic matter has been confirmed by Wang and Gao (2001) who found that Se is immobilized in a soil that constituted about 6–10% of organic matter; they also observed Se accumulation mainly in the surface layer where organic matter accumulates. Although soil organic matter plays a pivotal role in Se retention, it also immobilizes Se in a form that is unavailable for plant uptake (Fordyce, 2013).

- **Carbonates**

Selenium's association with soil carbonates has been previously reported. Of the most significant studies which indicate a direct link between carbonates and Se is that of (Aurelio et al., 2010). Their Extended X-ray Absorption Fine Structure (EXAFS) and theoretical modelling studies indicated that calcite is a large sink for Se. They also confirmed selenite ion substitution with the carbonate anion. The structure and size similarities between selenite and carbonate ions and the related ease of their exchangeability has been also documented by earlier studies such as (Cowan et al., 1990). Selenium adsorption on calcite under real environmental conditions in calcareous soils was also reported by Goldberg and Glaubig (1988). They found that the magnitude of Se sorption on calcite was four times that of kaolinite and eight times that of montmorillonite. They also found that if calcite is removed from a calcareous soil, it significantly affects the shape of the

Se sorption isotherm of the calcareous soils, which suggests the important role that calcite has in the sorption process.

- **Texture**

Several studies have demonstrated that soil particle size has a pronounced effect on Se sorption behaviour. Early examples include the study conducted by (Wells, 1967) who observed that clay soils retain more Se than sandy and loamy particles (Yläranta, 1983). Similarly, Vuori et al. (1989) documented a positive correlation for selenate sorption with fine, textured soils. In previous studies on selenite sorption on Danish soils, the greatest sorption was found on clays and silts while the sorption was lowest on sandy soils (Hamdy & Gissel-Nielsen, 1977). The type of clay mineralogy is also another significant factor that affects Se sorption capacity. Montmorillonite, kaolinite, and vermiculite have all exhibited some capacity for Se adsorption (Bar-Yosef & Meek, 1987; Goldberg & Glaubig, 1988; Hamdy & Gissel-Nielsen, 1977; Missana et al., 2009). Hamdy and Gissel-Nielsen (1977) studied selenium fixation as a function of time up to 10 days using kaolinite, vermiculite, and montmorillonite clay minerals. They found that kaolinite fixed the largest amounts of selenium as compared to the 2:1 type clay minerals. Among the 2:1 type clay minerals, vermiculite retained more selenium than montmorillonite. Bar-Yosef and Meek (1987) studied Se sorption by kaolinite and montmorillonite at different pH levels; the resulting adsorption isotherms suggested higher affinity at low Se concentrations. Both the studies of Bar-Yosef and Meek (1987) and of Hamdy and Gissel-Nielsen (1977) suggested that selenite fixation by clay minerals occurs in two distinct kinetic phases—an initial fast uptake is followed by a slower uptake. Goldberg and Glaubig (1988) studied selenium adsorption on calcareous and clay minerals. They compared two clay minerals, montmorillonite and kaolinite, and found that sorption was greater in kaolinite (twice more) compared with montmorillonite. They also found that the sorption behaviour of Se was dependent on the pH: a low pH enhanced sorption on clay minerals with maximum sorption at pH 5. Selenium adsorption on montmorillonite has been studied by the EXAFS and X-Ray Absorption Near Edge structure (XANES) spectroscopic studies conducted by (Peak et al., 2006); they observed the formation of bidentate, binuclear inner-sphere complexes of selenite oxyanions on montmorillonite.

- **Iron oxides and oxyhydroxides**

Iron oxides and oxyhydroxides are common soil constituents (Bergaya & Lagaly, 2013); in theory, goethite is the most common and thermodynamically stable iron (Fe) oxide in soils while haematite is the second most common Fe oxide (Sparks, 2003). Other soil Fe oxides include maghemite and ferrihydrite (Sparks, 2003). Iron oxides are usually formed from the weathering of Fe bearing silicates and sulphides (Bowles, 1997). These Fe oxides and oxyhydroxides are important for controlling the geochemistry of Se. Goethite tends to exhibit a high adsorption capacity for selenite (Zhang & Sparks, 1990a). Batch adsorption experiments have indicated that the adsorption capacity of the iron oxyhydroxides is strongly related to the positive surface charge density which increases as pH falls below the point of zero charge of the mineral. Selenite adsorption on goethite has been confirmed by several studies, including the X-ray absorption fine structure (XAFS) studies of (Hayes et al., 1987) and Manceau and Charlet (1994); both studies describe the adsorption mechanism as an inner-sphere complexation. Similarly, Duc et al. (2003) described selenite sorption as an inner-sphere surface complex while selenate was sorbed as an outer-sphere complex. Selenium adsorption on iron oxides (pzc c. 7-8) exceeds that of manganese dioxide (pzc c. 2-4) at a given pH and concentration. Balistrieri and Chao (1990) compared the adsorption of Se by amorphous iron oxyhydroxide and manganese dioxide in 0.1 M potassium chloride (KCl); sorption was measured as a function of time (5 min–24 hr) and under a range of pH values (4–11). They found that Se adsorption was greater on the amorphous iron oxyhydroxide compared with the manganese dioxide and that the adsorbed Se species was mainly selenite.

- **Manganese oxides**

Manganese oxides are common soil constituents which can act as an adsorbent material for trace elements including Se. The most common form of Mn oxide in the soil is birnessite (Mc Kenzie, 1989; Sparks, 2003). Generally, Fe, Al, and Mn oxides play a pivotal role in Se mobility in moist and acidic soils, while alkali metal carbonates (mainly $CaCO_3$) control sorption under alkaline and arid conditions (Barrow & Whelan, 1989; Jezek et al., 2012; Mathers et al., 2017).

Selenium associations with Mn oxides have been reported by Balistrieri and Chao (1990) who examined sorption onto these oxides as a function of pH, concentration, and oxidation states. Their data revealed that Se sorption was significant but was less than that of the Fe oxides. According to their interpretation, selenite was strongly bound as compared with selenate, suggesting the formation of inner-sphere and outer-sphere complexes, respectively. Several other studies have

demonstrated that the Fe and Mn oxides bound Se to be the dominant Se fraction (31–91%), according to the sequential fractionation of soils (Wang et al., 2012).

- **Aluminium oxides**

Aluminium oxides are another important soil constituent capable of binding Se in the soil. Lévesque (1974) studied Se sorption on a wide range of surfaces and found a significant positive correlation between soil Se and the Al oxide content (Goldberg, 2013). Peak (2006) described selenite adsorption on amorphous Al oxide and found both inner-sphere and outer-sphere complexation mechanisms. On the other hand, Wijnja and Schulthess (2000) found only outer sphere complexation mechanisms between selenate and aged γ -Al_2O_3 surfaces. Several other studies have also found evidence of the association between soil Se and the Al oxides; for example, (Mathers et al., 2017) reported stronger ^{77}Se retention in a soil containing higher Fe and Al oxide concentrations. Goldberg (2013) described Se adsorption envelopes on amorphous Al oxides using the triple layer model of surface complexation and discovered the maximum adsorption was at pH 7 (Goldberg, 2013) and pH 8 (Gabos et al., 2014).

1.2.4.2. Fixation reactions

Selenium can be apparently 'fixed' by soil constituents – that is, rendered chemically and biologically non-labile or inert. The predominant soil constituents that can incorporate Se in non-reactive forms are soil organic matter, some clay minerals, metal oxides and possibly calcite, although the magnitude and the nature of 'fixation' probably differs between the various adsorbents (Aurelio et al., 2010; Gissel-Nielsen et al., 1984; Mikkelsen et al., 1989; Montes-Hernandez et al., 2011).

For example, a study conducted by Coppin et al. (2009) revealed that fixation capacity was greater with soil organic matter compared to clay and Fe-(hydr)oxide minerals. Knowledge regarding the mechanism of fixation is important. Balistrieri and Chao (1990) attributed Se fixation by clay and Fe-(hydr)oxides to the formation of strong inner-sphere surface complexes. By contrast, fixation in calcite may involve incorporation into the carbonate matrix, and in soil humus covalent, carbon bonding to Se may be a relevant mechanism.

Understanding Se fixation may be important in assessing the likely fate of applied Se and refining fertilizer application rates on different soils. One difficulty in quantifying the fate of soil-applied

Se is the identification and measurement of Se originating from the applied fertilizer against a larger soil Se background. An application of 10 g ha^{-1} of Se may add only 4 µg kg^{-1} to a background soil Se concentration of approximately 200 µg kg^{-1} (assuming 2,500 t ha^{-1} of soil). However, enriched stable Se isotopes can be used to trace the fate of applied Se and discriminate between soil-derived and fertilizer-derived Se. In an isotopically labelled experiment, Mathers et al. (2017) quantified the retention of a single, realistic Se biofortification application (10 g ha^{-1}) on three contrasting soils over two growing seasons, by utilizing an enriched stable Se isotope (^{77}Se). They found that the retention at harvest was higher with topsoil (c. 15 – 31%) as compared with the subsoils (2-4%), suggesting rapid immobilization. Top soils have more organic matter content than subsoils and it is likely that the fixed (added) Se was held in its organic form. Evidence of selenium fixation by other phases is limited, but fixation in calcite, which is relevant to Somali soils, has been reported by Aurelio et al. (2010) and Montes-Hernandez et al. (2011).

1.2.4.3. Leaching from soil

The fate of added Se and knowledge regarding its leaching characteristics are important. Previous studies evaluating leaching of added Se observed that less than 0.2% of the Se added in the form of sodium selenite or sodium selenate was leached through a 20 cm column of either clay soil or fine sandy soil (Yläranta, 1982). In the case of a peat soil, more than 7% of the selenite and 84% of the selenate was leached (Yläranta, 1982). Rapid selenate losses from the soil are also confirmed by the field trials of Mathers et al. (2017). They suggested that after an application, approximately 40% of the applied $^{77}Se^{VI}$ was leached rapidly, and the remainder was distributed between crop tissues or transformed into non-available forms bound to humus. Thus, at field capacity (c. 800 m^3 water in topsoil per hectare), this is equivalent to a loss of 4 g ha^{-1} from 10 g ha^{-1} application or a solution concentration of 5.0 µg L^{-1}. Concentrations in this range could have implications regarding risks to water supplies (Mathers et al., 2017) but should also be seen in the context of the current drinking water regulations (50 µg L^{-1} and 10 µg L^{-1} (Inspectorate, 2010; US EPA, 2009).

1.2.4.4. Volatilization

Volatilization of reduced organic Se from sediments may occur as dimethylselenide (DMSe), diethylselenide (DESe), and dimethyldiselenide (DMDSe; see Ashworth & Shaw, 2006b; Chasteen & Bentley, 2003; Losi & Frankenberger, 1997; Peitzsch et al., 2009). However,

volatilization from aerobic soils is probably very limited because of redox conditions and strong sorption reactions. Thus, for example, no selenium volatilization was observed according to a lab-based incubation experiments conducted by (Yläranta, 1982). They found that an addition of 1 mg kg^{-1} of selenite and selenate to either clay or sandy soils did not result in any Se loss during three months of incubation.

1.2.5. Uptake by plants

1.2.5.1. Concentration of Se in crop plants and diet

Selenium concentrations in food crops are highly variable as a result of the variation in (i) underlying geology and soil conditions and composition; (ii) plant species and metabolism in plants; and (iii) fertilizer application rates (Gissel-Nielsen et al., 1984). To increase human intake of Se, increasing Se concentration in locally consumed crops either through the use of Se fertilizers (agronomic biofortification) or by genetic improvement is necessary (Marschner, 2011). According to their response to Se, plants can be categorized into three classes: Se-accumulators, Se-indicators, and Se non-accumulators. Non-accumulators rarely accumulate more than 100 mg kg^{-1} Se (dry weight), whereas Se-accumulators highly tolerant to Se can contain up to 40,000 mg kg^{-1} Se (dry weight) when grown in seleniferous environments (Jacobs, 1989). The only Se-accumulator plant which is commonly used as a food source is the tree *Bertholletia excelsa* (which produces Brazil nuts). These nuts are among the richest plant Se sources (Cardoso et al., 2016). However, some common crop species are secondary Se-accumulators, including the Brassica (rapeseed, calabrese or broccoli, and cabbage) and the Allium species (garlic, onions, leeks, and wild leeks) whereas cereal crops such as wheat, oats, rye, and barley are non-accumulators (Broadley et al., 2006; Fordyce et al., 2010; WHO, 1987).

1.2.5.2. Plant uptake pathways

Selenium uptake from the soil solution by plants depends on the bioavailable Se fraction in the soil which is in turn influenced by soil conditions such as soil pH, redox potential, clay content, metal oxide content, organic matter content, calcite, and the availability of competitive anions, such as sulphate, phosphate, and organic acid anions (Aurelio et al., 2010; Fordyce, 2013b; Mikkelsen et al., 1989; Øgaard et al., 2006; Wijnja & Schulthess, 2000). A soil might have relatively low total Se content, but it may produce a high Se concentration in plants due to high bioavailability, for example selenate under well-aerated calcareous conditions (pH 7–8.5; see

(Rodriguez, Rivero, & Ballesta, 2005). According to solution culture studies reported by Zayed et al. (1998) and Kikkert and Berkelaar (2013), plant Se uptake follows the ascending order of selenite, selenomethionine, selenocystine, and selenite. Selenium transfer within plants is easier than iodine, because it is more phloem mobile than iodine (Lyons, 2018). The uptake is mediated by transporters present in root cell membranes but varies depending on the Se species. For example, selenite is transported through the phosphate transporters (H. Li et al., 2008) whereas selenate is transported through sulphate transporters (Feist and Parker, 2001; Zhang et al., 2003).

1.2.5.3. Uptake in response to biofortification

Enriching grain Se concentration can be done by foliar application or Se application to the soil. For instantaneous plant uptake, selenium can be applied in the most bioavailable forms of sodium selenate and potassium selenate; Se can also be applied as selenite or less-mobile selenates, for example $BaSeO_4$, for long-term effects (Broadley et al., 2006; Gissel-Nielsen, 1998; Gupta & Gupta, 2002). Once Se is added in the form of selenite (i) it is first transported through phosphate transporter cells; (ii) then it is transformed to organo-selenium compounds in the root. The uptake of selenate is different: (i) it is transported through sulphate transporters; (ii) then it is transported to the xylem and to the shoot (Broadley et al., 2006; Terry et al., 2000; P. J. White & Broadley, 2009). Results have indicated that foliar application is more efficient compared to the soil Se application; this is due to the ease of phloem mobility (Lyons, 2018; Ramkissoon et al., 2019).

1.3. Iodine

Understanding the environmental behaviour of iodine (I) is crucial because of its role in human and animal nutrition. Iodine is essential for the synthesis of thyroid hormones that regulate various physiological processes (Zimmermann & Köhrle, 2002). Iodine is a non-metallic element and is a member of the halogen family. It has an atomic number of 53 and an atomic mass of approximately 127. Unlike Se, I has only one stable isotope, ^{127}I, that exists in nature; there are more than 20 radioactive isotopes. Iodine naturally exists in several oxidation states ranging from −1 to +7. In reducing environments, I exists as iodide (I^-) and under more oxidizing conditions as iodate (IO_3^-; see (Preedy et al., 2009).

1.3.1. Importance of iodine in human health

Environmental iodine deficiency may result in a number of health complications collectively known as iodine deficiency disorders (IDD), such as goitre, miscarriage, infertility, and intellectual disability (Delange et al., 2001; Longombe & Geelhoed, 1997). Iodine deficiency not only threatens humans' health, but it has become a threat to the social and economic development of many countries (Preedy et al., 2009). While the number of countries affected by iodine deficiency is steadily decreasing, the number of countries with excessive intake has doubled recently over several years (Zimmermann, 2013); this is possibly due to over-iodized salt or a high content of iodine in groundwater, such as in Somalia (Mannar & Hurrell, 2018). Excessive iodine intake may induce thyroid dysfunction, which may lead to both hypo- and hyperthyroidism (Leung & Braverman, 2014).

Globally, approximately 2 billion people are estimated to be iodine deficient. For comparison, 1.1 billion have zinc (Zn) deficiency, and about 1 billion are estimated to have low dietary Se intake. In sub-Saharan Africa, the deficiencies of these elements are widespread; for example, in eastern Africa alone, according to food supply data from the Food and Agriculture Organization, the estimated deficiency risks were 75%, 52%, and 26% for Zn, Se, and I, respectively (Joy et al., 2014a; Kumssa et al., 2015; White & Broadley, 2009; Zimmermann et al., 2008). Iodine is required in small amounts, and the recommended daily intake varies depending on the age and the reproductive status of the individual; for example, the recommended daily dietary allowance (RDA) is 120 μg for school age children (6–12 years old), 150 μg for adult men and women, and 250 μg for pregnant women (World Health Organization, 2004). The overall iodine status of a population can be accurately characterised by the median urinary iodine concentration (UIC), which is the most reliable, widely-used biomarker of iodine intake in populations. According to the WHO criteria, UIC < 150 μg L^{-1} is insufficient, 150–249 μg L^{-1} is adequate, and ≥ 300 μg L^{-1} is excessive (World Health Organization, 2001). Kassim et al. (2014) reported that iodine intake in Somalia is among the highest levels in the world, the fifth highest globally, and is classed as excessive according to the guidelines of the WHO, UNICEF, and the International Council for Control of Iodine Deficiency Disorders (ICCIDD) with > 300 μg L^{-1}. The ICCIDD reported that the median UICs for non-pregnant women and children were 329 and 416 μg L^{-1}, respectively. Though excessive iodine intake has been reported in Somalia, there has not yet been a geochemical study to investigate the contribution of drinking water to the dietary iodine intake. Therefore, one

aim of this study is to determine the iodine content of drinking and irrigation water in Somalia and to examine the variations in iodine concentration between groundwater and surface water. The study calculates the estimated iodine intake from drinking water and investigates the association between water iodine concentration and the excessively high UICs reported in the literature. A further aspect of the study concerns the fate of iodine in soil when irrigation with ground and surface water is practiced in Somalia. The change in bioavailability and capacity of soils in Somalia to fix iodine into calcite and gypsum is assessed by an adsorption-desorption and isotopic dilution experiments using ^{129}I as a tracer.

1.3.2. Dietary iodine

Diet is the main source of iodine, with seafood, dairy products, iodized salts, and drinking water being the most iodine-rich sources. Several studies have demonstrated that both insufficient and excessive iodine intakes exist. The body of literature includes studies that indicate excessive iodine intake in populations that drink iodine-rich water in some locations such as China (Zhao et al., 1998) and Somalia (Kassim et al., 2014). Iodine intake is also high in populations that consume (i) iodine-rich seafood as in Japan (Suzuki et al., 1965), (ii) iodine-rich meat and dairy products as in Iceland (Sigurdsson & Franzson, 1988), and (iii) iodized salts in some African and American countries (Zimmermann, 2009). Generally, I from drinking water is unlikely to provide more than 10% of the daily requirements for adults (Fuge, 2013). However, drinking water can be a direct source of I intake, which may eventually govern iodine intake levels and become a source of regional variations in a population's iodine status. Iodine-rich ground water has been reported in many places in the world and has been found to contribute to the iodine excessive disorders (IED; see Andersen et al., 2002; Fordyce et al., 2000; Watts et al., 2010). The significance of grains and vegetable is also noted; for example, (Hou et al., 1997) reported that 52–70% of the total iodine intake in four provinces in China is obtained from grains and vegetables.

1.3.3. Sources of iodine in agriculture

1.3.3.1. Parent material

A recent and extensive review of iodine geodynamics has been provided by (Humphrey et al., 2018). They found that iodine content in the soil is generally much higher than that of the parent material, which suggests that the role of the parent rock is not as significant as inputs from wet and dry deposition, for example, of volatilised iodine compounds from oceans (Fuge & Johnson, 2015).

Johnson (2003) reproduced data from Fuge et al. (1998) summarising the iodine content of common rock types and demonstrated that the mean iodine concentration tends to be higher in sedimentary rocks as compared to igneous rock types. According to Fuge and Johnson (1986), the iodine concentration in different rocks is normally in the following ascending order: igneous rocks < sandstones < shales < carbonates < recent sediments. Average concentrations (mg kg^{-1}) are: 0.24 for igneous rocks, 0.8 for sandstones, 2.3 for shales, 2.7 for carbonates, 5–200 mg kg^{-1} for recent sediments. In sedimentary rocks concentrations (mg kg^{-1}) are typically: (Shales 2.3); (Sandstones 0.8); (Limestones 2.7); (Organic-rich shales 16.7). In igneous rocks the corresponding values are: (Granite 0.25); (All other intrusive 0.22); (Basalts 0.22); (All other volcanic 0.24); (Volcanic glasses 0.52). Other studies have found elevated iodine concentrations in sedimentary rocks such as organic-rich shales, e.g. Kimmeridge Shale, Dorset, England with 23.3 mg kg^{-1} (Fuge et al., 1978).

1.3.3.2. Precipitation

There is evidence supporting the importance of rainfall for iodine enrichment of the soil, in particular soils that occur in close proximity to the ocean (Fuge, 1996). Although wet deposition has a significant role, the fate of the added iodine is also heavily influenced by soil characteristics that affect its retention, release, and speciation (Humphrey et al., 2018). According to Johnson (2003), the total iodine concentration in rainwater and snow demonstrates a range of values between 0.5–20 µg L^{-1}. The quantity of iodine added to the soil by rainfall can be predicted from the average annual rainfall and the iodine concentration of rainwater. For example, (Whitehead, 1979) predicted the iodine input from the annual rainfall of 900 mm in the UK and an average rainwater iodine concentration of 1.5 µg L^{-1}. According to this prediction, the input from rainfall is up to 6 mg kg^{-1} to a depth of 15 cm during a period of 1,000 years. Iodide accounts for up to 50% of the I in rainwater, and iodate is the second dominant iodine species (Fuge, 2013).

1.3.3.3. Irrigation water

Irrigation water from rivers, lakes, and groundwater also contributes to the iodine content of a soil. Rivers play an essential role by carrying water and nutrients, and agricultural usage accounts for more than 70% of abstraction from fresh water (Wisser et al., 2008). According to Johnson (2003), the iodine concentration in river water ranges 1–10 µg L^{-1}. The iodine concentrations in freshwater lakes are similar to those of rivers (1–10 µg L^{-1}; Johnson, 2003). However, in some areas, the

groundwater may be used for drinking, which may contain much higher levels of I that could potentially lead to concerns of excessive I intake by human populations (Shen et al., 2011). Some studies have reported high I concentrations in saline waters such as in coastal and arid or semi-arid areas (Smedley, 2000). The sources of I in groundwater are closely linked to the hydrochemical characteristics of groundwater and the lithological features of the aquifer (Shand & Frengstad, 2001). In freshwater, I exists as iodide, iodate, and organic I; the concentration of organic I is also generally comparatively high in freshwater, such as in river water, lake water, and rain (Abdel-Moati, 1999; Gilfedder et al., 2007; Reifenhäuser & Heumann, 1990; Truesdalea & Jones, 1996). However, iodine concentrations in freshwater are normally much lower (approximately 10 times lower) than that in seawater. Seawater is considered to be the largest source of I (Fuge & Johnson, 1986; Muramatsu & Wedepohl, 1998).

'Iodination' (iodine enrichment) of irrigation water has been reported to be a useful tool to tackle iodine deficiencies. Cao et al. (1994) proved the possibilities of producing iodine-enriched food through the irrigation of paddy soils with iodized water in Xinjiang, China. Several other laboratory studies with, or without, soils (culture media) have described the effect of enrichment of different iodine species through irrigation on iodine uptake by different plant species. For example, Li et al. (2017) conducted iodine biofortification hydroponic experiments to evaluate the effect of iodide and iodate on the quality and growth of strawberries. Other important studies include those of Cakmak et al. (2017) and Lyons (2018); these studies described the possibilities of iodine biofortification for cereal crops.

1.3.3.4. Biofortification inputs

The biofortification of crops by applying iodized fertilizer can increase the iodine concentration of food and, therefore, improve iodine dietary intake. One of the landmark studies that evidenced the effectiveness of agronomic biofortification is the case study reported in the Xinjiang province in north-west China (Lyons, 2018). Iodate in the form of potassium iodate was added to the irrigation water, and this resulted in a significant increase in the soil I content (three-fold), in crops and plants as well. Furthermore, according to a longer-term study, it resulted in better health in the human population with a 50% reduction in infant mortality (Lyons, 2018; Xin-Min et al., 1997). In a greenhouse experiment, Cakmak et al. (2017) investigated the feasibility of iodine biofortification of wheat, rice, and maize through fertilizer application. Their study demonstrated

increased I concentrations in whole grain of rice, maize and wheat as well as in polished rice and wheat endosperm. Lyons (2018) reviewed the agronomic biofortification of cereals with Se and I and proposed a simultaneous application of these micronutrients since their concurrent deficiencies are widespread.

1.3.4. Chemistry of iodine in soil

Several studies have been devoted to the geochemistry of iodine in soils, because it links between the food chain and the environment. The average concentration of iodine in topsoils worldwide is around 5 mg kg^{-1} (Fleming, 1980). Johnson (2003) compiled a database of published iodine literature for soils from all over the world. Iodine is present in soils as iodide, iodate, and organic iodine compounds. Little iodine is present in the soil solution, and most soil iodine is associated with organic matter with lesser amounts sorbed on clays and oxides of Fe and Al (Fuge & Johnson, 1986). The prevalent form of iodine in the soil solution is often iodide and soluble organic iodine, but iodate may also occur depending on pH and redox conditions (Fuge & Johnson, 1986; Kodama et al., 2006; Mackowiak & Grossl, 1999).

Marine sediments are the largest store of I (70%) due to the seawater iodine concentration (Muramatsu & Wedepohl, 1998). The amount of I in surface soils typically declines as the distance from the sea increases. Iodine deficiencies also exist in regions where I-containing topsoil has been removed by glacial movement or soil erosion due to heavy rain or flooding (Delange, 2000).

1.3.4.1. Factors affecting adsorption of iodine in soils

Sorption processes are one of the main factors that influence iodine and other micronutrients' fixation on soil components. Soil organic matter, oxide minerals, and clays are all known for their abilities to retain iodine in soils (Johnson, 2003). Knowledge regarding the mechanisms governing iodine interaction with these soil constituents is important to understand iodine solubility and plant uptake mechanisms as well (Humphrey et al., 2018).

- **Effect of pH and redox potential**

The pH and Eh (redox potential) are important factors that govern the biogeochemical dynamics of iodine. An inverse correlation between soil iodine concentration and pH has been reported in the literature (Humphrey et al., 2018). This may be due to the pH-dependence of the anion exchange capacity of pH-dependent charge soils (Xu et al., 2016), but it is also likely to reflect

conditions affecting iodine binding by soil humus (Shetaya et al., 2012). Iodine speciation is also affected by pH and Eh. Johnson (2003) reported that under acidic conditions, iodide is the dominant inorganic iodine species while iodate exists in alkaline soils. The study conducted by (Shetaya et al., 2012) reported that the initial iodate sorption rate is strongly influenced by the soil pH.

- **Soil organic matter**

The soil iodine content is often found to be related to the soil organic matter content (Yamada et al., 1999). Most studies in the literature confirm the impact that the soil organic matter has on iodine retention based on the soil, its speciation, and fixation (Johnson, 2003; Sheppard & Thibault, 1992). Therefore, peat soils tend to be the most iodine-rich soils within regions. The mechanisms that govern iodine retention by soil organic matter probably involve both biotic and abiotic processes that affect the bonding of iodine to humic substances (HS) including humic acids (HA), fulvic acids (FA), and humin (Humphrey et al., 2018). Shetaya et al. (2012) reported that soil organic matter is the primary influence on the time-dependent sorption of added iodate.

- **Carbonates**

Understanding the geochemistry of iodine in carbonate environments is important. Several studies have demonstrated experimentally the interaction between iodine and carbonates, mainly on calcite. The study reported by Feng and Redfern (2018) indicated that iodine is most easily accommodated as iodate (IO_3^-) onto the carbonate. Kerisit et al. (2018) have reported the incorporation modes of iodate in calcite. They found that pH was an important parameter and observed that iodate is mainly incorporated at the surface of the calcite and, therefore, has the potential to be easily remobilized. Iodate incorporation onto carbonates can be used in the remediation of contaminated acquirers (^{129}I); for example, manipulating the pH of contaminated aquifers promotes calcite precipitation, and as a result, iodate immobilization can be achieved (Kerisit et al., 2018).

- **Texture**

Studies, such as that of Johnson (2003), have confirmed the importance of texture on iodine retention in soils. The relative strength of sorption according to soil texture has been classified as the following: peat (7.0) > clay (4.3) > silt (3.0) > sand (2.2; see Johnson, 2003). Clay soils have

higher soil organic matter (SOM) than sandy and silt soils; therefore, they tend to bind to iodine more strongly

- **Iron, manganese and aluminium oxides**

Studies indicate that, in addition to retention on soil organic matter, binding on iron and aluminium oxides may also be important (Whitehead, 1973, 1979, 1984). This is supported by Fuge et al. (1998) who reported that iron-rich soils appear to accumulate iodine. Similarly, Sheppard and Thibault (1992) reported an association between some of the neutral or positively charged species of iodine and the Fe-Mn oxide fraction of the soil.

1.3.4.2. Fixation reactions

The soil organic and inorganic constituents can influence iodine fixation reactions, therefore reducing the concentration of the water-soluble iodine and its bioavailability for plants' uptake (Whitehead, 1974). This fixation process not only reduces the bioavailability but would also reduce losses through volatilization (Whitehead, 1974).

1.3.4.3. Losses from soil

Several studies have suggested that iodine can be leached from rocks or soil (Fuge & Johnson, 1986; Tagami et al., 2010; Whitehead, 1984) and have estimated the plant-unavailable iodine concentrations in agricultural fields. They found that total (X-ray fluorescence; XRF) and TMAH-extractable I in lowland paddy field samples were 1.9 and 1.1 mg kg^{-1}, respectively, whereas in upland fields they were 5.7 and 4.2 mg kg^{-1}, respectively. They suggested these variations could be explained by the low redox potential of the paddy fields and that iodine was being lost by leaching or volatilization. Iodine leaching from the soil profile in the form of iodide (I^-) has been reported by (Horel et al., 2014).

1.3.4.4. Volatilization

Iodine volatilization is important for transfer from the sea to the atmosphere, and then I is washed from the atmosphere, through rainfall, into soil. Its re-volatilization as iodine gas from soils to the atmosphere may then also occur (Fuge, 2013). Not all published studies agree on the magnitude of this volatilization; however there is agreement that the amount of iodine that is volatilized from soils is significant (Fuge, 2013). The research by Tagami et al. (2010) regarding the plant-

unavailable iodine concentrations in agricultural fields confirms that iodine can be lost from paddy fields by volatilization.

1.3.5. Uptake by plants

1.3.5.1. Concentrations in crop plants

The iodine content in grain crops is generally very low, ranging from 2 to 30 μg kg^{-1}; this concentration is too low to meet the daily requirement of human populations (Cakmak et al., 2017). Iodine concentration in plants varies depending on the soils they are grown in; for example, the iodine content in plants grown in I-deficient soils may be as low as 10 μg kg^{-1} compared to the 1,000 μg kg^{-1} in plants grown in an I-replete soil (Hetzel & Pandav, 1994).

1.3.5.2. Plant uptake pathways

Iodine uptake by plants is quite different from the uptake of most elements in which the pathway is through the root system followed by translocation to the upper part of the plants. However, with iodine, the uptake occurs in two ways: (i) through the roots or (ii) through leaf stomata; the stomatal pathway is more important (Fuge, 2013). Uptake through roots depends on the iodine speciation in the soil. According to Fuge (2013), iodide can be uptaken through the root system of plants more easily than iodate. However, another key problem is that there is little translocation from the roots to the aerial parts of plants. Thus, it is possible that the primary iodine uptake pathway could be from the atmosphere through rainfall or gaseous transfer (Fuge, 2013).

1.3.5.3. Uptake in response to biofortification

Foliar application of iodine fertilizer may be the most successful route for biofortification (Cakmak et al., 2017; Fuge, 2013). The effectiveness of foliar application has been reported by (Comandini et al., 2013). The review by Lyons (2018) confirms that in agronomic biofortification programs foliar iodate application is more effective than iodide (Cakmak et al., 2017; Dai et al., 2006; Lawson et al., 2015; Mackowiak & Grossl, 1999; Medrano-Macías et al., 2016; Smoleń et al., 2016). Thus, biofortifying leafy vegetables is easier (Smoleń et al., 2014) than grains, seeds, roots, and tubers (Gonzali et al., 2017; Hurtevent et al., 2013; Mackowiak & Grossl, 1999; Mao et al., 2014; Medrano-Macías et al., 2016). This is because iodine is transported mostly through xylem tissue but is less phloem-mobile (Mackowiak & Grossl, 1999). However, the research by Cakmak et al. (2017) indicates that there is evidence of phloem-iodine mobility. They demonstrated that grain iodine content can be enhanced through foliar application, which can be then translocated to

the rest of the plant (Fuge, 2013). This supports the evidence of the phloem mobility of I reported in wheat (Hurtevent et al., 2013) and vegetables (Kiferle et al., 2013; Li et al., 2017; Smoleń et al., 2014).

1.4. Objectives and outline of the thesis

The aim of this PhD thesis is to assess the status of Se and iodine in Somali agricultural soils, from both rain-fed and irrigated land. This involves examining both elements in soil, water and crops and, specifically, investigating their fractionation, speciation and the factors controlling sorption and retention in Somali soils. The most specialised part of the work presented is a study of the principal adsorbents, calcite and gypsum, in terms of their sorption and fixation of Se and iodine using enriched ^{77}Se and ^{129}I isotopes as tracers.

The experimental objectives of the thesis are listed below.

- To determine the total Se and iodine concentrations, speciation and associated hydrogeochemical properties of groundwater and surface water in the study area of south Somalia (Chapter 3).
- To develop and understanding of Se and iodine fractionation and speciation in agricultural soils from selected sites in south Somalia and to identify the major soil parameters that control Se and iodine concentrations and bioavailability in the soils (Chapter 4).
- To survey Se and iodine concentrations in soils and in a range of staple crops from selected demonstration plots established by the Somali Agriculture Technical Group (SATG) in order to investigate plant uptake of native Se and iodine and the major soil properties that control this (Chapter 5).
- To investigate selenite and selenate sorption on calcite, gypsum and on calcareous and gypsiferous soils. In particular, to explore the time-dependency of sorption reactions and, by measuring the lability (isotopic exchangeability of $^{74}Se^{VI}$ and $^{77}Se^{IV}$) of adsorbed Se, to investigate the kinetics and mechanisms associated with Se fixation reactions both on pure minerals (i.e. calcite and gypsum) and soils. EXAFS measurements were used to further investigate sorption/fixation reactions. (Chapter 6).
- To understand iodate/iodide sorption on the pure calcite and gypsum. As for Se in Chapter 6, to explore the time dependency of sorption reactions and estimate lability in order to

examine fixation reactions by utilizing the radioactive isotopes ($^{129}I^-$ and $^{129}IO^-_3$) as tracers. (Chapter 7).

The plan of the thesis and the approaches used in each chapter are described below.

This thesis is divided into eight chapters, starting with a literature review of the current knowledge regarding iodine and selenium chemistry and the status of I and Se in Somalia. This is followed (Chapter 2) by a general description of materials and methods. The experimental work is then presented in five Chapters (3-7) which address the specific objectives listed above and the dissertation ends with a general discussion and conclusions (Chapter 8).

In Chapter 3, total Se and iodine concentrations in groundwater and surface water arising from the Shabelle river and collected from agricultural land in south Somalia were measured using ICP-MS. In addition, Se and iodine speciation were also measured in unpreserved portions of each sample using HPLC-ICP-MS. To investigate the factors affecting both total concentrations and speciation of the two micronutrients the water temperature, pH and electrical conductivity (EC) were measured in the field and, in the lab, the DOC, DIC were determined and multi-elemental analysis was performed.

In Chapter 4, the total Se and iodine concentrations in soils from 12 sites located in agricultural land in south Somalia (including both rain-fed and irrigated fields) were measured after HF digestion and TMAH extraction respectively. In addition, a three-step sequential extraction procedure including dissolution in 0.01 M KNO_3, 0.016 M KH_2PO_4 and 10% TMAH was performed to determine the operationally defined 'soluble', 'adsorbed' and 'organic' Se and iodine respectively (Wang et al., 2020). Speciation of Se (selenate and selenite) and iodine (iodate and iodide) was determined for the soluble and exchangeable fractions using HPLC coupled to ICP-MS. A (4^{th}) 'residual' Se fraction was also calculated from the difference between total soil Se content (HF digestion) and the sum of the soluble, exchangeable and organically bound Se fractions. In addition, aqua regia digestions were performed to determine elemental composition of the soils including Se, this enabled us to compare the Se pool in the aqua regia digestion with the above three step sequential extraction. Moreover, several leaching trials i.e. acid and alkaline column leaching were conducted to study the fractionation of Se and iodine and their release pattern from the soil organic matter and from the carbonate minerals. Finally, the efficiency of the

tetramethyl ammonium hydroxide extraction method was tested under different soil processing procedures (i.e. agate ball milled vs < 2 mm sieved soils) and under different soil-to-solution ratios.

In Chapter 5, in a pilot study, soil samples and their corresponding crops (maize, mung bean and cowpeas) were sampled from demonstration field plots managed by the Somali Agriculture Technical Group (SATG). The plots had received urea and diammonium phosphate (DAP) fertilizers; no Se or iodine fertilizers were applied to these soils before sampling. Multi-elemental analysis including Se and iodine, were undertaken on the crop samples. The corresponding soils were characterized as described in chapter 4. The data were used to investigate the soil factors that influence the bioavailability of trace elements.

In Chapter 6, sorption experiments were conducted to investigate the adsorption kinetics of calcite and gypsum for selenate and selenite. Batch experiments were conducted at room temperature, at constant ionic strength using 0.01 M Ca $(NO_3)_2$ or 0.01 M $CaCl_2$ as the background electrolyte; and contact times of up to 21 days. In addition, enriched Se stable isotopes ($^{77}Se^{IV}$ and $^{74}Se^{VI}$) were applied to differentiate between labile and non-labile Se pools. EXAFS investigations were undertaken at the Diamond Light Source synchrotron facility to investigate the Se bonding mechanisms on pure minerals as well as in the calcareous soils from Somalia. Moreover, sorption and fixation as affected by changing the partial pressure of CO_2 were investigated from the calcareous systems. The partial pressure of CO_2 was controlled, by employing three bubbling systems, (i) continuous bubbling of 4% CO_2, (ii) continuous bubbling of air and (iii) swapping between bubbling of 4% CO_2 and air at three-day intervals; the latter was to investigate the possible role of occlusion in precipitating calcite as a possible fixation mechanism.

In Chapter 7, similar sorption experiments were conducted for the two inorganic iodine species (iodate and iodide) using ^{129}I as a tracer. The procedures used were similar to those of Chapter 6, except that EXAFS studies were only undertaken for Se sorption studies.

In Chapter 8, the major findings in each chapter of this thesis are discussed; remaining gaps in knowledge and areas for future work are also highlighted.

2. General materials and methods

2.1 Introduction

Calcareous soils from Southern Somalia have been used for the main body of this work, to characterize how selenium and iodine interact with carbonate rich soils. This chapter describes general methods and approaches used throughout this thesis including the field sampling protocols for water, soil and plant samples, sample processing and preservations methods, experimental and analytical approaches.

2.2 Sample Collection

2.2.1. Water

The main water sources in Somalia are groundwater, the Shabelle and Jubba Rivers, seasonal wadis and rainfall (see section 1.1.2). In this study samples were collected along the Shabelle River (at *Belet-weyn*, *Bulo-burte, Jowhar, Bal'ad*, and *Afgoi*) from canals, boreholes, shallow and tube wells and barkeds (local constructions used to store fresh water) (Figure 1). Groundwater samples were collected only where accessible. River water sampling strategy was to collect samples directly from the mainstream at three points in each settlement; where the river enters the settlement, the middle of the settlement and from where the rivers left the settlement. In the important agricultural zone of Baidoa (Somalia's sorghum belt) rain-fed agriculture is practiced and groundwater samples from shallow wells, tube wells and tap water were sampled.

Surface water samples were collected from the main flow using a clean bucket that was rinsed with the water to be sampled. At each location two samples were collected, one was used for onsite characterizations (pH, EC and temperature measurements), the other was filtered (<0.45µm) into a universal tube (20 ml), labelled and stored in a black plastic bag for transport to a local Somali Agricultural Technical Group (SATG) laboratory. Water pH and electrical conductivity (EC) were measured using a portable HANNA instruments meter. Calibration for pH used buffers at pH 7.00 and pH 4.01 and for EC used a 0.1 M KCl conductivity standard (12.8 DS m^{-1}). Samples for analysis were shipped to the University of Nottingham, UK and stored in the dark at 4^{o}C prior to analysis.

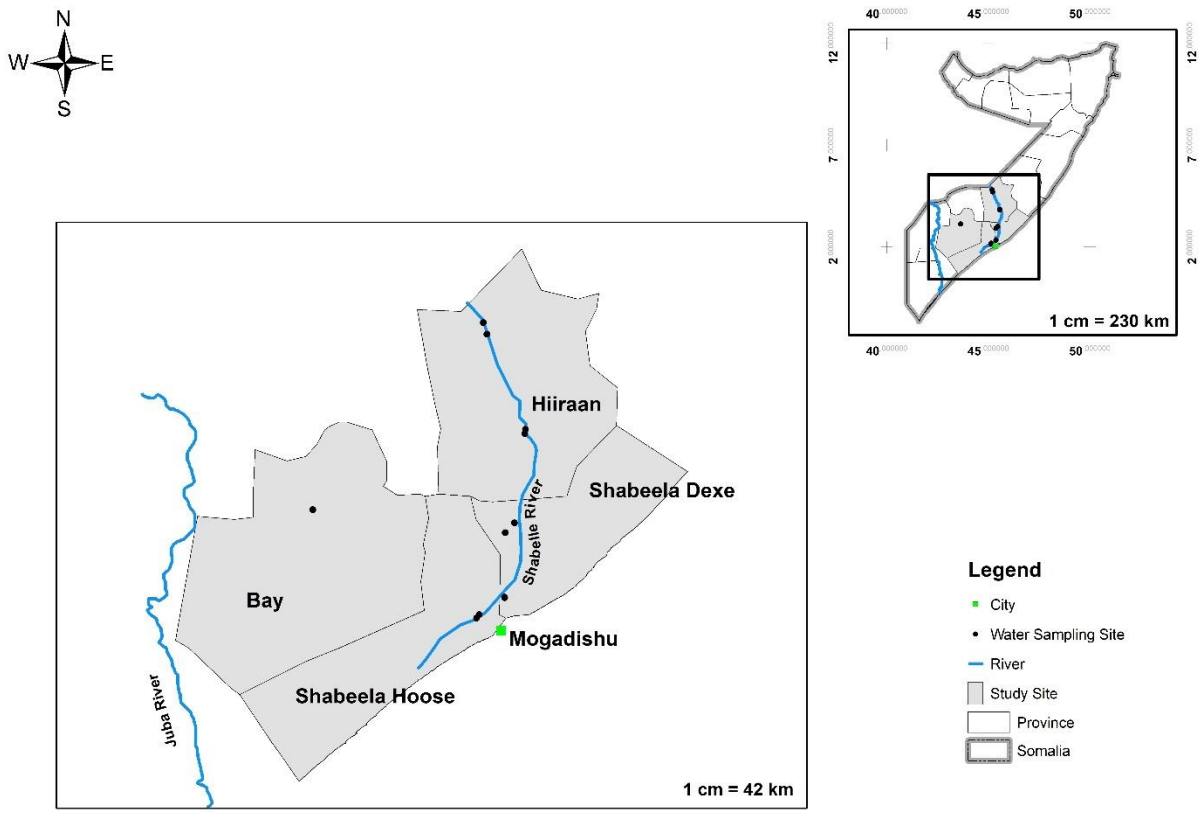


Figure 2.1. Sampling points of drinking and irrigation water in south Somalia during the field survey conducted in 2016/2017. Samples comprised both groundwater and surface water samples. The surface water samples were collected from the Shabelle River; the river was sampled from three points in each major city, i.e. entry, mid and end points. The R package was used to produce the map.

2.2.2. Soil

Two phases of soil sampling were undertaken. In the first phase soils, and their corresponding plants, were sampled from nine agricultural demonstration plots in lower Shabelle. In the second phase twelve sites with contrasting land uses in southern Somalia were selected to give soil samples that differed in their properties as well as their distance to the coast and the Shabelle River. Sites were selected after consulting the Food and Agricultural Organization (FAO) classification for the agricultural areas and with the help of the Somali Agricultural Technical Group (SATG). The criteria for site selection was:

- To collect samples from accessible districts in the main agricultural zones alongside the Shabelle river.

- To sample from fields currently or previously under cultivation.
- Samples to include both rain-fed and irrigated sites i.e. from each district at least one sample should be from a site that was irrigated by rainwater and the other from a ground/well water irrigated site.

The sampling protocol was adopted from the sampling concept described by (Bowley, 2013). Samples of topsoil (0-15 cm) depth, the main rooting zone for the crops, was collected using a spade. Each sample comprised five sub-samples (c. 2 kg in total) taken from the centre and corners of a 10 x 10 m square and placed in a plastic bag for transport to the laboratory. At each sampling site GPS coordinates and other observations such as land use and other features required for data interpretation were recorded. Soil samples were collected from both vegetated and un-vegetated sites. In the laboratory, the samples were air dried at room temperature (~28°C) in an aluminium tray, and < 2 mm sieved before a subsample was shipped to the University of Nottingham for analysis.

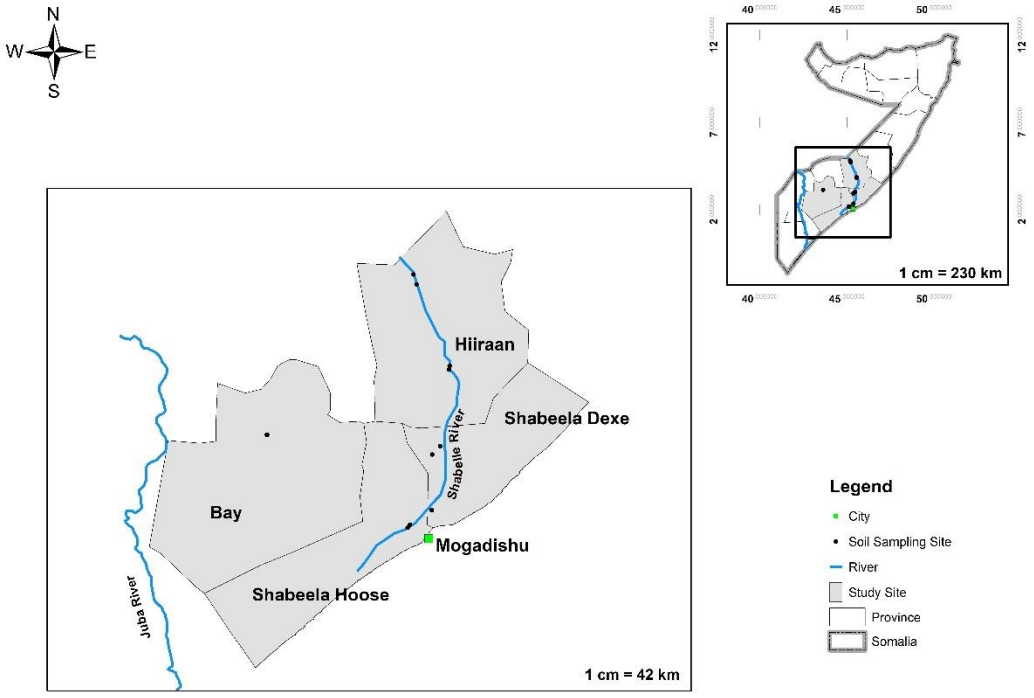


Figure 2.2. Map showing the locations of sampling of the agricultural soils in south Somalia during the field survey conducted in 2016/2017 (n=12). In each district two samples were collected i.e. both rainfed and irrigation systems. Each sample is made up from five sub-samples. The R package was used to produce this map.

2.2.3. Plant Sampling

Plant samples were collected from nine agricultural demonstration plots in Afgoi and nearby villages. The purpose of the demonstration experiments run by SATG was to evaluate the yield and other agronomic characteristics of some varieties of maize, cowpeas and mung beans at the Agri-Business Incubation Centre (ABIC) in Afgoi and at demonstration sites in farmers' fields. Sampling was therefore opportunistic and designed only to establish the concentrations of I and Se present in the crops and their associated soils. Four maize plots, three mung bean and two cow pea plots were selected for analysis. Plots were planted during the deyr season (October to December) and consisted of uniform rows of plant with timely irrigation, nitrogen fertilizer application (urea 75 kg ha^{-1}) and diammonium phosphate (DAP) 200 kg ha^{-1} before planting. The DAP was applied to all plots, whereas urea was only applied to the maize plots. This is because Somali soils are nitrogen and phosphorus deficient. However, legumes can fix substantial quantities of nitrogen (N), therefore it was not considered necessary to add urea to the legume plots. Spacing between rows was 0.75 m and 0.30 m between plants within a row.

Samples were collected from the plots during January and February (2016). In each field six plants in the inner rows of the trial were randomly selected to avoid border effects. The protocol for maize sampling was to collect six dry and ready to harvest cobs from each plot, and for the cow peas and mung beans 15 dry pods from each plot. The grains were shelled by hand and bulked together. After drying a subsample of 50 g of grain from each location was shipped to the UK for analysis.

2.3 Sample characterization

2.3.1. Water Samples

Water samples were split in the laboratory into three sub samples. One subsample was unpreserved and used for anion analysis using ion chromatography, dissolved carbon analysis and determination of inorganic I and Se species. A second subsample was preserved in 2% nitric acid for multi-element analysis (including Se). A third subsample was preserved in tetra-methyl ammonium hydroxide (TMAH) iodine determination. Prior to analysis all unpreserved samples were kept in the dark at 4°C.

2.3.2. Soil Samples

Measurements of pH, loss on ignition (LOI), cation exchange capacity (CEC) and sequential extraction for I and Se fractionation were undertaken on air dried < 2 mm sieved soil. A portion

(c. 10 g) of each soil was also finely ground using agate ball mill (PM 400, Retsch, Haan, Germany) for total elemental analysis after HF digestion and determination of total carbon, total nitrogen and inorganic carbon.

2.3.2.1. pH

About 5 g soil of < 2 mm sieved soil was equilibrated in 12.5 mL deionized water (1:2.5 soil/deionized water ratio) and shaken for 30 minutes on a rotary shaker. The pH of the soil suspension was measured using a combined pH meter (HI 209 pH meter, Hanna instruments Ltd, UK). Prior to each set of pH readings the electrode was calibrated using pH 7.00 and pH 4.01 buffers.

2.3.2.2. Loss on Ignition (LOI)

A sample of ~2 g of < 2 mm sieved soil was first oven dried at 105^0C overnight until a constant weight is achieved, then LOI was determined gravimetrically by further heating in a muffle furnace at 550 ^{0}C for 8 h. The % LOI was calculated from the difference between the pre- and post-ignition mass.

2.3.2.3. Cation Exchange Capacity (CEC)

The cation exchange capacity (CEC) of a soil represents soil's ability to hold positively charged ions. In this study cation exchange capacity was measured after extraction according to the procedure described by (Stuanes et al., 1984). Alternative methods determination of CEC are described elsewhere in the literature e.g. Chapman, (1965), Rhoades, (1982) using a range of extractants. For example, Polemio and Rhoades, (1977) developed method for determining the CEC of calcareous and gypsiferous soils by first saturating cation exchange sites with sodium and Coleman et al., (1959) used a potassium chloride extraction. Extraction with NH_4NO_3 salt is preferred over NH_4Ac because NH_4Ac does not compete effectively with multi-valent base cations (Borge, 1997). Therefore, in this study a portion of 1 g of air-dried soil (< 2 mm sieved) was equilibrated in 10 mL of 1 M NH_4NO_3 for 2 h. After extraction exchangeable cations (K, Ca, Mg & Na) were measured by ICP-MS following 1-in-10 dilution with Milli-Q water.

2.3.2.4. HF digestion

For multi-elemental total analysis, finely ground soil (0.2 g dry weight, DW) was digested with 2 mL of concentrated HNO_3 (70% TAG) and 1 mL of $HClO_4$ (70 % TAG) at 80°C for 8 h and then at 100°C for a further 2 h. An aliquot (2.5 mL) of HF (40 %) was then added and the samples were

heated to 120°C for 8 hr. A further 2.5 mL of HNO_3 and 2.5 mL Milli-Q water was added to the dry residue and the vessels heated at 50°C for 30 min. After the digestion was complete the final volume was made up to 50 mL using Milli-Q water (18.2 MΩ cm). Samples were diluted 1-in-10 with Milli-Q water prior to multi-element analysis by ICP-MS.

2.3.2.5. Aqua regia digestion

Hotplate aqua regia digestion method was used by treating a soil sample (2 g of ball milled soil) with a 3:1 mixture of hydrochloric (HCl) and nitric (HNO_3) acids in a fume hood. The sample was left to boil until about 5 ml is left. Samples were then removed from the heat source and a small amount of MilliQ water were added allowing them to cool. Further samples were filtered and diluted in Milli-Q water into a final volume of 50 ml. Prior to ICP-MS analysis samples were diluted 1:10 with MilliQ water.

2.3.2.6. Sequential Extraction

A three-stage sequential extraction procedure (SEP) was used to determine the concentrations of the operationally defined 'soluble', 'adsorbed' and 'organically bound- fractionations of Se and I in the air dried, < 2 mm sieved, soil (Wang et al., 2020). The soluble fraction was extracted with 0.01 M KNO_3, the adsorbed (exchangeable) pool using 0.016 M KH_2PO_4, and an organically bound fraction with tetra-methyl ammonium hydroxide (TMAH). Residual Se (that present in primary minerals) was calculated by taking the total Se concentration (measured after HF digestion, see section 2.3.2.6) and subtracting the sum of the nitrate, phosphate and TMAH extractable portions.

- Nitrate extraction (0.01 M KNO_3)

Soil (c. 4.0 g) plus 20 mL of 0.01 M KNO_3 was shaken together in a 50 mL centrifuge tube for 2 hr on a reciprocal shaker, centrifuged (30 min at 3500 rpm), and the supernatant filtered through a 0.22 μm PTFE syringe filter. A 1 mL sample of the supernatant was placed in a speciation vial for determination of concentrations of inorganic I and Se species. The remaining supernatant solution was preserved with TMAH to give a final concentration of 1%.

- Phosphate extraction (0.016 M KH_2PO_4)

A total of 20 mL of 0.016 M KH_2PO_4 was added to the soil remaining after the nitrate extraction. The tubes were then shaken for a further 1 hr and then centrifuged at 3500 rpm for 30 min before the supernatant was filtered through 0.22 μm PTFE syringe filters. A 1 mL aliquot of the

supernatant was then transferred into a speciation vial for speciation analysis. The remaining supernatant solution was preserved with TMAH to give a final concentration of 1%. Calculation of phosphate extractable I and Se accounted for carry over from the previous KNO_3 equilibration on a gravimetric basis.

- TMAH extraction (10% TMAH)

The remaining soils was then extracted with 10% TMAH using a method adapted from (Watts & Mitchell, 2009). A 10 mL aliquot of 10% TMAH was added to the residue from the phosphate extraction. The centrifuge tubes with lids loose, were placed in an oven at 70^0 C for 3 hr, with gentle shaking of the tubes after 1.5 hr. Samples were then centrifuged at 3500 rpm for 30 min before the supernatant was filtered (0.22 μm). Extracts were analysed by ICP-MS (see section 2.4.6) for total iodine and organically bound selenium (Se_{TMAH}). Alkaline extraction using TMAH is a well-established method for determination of 'total' iodine analysis as the vast majority of iodine in soils is organically bound. TMAH is preferred over other inorganic extractants because high pH can be achieved without increasing the salt concentrations in the supernatants therefore reducing the possibility of precipitation in the ICP torch and the nebulizer during analysis (Shetaya et al., 2012).

2.3.3. Plant Samples

Upon receipt plant samples were first placed into a freezer at – 18 °C for 48 hr in order to kill any viable insects that they contained. Defrosted grain samples were then milled in a centrifugal mill (Retsch ZM 200) and stored in re-sealable polythene bags at room temperature prior to microwave digestion in both acidic and alkaline conditions and subsequent ICP-MS analysis.

2.3.3.1. Microwave digestions

Milled grain (0.2 g, DW) was digested with either 6.0 mL of conc. HNO_3 or 10 mL of 10% TMAH under microwave heating using an Anton Paar (Anton Parr, GmbH, Austria) Multiwave 3000 platform with a 24-vessel 24HVT50 rotor. Digested samples were diluted to 20 mL with Milli-Q water (18.2 MV cm) and stored at room temperature pending analysis.

2.4 Analytical Methods

2.4.1. Ion Chromatography

Concentrations of chloride, sulfate and nitrate were measured using ion chromatography (Dionex ICS-1100) employing an IonPac AS14A analytical column, IonPac AG14A guard column and the flow rate of 1.4 mL min^{-1}. Groundwater samples were diluted 1 in 100 or 1 in 10 for chloride and sulfate measurements when required due to their higher concentrations of anions.

2.4.2. Dissolved Carbon Analysis,

The Shimadzu TOC-V TN is used to measure total carbon, inorganic carbon and organic carbon in the groundwater and surface water samples. First the total dissolved carbon (TC) was measured, this was done by introducing the sample into the catalyst-filled combustion tube and heating them to 680 ˚C, this causes CO_2 production, which is then detected using non-dispersive infrared detector (NDIR). At the same time the dissolved inorganic carbon (DIC) is measured by acidifying the sample with phosphoric acid to obtain a pH less than 3. All the inorganic carbon in the sample are converted to CO2, which is then detected using the same NDIR detector. The dissolved organic carbon (DOC) is then internally calculated by the system (DOC = TC - DIC).

2.4.3. Total Carbon and Nitrogen Analysis

Total carbon (TC) and total nitrogen (TN) were determined simultaneously using an Elementar VarioMax CN analyser on samples of finely ground soil. Samples were quantified against standards using ~10 mg Aspartic Acid as a bypass and ~20 mg of peaty soil as a quality control standard.

2.4.4. Total Organic Carbon Analysis

Soils were analysed for total inorganic carbon (TIC) using a Shimadzu SSM-5000A model. The soils samples were first weighed into ceramic boats, the boats were first washed and then heated in the furnace (8h 450˚C) to make sure that they were completely free of any organic residue. In the instrument the soil sample is then acidified to obtain a pH less than 3, this converts all carbonates in the sample to CO2 which is detected by NDIR detector. The total organic carbon (TOC) concentration was then calculated in excel by subtracting the inorganic carbon (IC) concentration from the TC concentration.

2.4.5. Total Elemental Analysis

Major and trace element concentrations (31 elements, excluding I) in the extracted or digested soils, plants and water samples were determined using ICP-MS (Thermo-Fisher Scientific iCAP-Q; Bremen, Germany). The instrument was run employing three operational modes, including (i) a collision-cell (Q cell) using He with kinetic energy discrimination (He-cell) to remove polyatomic interferences, (ii) standard mode (STD) in which the collision cell is evacuated and (iii) hydrogen mode (H_2-cell) in which H_2 gas is used as the cell gas. In-sample switching was used to measure B and P in STD mode, Se in H_2-cell mode and all other elements in He-cell mode.

Two sets of external calibration standards namely major (10, 20 and 30 mg L^{-1}) and trace (0 – 100 µg L^{-1}) were used. Phosphorus, B and S calibration utilized in-house standard solutions. Internal standards containing Ir (5 µg L^{-1}), Rh (10 µg L^{-1}), Ga (25 µg L^{-1}) and Sc (50 µg L^{-1}) were included to the sample stream on a separate line via an ASXpress unit. Samples and calibration standards were diluted 1-in-10 with 2% HNO_3 unless stated elsewhere and a 2% HNO_3 wash solution was used to clean the sample probe and line between samples. Quality control was assured using certified reference materials (CRMs) alongside samples during digestions and sample blanks were also included. Data processing was undertaken using Qtegra™ software (Thermo-Fisher Scientific).

For ^{77}Se and the isotopic exchangeability, the data were processed using the approach described by Mathers et al., (2017), the ^{77}Se, ^{78}Se and Re (the internal standard) raw intensity data as counts-per-second (cps) were exported from the ICP lab book for further processing in excel. First the internal standard (Re) data was converted from intensities (cps) to blank proportion, then the ^{77}Se and ^{78}Se data (cps) were corrected for blanks and internal standards. Another potential source of error when measuring Se isotopes by ICP-MS in H_2-cell mode is the formation of Se hydride (SeH), therefore further corrections for hydride formation (^{77}SeH) were made. Before describing how the hydride correction is carried out it is important to know that the natural isotopic abundances are: Se total=1; ^{78}Se=0.237; ^{77}Se=0.076; ^{76}Se=0.092. Mathers et al., (2017) showed in their experiments how ^{77}Se, the $^{77}(m/z)$ signal is subject to loss and gain from the formation of $^{77}SeH^+$ and $^{76}SeH^+$ respectively, on the otherhand loss from ^{77}Se inturn increases the $^{78}(m/z)$ signal. To overcome this, pure ^{77}Se standards (c. 100% isotope abundance) were analysed, then

the ratio of $^{77}SeH^{+}$ (reported as ^{78} *m/z*) to ^{77}Se (reported as ^{77} *m/z*) was calculated using the equation below.

$$Hr = \frac{78_{(m/z)}}{77_{(m/z)}} \qquad \text{Equation 2.1}$$

Where Hr is the hydride ratio, ^{78}(*m/z*) and ^{77}(*m/z*) are the signals (cps) measured. The hydride ratio was equal to 0.05.

The $^{78}Se_{cps}$ was first corrected for the $^{77}SeH^{+}$ that was formed from the enriched ^{77}Se using equation below:

$$78_{Se_{cps}} = [78(^{m}/_{z}) - (77(^{m}/_{z}) \times Hr)]\left(1 + \frac{Hr\ 78_{Se_{ia}}}{77_{Se_{ia}}}\right) \qquad \text{Equation 2.2}$$

Where $^{78}Se_{cps}$ is the corrected ^{78}(*m/z*) signal and $^{77}Se_{ia}$ and $^{78}Se_{ia}$ are the naturally occurring isotopic abundances of ^{77}Se and ^{78}Se respectively.

Then a mass discrimination factor (MDF) was applied to correct for ^{76}Se using the following equation:

$$76_{Se_{cps}} = 78_{Se_{cps}}\left(\frac{76_{Se_{ia}}}{77_{Se_{ia}}}\right) \times MDF \qquad \text{Equation 2.3}$$

Where, $^{76}Se_{ia}$ is the isotopic abundance of ^{76}Se, the mass discrimination factor (MDF) for ^{76}Se was equal to 1.14 and was obtained by this equation:

$$MDF = 1 - [(1 - 1.0690) \times 2] \qquad \text{Equation 2.4}$$

The value 1.0690 is the mass discrimination per mass unit for Se isotopes, this was determined under optimized instrumental conditions by analysing multi-isotopic standard; the value 2 is the mass difference (78-76).

Total iodine concentration in the TMAH extracts and TMAH preserved water samples were quantified by ICP-MS operated in standard mode using ^{72}Ge, ^{185}Re and ^{103}Rh as internal standards. A wash of 1% freshly prepared TMAH solution was used to ensure I wash-out between samples. Stock I standards (1000 mg L^{-1}) were prepared from oven-dried analytical grade potassium iodide (KI) or iodate (KIO_3), preserved in 1% TMAH and stored in the refrigerator at 4 ^0C. Working standards 0-100 μgL^{-1} were prepared from the stocks by serial dilutions.

For ^{129}I corrections, first both concentrations ($\mu g\ L^{-1}$) and raw intensity data as counts-per-second (cps values) for ^{127}I and ^{129}Xe were exported from the ICP lab book to excel for further processing. The ^{129}I concentrations were obtained by multiplying the ratio of the ^{127}I intensity and concentration data by the ^{129}Xe intensity data as shown in the equation below:

$$^{129}I = \left(\frac{^{127}I_{con}}{^{127}I_{cps}}\right) \times {}^{129}Xe_{cps} \qquad \text{Equation 2.5}$$

2.4.6. Speciation Analysis

Inorganic I and Se species were quantified in experimental solutions, natural waters and 'soluble' and 'adsorbed' soil fractions using coupled liquid chromatography ICP-MS (LC-ICP-MS). Speciation analysis were done as soon as possible after sampling to minimise and speciation changes. A Hamilton PRP-X100 anion-exchange column (100 x 4.1 mm; 5 µm particle size) was used to separate the iodine and selenium species. The mobile-phase (flow rate 1.5 mL min^{-1}) was 50 mmol L^{-1} NH_4NO_3, 1 x 10^{-5} mol L^{-1} NH_4EDTA, 2% v/v methanol and 0.1M TRIS. Data were captured using Qtegra software and peaks of the individual species were integrated manually. Organically bound species were calculated from the totals minus the sum of inorganic species.

2.4.7. Preparation of working stock solutions

Working stocks were $^{78}Se^{IV}$, $^{78}Se^{VI}$, $^{77}Se^{IV}$, $^{77}Se^{VI}$, $^{129}IO_3^-$, $^{129}I^-$, $^{129}IO_3^-$ and $^{129}I^-$, these stocks compromised both natural isotopes and tracers of the four species. They were freshly prepared in

the lab by dissolving in a MilliQ water; in particular the Se stock was not preserved in acid in order to avoid the acidification of the system.

The $^{78}Se^{IV}$, $^{78}Se^{VI}$ stocks of 1000 mg L^{-1} were prepared by dissolving sodium selenate and sodium selenite salts respectively in MilliQ water and was further diluted as appropriate for each experiment. On the other hand, IO_3^- and I^- stock solutions were prepared by diluting the 1000 mg L^{-1} stock that was prepared by dissolving the sodium iodide and sodium iodate salts respectively in MilliQ water, and similarly further dilutions were made as appropriate for the experimental stock preparations.

The concentration of the enriched isotope stock solutions was determined prior to spiking and were labelled properly with their measured concentrations, further a check standard was included with each ICP experiment for calibration purpose. This was done for both ^{77}Se and ^{78}Se in H_2 mode after appropriate dilutions to check their actual concentrations. The measured concentrations of the stocks used in this experiment were: ^{77}Se-selenite (4024 µg L^{-1}), ^{77}Se-selenate (640 µg L^{-1}), ^{129}I-iodate (5000 µg L^{-1}) and ^{129}I-iodide (122 µg L^{-1}). High stock concentration was used for the Se^{IV} and IO_3^- batch experiments, but for the Se^{VI} and I^- lower concentration stocks were used because the preliminary sorption experiments demonstrated that the adsorption was less.

2.4.8. Sample preservations

Filtered supernatants were preserved either in 2% HNO_3 or 0.05M A. EDTA for selenium and iodine samples respectively. All samples were kept in the cold room until analysis or otherwise were analysed immediately after preservation.

2.4.9. Determination of isotopically exchangeable I and Se

The concentration of the labile Se (E-values) were determined using the approach described by Mathers et al., 2017. After hydride corrections were made (described in section 2.4.5) and corrected ^{76}Se, ^{77}Se and ^{78}Se in counts per seconds were obtained, it was necessary to differentiate between the ^{77}Se coming from the spike and that originating from the multi-isotopic Se. Therefore, the ^{77}Se NON-spike was calculated using the following equation:

$$77_{\mathrm{Se_{ns}}} = 78_{\mathrm{Se_{cps}}} \times MDF \times \left(\frac{77_{\mathrm{Se_{ia}}}}{78_{\mathrm{Se_{ia}}}}\right) \qquad \text{Equation 2.6}$$

Where $^{77}Se_{ns}$ is the non-spike ^{77}Se and $^{78}Se_{cps}$ is ^{78}Se corrected for hydride.

Then Se_{tot} and ^{77}Se values (cps) were converted into µg L^{-1} by dividing their respective sensitivities, as shown in the equations below:

$$Se_{tot} = \frac{78_{Se_{cps}}}{78_{Se_{sen}}} \qquad \text{Equation 2.7}$$

$$77_{Se_{tot}} = \frac{\left(77_{(m/z)} - 76_{Se_{cps}} \times Hr\right)}{77_{Se_{sen}}} \qquad \text{Equation 2.8}$$

Where, $^{77}Se_{sen}$ and $^{78}Se_{sen}$ are the slopes or the measured sensitivities of ^{77}Se and ^{78}Se respectively, their values are expressed in cps ppb^{-1}. The concentration of $^{77}Se_{tot}$ represents all ^{77}Se in the suspension i.e. from both multi-isotopic Se and the enriched spike.

The concentration (µg L^{-1}) of ^{77}Se coming from the addition of the enriched ^{77}Se isotope was then calculated as described in the equation below:

$$77_{Se_s} = 77_{Se_{tot}} - 77_{Se_{ns}} \qquad \text{Equation 2.9}$$

Where $^{77}Se_s$ is the Se coming from the spike; then the adsorbed Se was calculated by converting the solution concentration to a gravimetric basis (µg kg^{-1}) for individual treatment.

Labile adsorbed $^{77}Se_E$ was then calculated after first getting the K_d value in the following manner:

$$77_{\mathrm{Se_{kd}}} = \frac{77_{\mathrm{Se_s}}}{77_{\mathrm{Se_{ads}}}} \qquad \text{Equation 2.10}$$

Where $^{77}Se_{kd}$ is the solid-liquid partition coefficient (L kg^{-1}) and $^{77}Se_{ads}$ is the adsorbed Se in (μg kg^{-1}).

$$77_{Se_E} = 77_{\mathrm{Se_{kd}}} \times \mathrm{Se_{tot}} \qquad \text{Equation 2.11}$$

The ^{129}I and hence the isotopically exchangeable iodine was calculated as described by Shetaya et al., 2012. The initial ^{129}I concentration was first calculated using the following equation:

$$^{129}\mathrm{I_{ic}} = \left(\frac{^{129}\mathrm{I}_{\ \mathrm{s.vol.}} \times\ ^{129}\mathrm{I}_{\ \mathrm{s.con.}}}{\mathrm{Vol_{tot}} + {}^{129}\mathrm{I}_{\ \mathrm{s.vol.}} \times 0.001}\right) \qquad \text{Equation 2.12}$$

Where $^{129}I_{ic}$ is the initial concentration in μg L^{-1}, the $^{129}I_{s.vol.}$ is the spike (^{129}I) volume pipetted to the supernatants, $^{129}I_{s.conc.}$ is the concentration of the experimental stock, and vol_{tot} is the total volume of the solution. The total adsorbed amount ($^{129}I_{Ads.}$) was determined by subtracting the initial concentrations and the final concentrations as shown in the equation below:

$$^{129}\mathrm{I_{Ads.}} = \left(129_{\mathrm{I_{ic}}} - 129_{\mathrm{I_{fc}}}\right) \times \left(\frac{\mathrm{Vol_{tot}} + {}^{129}\mathrm{I}_{\ s.vol.} \times 0.001}{\mathrm{W}}\right) \qquad \text{Equation 2.13}$$

The labile iodine fraction (E-values) were then calculated from the ^{129}I in the solution μg L^{-1}, and the adsorbed amount in μg kg^{-1} using the following equation:

$$\mathrm{E-Value} = \left(\frac{127_{\mathrm{I_{fc}}} \times {}^{129}\mathrm{I}_{Ads.}}{129_{\mathrm{I_{fc}}}}\right) \qquad \text{Equation 2.14}$$

Further for comparison purposes, the percentages of the labile iodine pools after 7, 14 and 21 days of equilibration were calculated for all treatments using the following equation:

$$\%\ ^{127}\mathrm{I_E} = \left(\frac{\mathrm{E - Value}}{^{127}\mathrm{I}_{Ads.}}\right) \times 100 \qquad \text{Equation 2.15}$$

The analysis of high iodine concentrations were in some cases a problematic in the preliminary experiment were in some treatments up to a 1000 μg L^{-1} was added, in some occasions the detector tripped from the pulse counter mode to the analogue mode, and this was accounted when processing the data by excluding the high STD 100 μg L^{-1} from the calibration curve for the low concentration values, and excluding low STD 20 and 50 μg L^{-1} for high concentration values, and then finally the two data were combined and was considered as true ^{127}I corrected values.

There are other complications when using ICP-MS for iodine analysis, for example the analytical sensitivity is reduced due to the relatively high first ionization potential (10.45 eV). Furthermore, it has been reported in the literature that argon impurity ^{129}Xe can significantly interfere with ^{129}I (Beals et al., 1992; Brown et al., 2007; Haldimann et al., 2000). To overcome this a correction factor based on the natural abundances of ^{131}Xe and ^{129}Xe can be applied (Haldimann et al., 2000; Shetaya et al., 2012).

2.5 Statistical analysis

All statistical data processing was performed using MS Excel 2013, Minitab 17.2.1 and in some occasions IBM SPSS version 22. MS Excel 2013 was used to plot the sorption isotherms. Freunlich and Langmuir modelling were also done using Excel. Explore function of SPSS was used to get mean, median, standard deviation, minimum, maximum and percentiles of the groundwater and surface water samples. The EMMEANS subcommand of the SPSS is used to provide pairwise comparisons. This allowed to distinguish between the effect of the region, the effect of the source (ground or surface water) and their interactions.

3. Selenium and iodine in drinking and irrigation water of south Somalia

3.1. Introduction

Selenium (Se) and iodine (I) are essential micronutrients for animals and humans and play important roles in the physiological and metabolic processes of cell systems. They are both vital for the synthesis and function of the thyroid hormones that regulate various physiological processes (Zimmermann and Köhrle, 2002). In addition, Se also plays critical roles in the immune system, and in cognitive health, as a component of antioxidant selenoproteins (Rayman, 2012).

Diet is the main source of these two micronutrients. Seafood, dairy products, iodized salt and drinking water are the most common iodine-rich sources (Fuge and Johnson, 2015). Selenium, on the other hand, is mainly derived from organ meats, muscle meats, seafoods, garlic, mushrooms and cereals; white bread contains less Se than wholemeal bread. In addition, brazil nuts are also known to contain high, but variable, levels of selenium (Fordyce, 2013). The Se content in foodstuffs is described in detail by (Rayman, 2008; Reilly, 2006).

Both elements have a fairly narrow margin between dietary deficiency and toxicity. In particular, the limit for Se dietary deficiency is <40 μg day^{-1} while toxicity is likely at >400 μg day^{-1} (WHO, 1996). Iodine and Se deficiency, and to a lesser extent toxicity, present a threat to human health and to the social and economic development of many countries. Globally, it is estimated that 1.88 billion people are iodine deficient while about 1 billion are estimated to have insufficient dietary Se intakes (Andersson et al., 2012; Fordyce, 2013). In sub-Saharan Africa the deficiency of these elements is widespread. For example, according to food supply data from the FAO, in eastern Africa the estimated risks of deficiency are 52% and 26% for Se and iodine respectively (Joy et al., 2014).

Selenium intake

In general, Se intake by humans in most parts of Africa is low, especially in the sub-Saharan African countries, typically < 50 μg day^{-1}. There are very few countries in Africa where Se intake falls within the optimum range of 80 – 260 μg day^{-1} (Hurst et al., 2013). The lowest average Se intake (i.e. 27 μg day^{-1}) is reported for Djibouti, which is a country neighbouring Somalia. According to Hurst et al. (2013), Se intake in Ethiopia and Kenya are similar to the level reported for Djibouti; their Se intake ranges between 27 and 45 μg day^{-1}. The risk of dietary Se inadequacy

is therefore high in SSA countries, reaching up 80% in Malawi, >60% in seven other countries in Southern Africa, and 22% across Africa as a whole (Hurst et al., 2013). According to USA guidelines the recommended dietary allowance (RDA) for Se is 55 μg day^{-1} for both men and women (Monsen, 2000). The UK reference nutrient intakes (RNI) for Se are 75 and 60 μg day^{-1} for adult males and females respectively (Foundation, 2001; Rayman, 2004). There are no data for Se intake by the Somali population; studies regarding the geochemistry of selenium of the Somali groundwater, surface water and soils are also lacking.

Iodine intake

Recently, while the number of countries affected by iodine deficiency has been steadily decreasing, the number of countries with excessive intake has doubled over several years (Zimmermann, 2013). Excessive iodine intake may induce thyroid dysfunction which may lead to both hypo- and hyperthyroidism (Leung and Braverman, 2014). Published literature shows excessive iodine intake from iodine-rich water in China (Zhao et al., 1998) and Somalia (Kassim et al., 2014), and from iodine rich seafood in Japan (Suzuki et al., 1965), iodine rich meat and dairy products in Iceland (Gunnarsdottir et al., 2009), and iodized salts in some African and American countries (Zimmermann, 2009). The overall iodine status of a population can be quantified by the median urinary iodine concentration (UIC), which is the most reliable and widely used biomarker of the iodine status of populations. According to the WHO categorization of UIC, <150 μg L^{-1} is insufficient, 150-249 μg L^{-1} is adequate and ≥ 300 μg L^{-1} is excessive (Kassim et al., 2014).

Kassim et al. (2014) reported that iodine intake in Somalia is among the highest in the world (the fifth highest globally) and is 'excessive' (>300 μg L^{-1}) according to the WHO guidelines, UNICEF and the International Council for Control of Iodine Deficiency Disorders (ICCIDD). The median urinary iodine concentrations for non-pregnant women and children were 329 and 416 μg L^{-1} respectively (Kassim et al., 2014).

It is useful to survey the iodine and Se content of groundwater and surface water in order to understand their likely contribution to dietary intake and input to agricultural soils through irrigation. For example, Watts et al., (2015) studied the iodine sources in the Malawian diet, and found that iodine concentrations from hand-dug wells or boreholes were in the range 1.0 to 54.2 μg L^{-1}, with a median iodine concentration of 12.6 μg L^{-1}. Higher iodine concentrations have been

reported in drinking water samples from groundwater sources in Argentina (>100 $\mu g\,L^{-1}$). In Ethiopia, Reimann et al., (2003) reported a wide range of iodine concentrations in water samples from spring, well and river sources taken along the Rift Valley (0.31–961 $\mu g\,L^{-1}$, n = 138). It is also important to investigate the geochemical factors that control the movement of Se and iodine into groundwater and surface water from aquifer sediments, parent rocks and soils.

In relation to Somalia, excessive dietary iodine intake has been reported (Kassim et al., 2014), but there is limited understanding of the geochemical basis for this. Therefore, the overall aim of this chapter was to determine the Se and iodine status of groundwater and surface water in South Somalia.

The specific objectives of this chapter are listed below.

i. To gain knowledge about the Se and iodine concentrations in groundwater and surface water (Shabelle river) collected from selected sites in Southern Somalia.
ii. To understand the role of geochemical factors such as the pH, DOC, DIC, anion composition etc on total iodine and Se concentrations and speciation.
iii. To estimate human intake from water sources and relate this to the high urinary iodine reported in the literature.
iv. To assess the input of Se and iodine to soils from irrigation with groundwater and surface water sources.

In order to fulfil these objectives, this study consisted of a field survey and laboratory measurements. Groundwater and surface water were collected from selected sites in Southern Somalia, the surface water samples were collected from the Shabelle river. In the lab quantitative measurements of multi-elements including Se and iodine were carried out. In addition, Se and iodine species were assayed using HPLC-ICP-MS. The pH, EC, DOC, DIC and major anions were measured to understand the role of these geochemical factors.

3.2. Materials and methods

3.2.1. Study area

This study was conducted in southern Somalia, at locations along the Shabelle river. In addition, groundwater samples were collected from Baidoa, in the Bay region. Two rivers, the Shabelle and Juba, flow through Somalia. The Shabelle and Juba Basin covers an area of 174,600 km^2. The most fertile soils in Somalia are found in these riverine areas in southern Somalia, between 41°53' and 46°09' east of the Prime Meridian; and between 0°16' south of the Equator and 5°04' north of the Equator (Venema and Vargas, 2007). This study was limited to the main cities of the Shabelle river.

The climate of Somalia is determined by the north and south movement of the inter-Tropical Convergence Zone (ITCZ) and by the monsoon winds. As a result, the climate varies from arid to semi-arid. In the southern parts, where the current study was carried out, the climate is relatively moist semi-arid. The mean annual rainfall varies between 300 to 600 mm. The annual potential evapotranspiration is also high as in other arid areas, 1500 – 2000 mm. The mean annual temperature of the study area is 26 to 28 °C (Muchiri, 2007). The land in Southern Somalia is described as low-lying and uniformly flat (Houghton-Carr et al., 2011).

3.2.2. Field sampling

In Somalia groundwater is the main water resource for domestic water supplies, livestock and irrigation. Surface water is mainly used in areas along the Shabelle and Juba rivers, all other regions rely on groundwater sources (BGS, 2020). Therefore, a sampling strategy was developed to ensure that samples were collected from wells, boreholes, tap water, river and canals. Groundwater and surface water samples were collected from 30 sampling points of six districts in Somalia in a survey carried out during October 2016 (Fig 3.1). The sampling process was logistically challenging due to the time and resources needed and restricted access to certain places. Two sets were collected in each sampling point, one set was processed and transported to the University of Nottingham for analysis, and the other set was used for on-site pH, EC and temperature measurements. Global positioning system (GPS) was used to record the location of the sampling points.

3.2.3. Sample processing

Samples were collected into 25 ml universal tubes and were syringe-filtered onsite to < 0.45 μm in order to remove suspended particulates and microorganisms and thereby preserve ambient analyte concentrations and ensure preservation of the chemical speciation of trace elements (Wilde et al., 1998). Samples were then stored in a cold room (c. 4^{o}C) prior to analysis. Samples for analysis of total Se and other elements were preserved in nitric acid (c. 2%) while samples for total iodine analysis were preserved in 1% TMAH.

3.2.4. Water characterization

pH and EC

The pH, EC and temperature were measured on-site from the source of the water using HANNA portable instruments. For the pH measurement the electrode was calibrated using pH 7.00 and pH 4.01 buffers, and for the EC measurement calibration was done using a 0.1 M KCl conductivity standard (12.8 mS cm^{-1}).

Anions

The concentration of chloride, sulfate and nitrate in the water were measured using ion chromatography (Dionex ICS-1100). The columns used were IonPac AS14A analytical column, IonPac AG14A guard column and the flow rate was 1.4 mL min^{-1}. Due to the higher anionic concentrations, groundwater samples were diluted 1-100 or 1-10 for chloride and sulphate measurements respectively.

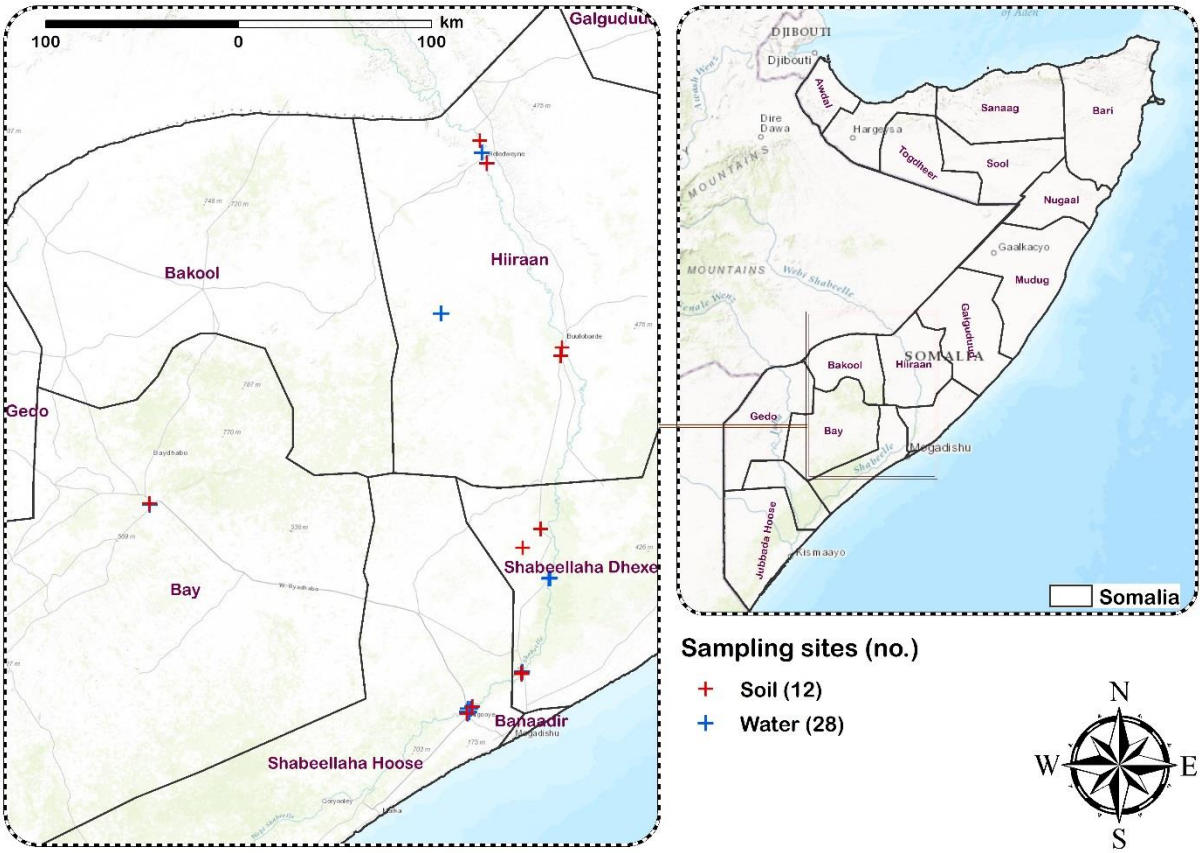


Figure 3.1. The soil and water sampling locations in southern Somalia.

DOC and DIC

Dissolved inorganic carbon (DIC) and dissolved organic carbon (DOC) were analysed using a Shimadzu TOC-V/TN system. All samples were diluted with Milli-Q water prior to analysis (detailed description is in section 2.3.4 in Chapter 2).

3.2.5. Iodine determination

Total iodine

The measurement of iodine in water by ICP-MS operating in standard mode was based on that of (Watts & Mitchell, 2009); detailed description in Chapter 2. The iodine samples were first spiked with 25 % tetramethyl ammonium hydroxide (TMAH: Sigma-Aldrich, Kent, UK) to result in a final solution of 1 % TMAH (0.2 mL of 25% TMAH in 5 mL). The quality control used in this experiment was blanks, iodine standards and replicate analysis. The blank was 1% TMAH; iodine calibration standards (1, 10 and 100 μg L^{-1}) were prepared after serially diluting from an iodine stock solution (1000 μg L^{-1}). Analyses were performed using a 1% TMAH matrix, the background

iodine in the blank solution was 3 μg L^{-1}. Due to the high iodine content in the groundwater, samples were diluted either 10 or 100 times depending on their concentration.

Iodine speciation in ground and surface water samples

Inorganic iodine species (iodate and iodide) in the unpreserved water samples were quantified using HPLC-ICP-MS. A Hamilton PRP-X100 anion-exchange column (100 x 4.1 mm; 5 μm particle size) was used for the separation of iodate and iodide species. The mobile-phase (flow rate 1.5 mL min^{-1}) was 50 mmol L^{-1} NH_4NO_3, 1 x 10^{-5} mol L^{-1} NH_4EDTA, 2% v/v methanol and 0.1M TRIS. Data were captured using Qtegra software and peaks of the individual species were integrated manually. Organically bound iodine was determined from the difference between total iodine and total inorganic iodine (I^- + IO_3^-).

3.2.6. Selenium determination

Total Se concentration

Selenium measurements were performed by using three sets of standards, including: (i) multiple trace elements including Se (20, 40 and 100 μg L^{-1}); (ii) BPS (boron, phosphorus and sulphur; 5, 10, 20, 40 mg L^{-1}); major elements, Ca, Mg, Na, K (10, 20 and 30 mg L^{-1}). The Se detection limit was 0.01 μg L^{-1}; the r^2 of the Se calibration curve was 0.9995.

Se speciation in ground and surface water samples

Selenite and selenate species were quantified simultaneously with the iodine species using HPLC-ICP-MS. Organically bound Se was determined by calculating the difference between total Se and total inorganic Se (selenite and selenate). Total Se was determined for the nitric acid preserved samples by ICP-MS in hydrogen mode.

3.2.7. Multi-elemental analysis

Multi-elemental analysis was performed using ICP-MS as described in section 2.3.1 in Chapter 2.

3.2.8. Hydrogeochemical characterization

After determining the major cations and anions, piper diagrams were plotted for hydrogeochemical characterization of the ground and surface water samples. The piper diagram is used to categorize the composition of the water samples and, potentially, help understand its evolution through time and space. In this study the Geochemist's Workbench was used to plot the piper diagrams. The

major ions are plotted in the two base triangles as cations (Ca^{2+}, Mg^{2+}, Na^{+}, K^{+}) and anions (Cl^{-}, SO_4^{2-}, $CO_3^{2-} + HCO_3^{-}$), samples are then projected onto the diamond area to give the percentages of these ions.

3.3. Results and discussion

3.3.1. General properties of the surface and groundwater samples

The general properties of the water samples, such as the pH, EC, DOC, DIC, anion and cation concentrations that influence the Se and iodine speciation were measured. Tables 3.1 and 3.2 summarize the chemical properties of the ground and surface water. In general, the Somali groundwater and surface water samples were slightly basic, the mean pH values of the groundwater and surface water were 7.64 ± 0.03 and 7.90 ± 0.02 respectively. The pH of the well samples varied 7.13 to 8.23 with an arithmetic mean of 7.82; the pH of the tap water ranged from 6.99 to 8.23 with an arithmetic mean of 7.63; the pH values of the borehole and tube well water samples were 7.58 and 7.03 respectively. The pH of the samples collected directly from the river varied from 7.11 to 8.18 with an arithmetic mean of 7.76; the median pH of the river samples was 7.94. The pH of the water collected from the canals off the river varied from 7.06 to 8.22 with an arithmetic mean of 7.98. Samples were also collected from surface water storage constructions locally known as 'Barkad' and their pH varied from 7.11 to 8.18, with an arithmetic mean of 7.76. These findings indicate that in general the pH of these water samples reflects their alkalinity, and this may be attributed to their $CaCO_3$ contents, fig 3.2.

The electrical conductivity (EC) indicates the extent of salinization of the freshwater samples. The ECs of the groundwater and surface water were, on average, 2340 µS cm^{-1} and 1190 µS cm^{-1} respectively. These are comparable to values (1,300 to 5,000 µS cm^{-1}) reported by Muthusi (2007) for a rural water survey in Somalia. The chemistry of these water types was further described using piper diagrams (Fig 3.3). In general, the chemistry of these water samples is mainly influenced by either NaCl, or $CaSO_4$ which can be attributed to sea water intrusion or geological influences.

Groundwater from Afgoi areas may be classified as being 'NaCl type'. The major anion is Cl (65%), followed by SO_4 (30%) and HCO_3+CO_3 (5%). The major cations are Na+K (65%), Mg (20%) and Ca (15%). Groundwater samples from the Baidoa region, comprising samples from wells, tap water & tube wells, were also classed as NaCl and $CaCl_2$ water types. The major anions were Cl (75%), SO_4 (15%), and HCO_3+CO_3 (<10%), the major cations were Na+K (45%), Ca

(40%) and Mg (15%). Groundwater samples from the Bal'ad zone were also influenced by NaCl and $CaCl_2$ water types; Cl was the dominant anion (70%) in these samples, followed by SO_4 (25%), and HCO_3+CO_3 (<5%); the major cations were Na+K (40%), Ca (35%) and Mg (25%).

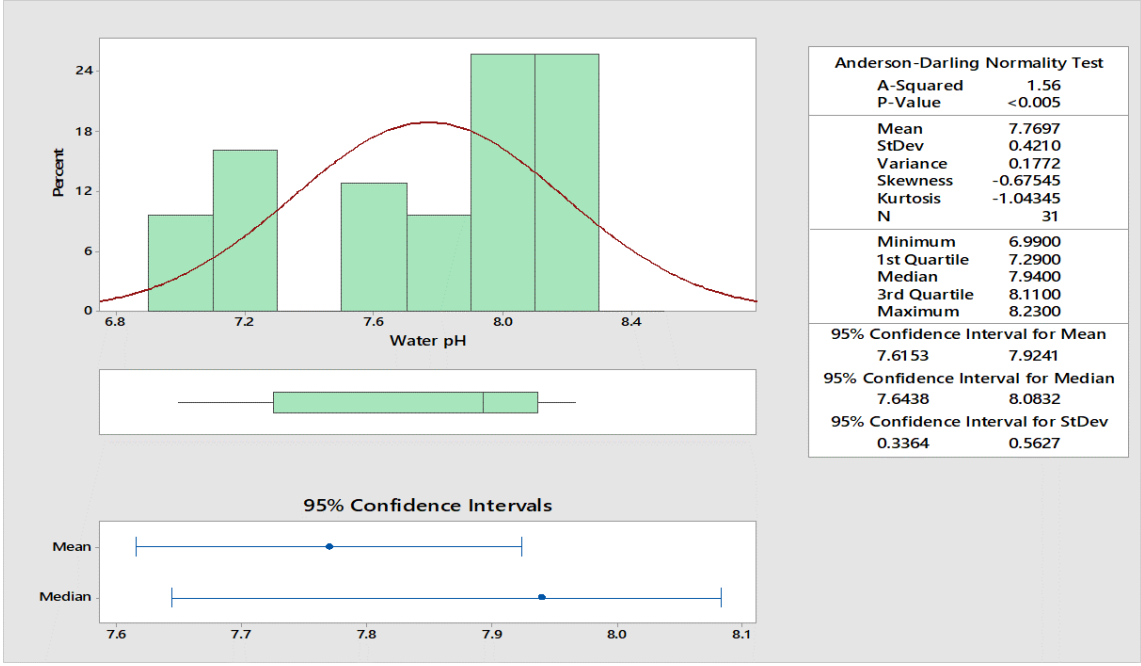


Figure 3.2. The frequency distribution of the pH of groundwater and surface water. The assessment of the compatibility of distributions for fitting was made using the Anderson–Darling (A–D) test for a significance level of $\alpha = 0.05$.

For some samples, the groundwater type was $CaSO_4$ type; for example, borehole samples from Afgoi differed from the well and tap water from Afgoi, the borehole water was a $CaSO_4$ type. The major anion was SO_4 (75%), followed by Cl (20%) and HCO_3+CO_3 (<5%). The major cations were Ca (55%), Mg (25%) and Na+K (20%). Groundwater samples collected from the Beletweyn region were also of the $CaSO_4$ water type, the major anions were SO_4 (70%), Cl (25%) and HCO_3+CO_3 (<5%), whereas the major cations were Ca (55%), Na+K (30%), Mg (15%). The main $CaSO_4$ sources are from the lithology of the acquifer in which dissolution of gypsum or anhydrite controls the Ca^{2+} and SO_4^{2}- concentrations.

The chemistry of the surface water samples was mainly influenced by $CaSO_4$ but there were also instances of $CaCl_2$, NaCl and $MgCl_2$ water types. Approximately 90% of these anions were SO_4-Cl, of which more than 50% were SO_4, 35% were chloride and less than 10% were HCO_3+CO_3. The major cations were mainly Ca + Mg (representing 70%), Ca was the dominant cation (50%),

followed by Na+K (30%) and Mg (20%). Surface water samples from Bal'ad differed from other samples in that the major anions were SO_4-Cl (95%); Cl was the dominant anion (55%), followed by SO_4 (40%) and less than 5% were HCO_3+CO_3. The major cations were also different from the other surface water samples, Bal'ad samples had more Na+K (45%) with Ca (35%) and Mg (~20%) making up the balance.

Median values of dissolved organic carbon (DOC) in the groundwater and surface water samples were 5.15 mg L^{-1} and 7.06 mg L^{-1} respectively. In general, the DOC values were slightly higher in samples collected from tube wells (7.13 mg L^{-1}), rivers (7.44 mg L^{-1}), canals (7.03 mg L^{-1}) and barkad (8.04 mg L^{-1}). Surface water samples had, on average, slightly higher DOC values (7.23 mg L^{-1}) compared with groundwater samples (5.70 mg L^{-1}). In all cases however, the DOC concentrations were low suggesting that soil organic matter in the area was low and/or relatively flocculated.

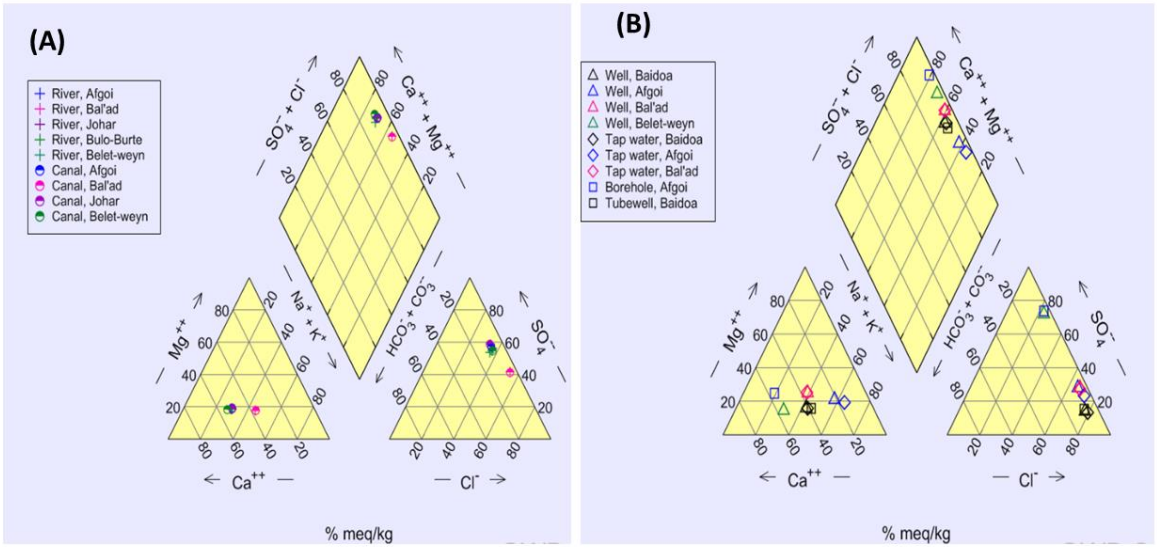


Figure 3.3. Piper diagram describing the hydro-geochemical properties of (A) Shabelle river water samples; (B) groundwater from Shabelle riverine areas and Bay region.

Table 3.1. The main physico-chemical properties of the groundwater samples from South Somalia. Data are means ± standard deviation for each measured parameter.

Characteristics	Well	Tap water	Borehole	Tube well
pH	7.82 ± 0.410	7.63 ± 0.52	7.58	7.03
EC (dS m^{-1})	2.20 ± 0.560	2.63 ± 0.85	2.28	1.88
Cl^-(mg L^{-1})	438 ± 244	597 ± 327	133 ± 12.0	216 ± 20.0
NO_3-N (mg L^{-1})	16.2 ± 13.3	16.2 ± 11.0	n. d	6.43 ± 0.13
SO_4-S (mg L^{-1})	108 ± 57.3	87.1 ± 55.0	193 ± 13.2	19.5 ± 0.210
S (mg L^{-1})	139 ± 64.3	123 ± 84.0	219 ± 3.31	18.6 ± 0.170
TOC (mg L^{-1})	4.75 ± 3.00	6.15 ± 3.35	4.75 ± 1.43	7.13 ± 0.48
TIC (mg L^{-1})	64.3 ± 23.1	65.5 ± 25.7	36.3 ± 1.05	39.9 ± 2.56
B (mg L^{-1})	0.700 ± 0.360	0.700 ± 0.310	0.190 ± 0.000	0.400 ± 0.02
Na (mg L^{-1})	323 ± 212	424 ± 334	87.1 ± 1.50	115 ± 0.53
Mg (mg L^{-1})	75.2 ± 43.2	86.3 ± 49.7	60.6 ± 0.800	20.8 ± 0.110
K (mg L^{-1})	10.9 ± 9.50	21.7 ± 26.4	4.12 ± 0.0700	0.220 ± 0.01
Ca (mg L^{-1})	180 ± 57.3	172 ± 57.2	229 ± 2.79	82.2 ± 3.02
Li (µg L^{-1})	12.8 ± 7.63	14.0 ± 11.3	13.7 ± 0.220	2.21 ± 0.0900
Al (µg L^{-1})	2.75 ± 1.65	5.35 ± 7.40	1.70 ± 0.560	1.19 ± 0.260
V (µg L^{-1})	9.14 ± 6.49	9.64 ± 7.36	40.8 ± 0.520	1.39 ± 0.0200
Cr (µg L^{-1})	2.07 ± 2.31	0.740 ± 0.550	0.880 ± 0.0200	0.160 ± 0.000
Mn (µg L^{-1})	31.5 ± 42.0	27.4 ± 33.6	61.4 ± 19.0	0.0900 ± 0.0100
Fe (µg L^{-1})	3.71 ± 8.07	3.00 ± 3.46	n. d	n. d
Co (µg L^{-1})	0.410 ± 0.600	0.650 ± 0.540	0.320 ± 0.0300	0.0200 ± 0.000
Ni (µg L^{-1})	11.6 ± 21.8	15.5 ± 21.4	0.910 ± 0.150	0.110 ± 0.0400
Cu (µg L^{-1})	2.93 ± 3.21	1.86 ± 1.53	0.390 ± 0.0200	0.130 ± 0.0100
Zn (µg L^{-1})	87.7 ± 146	124 ± 155	0.220 ± 0.530	0.0400 ± 0.170
As (µg L^{-1})	1.03 ± 0.940	1.64 ± 2.05	0.780 ± 0.0300	0.0500 ± 0.0100
Br (µg L^{-1})	32.8 ± 16.0	44.8 ± 20.9	13.3 ± 0.0700	22.4 ± 0.140
Rb (µg L^{-1})	2.23 ± 2.28	5.41 ± 6.44	0.730 ± 0.030	0.430 ± 0.0100
Sr (µg L^{-1})	2647 ± 1300	2515 ± 1770	3167 ± 27.5	366 ± 2.27
Mo (µg L^{-1})	5.43 ± 2.76	4.66 ± 4.33	4.12 ± 0.220	2.71 ± 3.82
Cd (µg L^{-1})	0.0300 ± 0.0200	0.0400 ± 0.0200	0.0100 ± 0.000	0.0100 ± 0.0100
Cs (µg L^{-1})	0.0100 ± 0.0100	0.0100 ± 0.0100	n. d	0.0100 ± 0.000
Ba (µg L^{-1})	54.8 ± 7.88	50.2 ± 5.71	34.7 ± 0.300	34.8 ± 0.350
Pb (µg L^{-1})	0.340 ± 0.120	0.310 ± 0.110	0.260 ± 0.000	0.260 ± 0.000
U (µg L^{-1})	3.85 ± 2.59	4.44 ± 2.72	4.17 ± 0.0200	0.910 ± 0.0100
Se (µg L^{-1})	4.31 ± 3.56	4.73 ± 2.73	0.980 ± 0.0100	1.66 ± 0.0200
I (µg L^{-1})	1810 ± 1340	2230 ± 2030	963 ± 47.4	460 ± 15.3

Table 3.2. The main physico-chemical properties of the surface water samples from South Somalia. Data are means ± standard deviation for each measured parameter.

Characteristics	River	Canals	Barkad
pH	7.76 ± 0.380	7.98 ± 0.360	7.76 ± 0.380
EC (dS m^{-1})	1.16 ± 0.470	1.34 ± 0.570	1.16 ± 0.470
Cl^-(mg L^{-1})	102 ± 74.0	99.0 ± 68.0	60.0 ± 10.0
NO_3-N (mg L^{-1})	2.18 ± 0.420	2.16 ± 0.510	1.90 ± 0.0500
SO_4-S (mg L^{-1})	53.8 ± 16.7	56.4 ± 12.6	43.5 ± 0.170
S (mg L^{-1})	61.9 ± 27.6	64.0 ± 23.9	61.9 ± 27.5
TOC (mg L^{-1})	7.44 ± 1.84	6.46 ± 1.75	7.44 ± 1.84
TIC (mg L^{-1})	28.6 ± 3.31	28.3 ± 3.32	28.6 ± 3.31
B (mg L^{-1})	0.100 ± 0.0500	0.110 ± 0.0500	0.100 ± 0.0500
Na (mg L^{-1})	75.3 ± 57.3	72.5 ± 52.7	75.3 ± 57.3
Mg (mg L^{-1})	20.5 ± 9.43	20.7 ± 8.66	20.5 ± 9.43
K (mg L^{-1})	5.06 ± 0.750	5.24 ± 0.68	5.06 ± 0.75
Ca (mg L^{-1})	84.3 ± 25.5	86.8 ± 22.1	84.3 ± 25.5
Li (µg L^{-1})	1.53 ± 1.13	1.66 ± 1.12	0.770 ± 0.0200
Al (µg L^{-1})	3.43 ± 0.670	3.44 ± 1.25	4.19 ± 0.620
V (µg L^{-1})	12.6 ± 1.56	11.5 ± 1.94	11.2 ± 0.120
Cr (µg L^{-1})	0.550 ± 0.180	0.610 ± 0.180	0.480 ± 0.0100
Mn (µg L^{-1})	0.610 ± 1.65	0.450 ± 0.670	0.620 ± 0.640
Fe (µg L^{-1})	n. d	n. d	n. d
Co (µg L^{-1})	0.0700 ± 0.0100	0.0600 ± 0.0100	0.0700 ± 0.0100
Ni (µg L^{-1})	1.09 ± 0.160	1.49 ± 1.41	1.16 ± 0.0900
Cu (µg L^{-1})	1.60 ± 0.240	1.56 ± 0.230	1.67 ± 0.290
Zn (µg L^{-1})	0.630 ± 2.40	4.42 ± 12.5	0.410 ± 0.120
As (µg L^{-1})	0.660 ± 0.0900	0.630 ± 0.100	0.620 ± 0.0200
Br (µg L^{-1})	9.21 ± 6.18	8.90 ± 5.64	6.23 ± 0.0700
Rb (µg L^{-1})	1.63 ± 0.170	1.62 ± 0.190	1.44 ± 0.0400
Sr (µg L^{-1})	913 ± 315	943 ± 275	780 ± 2.68
Mo (µg L^{-1})	3.41 ± 0.330	4.34 ± 4.54	3.83 ± 0.680
Cd (µg L^{-1})	0.0100 ± 0.000	0.0100 ± 0.000	0.0100 ± 0.000
Ba (µg L^{-1})	88.8 ± 25.4	87.6 ± 23.4	79.5 ± 0.600
Pb (µg L^{-1})	0.270 ± 0.0100	0.270 ± 0.0100	0.280 ± 0.000
U (µg L^{-1})	1.98 ± 0.24	1.85 ± 0.240	2.32 ± 0.0200
Se (µg L^{-1})	0.590 ± 0.100	0.600 ± 0.220	0.650 ± 0.0200
I (µg L^{-1})	217 ± 78.5	220 ± 79.4	223 ± 1.95

3.3.2. Comparisons between major anions of the different water types

The anion concentrations in the water generally followed the order chloride > sulphate > nitrate > bicarbonate. These anionic constituents were present at (elemental) concentrations in the range of a few mg L^{-1} to up to more than a thousand mg L^{-1}. The Cl concentration found in several wells from different regions varied from 95 to 740 mg L^{-1}, with the arithmetic mean of 440 mg L^{-1}. These are concentrations in excess of the WHO guidelines for drinking water of 250 mg L^{-1}. Large concentrations of Cl were found in most wells but there were variations between the regions; for example, samples from Afgoi and Bal'ad had greater Cl concentrations (630 mg L^{-1}) than measured in Baidoa samples (220 mg L^{-1}).

The Cl concentrations in tap water ranged from 230 to 1000 mg L^{-1} with an arithmetic mean of 600 mg L^{-1}. There were regional variations, for example tap water from Afgoi had the greatest Cl concentration (1000 mg L^{-1}) followed by Bal'ad (530 mg L^{-1}) and Baidoa (250 mg L^{-1}). Surface water samples had lower Cl concentrations; river water samples varied from 50 mg L^{-1} to 260 mg L^{-1}, with an arithmetic mean of 100 mg L^{-1}; samples from the canal had similar concentrations (Fig 3.4).

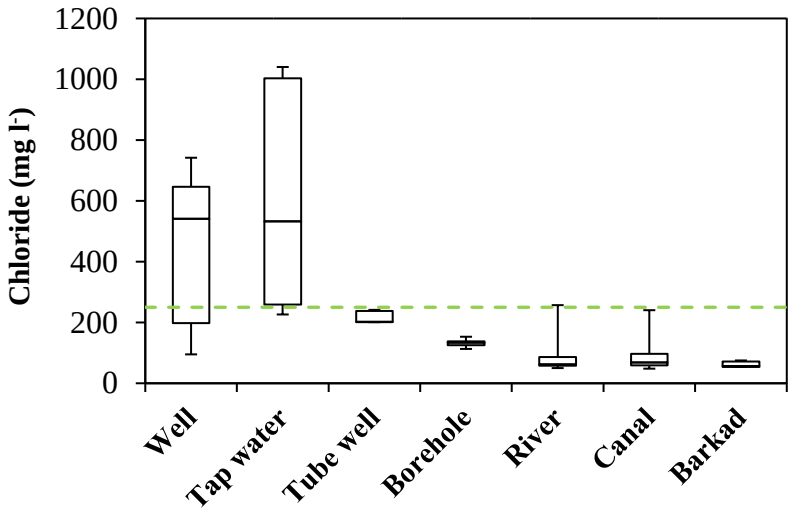


Figure 3.4. Box and whisker plot of measured chloride concentration in groundwater and surface water samples collected in a survey in Somalia, the dashed reference line is the maximum permissible limit in drinking water (WHO).

Sum of the anions Cl, SO_4-S and NO_3-N were plotted against the EC (µS cm^{-1}) in order to further characterize and determine the salinization of the water samples. It can be seen (Fig. 3.5) that these samples have EC exceeding EC 1000 µS cm^{-1}, are most likely affected by sea water intrusion into freshwater aquifers. There is a good agreement between the EC and the sum of the Cl, SO_4-S and NO_3-N anions (R^2= 0.5057; $p < 0.001$), as shown in Fig.3.5. Chloride concentrations strongly positively correlated with the Na ions with a correlation coefficient of R^2=0.9343; $p < 0.001$; the Na: Cl ratio varied from 0.5 to 1.1. Good agreements were also found to exist between the Cl contents and Ca (R^2= 0.5139; $p < 0.001$) and Mg (R^2= 0.9055; $p < 0.001$) contents of these samples (Fig. 3.6). This was further confirmed with the good agreements found in the scatter plot between the sum of (Ca and Mg) vs (Cl and SO_4) contents (R^2= 0.8861; $p < 0.001$; Fig 3.7), probably there was significant calcium sulfate content in these water samples (R^2= 0.7137; $p < 0.001$; Fig 3.7).

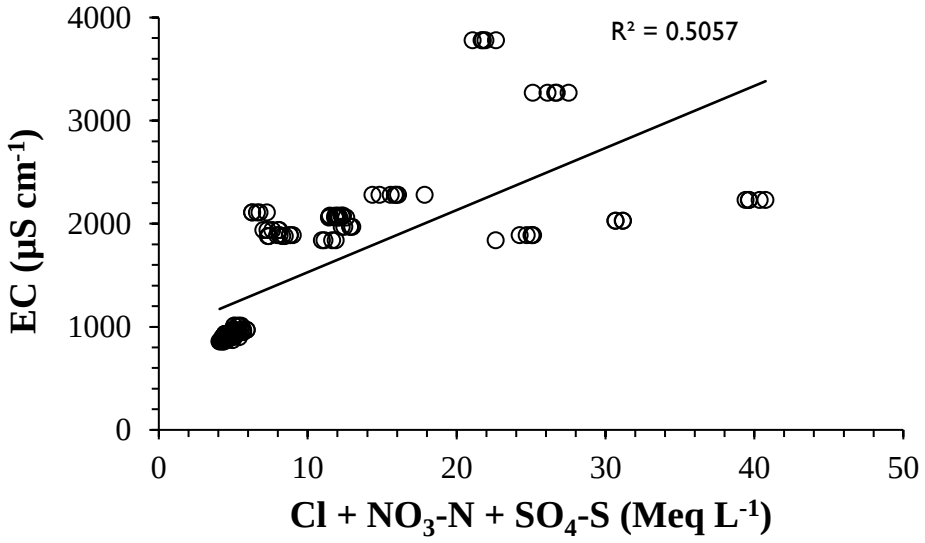


Figure 3.5. Relationship between total anions (Cl, SO_4-S and NO_3-N) and the electrical conductivity (EC) of the surface water and groundwater samples collected from south Somalia.

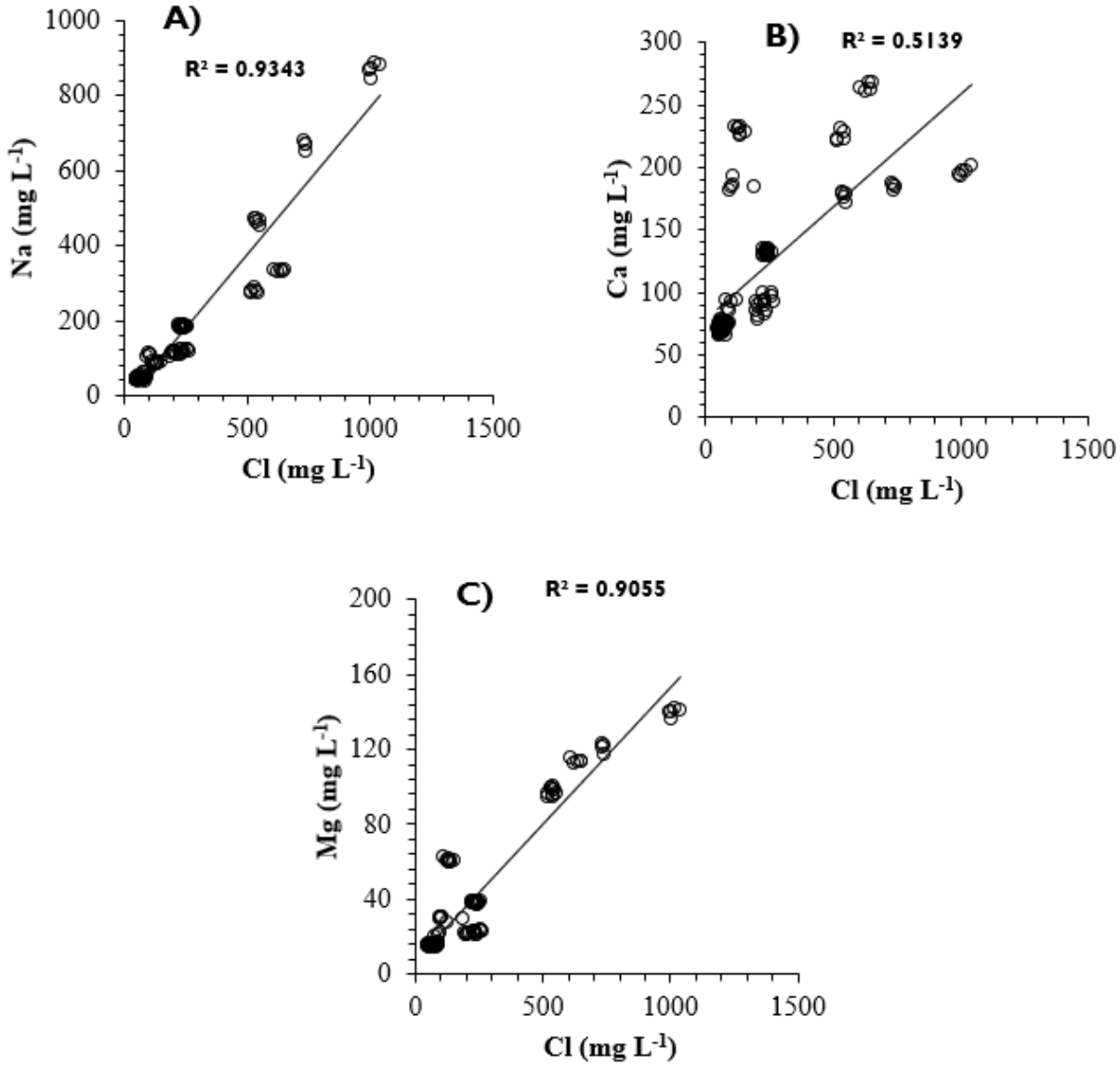
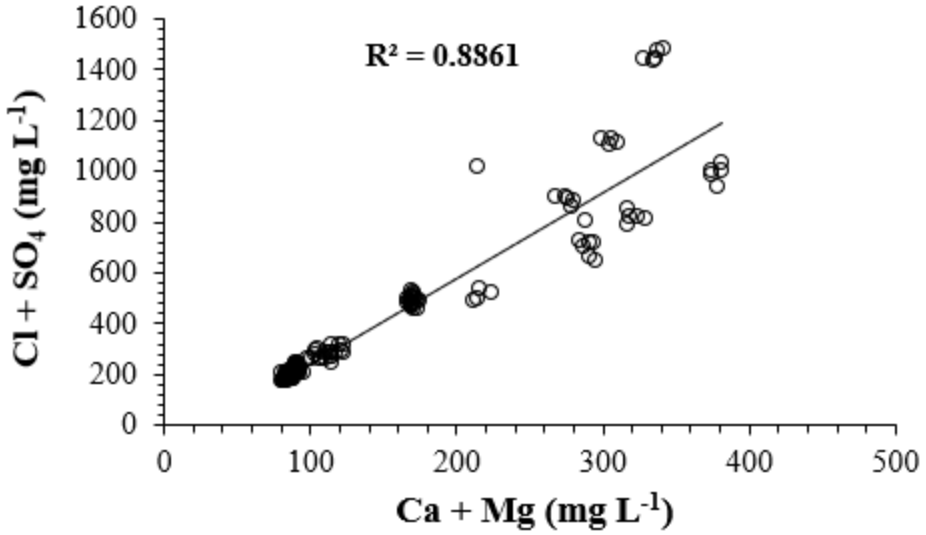


Figure 3.6. Scatter plot showing the correlation between Cl and major cations: a) Na; b) Ca and c) Mg present in the surface and groundwater systems of the study area.

(a)



(b)

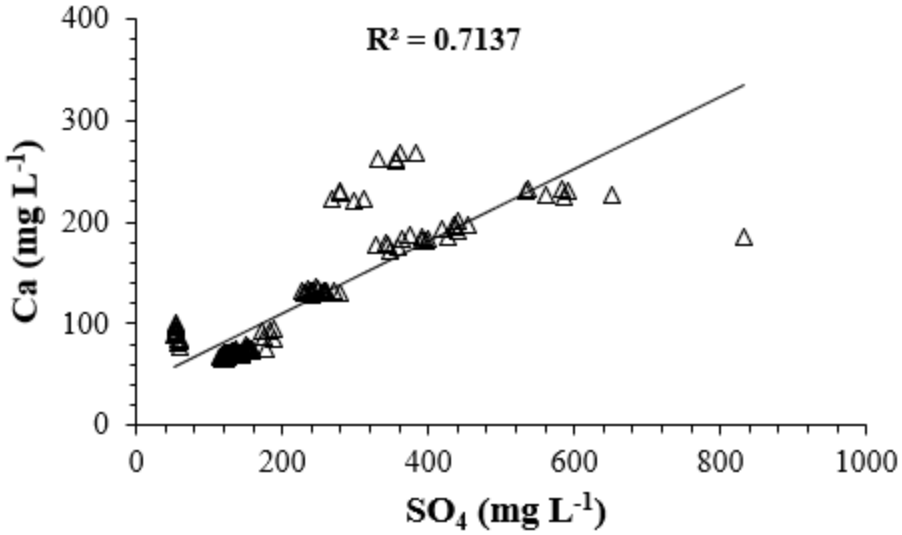


Figure 3.7. Scatter plot of a) cations (including Ca and Mg) versus anions (Cl and SO_4); b) The scatter plots of Ca versus SO_4 in groundwater and the Shabelle river, Somalia.

Likewise, sulphate concentrations were also high in the groundwater, higher than the permissible levels (i.e. 250 mg L^{-1}) recommended by USEPA for drinking water (Abernathy et al., 2003). The highest SO_4 concentrations were recorded in borehole samples (580 mg L^{-1}), followed by well (320 mg L^{-1}), and tap water (260 mg L^{-1}). Surface water (i.e. from river, canals and barkad storage) had relatively lower SO_4 (average 160 mg L^{-1}), the concentrations varied from 115 to 278 μg L^{-1}. The sources of the SO_4 can be from the lithology of the aquifers, from gypsum and anhydrite

dissolution. The SO_4/Cl ratio varied from 0.20 to 4.75 suggesting that the fresh water has mixed with sea water, generally this ratio increases with a decrease in salinity. In general, the abundance of sulphur in these groundwater and surface water can be from carbonate and marine sediments. It has been reported that carbonates have sulphur contents of 1,200 mg L^{-1}, while deep sea sediments have 1,300 mg L^{-1} (Field, 1972).

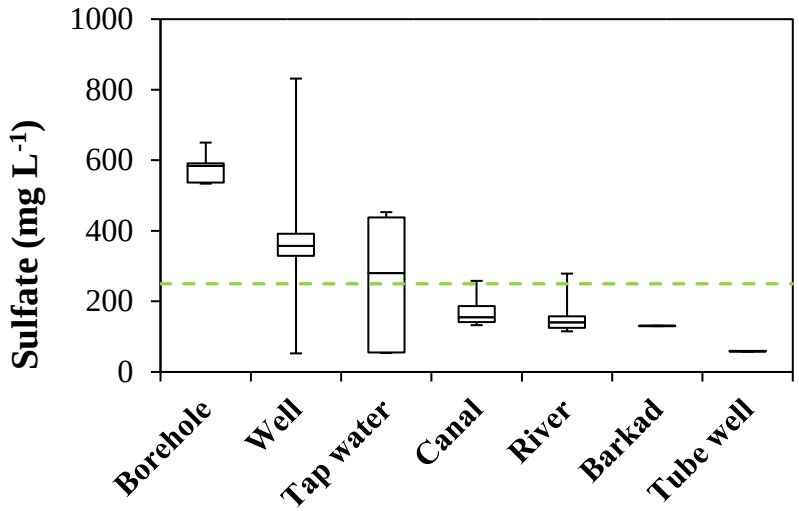


Figure 3.8. Measured sulphate concentrations in groundwater and surface water samples collected from south Somalia; the dashed line represents the maximum permissible limit in drinking water (WHO).

The average nitrate concentrations of well, tap water and surface water were 71.6 mg L^{-1}, 71.5 mg L^{-1} and 10 mg L^{-1}, respectively; these levels in groundwater are higher than the accepted limit of 10 mg L^{-1} of NO_3-N (US EPA, 2009). The anions HCO_3+CO_3 were ≤ 5% in most of the samples except for groundwater from Baidoa and in the river water samples where it reaches 8% of the total anion concentration. Other anions such as fluoride and phosphate were not detected in any of the samples. The absence of fluoride from the Somali water samples contradicts with the high concentrations reported in Ethiopia particularly in the Rift Valley region, where fluoride problem is more acute reaching up to 12 mg L^{-1} (Reimann et al., 2003). Elevated fluoride levels are common in groundwaters in the rift valley regions of Kenya and Tanzania as well (Adelana and MacDonald, 2008).

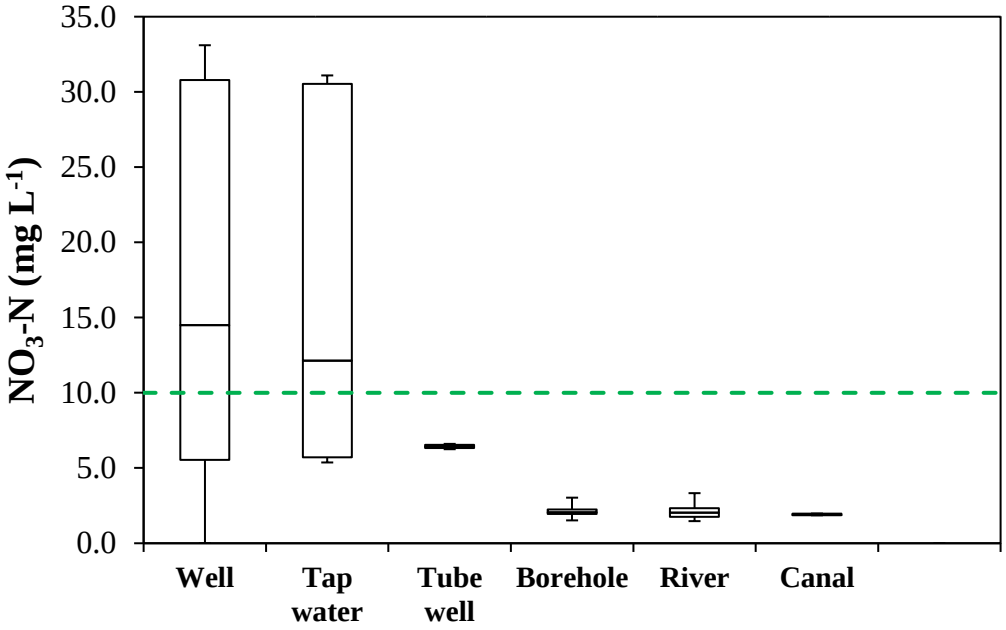


Figure 3.9. Nitrate-nitrogen concentration in groundwater and surface water samples collected in a survey in Somalia, the dashed reference line (10 mg L^{-1} of NO_3-N) is the maximum permissible limit in drinking water according to the US Environmental Protection Agency (EPA).

3.3.3. Iodine

3.3.3.1. Total Iodine in ground and surface water

The iodine concentration in groundwater samples collected from four districts in Somalia varied between 404 and 5160 μg L^{-1}, with an arithmetic mean of 1690 μg L^{-1}, a median of 990 μg L^{-1}. Concentrations in surface water samples collected from the Shabelle river varied between 133 and 388 μg L^{-1}, with a mean of 218 μg L^{-1} and a median of 187 μg L^{-1}.

Total iodine concentrations were six times higher in groundwater ($P<0.001$) than in the surface water. The iodine concentrations in samples collected from the main river did not differ significantly ($P=0.086$) from those from the canals and barkad (water storage constructions).

Duncan's multiple range tests showed that water samples collected from tap (2230 μg L^{-1}), well (1811 μg L^{-1}) and borehole (963 μg L^{-1}) had significantly greater ($P<0.001$) iodine concentrations than water samples collected from river (217 μg L^{-1}), canal (220 μg L^{-1}), barkad (222 μg L^{-1}) and tube well (459 μg L^{-1}) sources. Tap water had the highest iodine content, followed by samples

collected from wells and boreholes, Fig. 3.10 shows iodine concentrations of the different water types; details of the speciation data are summarized in Table 3.3.

Ground water samples showed a geographical variation, with significance differences ($P<0.001$) between the study regions, the iodine concentrations were greatest in samples from Afgoi (2944 μg L^{-1}), followed by Bal'ad (1484 μg L^{-1}), Baidoa (471 μg L^{-1}) and Beletweyn (441 μg L^{-1}). There was a negative correlation between the total iodine concentration of the water and the distance from the Indian Ocean coastline, although plotting the whole data did not show a correlation. (Fig. 3.11). Geographical variation in the iodine content of ground water is common and where reported elsewhere. For example, in Denmark iodine concentration in ground water varied largely between regions (Pedersen et al., 1999). Compared to the results from the current study, the iodine concentrations in tap water were low in Denmark (1 to 139 μg L^{-1}) and Malawi (1 to 54 μg L^{-1}) but higher in the Guanzhong Basin, China (2 to 28,620 μg L^{-1}). Generally, worldwide iodine concentrations in surface and ground waters vary from 0.01 to 70 μg L^{-1}, with higher concentrations in coastal, arid or semi-arid areas (Duan et al., 2016; Pedersen et al., 1999; Rosenthal and Mates, 1986; Smedley, 2000; Watts et al., 2015).

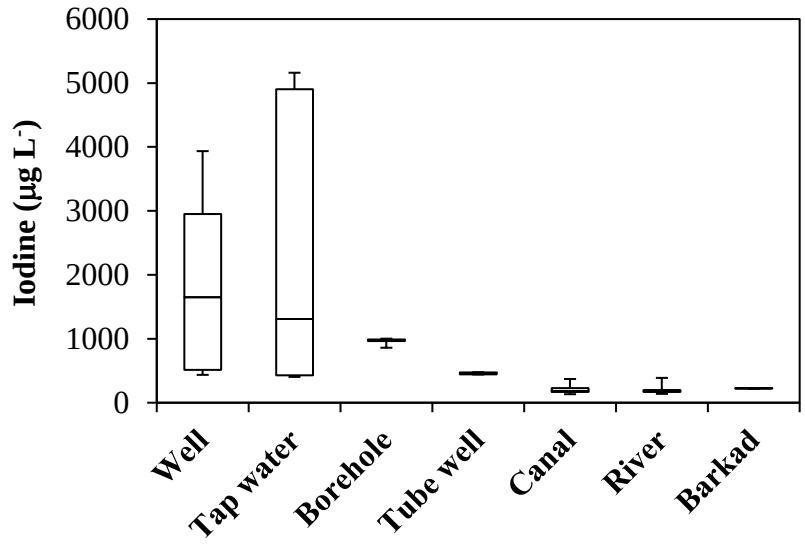


Figure 3.10. Box and whisker plot for total iodine concentration in groundwater and surface water samples in south Somalia; the Box and whisker plot data is classified by water type. The recommended daily intake (RDI) is 150 μg day^{-1} (WHO, 2006).

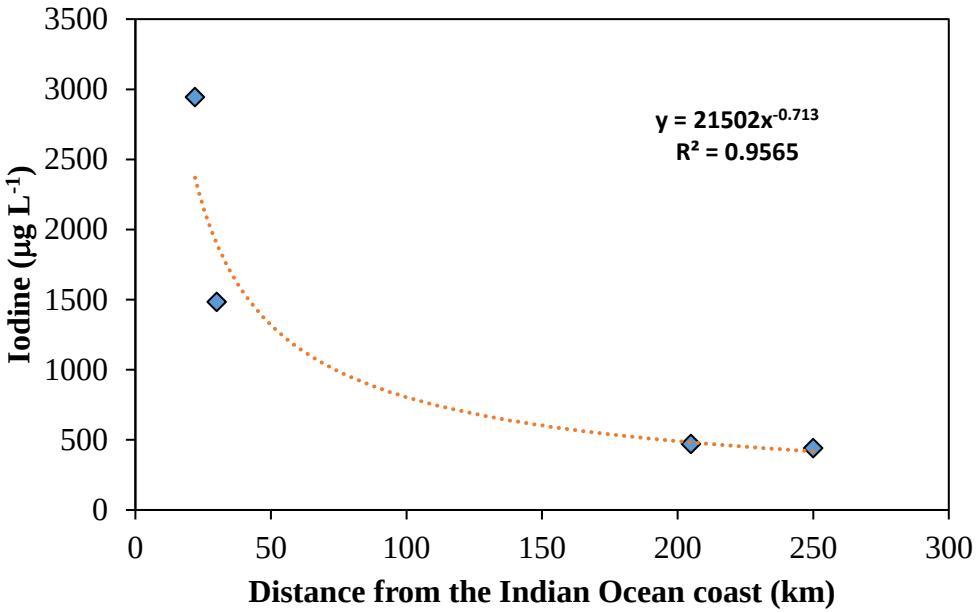


Figure 3.11. Correlation between total iodine concentration of the water samples and the distance from the Indian Ocean coastline, these are mean values of the groundwater from four districts.

3.3.3.2. Iodine speciation

The different iodine species in groundwater and surface water are summarized in Tables 3.3 and 3.4. Speciation analysis revealed that the majority of the iodine was organically bound I (88 % - 94 %). Organic matter is the single most important factor controlling iodine content in soils (Johnson, 2003); the importance of iodine sorption onto organic matter (OM) has been demonstrated by (Bowley, 2013) and (Shetaya et al., 2012). The dominant inorganic iodine species was iodide, ranging between 1.4 % and 8 % of the total iodine content. Only two samples (from well and tube well) had high iodate concentrations. On average, iodate and iodide accounted for 3.5% and 5.6% of the total iodine concentration, respectively. This finding is in line with the study of Voutchkova et al. (2017) that reported the predominance of I^- and organically bound iodine in Danish groundwater. Previous contradicting literature has shown that in arid alkaline environments the dominant iodine species is iodate, very insoluble iodide species have been reported in the weathered areas of mineral deposited in arid environments (Johnson, 2003).

3.3.3.3. Factors influencing the concentration and speciation of iodine

The pH did not significantly affect iodate concentration, but there was a weak positive correlation between the pH and I^- (r = 0.204), organically bound iodine (r = 0.166) and total iodine (r = 0.165). The effect of the EC was much stronger, there was a strong positive correlation between the EC and IO_3^- concentration (r = 0.589), but the correlations between EC and organically bound IODINE (r = 0.461) and total iodine (r = 0.466) were weaker. Dissolved organic matter (DOC) was strongly negatively correlated with IO_3^- (r = -0.587), but a weak negative correlation with organically bound iodine (r = -0.351) and total iodine (r = -0.350) was observed. This contradicts a previous study where a positive relationship (r = 0.85) between DOC and total iodine, I^- and dissolved organic iodine was reported in Danish water samples (Voutchkova et al., 2017). In the current study most of the dissolved carbon was present as DIC (average; 83.3%) and only 16.7% was in the form of DOC. Dissolved inorganic carbon was positively correlated with IO_3^- (r = 0.804), I^- (r = 0.673), organically bound iodine (r = 0.952) and total iodine (r = 0.953). Similarly, the Ca concentration of the water was also positively correlated with the different iodine species, although the relationship with I^- was relatively weak (r = 0.407). Sodium, Mg, Cl and NO_3 all showed a strong and positive correlation with the concentration of total iodine and iodine species. Values of the Pearson correlation coefficient 'Pearson's r' are summarized in Table 3.8.

3.3.3.4. Iodine inputs through irrigation (ground or surface water)

The main iodine input to the topsoil is normally from atmospheric wet and dry deposition (Whitehead, 1984). However, in Somalia where iodine rich groundwater is commonly used in irrigation it is important to know how much iodine is added to the soils via irrigation water. The annual iodine input to soils from groundwater and surface water was calculated according to the procedure described by (Bowley, 2013). The iodine input from groundwater and surface water per year (I_{in}, g ha^{-1} yr^{-1}) is obtained using equation 3.1.

$$I_{in} = \frac{I_{irr} \times V_{irr}}{100} \qquad \text{Equation 3.1}$$

Where I_{irr}= iodine content of the irrigation water (μg L^{-1}) and V_{irr} = volume of the irrigation water (mm yr^{-1}). The volume of irrigation water required by maize plants during the entire growing season is 500 – 800 mm (Critchley et al., 1991) so using a mean I_{irr} value of 1685 μg L^{-1}, I_{in} can

be estimated as 8,425 g ha^{-1} yr^{-1} – 13,480 g ha^{-1} yr^{-1}. This clearly indicates that the potential iodine input from Somali groundwater is very high. This would represent an annual increase in topsoil iodine concentration of 3.4 – 5.4 mg kg^{-1} assuming 2500 t topsoil ha^{-1}. The input from irrigation with the Shabelle river (i.e. 218 μg L^{-1}) is lower than that of the groundwater and is estimated to range between 1,090 g ha^{-1} $season^{-1}$ and 1,744 g ha^{-1} $season^{-1}$. The iodine input from the river water is 87% lower than that of the groundwater. By contrast, the input from approximately 700 mm of rainwater in the UK throughout a given year is only 14.0 g ha^{-1} yr^{-1} as estimated by (Bowley, 2013).

Table 3.3. Measured total iodine concentration and speciation (^{127}I; µg L^{-1}) in groundwater samples, south Somalia. Data are means ± standard deviation; "minimum", first quartile (Q1), median, third quartile (Q3), and "maximum".

	Well							Tap water						
Characteristics	Min	25%	Median	75%	Max	Av.	SD	Min	25%	Median	75%	Max	Av.	SD
Iodate	0.00	41.3	193	212	300	144	111	34.8	37.9	44.6	155	178.1	83.1	61.6
Iodide	3.77	6.34	19.83	47.7	260.6	58.8	91.6	0.00	2.62	3.74	535	557	183	263
Org I	393	466	1445	2635	3481	1609	1188	360	378	1126	4324	4586	1965	1799
Total I	435	516	1651	2951	3935	1811	1341	404	427	1308	4904	5161	2230	2034
	Borehole							Tube well						
Iodate	19.73	19.79	20.11	20.20	20.37	20.06	0.23	41.70	42.20	44.62	45.65	46.21	44.06	1.83
Iodide	66.4	85.6	90.7	94.0	95.2	87.7	10.0	5.84	5.97	6.62	6.96	7.19	6.49	0.54
Org I	774	851	864	878	886	855	38.0	392	395	412	421	424	409	13.5
Total I	860	962	973	990	1001	963	47.4	441	444	463	474	477	460	15.3

Table 3.4. Measured total iodine concentration and speciation (^{127}I; µg L^{-1}) in Shabelle river water samples, south Somalia. Data are means ± standard deviation; "minimum", first quartile (Q1), median, third quartile (Q3), and "maximum".

	River							Canal						
Characteristics	Min	25%	Median	75%	Max	Av.	SD	Min	25%	Median	75%	Max	Av.	SD
Iodate	0.07	0.21	0.40	0.50	1.30	0.50	0.39	0.00	0.21	0.43	1.20	24.81	2.02	5.01
Iodide	0.00	7.61	10.4	13.0	35.2	13.6	10.4	0.01	2.24	8.01	13.1	34.3	11.1	11.1
Org I	138	161	175	186	355	203	68.0	133	158	175	219	345	207	68.8
Total I	139	170	185	198	388	217	78.5	133	166	186	230	371	220	79.4
	Barkad													
Iodate	0.27	0.27	0.28	0.28	0.28	0.28	0.01							
Iodide	13.0	13.2	14.4	14.9	14.9	14.2	0.87							
Org I	206	206	208	211	211	208	2.36							
Total I	220	221	223	224	224	223	1.95							

3.3.4. Selenium

3.3.4.1. *Total Se in ground and surface water*

The concentrations of Se ranged from 0.09 to 9.25 µg L^{-1} and 0.40 to 1.60 µg L^{-1} for the groundwater and surface water samples, respectively. The Se concentrations in groundwater were significantly higher than those from the surface water sources, according to the adjusted P values ($P<0.001$) from the multiple comparison's tests. Concentrations were also slightly greater than the global mean Se concentration in fresh water of 0.02 µg L^{-1} (Fordyce, 2005). In some areas in the world, Se concentrations may approach 50–300 µg L^{-1} such as in U.S. seleniferous water samples (Fordyce, 2005). Similarly, quite high Se levels have been reported in Argentina surface water (2–19 µg L^{-1}), Slovakia groundwater (0.5–45 µg L^{-1}) and China seleniferous surface water (0.46–275 µg L^{-1}). Lower Se concentrations than the Somali groundwater and surface waters have also been reported in Spain with freshwater samples in the range 0.001–0.202 µg L^{-1}) and U.S. drinking water (0.0–0.01 µg L^{-1}) (Fordyce, 2005). In general, the Se concentrations in the Somali groundwater and surface water were very similar to those reported in Ethiopia. Concentrations observed in Rift Valley drinking water samples ranged from 0.015 to 7.6 µg L^{-1} (median: 0.62 µg L^{-1}) (Reimann et al., 2003). The average Somali Se concentrations were lower than the iodine contents by three orders of magnitude (Fig. 3.12).

Lithology, among other factors, controls the geochemistry of water - including Se and iodine concentrations. Sedimentary rocks, generally, tend to have higher iodine concentrations with average iodine contents in recent sediments of 5–200 mg kg^{-1}, carbonates 2.7 mg kg^{-1}, shales 2.3 mg kg^{-1} and sandstones 0.8 mg kg^{-1} (Fuge and Johnson, 1986). Selenium contents of the sedimentary rocks on the other hand are much lower, for example the Se concentrations in limestone (0.03 mg kg^{-1} – 0.08 mg kg^{-1}), sandstone (< 0.05 mg kg^{-1}) and shale (0.05 mg kg^{-1} – 0.06 mg kg^{-1}) are all much lower than the iodine concentrations (Fordyce, 2005).

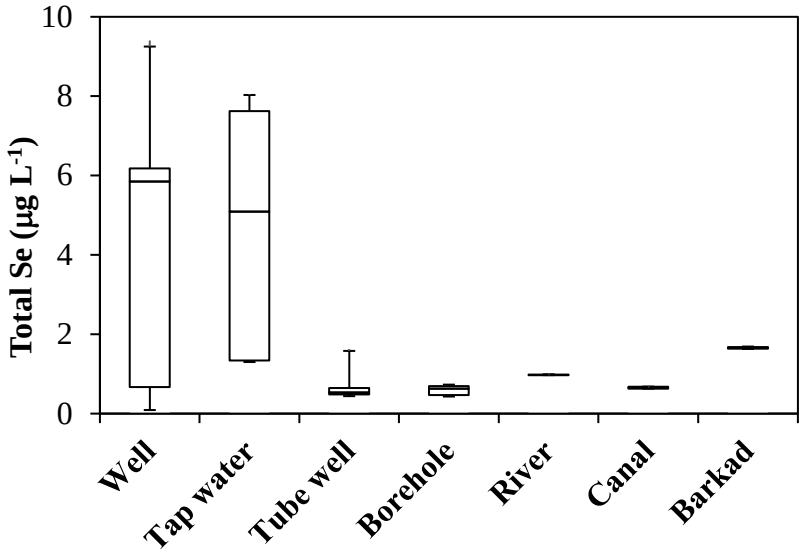


Figure 3.12. Box and whisker plot for total Se concentrations in surface water and groundwater samples of south Somalia. The data is classified by water type.

3.3.4.2. Se Speciation

Selenium speciation is important because it affects mobility and therefore bioavailability to plants. In the environment, in general, selenate is more mobile, soluble and less strongly adsorbed than selenite. In the Somali groundwater samples Se was mainly present as selenate accounting for 50 - 80% of the total Se. Thus, unlike iodine, most of the Se in the Somali groundwater and surface water appears to be inorganic. The organically bound Se was 20 -50% of total Se in river water and tube well samples but lower in groundwater sources which had high selenate concentrations of up to 80% of total Se. The different Se species in the Somali groundwater and surface water are tabulated in Tables 3.5 and 3.6.

3.3.4.3. Factors influencing total concentration and speciation of Se

The chemistry of groundwater and surface water is in general dependent on the underlying geology (Khatri and Tyagi, 2015). Previous studies have reported that the mobility and bioavailability in soils is influenced by bio-physicochemical factors such as the pH, redox potential, Se speciation, mineralogy, organic matter content and the presence of competing ions (Fordyce, 2005). A correlation analysis was used to determine associations with total Se and species. The pH of the water samples was very weakly positively correlated with organically bound Se ($r = 0.212$), total Se ($r = 0.150$) and selenate ($r = 0.137$). Similar positive relationship between pH and soil Se has been reported by Elrashidi (2018); the positive correlation of pH with total Se was mainly attributed to increasing content of $CaCO_3$. The main inorganic Se species was selenate, which is in line with the literature and with this correlation. It has been

reported in the literature that under oxidizing alkaline conditions selenate is the predominant inorganic phase, whereas selenite is predominant under reducing acidic conditions (Fordyce, 2005). A better correlation existed with EC; the EC was positively correlated with selenate (r = 0.717), organic Se (r = 0.647) and total Se (r = 0.712), but weakly correlated with selenite (r = 0.200). High negative correlations were observed between DOC and selenate (r = -0.530), organically bound Se (r = -0.502) and total Se (r = -0.523). This contradicts with the positive relationship between Se and soil organic matter that has been observed in many studies. It has been reported in the literature that selenium association with soil organic matter occurs via adsorption on to the reactive groups on soil organic matter i.e. directly or indirectly via metal ions or as part of the structure of organic matter molecules (Gustafsson and Johnsson, 1994; Qin et al., 2012). Around 70 to 100% (mean 83%) of total carbon in the water samples was carbonate/bicarbonate. Dissolved inorganic carbon (DIC) showed a strong positive correlation with selenite (r = 0.837), selenate (r = 0.562), organically bound Se (r = 0.819) and total Se (r = 0.853), which is supported by the positive strong correlation between the total Ca concentrations with the selenate (r = 0.734), organically bound Se (r = 0.669) and total Se (r = 0.731).

In addition, the cations Sodium and Mg and the anions Cl and NO_3 all correlated positively with the concentration of total Se and the individual Se species. Both Fe and Zn concentrations also showed a strong positive correlation with total Se and the different species. There was a strong and positive correlation between total Se, total iodine and their species (Table 3.8).

Table 3.5. Measured total selenium concentration and speciation (^{78}Se; µg L^{-1}) in groundwater samples from south Somalia. Data are means ± standard deviation; "minimum", first quartile (Q1), median, third quartile (Q3), and "maximum".

	Well							Tap water						
Characteristics	Min	25%	Median	75%	Max	Av.	SD	Min	25%	Median	75%	Max	Av.	SD
Selenate	0.00	0.25	4.69	4.98	7.76	3.42	3.01	1.06	1.17	3.57	5.95	6.43	3.62	2.13
Selenite	0.00	0.00	0.00	0.12	0.15	0.04	0.06	0.00	0.00	0.00	0.30	0.41	0.13	0.17
Org Se	0.09	0.28	1.06	1.28	2.03	0.85	0.59	0.00	0.24	1.17	1.35	2.07	0.98	0.65
Total Se	0.09	0.67	5.85	6.17	9.25	4.31	3.56	1.30	1.34	5.09	7.62	8.03	4.73	2.73
	Borehole							Tube well						
Selenate	0.70	0.71	0.74	0.75	0.76	0.73	0.02	1.33	1.34	1.37	1.39	1.40	1.37	0.03
Selenite	0.00	0.00	0.00	0.00	0.07	0.01	0.03	0.09	0.10	0.10	0.13	0.14	0.11	0.02
Org Se	0.17	0.21	0.24	0.27	0.28	0.23	0.04	0.15	0.16	0.19	0.21	0.23	0.19	0.03
Total Se	0.97	0.97	0.98	0.98	0.99	0.98	0.01	1.63	1.64	1.65	1.68	1.69	1.66	0.02

Table 3.6. Measured total selenium concentration and speciation (^{78}Se; µg L^{-1}) in Shabelle river water samples, south Somalia. Data are means ± standard deviation; "minimum", first quartile (Q1), median, third quartile (Q3), and "maximum".

	River							Canal						
Characteristics	Min	25%	Median	75%	Max	Av.	SD	Min	25%	Median	75%	Max	Av.	SD
Selenate	0.00	0.20	0.31	0.36	0.45	0.29	0.09	0.15	0.18	0.27	0.30	1.18	0.30	0.20
Selenite	0.00	0.00	0.00	0.00	0.10	0.01	0.03	0.00	0.00	0.00	0.00	0.09	0.00	0.02
Org Se	0.20	0.26	0.28	0.33	0.46	0.29	0.05	0.23	0.27	0.30	0.34	0.40	0.31	0.04
Total Se	0.43	0.47	0.63	0.69	0.73	0.59	0.10	0.44	0.48	0.53	0.65	1.58	0.60	0.22
	Barkad													
Selenate	0.26	0.27	0.31	0.34	0.35	0.31	0.04							
Selenite	0.00	0.00	0.00	0.04	0.05	0.01	0.03							
Org Se	0.29	0.30	0.34	0.37	0.37	0.33	0.04							
Total Se	0.63	0.63	0.65	0.68	0.68	0.65	0.02							

3.3.4.4. Selenium inputs through irrigation with ground or surface water

Selenium addition from the groundwater and surface water was calculated according to the procedure described by (Dhillon and Dhillon, 2003) *in* (Sparks, 2012). Selenium additions were obtained by multiplying the total amount of water required for a specific crop by the Se concentration of the irrigation water. The papers published by the Food and Agriculture Organization (FAO) are useful in specifying the water requirements of different crops. Calculations of inputs are based on the method described in (Critchley et al., 1991) and (Brouwer and Heibloem, 1986). Maize, sorghum and beans are the main staple crops in Somalia, according to (Critchley et al., 1991); the required water in a single growing period is 500 – 800 mm, 450 – 650 mm and 300 – 500 mm respectively. The growing periods varies from 3 months to 4 months depending on the species (Critchley et al., 1991). The current measurements of Se concentration in the water samples were 0.09 µg L^{-1} to 9.25 µg L^{-1} (median 1.7 µg L^{-1}) and 0.40 µg L^{-1} to 1.60 µg L^{-1} (median 0.6 µg L^{-1}) for the groundwater and surface water respectively. Therefore, the Se additions from irrigation of maize with groundwater or surface water can be estimated to be in the ranges 8.50 – 13.6 g ha^{-1} $season^{-1}$ or 3.00 to 4.80 g ha^{-1} $season^{-1}$ respectively (Table 3.7). The maximum Se recorded in groundwater was 9.25 µg L^{-1} which would add about 46.3 – 74.0 g ha^{-1} $season^{-1}$. Selenium additions from irrigation in the seleniferous region of northwest India were much greater, estimated at 9.4–262.5 g $ha^{-1}yr^{-1}$, with an arithmetic mean of 92 g $ha^{-1}yr^{-1}$ for maize (Dhillon and Dhillon, 2003). Nevertheless, considering typical Se biofortification inputs of 5-20 g ha^{-1} (Curtin et al., 2006), the annual inputs from irrigation water in Somalia, falling in the same general range as biofortification treatments, would certainly be expected to have a significant influence on Se concentrations in crops.

Table 3.7. Total Se addition from groundwater and surface water samples. Calculation of the added Se (g ha^{-1} $season^{-1}$) is based on the median Se concentrations (µg L^{-1}) in the water samples.

Crop	**Water requirement**	**Addition from GW**	**Addition from SW**
	(mm)	**(**g ha^{-1} $season^{-1}$**)**	**(**g ha^{-1} $season^{-1}$**)**
Maize	500 – 800	8.50 – 13.6	3.00 – 4.80
Sorghum	450 – 650	7.65 – 11.1	2.70 – 3.90
Beans	300 – 500	5.10 – 8.50	1.80 – 3.00

* GW: Groundwater; SW: Surface water; calculations are based on the median Se value

Table 3.8. Factors influencing total concentrations of selenium, iodine and their speciation in the Shabelle river water and groundwater samples from south Somalia.

	pH	EC	DOC	Na	Mg	Al	K	Ca	Mn	Fe	Zn	Ba	Cl	NO_3	SO_4	CO_3	Se (VI)	Se (IV)	Organo-Se	Total Se	IO^-_3	I^-	Organo-I
EC	-0.172																						
DOC	0.029	-0.473																					
Na	0.111	0.537	-0.330																				
Mg	0.133	0.729	-0.480	0.917																			
Al	0.255	0.086	-0.009	0.297	0.255																		
K	0.310	0.242	-0.049	0.863	0.703	0.394																	
Ca	0.031	0.858	-0.463	0.631	0.853	0.110	0.411																
Mn	0.111	0.663	-0.263	0.170	0.482	0.017	0.064	0.779															
Fe	0.213	0.559	-0.363	0.410	0.582	0.389	0.249	0.575	0.518														
Zn	0.146	0.714	-0.406	0.321	0.590	0.195	0.096	0.632	0.691	0.764													
Ba	-0.038	-0.123	0.165	-0.151	-0.243	0.088	-0.108	-0.202	-0.302	-0.147	-0.191												
Cl	0.060	0.684	-0.387	0.967	0.952	0.277	0.769	0.717	0.318	0.540	0.518	-0.199											
NO_3	0.099	0.435	-0.416	0.922	0.861	0.215	0.686	0.526	0.096	0.392	0.337	-0.305	0.897										
SO_4	0.151	0.549	-0.294	0.518	0.674	0.103	0.473	0.845	0.673	0.304	0.257	-0.120	0.505	0.374									
CO_3	0.110	0.602	-0.447	0.940	0.941	0.231	0.71	0.700	0.312	0.502	0.468	-0.357	0.951	0.959	0.519								
Se (VI)	0.137	0.717	-0.530	0.694	0.864	0.176	0.381	0.734	0.541	0.710	0.839	-0.350	0.815	0.770	0.400	0.837							
Se (IV)	-0.005	0.200	0.103	0.690	0.489	0.206	0.778	0.209	-0.088	0.082	-0.041	-0.228	0.635	0.543	0.192	0.562	0.222						
Organo Se	0.212	0.647	-0.502	0.714	0.852	0.294	0.462	0.669	0.464	0.671	0.801	-0.246	0.808	0.772	0.374	0.819	0.935	0.241					
Total Se	0.150	0.712	-0.523	0.720	0.879	0.203	0.420	0.731	0.526	0.707	0.833	-0.339	0.835	0.789	0.403	0.853	0.997	0.257	0.956				
IO^-_3	0.005	0.589	-0.587	0.612	0.753	0.012	0.197	0.625	0.374	0.524	0.619	-0.371	0.693	0.805	0.340	0.804	0.898	0.080	0.818	0.888			
I^-	0.204	0.237	-0.035	0.833	0.673	0.352	0.969	0.407	0.042	0.166	-0.008	-0.173	0.734	0.640	0.491	0.673	0.301	0.828	0.365	0.338	0.133		
Organo-I	0.166	0.461	-0.351	0.971	0.911	0.277	0.851	0.623	0.193	0.381	0.283	-0.327	0.925	0.940	0.553	0.952	0.693	0.679	0.709	0.719	0.643	0.840	
Total-I	0.165	0.466	-0.350	0.972	0.913	0.278	0.852	0.627	0.198	0.385	0.289	-0.328	0.927	0.939	0.555	0.953	0.697	0.680	0.711	0.721	0.643	0.841	1.000

Conclusion

So far, this study is the first study to describe the geochemistry of iodine and selenium in Somali groundwater and surface water. For the first time speciation information is reported for the groundwater and surface water samples of this region. Results from this survey have shown that the mean Se_{Tot} concentration was 3.63 μg L^{-1} and 0.595 μg L^{-1} for the groundwater and surface water respectively. Selenium speciation in the groundwater and surface water samples from Somalia also showed that selenate was the predominant Se species. Groundwater iodine was approximately three orders of magnitude greater than the typical range in potable groundwater, with an average concentration of 1690 μg L^{-1}, and a median of 990 μg L^{-1}. The average surface water iodine concentrations were above 200 μg L^{-1}; with an average of 218 μg L^{-1}, a median of 187 μg L^{-1}. This elevated I in groundwater confirm the excessive iodine intakes reported in the literature. It also highlights the urgent need for more research of iodine in groundwater. ^{127}I values from this study are higher than the typical range in drinkable groundwater 1 μg L^{-1} to 70 μg L^{-1}. Further iodine speciation analysis revealed that the dissolved ^{127}I was mainly present associated with (dissolved) organic matter (88 - 94 %), the rest of the iodine was present in the inorganic form. The dominant inorganic iodine species was iodide. Irrigation with the iodine-rich groundwater may also cause a substantial increase in the iodine content of soils and hence in the corresponding local crops, but further research in this area is needed.

4. Selenium and iodine in agricultural soils of South Somalia

4.1. Introduction

Selenium and iodine are two essential micronutrients for humans and animals. Both elements have a narrow margin between dietary deficiency and excess and both a shortage or a surplus of both elements can have serious health complications. Studies have shown that selenium and iodine status vary between regions as a direct result of their abundance and availability from local soils (Hartikainen, 2005). The variations in soils is often reflected in local food products (Johnson, 2003).

Selenium

Worldwide, the total Se concentration in most soils varies from 0.03 to 2.0 mg kg^{-1}, with an arithmetic mean of 0.40 mg kg^{-1} (Ure and Berrow, 1982). However, more elevated Se concentrations are reported in some seleniferous soils, such as in India (1–19.5 mg kg^{-1}), China (1.49–59.4 mg kg^{-1}) and USA (1–10 mg kg^{-1}) (Fordyce, 2013). Total Se concentrations as high as 5000 mg kg^{-1} have been reported in some seleniferous soils (Fordyce, 2013). In Africa, the total Se concentration is typically within the range reported by Ure and Berrow (1982). In South Africa for example, according to a map produced by Courtman et al. (2012), the soil Se status was in the range of 0.04 – 1.14 mg kg^{-1}. The total concentration of some micronutrients, such as selenium, is significantly influenced by the geological parent materials of the soils, atmospheric inputs and pedogenic processes (White and Zasoski, 1999). The association between the underlying geology and the Se concentration of soils has been documented. Fordyce (2013) reported the Se concentration of different rock types. Sedimentary rocks, particularly shales, coals and organic rich deposits, tend to have higher Se contents compared with igneous rocks (0.35 mg kg^{-1}) and volcanic rocks (0.35 mg kg^{-1}). However, some sedimentary rocks are exceptional, such as sandstone, limestone and carbonates which contain lower Se concentrations (Fordyce, 2013).

Clay soils in general tend to contain higher concentrations of Se than coarse-textured mineral soils (Keskinen et al., 2009). Moreover, soil Se may vary depending on climatic and pedogenic processes – especially those processes that affect inputs and retention of Se. Thus, Tan et al. (2002) showed the variability of Se content in soils from different climatic zones in China. The role of the soil organic matter content in retaining Se is also substantial (Fordyce, 2013). Selenium

association with soil organic matter is complex and is thought to arise from abiotic complexation (e.g. Se-metal-organic complexes) or via microbially mediated incorporation processes (Fernández-Martínez and Charlet, 2009; Gustafsson and Johnsson, 1994).

In addition to soil organic matter, carbonate minerals in calcareous soils can also incorporate Se, as reported by Aurelio et al. (2010) where selenite substitutes for carbonate. In terms of selenium speciation, Se exists in both inorganic and organic forms. Although the latter is dominant in most soils, it is the inorganic Se fraction which is considered bioavailable. Selenate (SeO_4^{2-}) and selenite (SeO_3^{2-}) are the most common inorganic species in oxidized alkaline or acidic soils respectively. Selenate is highly soluble, mobile, bio-available and potentially toxic at high concentrations. Inorganic Se may also include elemental Se (Se^0) and selenides (Se^{2-}) in highly reduced soils (Fordyce, 2013). Selenium speciation is more important than the total soil Se content, and is influenced by the pH, redox potential and soil microbial activity. Selenium that is directly available to plants and soil biota is present in the soil solution as a 'soluble fraction' and surface adsorbed as an 'exchangeable fraction'. Therefore, the available Se does not necessary correspond to the total Se content, but rather depends on the soil properties. For example, low Se soils in the semi-arid Mediterranean of Central Spain give rise to high Se concentrations in plants. This is probably due to the high pH values (7.1 to 8.7) and the subsequent high bioavailability of selenate in these soils (Rodriguez et al., 2005).

Iodine

Iodine concentrations vary greatly between different media and between regions of the Earth. The total iodine concentration in soils worldwide is in the range of 0.5–20 mg kg^{-1}, with an arithmetic mean of approximately 5 mg kg^{-1} worldwide (Whitehead, 1984). Unlike Se, most soil iodine is derived from volatilization from seawater which then enters the soil–plant system either through wet deposition or dry deposition (Fuge, 2013). This results in much greater iodine concentrations in soils than in parent rocks (Shetaya et al., 2012). The study of Johnson (2003) showed that the average iodine concentration in soils (5.1 mg kg^{-1}) was affected by soil texture and followed the order: peat (7.0) > clay (4.3) > silt (3.0) > sand (2.2). In general, clay-rich soils and organic rich soils tend to have much higher levels of iodine compared with sandy soils.

In aqueous and soil environments iodine naturally exists in several oxidation states ranging from −1 to +7. In reducing environments, I exists as iodide (I^-) and under more oxidizing conditions as

iodate (IO_3^-) (Preedy et al., 2009). The mobility of iodine and the distribution of its species depends on the soil conditions (i.e. soil characteristics such as the pH), iodide is more mobile and seems to be favoured by acidic soil conditions, while iodate is less mobile and is favoured by oxidizing alkaline conditions (Johnson, 2003).

Soil extractions using water, or weak electrolyte solutions, in combination with chemical speciation analyses of the supernatant solutions can be employed to determine the concentration and speciation of bioavailable Se and iodine pool in soils (Qin et al., 2012; Stroud et al., 2012). In addition, sequential extraction procedures (SEPs) may be employed to provide a complete fractionation of Se and I in soil (Chao and Sanzolone, 1989). Typically, SEPs start by first extracting with weak electrolyte solutions, and then the strength of the extraction solution is gradually increased to (sequentially) determine the concentrations of (for example) 'water-soluble', 'exchangeable', 'organically bound' and 'acid-soluble' (for Se only).

To date, the Se and iodine concentrations, and their chemical speciation, in Somali agricultural soils have not been studied. In Somalia, a major proportion of the soils are calcareous. For example, out of 800 soil samples collected from widely scattered locations of the Shabelle and Juba riverine areas, 30% comprised less than 10% calcium carbonate, 31% contained from 10 to 20% and 39% contained from 20 to 30% (Food, 1973). Gypsiferous soils are another important soil type in Somalia, covering 16% of the total area of the country (FAO, 1990). It is important to understand the fertility of the agricultural lands of Somalia and the availability of Se and iodine for uptake by food crops. Thus, this study is the first to explore the Se and iodine concentrations, and their chemical speciation, in agricultural soils from south Somalia.

4.2. Materials and methods

4.2.1. Study areas

The study area lies between longitude 43.64167 and 45.56682 east of the Prime Meridian; and between latitude 2.15139 and 4.81687 north of the Equator. The area extends to cover the main districts of the Shabelle valley and also includes two sites from Baidoa in the Bay region. The Juba and Shabelle riverine areas in southern Somalia have an estimated rural population of approximately two million, which is more than 40% of the total rural population of Somalia (Venema and Vargas, 2007). According to Venema and Vargas (2007) the geology of the study area is characterized by the metamorphic basement complex and by the presence of sedimentary

rock types. The metamorphic basement complex consists mainly of migmatites and granites, while the sedimentary rock types include limestones, sandstones, and gypsiferous limestones (Vargas et al., 2007). In some parts of the southern Shabelle, there are deposits that date back to late tertiary and comprise fluvio-lagunal deposits, which consists of clay, sandy clay, sand, silt, and gravel. In general, recent fluvial deposits are commonly found alongside the two rivers, the Juba and Shabelle, consisting of sand, gravel, clay and sandy clay (Vargas et al., 2007). The main landform in the study area is the presence of the perennial Shabelle river, originating from the highlands of Ethiopia and flowing towards the Indian Ocean (Vargas et al., 2007).

The soils of the study area are classified as deep seasonally poorly drained, medium to heavy textured, calcareous, alluvial Fluvisols, Cambisols and Vertisols. Haplic Vertisols (Chromic) predominate in the Shabelle valley. The salinity and alkalinity of these soils tends to increase as the alluvium of the lower Shabelle valley encroaches on the alkaline (Marine) Alluvial Plain. The Shabelle river swamps consist of clays and silty clays, with accumulated surface organic matter, but with low levels of salinity build-up despite the high rate of surface evaporation. Along the upper reaches of both the Juba and Shabelle there are extensive limestone outcrops, with more localised sandstones, marls and gypsum (Vargas et al., 2007).

The study area also includes two sampling sites in Baidoa in the Bay region. Biadoa is the main city and the capital of the Bay region; the region is located between the Juba and Shabelle rivers in South-central Somalia, but it is a non-riverine area. In this region rain-fed farming is practised alongside pastoralism in an agro-pastoral economic system. The climate of the Bay region follows a bimodal rainfall pattern: the light rainy season (‘Dayr’) usually begins by mid-October, and the heavy rainy season (‘Gu’) usually begins by mid-April. According to the main features and landform, the region has no natural perennial surface water. According to the soils and geology of the Bay region, there are five major geomorphological-ecological units: the Basement complex peneplain; the limestone plateau; a basement complex-limestone interface; coastal plain deposits; and clay plains. About 18% of the Bay region is occupied by the clay plains, the soils are predominantly Vertisols (Porter et al., 1988).

4.2.2. Soil sampling

Soil samples (i.e. surface soils) were collected from twelve agricultural sites from South Somalia in 2016 and 2017. The samples included six rain-fed and six irrigated soils and differed in their distance from the river. Soil sampling sites and sample processing are described in Chapter 2.

4.2.3. Soil characterization

All soils were analysed for their general properties, such as pH, carbonate content, organic matter content (LOI) and cation exchange capacity (CEC). In addition, the elemental composition of the soils (i.e. 31 elements) was determined by inductively coupled plasma mass spectrometry (ICP-MS) following HF-$HClO_4$-HNO_3 digestion; the digestion approach and the ICP-MS methodology are described in Sections 2.3.2.4 and 2.4.5 respectively. All results are reported as mean ± standard deviation in mg kg^{-1}; analysis was in triplicate, except the pH for which only duplicate samples were analysed.

4.2.4. Selenium and iodine fractionation

In addition to their total concentrations, fractionation of iodine and Se was undertaken to resolve their 'soluble', 'exchangeable' and 'organically bound' pools. Sequential extractions were performed using 0.01 M KNO_3, 0.016 M KH_2PO_4 and TMAH respectively (Wang et al., 2020). The method is described in Section 2.3.2.5.

4.2.5. Speciation of inorganic Se and iodine

In addition to fractionation, speciation analysis was applied to the soluble and exchangeable fractions to characterise the inorganic Se and iodine species and, by difference from the total concentration, to estimate the organic Se and iodine in these two fractions. Details of the speciation methods are described, in detail, in Section 2.4.6.

4.2.6. Chemical analysis

The pH was measured using a combined pH meter (HI 209 pH meter, Hanna instruments Ltd, UK) with a glass electrode (Beckman 511084), the approach is described in Section 2.3.2.1. Concentrations of Se and iodine, and other elements, were measured by ICP-MS (Thermo-Fisher Scientific iCAP-Q; Bremen, Germany), the approach is described in Section 2.4.5. Inorganic Se and iodine species were analysed using coupled liquid chromatography and ICP-MS (LC-ICP-MS), the approach is described in Section 2.4.6. Concentrations of the total inorganic carbon (TIC) were measured using a Shimadzu SSM-5000A model, (Section 2.4.4). Concentration of total

carbon (TC) and total nitrogen (TN) were determined simultaneously using an Elementar VarioMax CN analyser (Section 2.4.3).

4.3. Results and discussion

4.3.1. Soil characteristics

The general characteristics of the soil samples are presented in Table 4.1. The pH values of the soil samples from the study region were all above 7, ranging from 7.9 to 8.4, with an arithmetic mean of 8.1±0.1. The pH was highest in soils from Bal'ad district. Estimated soil organic matter content (% loss-on-ignition) ranged from 0.17% to 1.07%, with an arithmetic mean of 0.4%±0.2. The highest LOI was noted in samples from Baidoa, Bay region (1%±0.2), which was 5-fold more than that of Bal'ad soils. The high pH values and low LOI values are consistent with the calcareous and coarse textured nature of these soils. The LOI measurements may overestimate the organic matter content of the soils therefore the TOC and TIC were also determined. The mean values of TIC and TOC were 2.0% ±1.0 and 1.1%±0.4 respectively; the TIC content was approximately 60% of the total soil carbon. The four major exchangeable cations were calcium (Ca), magnesium (Mg), potassium (K), and sodium (Na) accounting for 82%, 12%, 5%, and 1% of the cation exchange capacity (CEC) respectively. The mean total exchangeable cation (Ca, Mg, K and Na) concentration was (53 cmolc kg^{-1}); the highest value of exchangeable Ca was recorded in a soil sample collected from a farm in Bulo-Burte (128.0 cmolc kg^{-1} ±4.30). However, almost certainly the 'exchangeable' Ca concentration was exaggerated by dissolution of $CaCO_3$ as these concentrations of (apparently) exchangeable Ca exceed the CEC of most 2:1 aluminosilicate clays.

Table 4.1. General characteristics of the twelve study soils (mean and coefficient of variation, or CV). Triplicate technical replications are used except for the pH measurements where duplicate measurement is used. Total concentrations of Zn (Zn_{Tot}), Se (Se_{Tot}) and I (I_{TMAH}) are in units of mg kg^{-1}).

Site/ Land use		**Codes**	**pH**	**LOI**	**TIC**	**TOC**	**Exchangeable cations**				**Zn_{Tot}**	**Se_{Tot}**	**I_{TMAH}**
				(%)	**(%)**	**(%)**	**(cmolc kg^{-1})**						
							Na	Mg	K	Ca			
Beletweyn	Rainfed	BW-R	8.02	0.30	3.03	0.78	0.60	6.80	1.70	37.4	65.0	351	2860
Beletweyn	Irrigated	BW-I	8.14	0.21	2.96	0.79	0.40	4.10	1.40	28.0	51.6	300	2120
Buloburte	Rainfed	BB-R	8.23	0.22	3.31	0.78	0.10	4.30	1.90	30.4	47.5	318	5300
Buloburte	Irrigated	BB-I	7.87	0.26	2.30	0.65	0.70	2.80	1.50	128	46.5	332	3890
Jowhar	Rainfed	JH-R	7.95	0.26	2.08	1.50	0.30	5.70	3.10	30.6	58.9	439	3830
Jowhar	Irrigated	JH-I	8.06	0.29	2.79	1.39	0.60	6.60	2.30	35.3	57.5	381	4800
Bal'ad	Rainfed	BA-R	8.41	0.18	0.87	0.73	0.10	2.60	1.40	22.3	33.4	359	1890
Bal'ad	Irrigated	BA-I	8.07	0.35	1.31	1.39	1.50	4.30	4.70	34.5	112	434	5890
Afgoi	Rainfed	AF-R	8.18	0.28	2.21	1.02	0.40	6.40	2.20	38.5	65.9	439	5310
Afgoi	Irrigated	AF-I	8.11	0.50	2.18	1.15	0.90	6.60	2.10	38.9	67.5	396	6140
Baidoa	Rainfed	BD-R	8.13	1.00	0.48	1.64	2.50	8.90	1.20	50.8	29.7	517	7210
Baidoa	Irrigated	BD-I	8.04	0.78	0.26	1.12	0.40	6.80	0.80	56.1	27.1	516	7740
CV (%)			1.70	64.3	51.3	35.6	93.5	32.5	50.1	61.4	40	18	40

4.3.2. Multi-elemental analysis

The acid digests of all the soil samples were analysed for multi-elements by ICP-MS. This was to examine possible relationships between the chemical constituents of the soils and soil Se and iodine concentrations and also to assess whether the soils from the different land use systems (i.e. rainfed and irrigated lands) varied in terms of elemental composition. As quality control measures, triplicate analysis were undertaken and a soil certified reference material (Montana II Soil, 2711a) was analysed for which the mean elemental recoveries ranged from 70% to 105% (Table 4.2).

The Ca concentration in these soils originates from calcium carbonate (calcite) and calcium sulfate (gypsum), which occur in arid and calcareous soils (Bolan et al., 2005). In particular, these soils are characterised by high calcite contents. The average total Ca concentration (Ca_{Tot}) was 67,500 mg kg^{-1} (the range was 15,400 – 103,000 mg kg^{-1}; the concentration was highest in soils from

Bulo-Burta (BB), followed by Belet-Weyn (BW), Johar (JH), Afgoi, Baidoa (BD) and Bal'ad (BA).

In the Shabelle valley and Baidoa soil samples, aluminium and iron were the second and third most abundant cations, their averages were 45,800 mg kg^{-1} and 39,800 mg kg^{-1} respectively. Potassium was the fourth most abundant cation; mean K_{Tot} concentration was 11,900 mg kg^{-1}; the range was 1,430 mg kg^{-1} – 18,000 mg kg^{-1}; as also found for Ca_{Tot}, K_{Tot} was highest in soils from Belet-Weyn (BW) and Bulo-Burta (BB), while soils from Baidoa (BD) and Bal'ad (BA) had the lowest K concentration. Magnesium was the fifth most abundant cation, in the range of 5,640 mg kg^{-1} – 13,900 mg kg^{-1}, with an arithmetic mean of 10,700 mg kg^{-1}; Mg_{Tot} was highest in soils from Belet-Weyn (BW) and Bulo-Burta (BB), while soils from Baidoa (BD) and Bal'ad (BA) had the lowest Mg concentration. In general, the cations in the Somali agricultural soil samples followed the order Ca_{Tot} (mean: 67,500 mg kg^{-1}) > Al_{Tot} (mean: 45,800 mg kg^{-1}) > Fe_{Tot} (mean: 39,800 mg kg^{-1}) > K_{Tot} (mean: 11,900 mg kg^{-1}) > Mg_{Tot} (mean: 10,700 mg kg^{-1}) > Na_{Tot} (mean: 1,820 mg kg^{-1}) > Ti_{Tot} (mean: 1,600 mg kg^{-1}) > Mn_{Tot} (mean: 790 mg kg^{-1}) > P_{Tot} (mean: 546 mg kg^{-1}) > Ba_{Tot} (mean: 267 mg kg^{-1}) > Sr_{Tot} (mean: 243 mg kg^{-1}). In general, the multi-elemental contents of the soils may be categorized into (i) major nutrients; (ii) minor nutrients; (iii) potentially toxic elements and (iv) structural elements and are depicted in Figures 4.1 ─ 4.4.

The concentrations of these elements in the soils are related to several factors, such as geographic location, type of rock, pH, nature of drainage water, clay content, cation exchange capacity, weathering and climatic conditions (Dávila et al., 1999; Jo and Koh, 2004; Materechera, 1999; Pombo, 1995; Scheuner et al., 2004; Shallari et al., 1998; Yanai et al., 2005; Young et al., 1988).

Table 4.2. Validation of the HF digestion method. Triplicate samples of certified reference material (NIST SRM 2711a Montana II Soil) were HF digested and analyzed by ICP-MS.

Element	Accredited values ($mg\ kg^{-1}$)	Mean measured values ($mg\ kg^{-1}$)	Recovery (%)
Na	12000	10500	88
Mg	10700	7780	72
P	842	804	95
K	25300	22460	89
Ca	24200	19700	82
Al	67200	45100	67
V	80.7	68.0	84
Cr	52.3	35.9	69
Mn	675	548	81
Fe	28200	23500	83
Co	9.89	7.97	81
Ni	21.7	17.6	81
Cu	140	108	77
Zn	414	388	94
As	107	98.5	92
Se	2.00	1.75	88
Rb	120	90.0	75
Sr	242	199	82
Ag	6	5.61	93
Cd	54.1	56.6	105
Cs	6.7	5.61	84
Ba	730	731	100
Tl	3	2.42	81
U	3.01	2.21	74

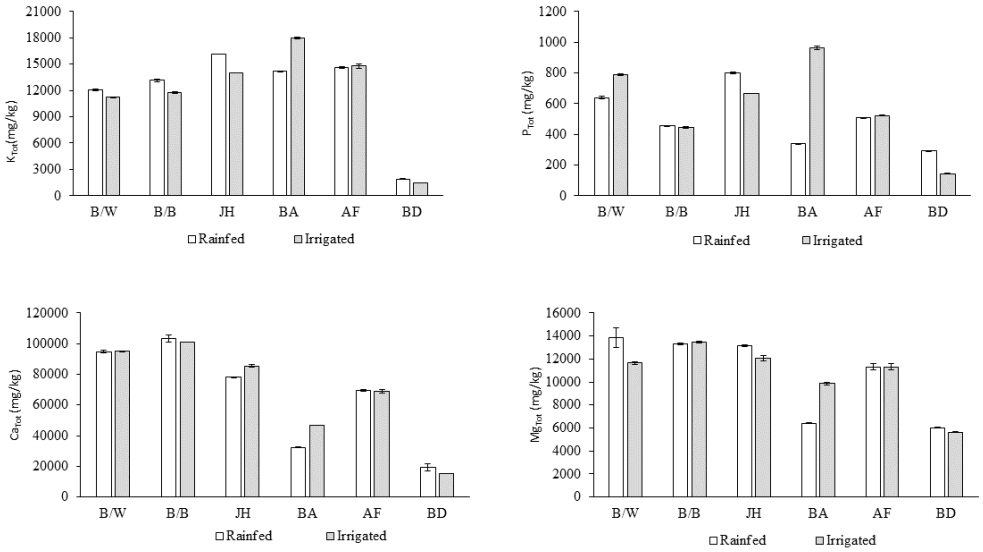


Figure 4.1. Major nutrients (Ca_{Tot}, K_{Tot}, Mg_{Tot}) of the soil root zone as determined by ICP analysis after HF digestion. Each bar represents the mean and corresponding standard error; n = 12; each value of the 12 is the mean of 3 replications. Rainfed (white), irrigated (grey); the soil codes are described in Table 4.1.

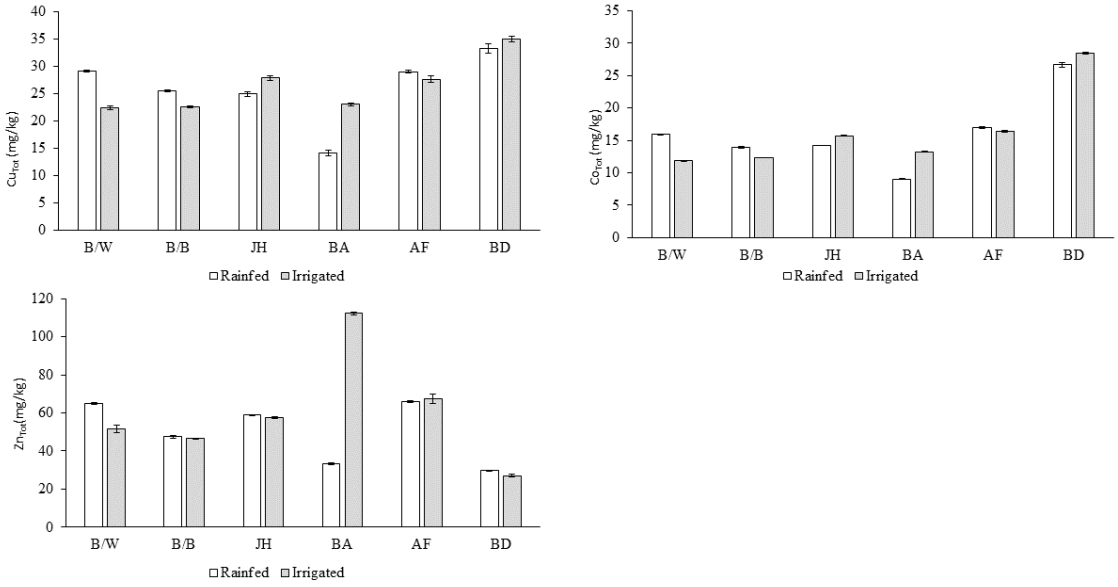


Figure 4.2. Minor plant nutrients (Cu_{Tot}, Co_{Tot}, Zn_{Tot}) of the soil root zone as determined by ICP analysis after HF digestion. Each bar represents the mean and corresponding standard error; n = 12; each value of the 12 is the mean of 3 replicates. Rainfed (white), irrigated (grey); the soil codes are described in Table 4.1.

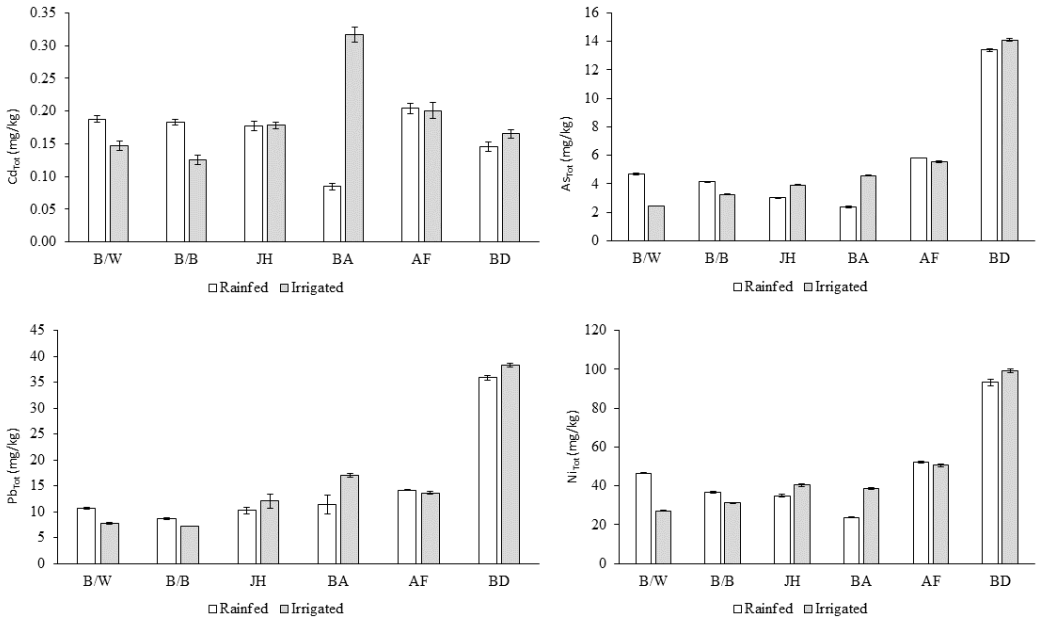


Figure 4.3. Potentially toxic elements (Cd_{Tot}, Pb_{Tot}, As_{Tot} and Ni_{Tot}) of the soil root zone as determined by ICP analysis after HF digestion. Each bar represents the mean and corresponding standard error; n = 12; each value of the 12 is the mean of 3 replicates. Rainfed (white), irrigated (grey); the soil codes are described in Table 4.1.

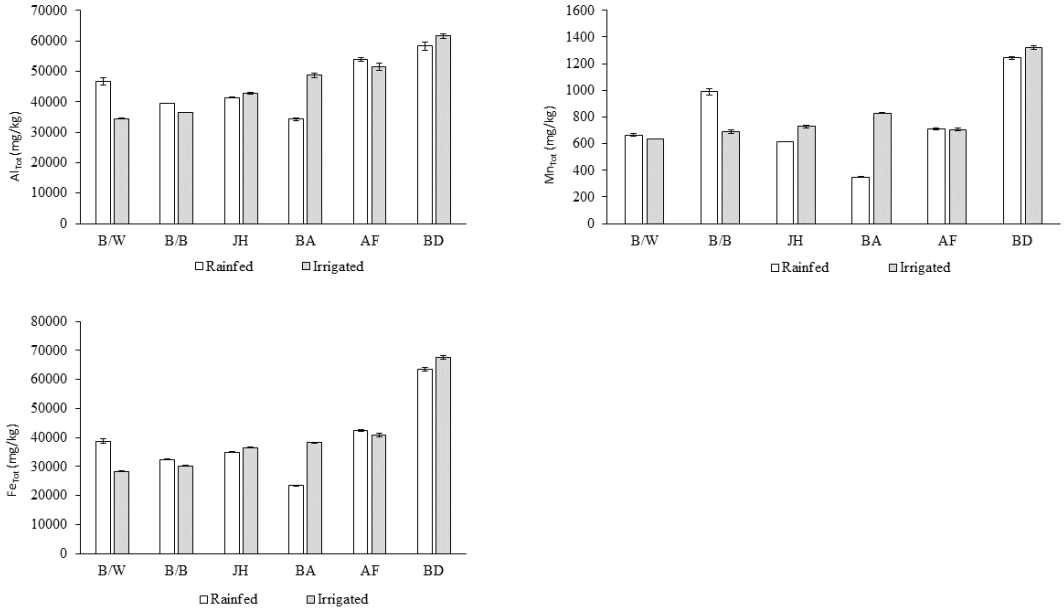


Figure 4.4. Structural elements (Al_{Tot}, Fe_{Tot} and Mn_{Tot}) of the soil root zone as determined by ICP analysis after HF digestion. Each bar represents the mean and corresponding standard error; n = 12; each value of the 12 is the mean of 3 replicates. Rainfed (white), irrigated (grey); the soil codes are described in Table 4.1.

4.3.3. Selenium

4.3.3.1. Total Se concentration (Se_{Tot})

Total Se concentration (Se_{Tot}) in the soil samples varied from 300 to 520 µg kg^{-1}, with an arithmetic mean of (400 µg kg^{-1}), the highest Se concentration was found in soils from Baidoa, Bay region (Fig. 4.5). The Se_{Tot} in samples from Beletweyn and Buloburte were 25% below the world average, however soils from Baidoa were 30% higher in Se than the world average. The average Se_{Tot} of 400 µg kg^{-1} is comparable to the Se content of UK soils (<1000 µg Se kg^{-1}) and identical to the world mean of 400 µg kg^{-1}, but is slightly higher than that of Malawi (190 µg kg^{-1}) or Finnish soils (10 µg kg^{-1}) (Broadley et al., 2006; Chilimba et al., 2011; Fordyce, 2005; Fordyce, 2013) According to Fordyce (2005), soils that have concentrations of Se < 600 µg kg^{-1} are considered Se deficient. Similarly, Gupta and Gupta (2002) reported that in general, a soil with less than 600 µg kg^{-1} of Se is considered Se-deficient. All the soil samples from the 12 agricultural sites contained less than 600 µg kg^{-1} Se; more than 50% of the measured soils contained less than 400 µg Se kg^{-1}. This indicates that agricultural soils in southern Somalia may be prone to problems related to Se deficiency in agricultural produce. The soils with the highest Se_{Tot} (i.e. >400 µg kg^{-1}) were typically characterized by a large organic matter content.

Correlation analysis was performed to attempt identification of the main soil factors influencing Se_{Tot}. Soil organic matter showed a strong correlation with Se_{Tot} whether expressed as LOI (R^2= 0.628; $p < 0.001$) or as TOC (R^2= 0.400; $p < 0.001$); Fig. 4.6 shows the relationship between LOI and Se_{Tot}. The presence of Se mainly in organically bound forms was also suggested by a very strong correlation between Se_{Tot} (HF digest) and Se_{TMAH} (r=0.901), although Fe_{Tot} and Al_{Tot} also showed a strong correlation with Se_{Tot}, (R^2= 0.742; $p < 0.001$ and R^2= 0.751; $p < 0.001$ respectively). By contrast, negative correlations were found between Se_{Tot} and TIC (r = -0.761), soil pH (r = -0.137) and Ca_{Tot} (r = -0.793) suggesting that calcareous conditions were not associated with Se sources or retention in the Somali soils. Availability, rather than total concentration, of Se in the soil is the key indicator of Se bioavailability to plants (Fordyce, 2013). Thus, Se fractionation and speciation were performed; methods are described in detail in Section 4.1.2.2.

Figure 4.7 shows a histogram of Se_{Tot}; it was found that the Se_{Tot} was not normally distributed according to the Anderson-Darling Normality Test (P value < 0.05). In order to see the effect of the land use (rainfed and irrigated systems) a paired T-test analysis was performed (Table 4.3);

there was no significant difference between the two systems (P value = 0.376). However, an ANOVA was also conducted to compare the Se concentrations of the regions, there was a significant effect of sampling location (i.e. area) on the Se content [F5, 30 = 40.07, P < 0.0005]. Pairwise comparisons between groups were assessed using Tukey's post-hoc test. Tukey Pairwise Comparisons showed that Se_{Tot} was in the following order BD> AF, JH, BA>BW and BB.

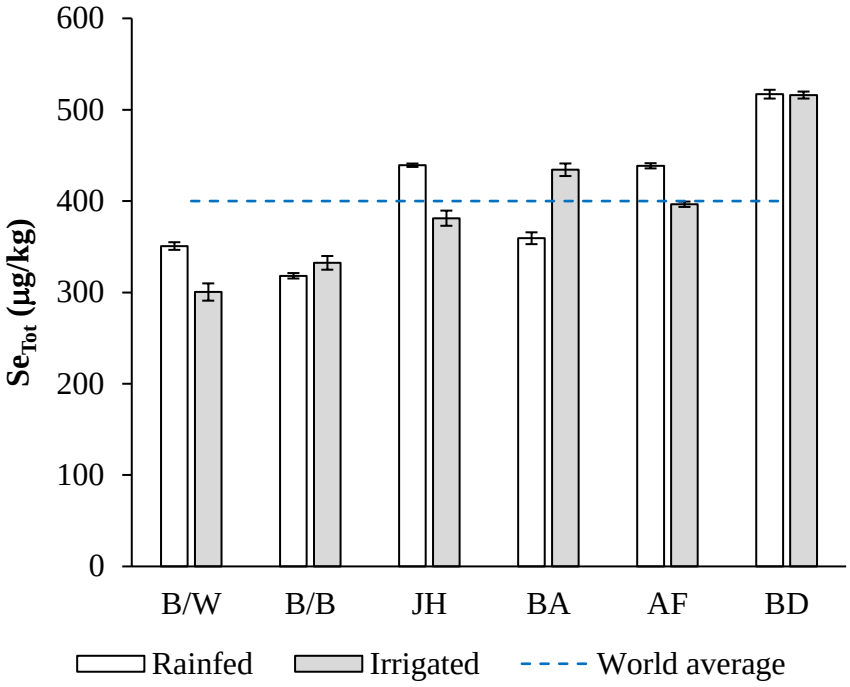


Figure 4.5. Total Se concentrations (Se_{Tot}) in Somali agricultural soils as determined by ICP analysis after HF digestion. Each bar represents the mean and corresponding standard error; n = 12; each value of the 12 is the mean of 3 replicates. Rainfed (white), irrigated (grey); the soil codes are described in Table 4.1.

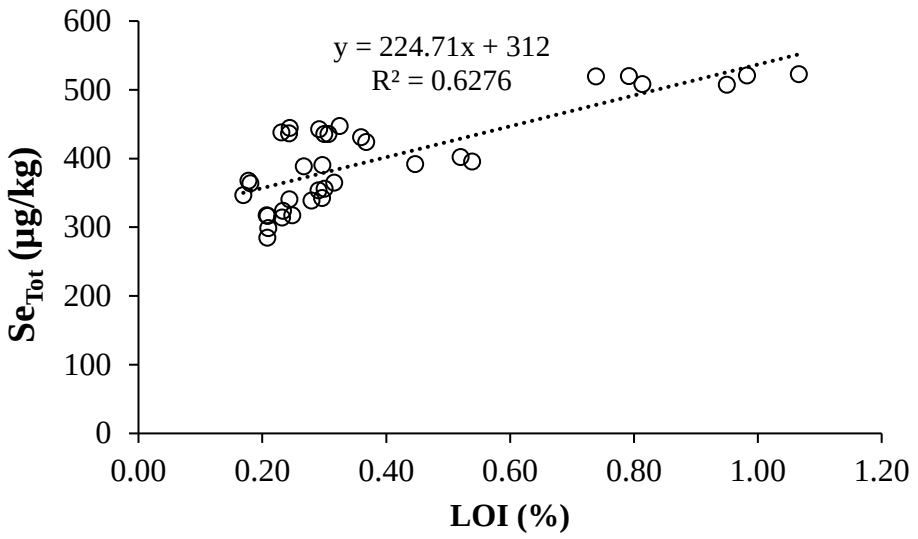


Figure 4.6. Relationship between loss on ignition (representing soil organic matter content) and total selenium (Se_{Tot}) in agricultural soil samples from south Somalia.

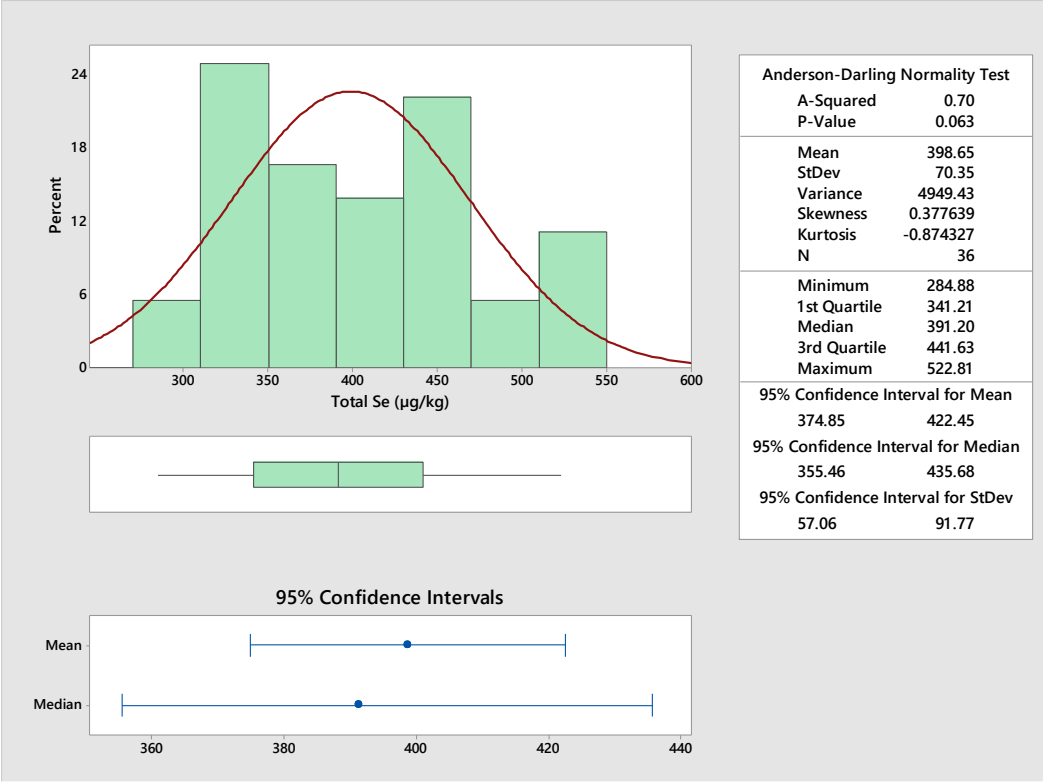


Figure 4.7. Histogram illustrating distribution of total selenium concentration in agricultural soil samples from south Somalia. The assessment of the compatibility of fitted distributions was made using the Anderson–Darling (A–D) test for the significance level of $\alpha = 0.05$.

Table 4.3. Comparison between the total Se concentrations (mg kg^{-1}) of rainfed and irrigated soils; a T-test was used to test for differences between the two land uses.

Land use	Number of samples	Mean	SD	SE
Rainfed	18	0.4038	0.0698	0.0165
Irrigated	18	0.3935	0.0725	0.0171
P-Value = 0.376				

4.3.3.2. Se fractionation and speciation

- Soluble Se (0.01 M KNO_3)

Concentrations of Se in the 0.01 M KNO_3 extraction (Se_{Sol}) were low, 2.00 to 5.00 µg kg^{-1} in the rainfed soils and 2.00 to 4.00 µg kg^{-1} in the irrigated soils (Table 4.4), with an arithmetic mean of 3.67 and 3.17 µg kg^{-1} for the rainfed and irrigated fields respectively. In general, the concentrations of Se_{Sol} accounted for less than 1.00% of Se_{Tot}, ranging from 0.48 to 1.51 %. The percent Se_{Sol} differed significantly ($p<0.05$) between sampling regions and Se_{Sol} was not correlated with Se_{Tot}. The Se_{Tot} from Baidoa region was 520 µg kg^{-1}; 30% higher than the mean Se_{Tot} (i.e. 400 µg kg^{-1}) in the Somali soil samples, however the Se_{Sol} fraction was only 3 µg kg^{-1}, representing 0.5% of the Se_{Tot}. The majority (70% of the Se_{Tot}) in Baidoa soils were bound to the organic matter as revealed by the TMAH extraction.

Selenium speciation was also performed for Se_{Sol} and Se_{Ads}. The speciation analysis showed that the inorganic soluble Se ($Se_{Sol\text{-}Inorg}$) varied from 31.2% to 66.9% of the total Se_{Sol} with an arithmetic mean of 50.7%, while the soluble organic Se ($Se_{Sol\text{-}Org}$) varied from 33.1% to 68.8, with an arithmetic mean of 49.3%. The $Se_{Sol\text{-}Inorg}$ contained both inorganic Se species i.e. 26% selenate (Se^{VI}) and 24% selenite (Se^{IV}). Table 4.4 summarizes the Se speciation in the soluble fraction and the proportion of the inorganic and organic Se. The soluble Se data was not normally distributed, the P-Value of the Anderson-Darling Normality Test was < 0.05, (Fig. 4. 8).

Table 4.4. Speciation of selenium in the soluble fraction (Se_{Sol}) and proportion of organic and inorganic Se in Se_{Sol}. Concentrations are given in µg kg^{-1}; proportions are expressed as percentages. Data are means ± standard deviation for each measured parameter.

Soil	Land use	Se_{Sol} (Total)	$Se_{Sol(IV)}$ (selenite)	$Se_{Sol(VI)}$ (selenate)	$Se_{Sol(IV)}$ (selenite)	$Se_{Sol(VI)}$ (selenate)	$Se_{Sol-Inorg}$	$Se_{Sol-Org}$
		µg kg^{-1}	µg kg^{-1}	µg kg^{-1}	%	%	%	%
BW-R	Rainfed	5.06	0.25	3.13	5.00	61.9	66.9	33.1
BW-I	Irrigated	3.04	0.46	0.93	15.3	30.6	45.9	54.1
BB-R	Rainfed	1.76	0.47	0.41	26.7	23.2	49.8	50.2
BB-I	Irrigated	3.91	0.76	0.86	19.3	22.0	41.3	58.7
JH-R	Rainfed	5.45	2.19	1.06	40.3	19.4	59.7	40.3
JH-I	Irrigated	3.65	0.67	1.56	18.3	42.8	61.1	38.9
BA-R	Rainfed	3.86	2.05	0.41	53.2	10.5	63.7	36.3
BA-I	Irrigated	2.14	0.63	0.16	29.7	7.43	37.1	62.9
AF-R	Rainfed	3.17	1.04	0.78	32.8	24.4	57.2	42.8
AF-I	Irrigated	2.59	0.70	0.48	27.1	18.6	45.7	54.3
BD-R	Rainfed	2.70	0.33	0.51	12.3	18.8	31.2	68.8
BD-I	Irrigated	2.63	0.33	0.94	12.4	35.7	48.2	51.8

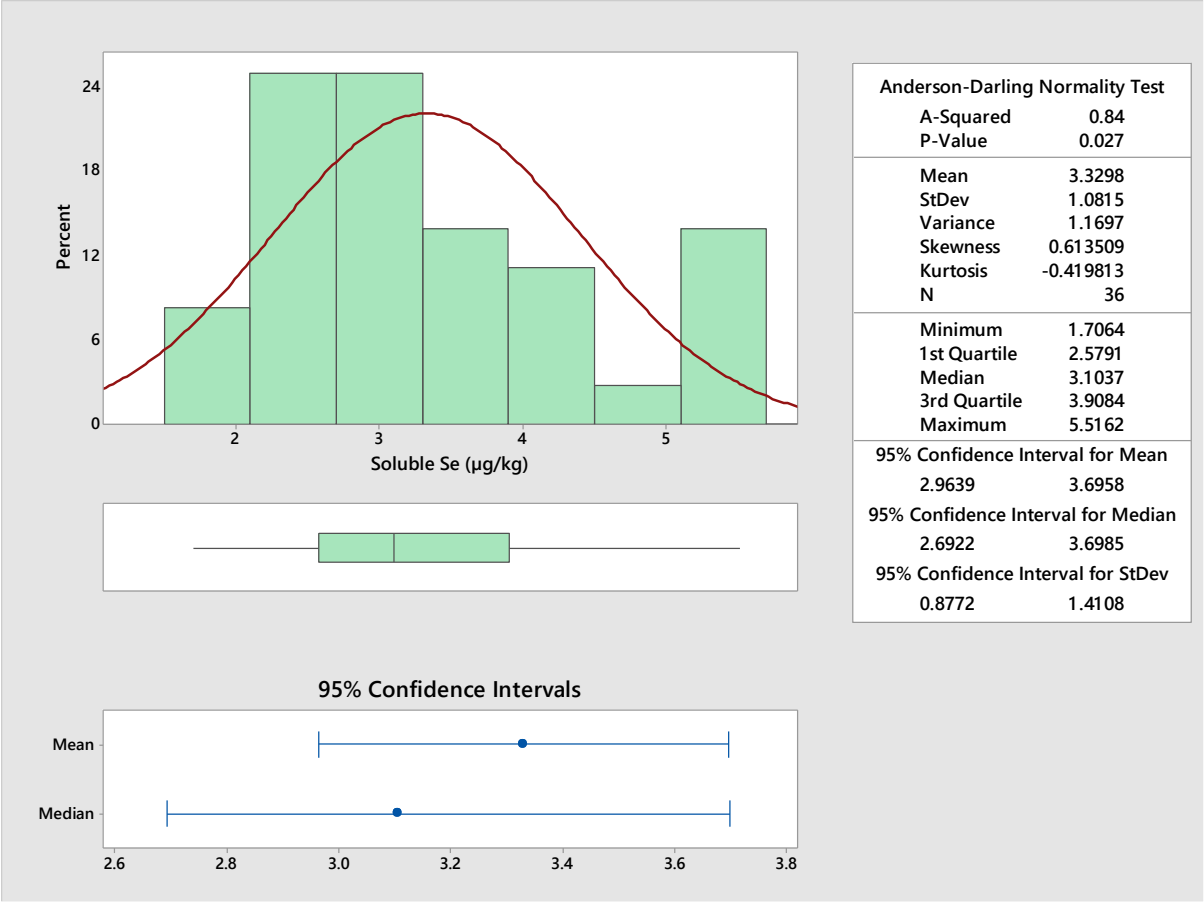


Figure 4.8. Histogram illustrating the distribution of soluble Se (Se_{Sol}) concentration in agricultural soil samples from south Somalia. The assessment of the compatibility of fitted distributions was made using the Anderson–Darling (A–D) test for the significance level of $\alpha = 0.05$.

Figure 4.9 shows the correlation of $Se_{Sol(IV)}$, $Se_{Sol(VI)}$ and organically associated Se in the Se_{Sol} and the (total) Se_{Sol}. There was a relatively stronger correlation between $Se_{Sol(VI)}$ and Se_{Sol} as compared with $Se_{Sol(IV)}$. Correlations were also used to test for a relationship between Se concentrations in the groundwater and surface water and the soluble soil Se (Se_{Sol}); Figure 4.10 shows that there was no significant relationship. The data shows that whereas the Se_{Sol} probably depends on local soil properties, and varies between soils, the concentration of Se in the water samples was much more spatially conservative by comparison.

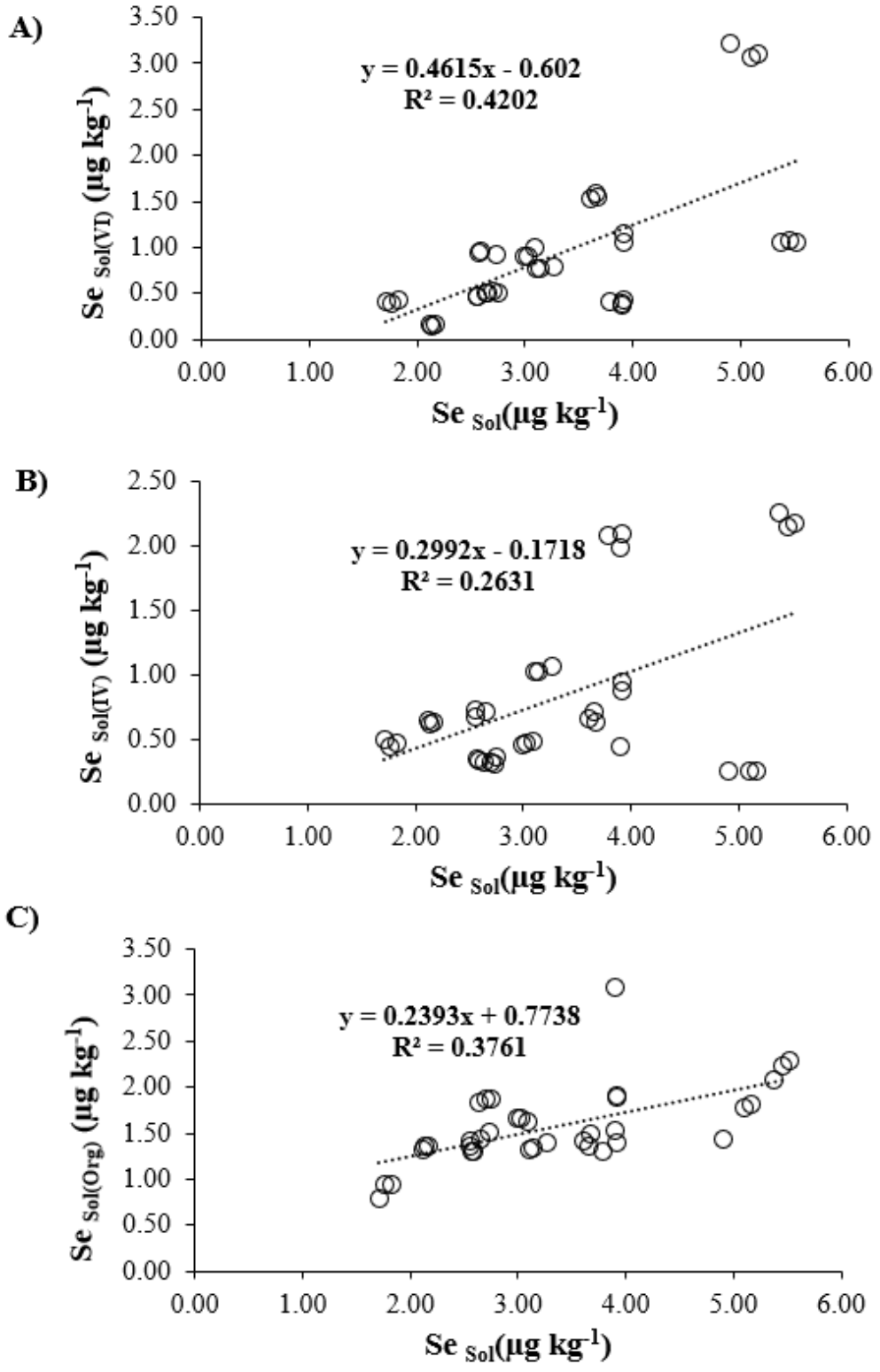


Figure 4.9. Scatterplot showing relationship between soluble selenium speciation a) selenate; b) selenite, and c) organic-Se and total soluble selenium (Se_{Sol}; µg kg^{-1}) in agricultural soil samples of south Somalia.

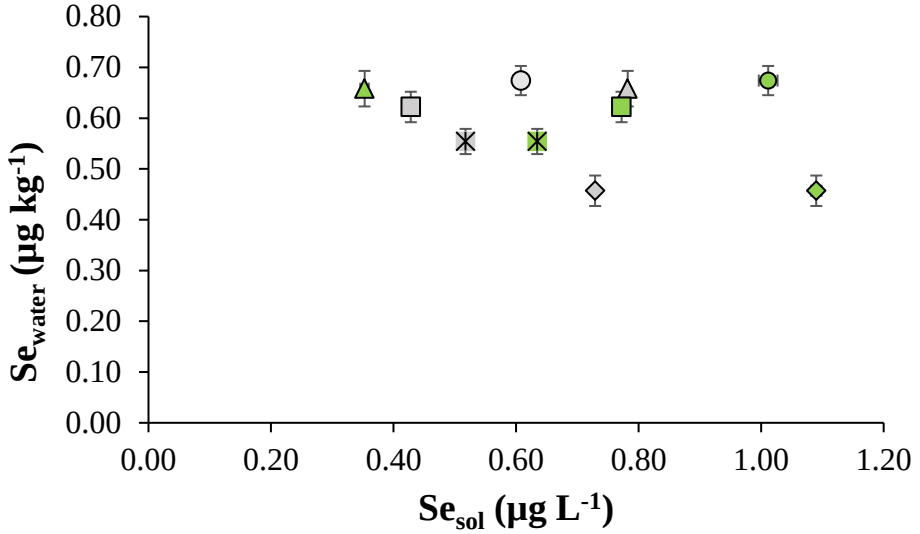


Figure 4.10. Correlation between Se in water samples (Se_{water}) and the soluble soil Se fraction (Se_{Sol}). Values of Sewater are averages for each region whereas soil data are the averages for both rainfed and irrigated soils; the circle, triangle, diamond, square and asterisk represent averages for Belet weyn, Bulo Burte, Jowhar, Balad and Afgoi respectively. Green colour represents rainfed sites and grey colour for irrigated sites.

In order to identify the main factors determining Se_{Sol} a correlation analysis was performed with soil properties. There was a weak negative correlation with pH ($r = -0.355$; P-Value < 0.05) and the soil organic matter content. ($r = -0.330$). This was consistent with the negative correlation seen between DOC and the Se concentration in groundwater and surface water samples (reported in Chapter 3). A positive correlation between organic matter and Se_{Tot} is expected if Se was being accumulated in humus but it might also be expected that the solubility of Se would be low in soils with a high organic matter content due to strong adsorption. A positive and weak correlation between the Se_{Sol} and the TIC ($r=0.177$), Mg ($r=0.348$) and Ca ($r=0.262$) was also seen.

- Adsorbed Se (0.016M KH_2PO_4)

Selenium in the adsorbed fraction was also measured, this fraction can be regarded as 'readily bioavailable' Se (or 'ligand-exchangeable') and possible originates from Se bound to Fe/Al oxides. The concentrations of the adsorbed Se (Se_{Ads}) accounted, on average, for 2.99% of the Se_{Tot},

ranging from 1.3 to 5.3%. Concentrations of the Se_{Ads} fraction were 3-fold higher than those of Se_{Sol}. Concentrations of extractable Se in UK agricultural soils were reported by Stroud et al., (2010), who found low extractable soil Se concentrations (2.4 –12.4 µg kg^{-1}). The Se_{Ads} in the Somali agricultural soils samples differed significantly ($P < 0.05$) between soils. For example, Se_{Ads} in soils from Jowhar were significantly ($P < 0.05$) greater than from other regions and accounted for 5% of the Se_{Tot}. As also seen for Se_{Sol}, the concentrations of Se_{Ads} in Baidoa soils were significantly lower from those from other regions, representing less than 2% of the Se_{Tot}.

Speciation of the adsorbed Se indicated that, on average, 71% of the Se_{Ads} was inorganic, while 29% was organic. The majority of the inorganic exchangeable Se was selenite; in fact, in most of the samples selenite was the only inorganic species measurable in the $Se_{Ads.}$ This finding confirms experimentally the literature view that Se^{VI} is more mobile than Se^{IV}; selenite tends to bond more strongly than selenate with amorphous Fe and Al oxides. Other similar studies that reported the magnitude of Se^{IV} sorption include that of Supriatin (2016) who carried out ammonium oxalate extraction on soils and found that inorganic Se was mainly present as Se^{IV} while Se^{VI} was not measurable. On average the sum of the Se_{Sol} and Se_{Ads} accounted for just 4% of the Se_{Tot}. Speciation of selenium in the adsorbed fraction is summarized in Table 4.5.

Table 4.5. Speciation of selenium in the adsorbed fraction and proportions of organic and inorganic Se. Concentrations are given in µg kg^{-1}; proportions are expressed as percentages. Data are means ± standard deviation for each measured parameter.

Soil	Land use	Se_{Ads}	$Se_{(IV)-Ads}$	$Se_{(VI)-Ads}$	$Se_{(IV)-Ads}$	$Se_{(VI)-Ads}$	Inorg	Org
		µg kg^{-1}	µg kg^{-1}	µg kg^{-1}	%	%	%	%
BW-R	Rainfed	4.74	2.77	0.28	58.5	5.85	64.4	35.6
BW-I	Irrigated	6.77	4.60	0.06	67.9	0.89	68.8	31.3
BB-R	Rainfed	7.45	5.46	0.00	73.2	0.00	73.2	26.8
BB-I	Irrigated	12.9	8.74	0.17	67.7	1.34	69.0	31.0
JH-R	Rainfed	22.9	17.4	0.00	76.0	0.00	76.0	24.0
JH-I	Irrigated	11.1	8.02	0.14	72.1	1.26	73.3	26.7
BA-R	Rainfed	17.5	13.1	0.00	74.9	0.00	74.9	25.1
BA-I	Irrigated	8.26	5.68	0.00	68.7	0.00	68.7	31.3
AF-R	Rainfed	19.5	14.8	0.00	76.0	0.00	76.0	24.0
AF-I	Irrigated	12.6	9.30	0.00	73.8	0.00	73.8	26.2
BD-R	Rainfed	8.22	5.15	0.05	62.6	0.61	63.2	36.7
BD-I	Irrigated	9.55	7.04	0.12	73.7	1.26	75.0	25.1

In order to identify the main factors influencing Se_{Ads}, Pearson correlation coefficients were determined. The Se_{Ads} data showed only a weak, non-significant negative correlation with both the soil organic matter content (R=-0.266) and the TIC (r=-0.157). A test for normality of the measured Se_{Ads} was conducted fig. 4.11, the data was not normally distributed P<0.005.

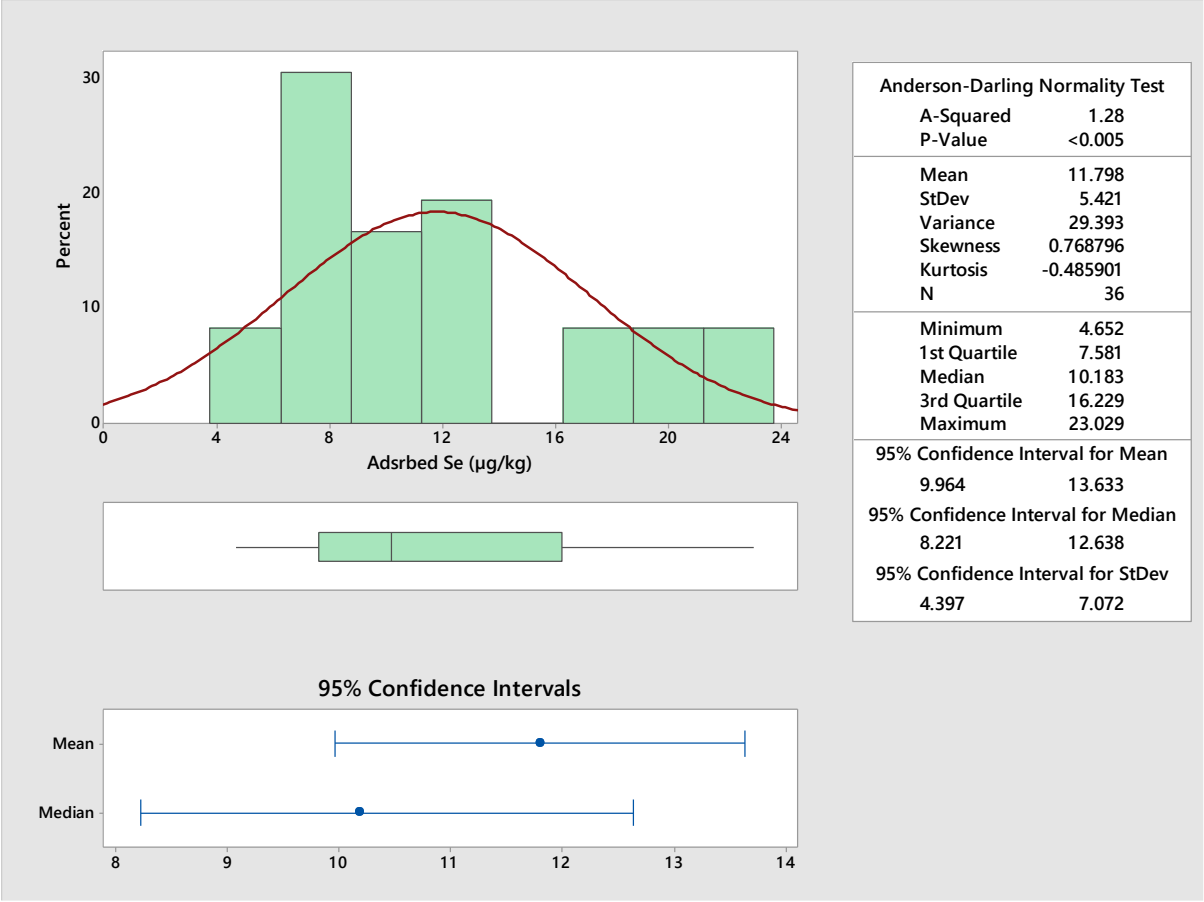


Figure 4.11. Normality test of the distribution of the adsorbed Se (Se_{Ads}) concentration in agricultural soil samples from south Somalia. Assessment of the compatibility of fitted distributions was made using the Anderson–Darling (A–D) test for a significance level of $\alpha = 0.05$.

- Organically bound Se, extractable with TMAH (Se_{TMAH})

On average, concentrations of organic matter bound Se (Se_{TMAH}) were tenfold greater than Se_{Sol} and Se_{Ads} fractions combined but still only accounted for 40% of the Se_{Tot}. Values of Se_{TMAH} also significantly differed between soils ($P < 0.05$). For example, Se_{TMAH} in soils from Baidoa (Bay region) were significantly ($P < 0.05$) greater than in other regions, accounting for 70% of the Se_{Tot}. On the other hand, Se_{TMAH} accounted for only 15% and 17% of the Se_{Tot} in samples from Beletweyn and Buloburte respectively.

The Se_{TMAH} was only weakly correlated with the soil pH (r=0.105) but the association with soil organic matter content was much stronger (r=0.844), which is supported by a positive correlation between the TOC and the Se_{TMAH} (r=0.529). There was also a negative and strong correlation between Se_{TMAH} and soil TIC (r=-0.877) and, as expected, with concentrations of Ca (r=-0.685) and Mg (-0.864). This supports the importance of soil organic matter in binding Se, as determined by TMAH extraction, and also suggests that calcite- or gypsum-bound Se is not extractable by TMAH. However, the aluminium and iron total concentration had positive and strong correlations with the Se_{TMAH}, r=0.732 (Al) and r=0.831 (Fe) respectively and the alkaline conditions of the TMAH extractant (pH 12) would be expected to solubilize oxide-bound selenite. Therefore, it is difficult to reach a definitive conclusion regarding the fractionation of Se in the soils sampled. In Fig 4.12 the normal distribution of the organically bound Se is presented and shows that the data was not normally distributed.

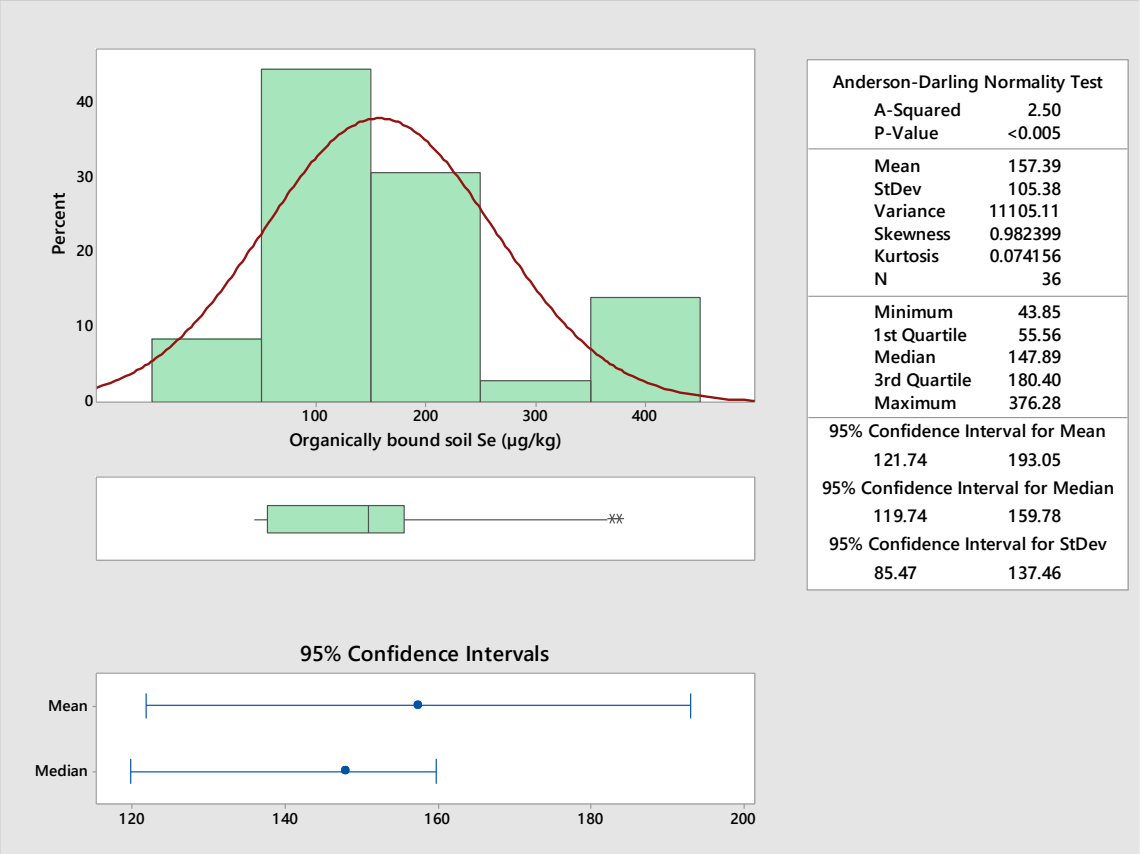


Figure 4.12. Normality test of the distribution of the organically bound Se (Se_{TMAH}) concentration in agricultural soil samples from south Somalia. The assessment of the compatibility of fitted distributions was made using the Anderson–Darling (A–D) test for the significance level of α = 0.05.

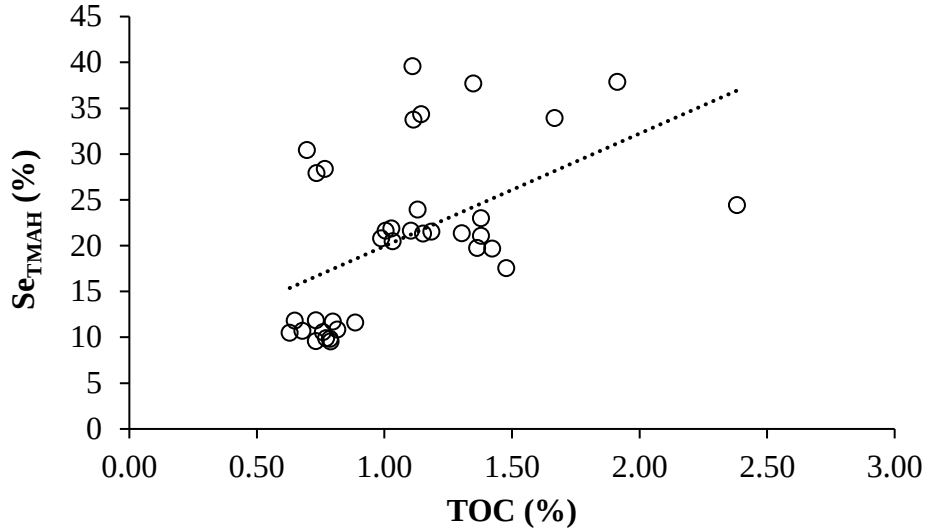


Figure 4.13. Scatter plot illustrating the relationship between the Se_{TMAH} (%) and total soil organic carbon (TOC; %).

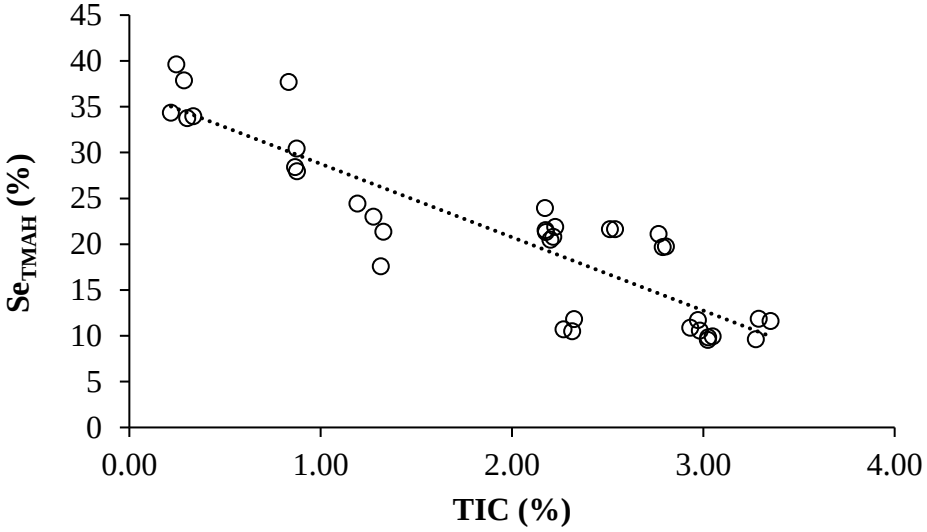


Figure 4.14. Scatter plot illustrating the relationship between the Se_{TMAH} (%) and total soil inorganic carbon (TIC; %).

- Residual Se

The residual Se ($Se_{Residue}$) was calculated by subtracting the Se_{Sol}, Se_{Ads} and Se_{TMAH} from the Se_{Tot}. Concentrations of $Se_{Residue}$ were generally greater than those of Se_{Sol}, Se_{Ads} and Se_{TMAH}. On average the $Se_{Residue}$ accounted for 60% of the Se_{Tot}. The $Se_{Residue}$ differed between soils and accounted for 80% of the Se_{Tot} in Belet-weyn and Buloburte and Jowhar but only 30% in the case of the Baidoa samples. There was a very strong relationship between Ca (mainly present as $CaCO_3$ or $CaSO_4$) and the $Se_{Residue}$ ($r = 0.801$). This indicates the importance of the carbonate minerals in containing $Se_{Residue}$, which means most of the selenium in the study soils probably existed as a carbonate-bound fraction which was not extractable with TMAH and therefore probably located within mineral matrices (Fig. 4.15).

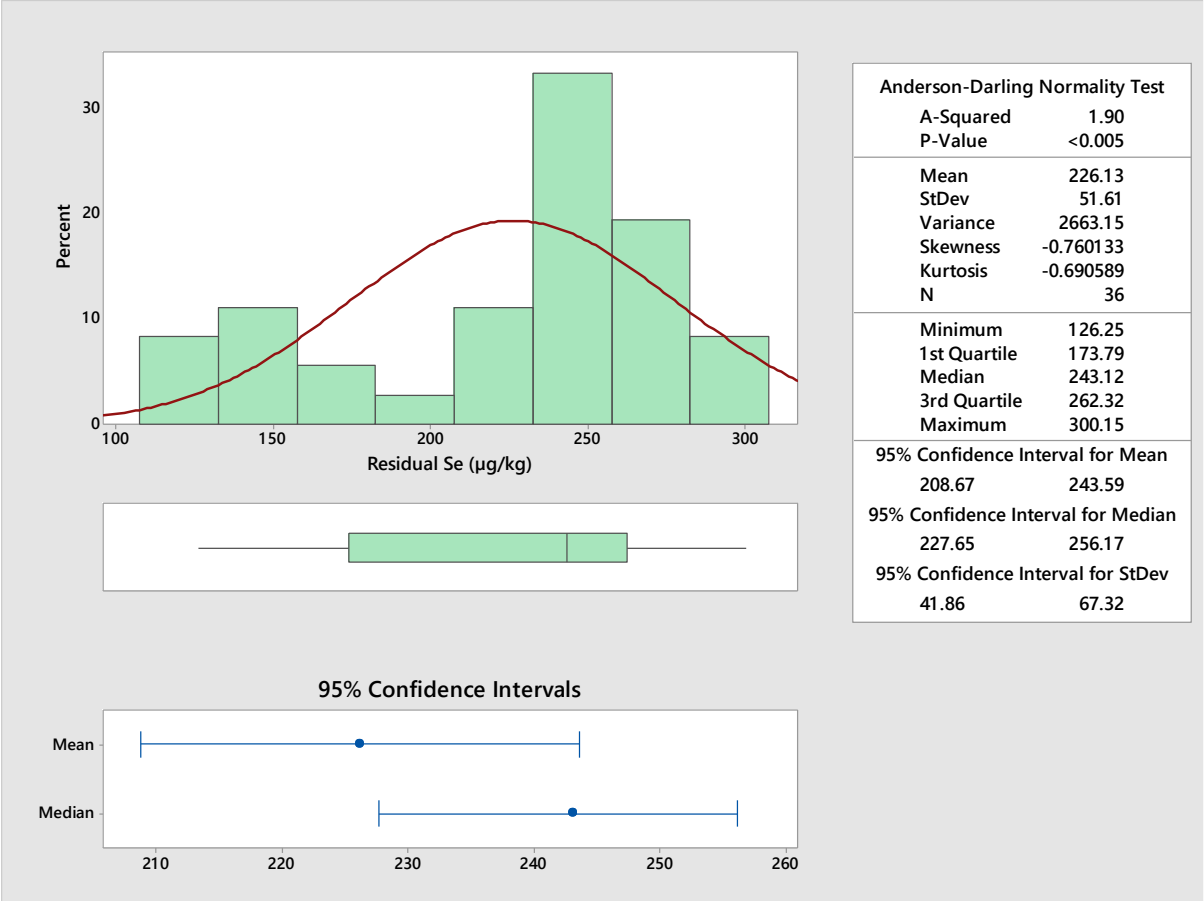


Figure 4.15. Histogram illustrating distribution of recalcitrant soil Se ($Se_{Residue}$) in agricultural soil samples from south Somalia. The assessment of the compatibility of fitted distributions was made using the Anderson–Darling (A–D) test for the significance level of $\alpha = 0.05$.

Possible relationships between soil Se and soil TOC and TIC properties have emerged. Fig. 4.13 shows that Se_{TMAH} had a weak correlation with % TOC but a strongly negative correlation with soil carbonate content (Fig. 4.14). Similarly, Fig. 4.16 shows a weak correlation between the ratio Se_{TMAH}: $S_{eResidue}$ and TOC. This suggests that Se_{TMAH} is mainly associated with the soil organic matter but the weak correlations underpinning this and the strong correlations between Fe/Al and Se_{TMAH} suggest that this Se fraction may be divided between humus and oxide minerals. In support of the trend shown in Fig. 4.14, the ratio Se_{TMAH}: $S_{eResidue}$ was strongly negatively correlated with the % TIC, (Fig. 4.17). These trends suggest that, whereas Se_{TMAH} may be divided between humus-bound and Fe/Al oxide-bound forms, $Se_{Residue}$ appears to be strongly associated with $CaCO_3$ in the Somali soils.

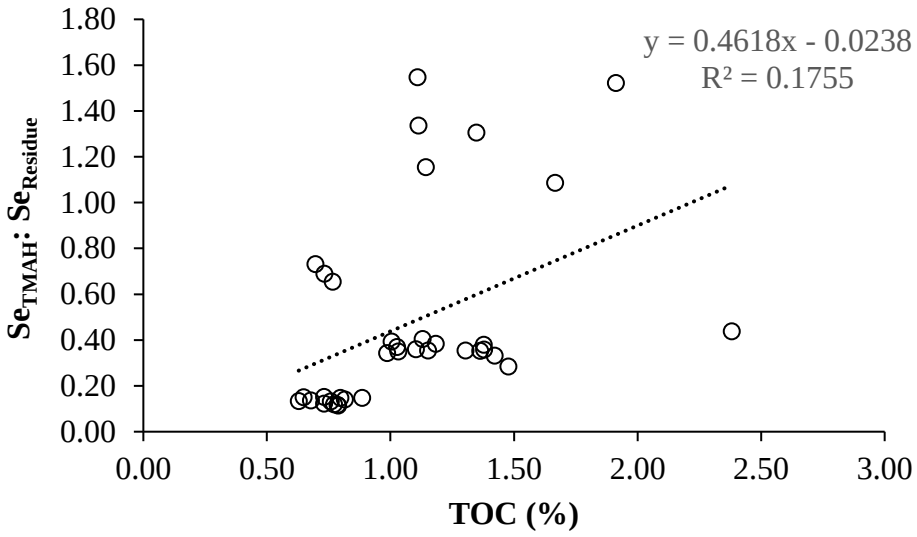


Figure 4.16. Scatter plot illustrating the relationship between soil organic carbon (TOC; %) and the ratio of Se_{TMAH}: $Se_{Residue}$.

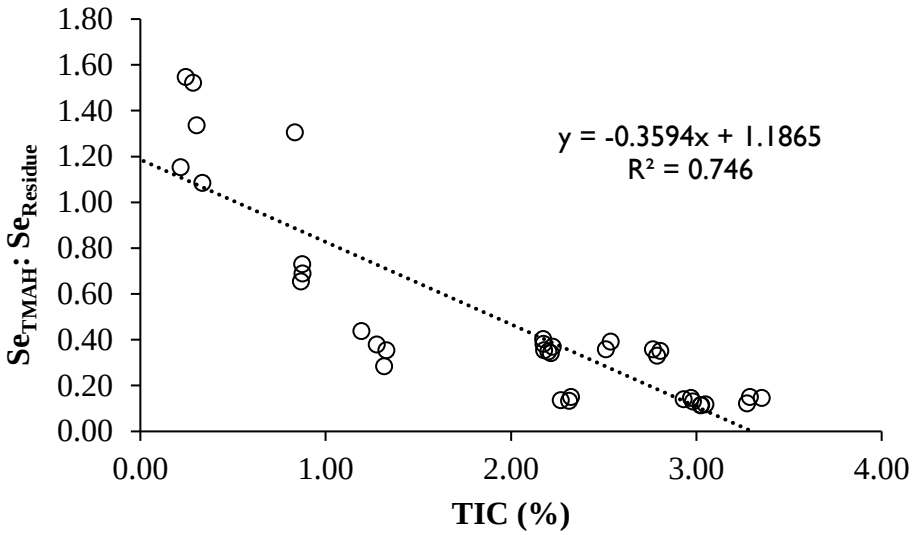


Figure 4.17. Scatter plot illustrating the relationship between soil organic carbon (TIC; %) and the ratio of Se_{TMAH}: $Se_{Residue}$.

Generally, the Se fractionation scheme has shown that selenium extractability in the different soils increased in the order of $Se_{Sol} < Se_{Ads} < Se_{TMAH} < Se_{Tot}$. The 0.01 M KNO_3 method extracted on mean 0.86% of the Se_{Tot}, this is similar to that reported by (Wang and Chen, 2003) and (Zhang and Moore, 1997). The 0.01 M KNO_3 extractable is also comparable to the water soluble fraction reported by (Kang et al., 1991; Séby et al., 1997). The fraction of Se extracted with 0.016 M KH_2PO_4 accounted on average for 2.99% of the Se_{Tot}, this extracts the exchangeable Se i.e. mainly inorganic Se adsorbed to soil mineral surfaces as a result of competition of phosphate for Se adsorption (Stroud et al., 2010). The Se_{Ads} is comparable to the findings of (Stroud et al., 2010). The Se fraction that is associated with the soil organic matter Se_{TMAH}, is higher than the two extractions accounting for 36.8%. Figure 4.18 and Table 4.6 summarize the distribution of Se fractions.

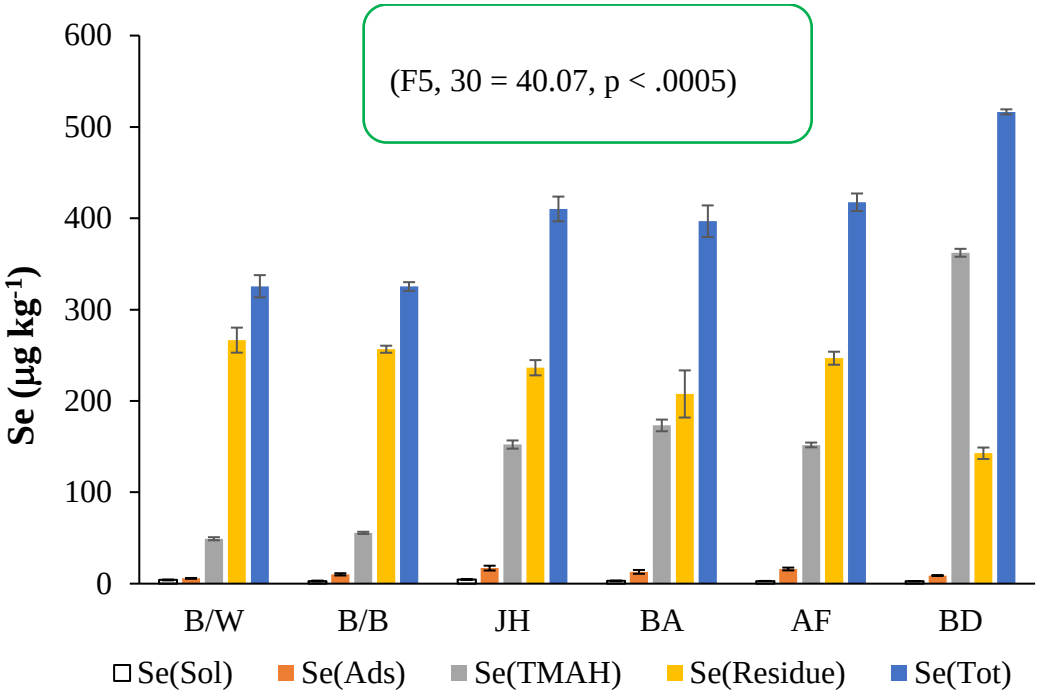


Figure 4.18. The mean concentration (µg kg^{-1}) of soluble, adsorbed, organically bound and total selenium measured in triplicate (± the standard error) is summarized for ease of comparison between these fractions. Data is produced after the sequential extraction for the soil samples and were determined by ICPMS (codes in Table 4.1).

Table 4.6. Selenium concentration (µg kg^{-1}) of the Somali Agricultural soil samples after a three-step sequential extraction. The operationally defined fractions include soluble Se, exchangeable Se, organic matter-bound Se, and the residual Se fraction. N=12; a is (rainfed soils) and b (irrigated soils).

	Sampling sites											
Fraction	BW^a	BW^b	BB^a	BB^b	JH^a	JH^b	BA^a	BA^b	AF^a	AF^b	BD^a	BD^b
Se_{Sol}	5.06	3.04	1.76	3.91	5.45	3.65	3.86	2.14	3.17	2.59	2.70	2.63
Se_{Ads}	4.74	6.77	7.45	12.9	22.9	11.1	17.5	8.26	19.5	12.6	8.22	9.56
Se_{TMAH}	45.8	52.5	57.8	53.4	160	144	187	159	155	149	359	365
$Se_{Residue}$	295	238	251	262	251	222	151	265	261	232	147	139
Se_{Tot}	351	300	318	332	439	381	359	434	439	396	517	516

BW: Beletweyn; BB: Buloburte; JH: (Jowhar); BA: Bal'ad; AF: Afgoi; BD: Baidoa; (a: rainfed; b: irrigated).

4.3.4. Iodine

4.3.4.1. Total iodine concentrations

The total iodine concentration (I_{Tot}) in the soil samples varied from 1.81 to 7.82 mg kg^{-1}, with an arithmetic mean of 4.75 mg kg^{-1}); the greatest I_{Tot} was found in soils from Baidoa, Bay region (Fig 4.19). The mean iodine concentration (4.75 mg kg^{-1}) is slightly greater than the worldwide geometric mean of 3.00 mg kg^{-1} (Johnson, 2003). Malawian and Pakistani soils with 2.06 mg kg^{-1} and 0.921 mg kg^{-1}, respectively, are substantially lower (Watts et al., 2015; Zia et al., 2015). A histogram showing the frequency distribution of the iodine concentration is presented in Fig. 4.20.

In order to investigate the soil factors controlling I_{Tot} correlation analyses were performed. Results were very similar to those for Se. I_{Tot} showed a positive correlation with the soil organic matter (% LOI) (r=0.772) and with total soil Se (Se_{Tot}; r=0.755) and Se_{TMAH} (r=0.684). There was also a positive correlation (r=0.505) between the TOC and I_{Tot}. As also found for Se, a negative correlation (r= -0.472) was found between the TIC and I_{Tot}. The data also showed a weak negative correlation between the pH and I_{Tot} and, similarly, the Ca_{Tot} concentrations were negatively correlated (r=-0.508) with I_{Tot}. Again, as for Se, total Fe and Al concentrations showed a strong correlation with I_{Tot} (r=0.834 and r=0.848 respectively).

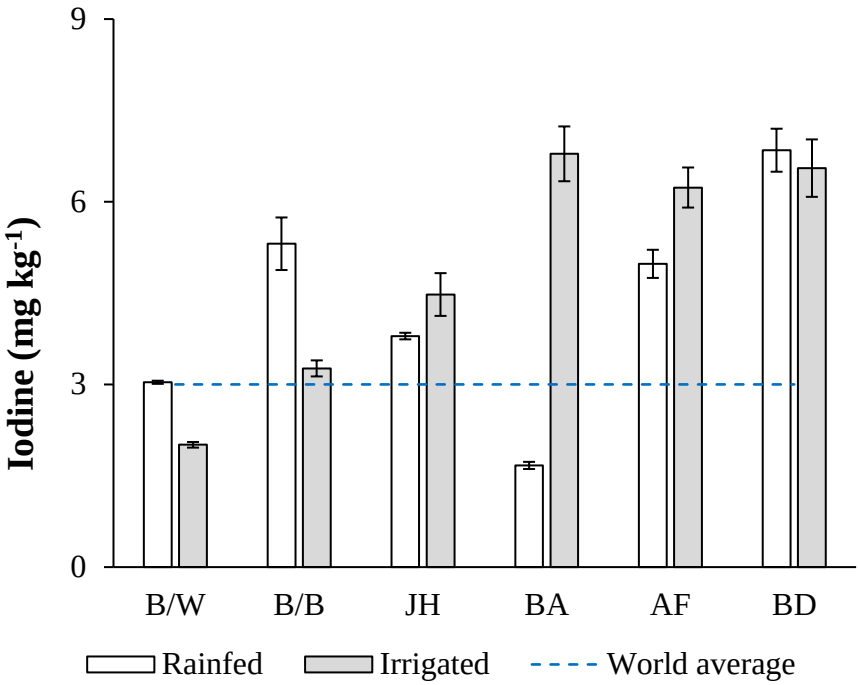


Figure 4.19. Total iodine concentration (I_{Tot}; mg kg^{-1}) in Somali agricultural soils as determined by ICP analysis after the sequential extraction. Each bar represents the mean and corresponding standard error; n = 12; each value of the 12 is the mean of 3 replicates. Rainfed (white), irrigated (grey); the soil codes are described in Table 4.1. The dashed line is the world geometric mean.

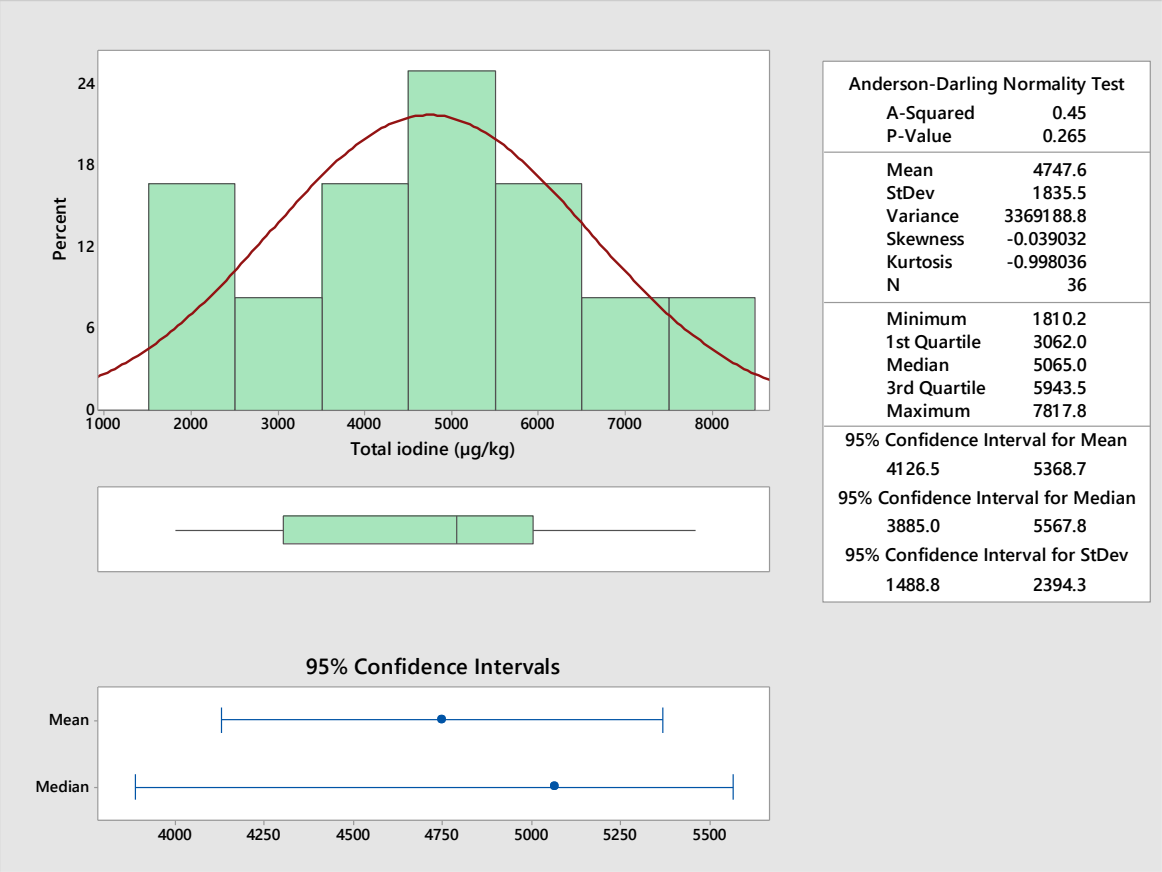


Figure 4.20. Histogram illustrating distribution of total iodine (I_{Tot}) concentration in agricultural soil samples from south Somalia. The assessment of the compatibility of fitted distributions was made using the Anderson–Darling (A–D) test for the significance level of $\alpha = 0.05$.

4.3.4.2. *Iodine fractionation and speciation*

- Soluble iodine (0.01 M KNO_3)

The concentrations of the soluble iodine (I_{Sol}) accounted, on average, for about 1.53% of the total soil iodine, ranging from 0.74 to 4.74% of I_{Tot}. Soluble iodine significantly ($P < 0.001$) differed between sampling regions and followed the order Baidoa>Bulo-Burte>Afgoi>Jowhar>Bal'ad and Belet-weyn. The distribution of I_{Sol} is shown in a histogram in Fig 4.21. There was no clear relationship between I concentration in water (I_{water}) and I_{Sol} in the surrounding soils (Fig. 4.22). In contrast to the results for Se, on average about 81.1% of the I_{Sol} was organic, and only 18.9% was inorganic existing as iodide (15.7%) and iodate (3.18%); Table 4.7 presents the speciation of iodine in the soluble fraction (I_{Sol}) and proportion of organic and inorganic I. The significant role that the soil organic matter has in the accumulation of iodine is well established in the literature (Johnson, 2003).

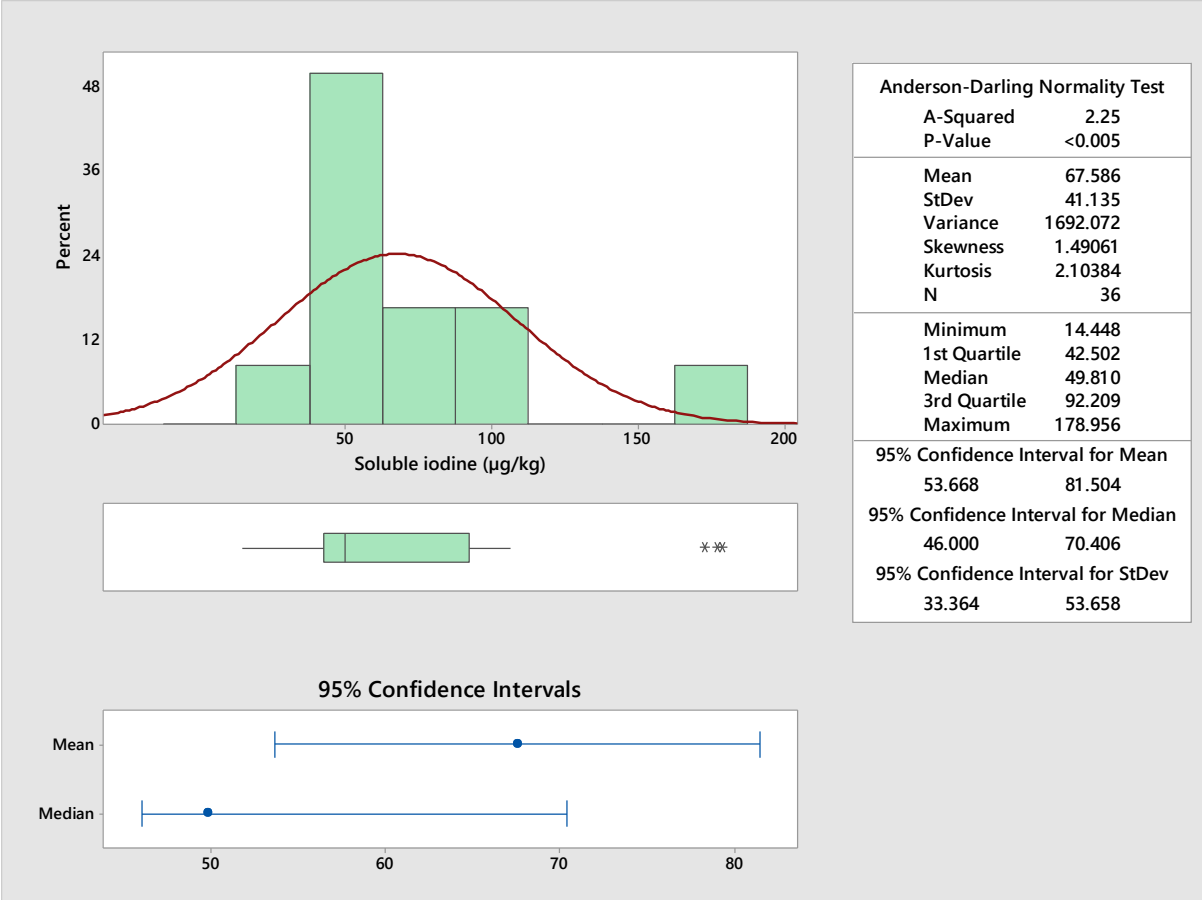


Figure 4.21. Histogram illustrating distribution of the soluble iodine (I_{Sol}) concentration in the agricultural soil samples from south Somalia. The assessment of the compatibility of fitted distributions was made using the Anderson–Darling (A–D) test for the significance level of $\alpha = 0.05$.

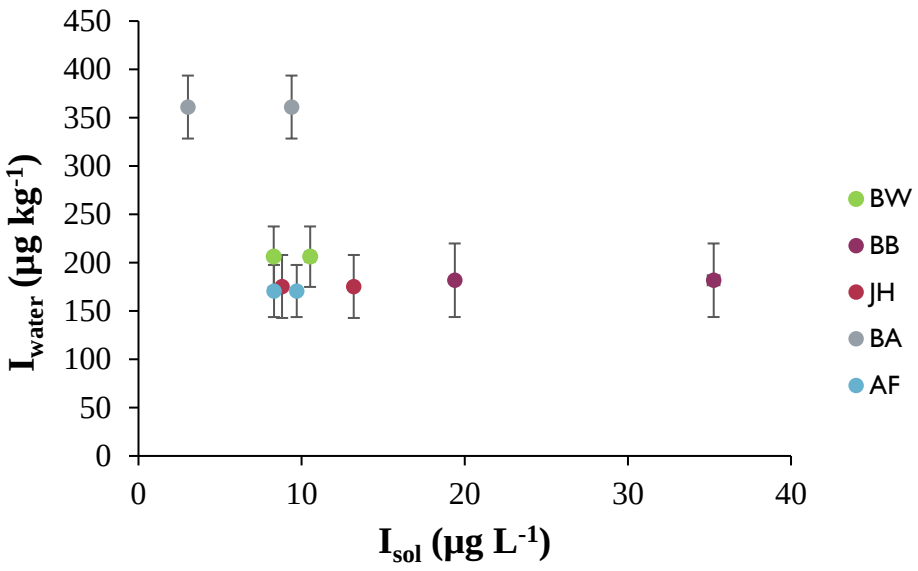


Figure 4.22. Relationship between total soluble iodine in the soil (^{127}Isol) and total iodine (^{127}Iwater) in surface water and groundwater samples.

Table 4.7. Speciation of iodine in the soluble fraction (I_{Sol}) and proportion of organic and inorganic I in I_{Sol}. Concentrations are given in µg kg^{-1}; proportions are expressed as percentages. Data are means ± standard deviation for each measured parameter.

Soil	Land use	I_{Sol} (Total)	$I_{Sol(IO^{3-})}$ (Iodate)	$I_{Sol(I^-)}$ (Iodide)	$I_{Sol(IO^{3-})}$ (Iodate)	$I_{Sol(I^-)}$ (Iodide)	$I_{Sol-Inorg}$	$I_{Sol-Org}$
		µg kg^{-1}	µg kg^{-1}	µg kg^{-1}	%	%	%	%
BW-R	Rainfed	52.6	1.20	8.62	2.28	16.4	18.7	81.3
BW-I	Irrigated	41.4	0.393	6.94	0.950	16.7	17.7	82.3
BB-R	Rainfed	96.9	9.85	13.2	10.2	13.6	23.8	76.2
BB-I	Irrigated	176	13.2	27.3	7.49	15.4	22.9	77.1
JH-R	Rainfed	66.0	1.73	9.33	2.62	14.1	16.8	83.2
JH-I	Irrigated	44.0	0.615	5.32	1.40	12.1	13.5	86.5
BA-R	Rainfed	15.1	0.237	1.98	1.57	13.1	14.7	85.3
BA-I	Irrigated	46.9	0.132	4.04	0.282	8.61	8.9	91.1
AF-R	Rainfed	41.5	1.08	10.1	2.60	24.4	27.0	73.0
AF-I	Irrigated	48.5	0.404	9.07	0.833	18.7	19.5	80.5
BD-R	Rainfed	79.1	4.18	13.8	5.28	17.4	22.7	77.3
BD-I	Irrigated	103	2.82	17.9	2.74	17.4	20.1	79.9

- Adsorbed iodine (0.016M KH_2PO_4)

The concentrations of the adsorbed iodine (I_{Ads}) accounted on average for about 2.66% of the I_{Tot} content, ranging from 2.13 to 3.97% of I_{Tot}. Adsorbed iodine significantly ($P < 0.001$) differed between soils, values of I_{Ads} from Bulo-Burte (137 µg kg^{-1}) were significantly ($P < 0.05$) higher than other regions. The distribution of the adsorbed I is shown in Fig.4.23.

Similarly, as in the case of the soluble fraction, 88.8% of I_{Ads} was organic, and only 11.2% was in inorganic forms including both iodate (5.35%) and iodide (5.86%) species. On average the sum of the soluble and adsorbed iodine accounted for 4.19% of the total soil iodine. Table 4.8 summarizes speciation of Iodine in the adsorbed fraction.

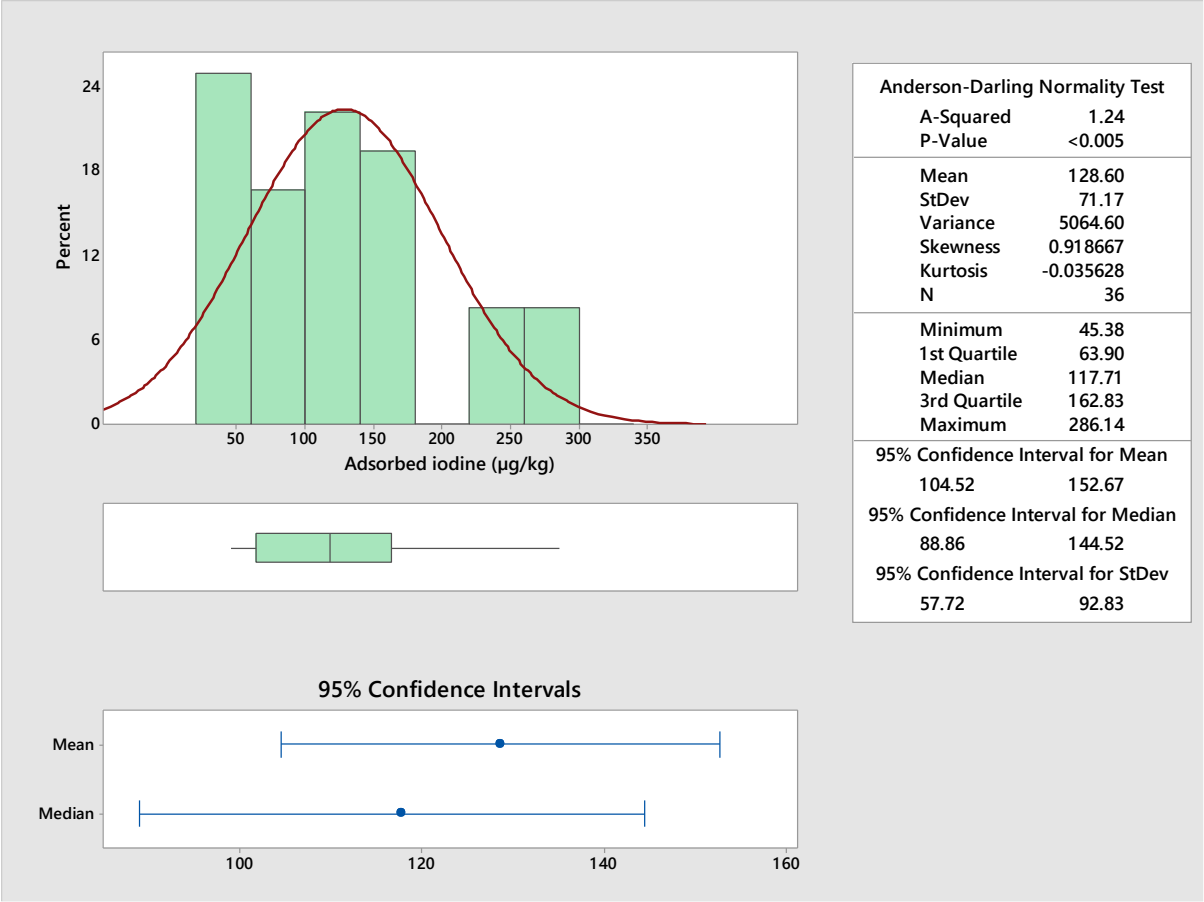


Figure 4.23. Histogram illustrating distribution of the adsorbed iodine (I_{Ads}) concentration in the agricultural soil samples from south Somalia. The assessment of the compatibility of fitted distributions was made using the Anderson–Darling (A–D) test for the significance level of $\alpha = 0.05$.

Table 4.8. Speciation of iodine in the soluble fraction (I_{Ads}) and proportion of organic and inorganic I in I_{Ads}. Concentrations are given in µg kg^{-1}; proportions are expressed as percentages. Data are means ± standard deviation for each measured parameter.

Soil	Land use	I_{Ads} (Total)	$I_{Ads(IO^{3-})}$ (Iodate)	$I_{Ads(I^-)}$ (Iodide)	$I_{Ads(IO^{3-})}$ (Iodate)	$I_{Ads(I^-)}$ (Iodide)	$I_{Ads-Inorg}$	$I_{Ads-Org}$
		µg kg^{-1}	µg kg^{-1}	µg kg^{-1}	%	%	%	%
BW-R	Rainfed	54.1	3.16	4.82	5.85	8.93	14.8	85.2
BW-I	Irrigated	58.4	1.32	3.62	2.25	6.22	8.47	91.5
BB-R	Rainfed	170	41.4	8.43	24.4	4.97	29.3	70.7
BB-I	Irrigated	149	21.0	20.0	14.1	13.4	27.5	72.5
JH-R	Rainfed	108	4.55	4.30	4.23	3.97	8.20	91.8
JH-I	Irrigated	92.9	2.20	5.62	2.36	5.96	8.31	91.7
BA-R	Rainfed	49.3	0.644	1.40	1.32	2.87	4.18	95.8
BA-I	Irrigated	81.0	0.477	3.05	0.585	3.74	4.32	95.7
AF-R	Rainfed	120	5.72	7.27	4.76	6.06	10.8	89.2
AF-I	Irrigated	139	2.21	8.18	1.59	5.90	7.49	92.5
BD-R	Rainfed	240	4.37	9.91	1.82	4.14	5.96	94.0
BD-I	Irrigated	282	2.82	11.5	1.00	4.07	5.07	94.9

- Organically bound iodine (TMAH extractable)

Concentrations of organic matter bound iodine (I_{TMAH}) were nine-fold greater than the soluble and adsorbed fractions together. Concentrations of I_{TMAH} accounted on average, for 90% of I_{Tot} and significantly ($P < 0.05$) differed between soils. The concentration of the I_{TMAH} is presented in Fig 4.24. The different I fractions are combined in a single graph in Fig 4.25 and in Table 4.9 for easy comparison.

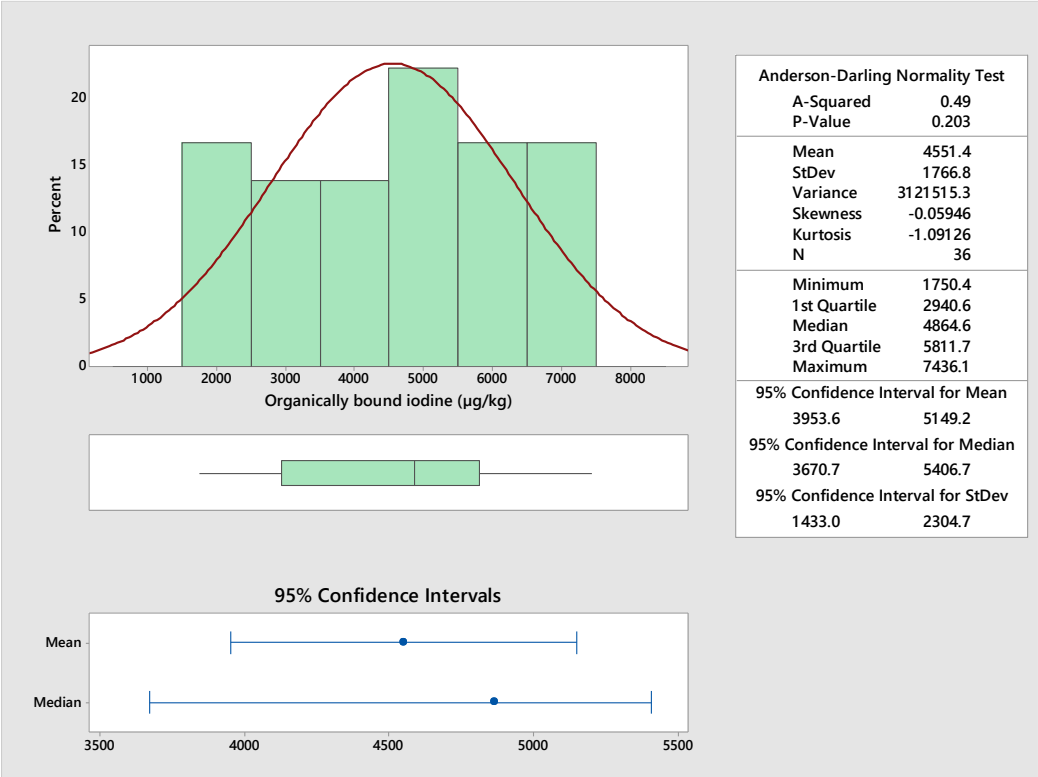


Figure 4.24. Normality test of the distribution of the organically bound iodine (I_{TMAH}) concentration in agricultural soil samples from south Somalia. The assessment of the compatibility of fitted distributions was made using the Anderson–Darling (A–D) test for the significance level of $\alpha = 0.05$.

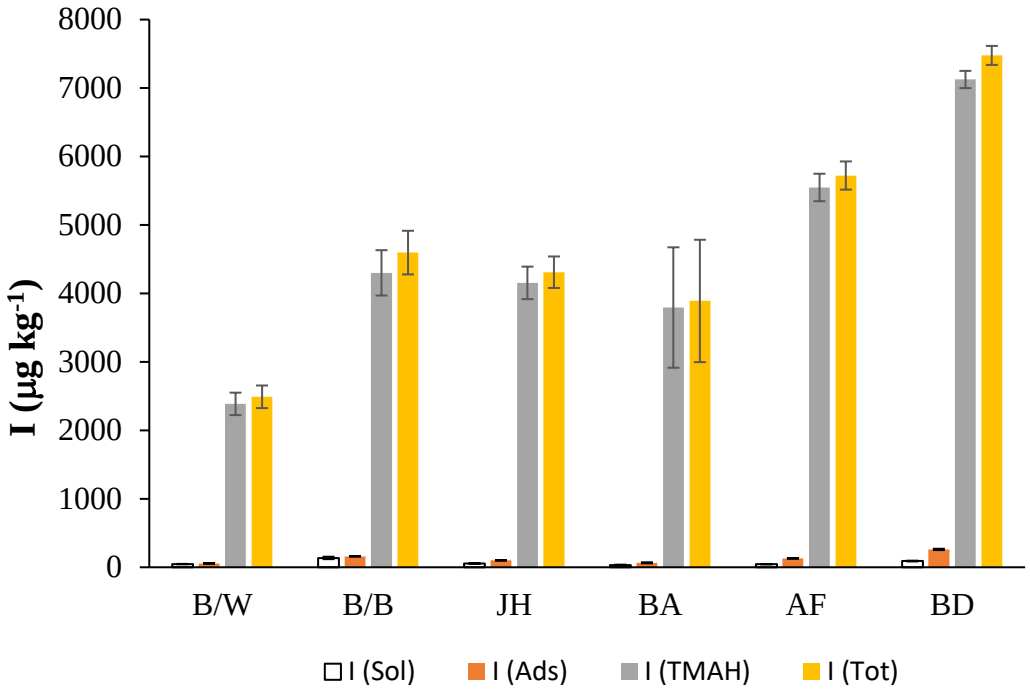


Figure 4.25. The mean concentration (µg kg^{-1}) of soluble, adsorbed, organically bound and total iodine measured in triplicate ± the standard error is summarized for ease of comparison between these fractions. Data was produced after ICP-MS analysis of the sequentially extracted soil samples. (codes in Table 4.1).

Table 4.9. Iodine content (µg kg^{-1}) of the Somali Agricultural soil samples after a three-step sequential extraction. The operationally defined fractions are soluble I, exchangeable I, organic matter-bound I and the residual I fraction. N=12; a is (rainfed soils) and b (irrigated soils).

	Sampling sites											
Fraction	BW[a]	BW[b]	BB[a]	BB[b]	JH[a]	JH[b]	BA[a]	BA[b]	AF[a]	AF[b]	BD[a]	BD[b]
I_{Sol}	52.6	41.4	96.9	176	66.0	44.0	15.1	46.9	41.5	48.5	79.1	103
I_{Ads}	54.1	58.4	170	149	108	92.9	49.3	81.0	120	139	240	282
I_{TMAH}	2750	2020	5030	3570	3650	4660	1830	5760	5150	5950	6890	7360
I_{Tot}	2860	2120	5300	3890	3830	4800	1890	5890	5310	6140	7210	7740

BW: Beletweyn; BB: Buloburte; JH: (Jowhar); BA: Bal'ad; AF: Afgoi; BD: Baidoa; (a: rainfed; b: irrigated)

4.4. Summary, discussion and conclusions

Selenium

The mean concentration of Se_{Tot} in the main agricultural lands in south Somalia was 400 µg kg^{-1}, ranging from 300 to 520 µg kg^{-1}, which is similar to the world average of soil Se_{Tot} of 400 µg kg^{-1}. According to Fordyce (2005) soils that have concentrations of Se < 600 µg kg^{-1} are considered Se deficient, thus it is possible that agricultural soils in southern Somalia may be prone to problems related to Se deficiency in agricultural produce. The fraction Se_{Sol} which is considered to be most available to plants was also measured. The mean concentration of the Se_{Sol} fraction was 3.33 µg kg^{-1}, ranging from 1.71 to 5.52 µg kg^{-1}. The proportion of the Se_{Sol} accounted on average for less than 1.00% of Se_{Tot}, ranging from 0.48 to 1.51 %. The ligand-exchangeable Se fraction (Se_{Ads}), which may be a significant Se fraction for plant uptake through replenishment of Se_{Sol}, was also measured. The mean concentration of Se_{Ads} was greater than the Se_{Sol} and varied from 4.65 to 23.0 µg $kg^{-1,}$ with an arithmetic mean of 11.8 µg kg^{-1} representing 2.99% of the Se_{Tot}. The Se concentration in the soluble and the adsorbed fractions are regarded as the readily available Se for plants uptake, the combination of these two fractions has accounted for 3.85% of the total soil Se (Se_{Tot}).

Selenium availability depends on its speciation, it can be organic or inorganic, the major inorganic Se species found in soil solutions are selenite (Se^{IV}) and selenate (Se^{VI}). Speciation of the Se_{Sol} revealed that 50.7% of the Se_{Sol} was present as inorganic anions, the $Se_{Sol\text{-}Inorg}$ contained both possible inorganic Se species i.e. 26% selenate (Se^{VI}) and 24% selenite (Se^{IV}). The proportion of Se_{Sol} that was associated with dissolved soil organic matter was 49.4%. By contrast, speciation of the Se_{Ads} indicated that 71% of the Se_{Ads} was inorganic, while only 29% was organic. The majority of the inorganic Se_{Ads} was Se^{IV} (70.4%) while Se^{VI} only represented 0.93% of the Se_{Ads}. This finding is in agreement with the common finding that Se^{IV} is more strongly adsorbed than Se^{VI}.

In addition, Se_{TMAH} (considered mainly organically bound Se) was also measured. The proportion of Se_{TMAH} was greater than that of Se_{Sol} and Se_{Ads} fractions combined together and accounted on average for 36.8% of the Se_{Tot}. The concentration of the Se_{TMAH} varied from 43.8 to 376 µg kg^{-1}. The large fraction (12.4% to 73.0%) of Se extracted in TMAH supports the conclusion that most of Se in the Somali agricultural soils exists as organic Se. However, a strong correlation between

Se_{TMAH} and Fe/Al concentration may imply that some of the Se extracted by TMAH might be associated with Fe/Al hydrous oxides.

The sequential extraction also showed that there is a large Se fraction that was present in a recalcitrant form in the soil which resisted extraction with 10% TMAH extraction. The recalcitrant Se ($Se_{Residue}$) varied from 126 to 300 µg kg^{-1}, with an arithmetic mean of 226 µg kg^{-1}. The $Se_{Residue}$ was greatest in carbonate rich soils (Belet-weyn soils; 82%) and lowest with soils with relatively high organic matter (Baiodoa soils; 28%). The $Se_{Residue}$ may be associated with the soil primary minerals such as the $CaCO_3$, possibly through Se^{IV} incorporation into the calcite structure (Aurelio et al., 2010), isomorphically replacing carbonate. Batch adsorption experiments and EXAFS studies were performed to investigate the mechanisms of Se incorporation into calcite and are described in Chapters 6 and 7.

Correlations between soil properties and the different Se fractions revealed the importance of the soil organic matter. Soil organic matter showed a strong correlation with Se_{Tot} whether expressed as LOI (R^2= 0.628; $p < 0.001$) or as TOC (R^2= 0.400; $p < 0.001$). The presence of Se mainly in organically bound forms was also suggested by a very strong correlation between Se_{Tot} (HF digest) and Se_{TMAH} (r=0.901). By contrast, negative correlations (Pearson correlation) were found between Se_{Tot} and TIC (r = -0.761), soil pH (r = -0.137) and Ca_{Tot} (r = -0.793) suggesting that calcareous conditions were not associated with Se sources or retention in the Somali soils. To some extent this conflicts with the apparent existence of a recalcitrant Se fraction with good evidence of an association with $CaCO_3$. Neither the Se_{TMAH} nor the $Se_{Residue}$ fractions are immediately plant-available and, as in most soils, the available fractions (Se_{Sol} and Se_{Ads}) are a very small proportion of the Se_{Tot}. Nevertheless, it would be interesting to investigate which of the two fractions (Se_{TMAH} and $Se_{Residue}$) would contribute more to replenishment of the available Se fractions in the long term. Although the $Se_{Residue}$ fraction is apparently locked up within mineral structures that resist alkaline extraction it is likely that it is present as (inorganic) selenite and so could potentially contribute to plant uptake if local rhizosphere conditions caused dissolution of the $CaCO_3$ particles. By contrast, rendering Se_{TMAH} bioavailable would require mineralisation of organic forms of Se bound to humus which appear to be recalcitrant in studies investigating the residual supply of Se in biofortification experiments. Finally, with limited data, a comparison of soluble Se and Se concentrations in local water systems showed no association. This probably suggests groundwater

geochemical control over Se dissolution in water systems and local soil chemical control over Se solubility. There was therefore no evidence of, for example, a steady state between local water supplies and soils, notwithstanding the fact that irrigation is a long standing and widely practiced part of the local agriculture.

Iodine

Many of the major trends seen with Se were also seen in fractionating and speciating the iodine in the Somali soils. The mean concentration of the I_{Tot} in the main agricultural lands in south Somalia varied from 1.81 to 7.82 mg kg^{-1}, with an arithmetic mean of 4.75 mg kg^{-1}. Total mean iodine concentration in the Somali agricultural soils (4.75 mg kg^{-1}) is slightly higher than the worldwide geometric mean of 3.00 mg kg^{-1} (Johnson et al., 2003), but is comparable to the mean iodine concentration in soils worldwide 5.00 mg kg^{-1}.

In order to provide useful and more direct information regarding uptake by plants, the total iodine concentration of the soil was further fractionated into I_{Sol}, I_{Ads} and I_{TMAH}. The I_{Sol} which is considered to be most available to plants was on average 67.6 µg kg^{-1}, ranging from 14.4 to 179 µg kg^{-1}. The proportion of the I_{Sol} accounted on average for 1.53% of I_{Tot}, ranging from 0.74% to 4.74%. The mean concentration of I_{Ads} was greater than the I_{Sol} and varied from 45.4 to 286 µg $kg^{-1,}$ with an arithmetic mean of 129 µg kg^{-1} representing 2.66% of the I_{Tot}. The I_{Sol} and I_{Ads} are regarded as the readily available I for plants uptake, the combination of these two fractions accounted for 4.19% of the I_{Tot}. The speciation analysis has also revealed that the dominant form of this fractions was the organically bound iodine. Contrary to the literature (Johnson, 2003), iodide (15.7%) in the soluble fraction was higher than the iodate (3.18).

A large fraction of the soil I was associated with the soil organic matter (I_{TMAH}). The proportion of I_{TMAH} was greater than I_{Sol} and I_{Ads} fractions combined and accounted on average for 96% of the I_{Tot}. The concentration of the I_{TMAH} varied from 1.75 to 7.44 mg kg^{-1}. This finding confirms previous studies which suggest that soil organic matter plays a principal role in retaining iodine. I_{Tot} showed a positive correlation with the soil organic matter and with the TOC. A negative correlation was found between the TIC and I_{Tot}. The data also showed a weak negative correlation between the pH and I_{Tot} and, similarly, the Ca_{Tot} concentrations were negatively correlated with I_{Tot}.

This survey is the first of its type in Somalia and the results may provide guidance on Se and iodine in the region. This chapter has shown Se and iodine fractionation and speciation in Somali agricultural soils and the contrasting roles that soil organic matter and inorganic carbon (calcite) play in determining the retention, fractionation, speciation and (potentially) the bioavailability of Se and iodine in these soils. The soil parameters measured in this study can be used to assist the Se and iodine fertilization projects. There is a need to conduct a well-structured survey of all soil types and major food crops to identify the Se and iodine status of these soils and the population.

Appendix A:

Assessment of the validity of the TMAH extraction method

Organic matter is well known to play an important role in the retention-release of many micronutrients including Se and iodine (Hooda, 2010). The organically bound Se and iodine can be extracted using alkaline solutions such as tetra methyl ammonium hydroxide (TMAH) (Shetaya et al., 2012; Watts and Mitchell, 2009; Yamada et al., 1996). Extraction with tetra methyl ammonium hydroxide (TMAH) has been widely used for extracting iodine from environmental samples including soils, sediments, plants, and food.

In this study the validity of the TMAH extraction for extracting Se and iodine was tested. Two contrasting calcareous topsoils from Somalia (0 – 20 cm) were tested, including ball milled and 2 mm-sieved samples. The two soils varied in their physical and chemical properties including total iodine and selenium concentration. Each soil sample was composed of five sub-samples taken in the field and bulked together to make one composite sample. The soils were air-dried and sieved to < 2 mm. A subsample (~10 g) of each soil was finely ground using an agate ball mill at 400 rpm for 4 minutes (PM 400, Retsch, Haan, Germany). Firstly, these study soils were characterized for their physical and chemical properties. Soil pH, loss on ignition (LOI), cation exchange capacity (CEC), total carbon (TC), inorganic carbon (IC), and multi-elemental analysis were performed. TMAH extractable selenium (Se_{TMAH}) and iodine (I_{TMAH}) were measured as described in Chapter 2. All analyses were performed in triplicate.

TMAH was then used to extract fractions (I_{TMAH} and Se_{TMAH}) using (i) different soil-to-solution ratios, and (ii) with and without agate ball-milling of the soil. A total of 16 treatments consisting of two soils and four levels of soil-to-solution ratios (1:10, 2:10, 3:10, 4:10) and two soil processing steps (< 2 mm sieved, or agate ball milled) were evaluated. The extraction was done with two replicates. TMAH extraction was undertaken by adding 10 ml of 10% TMAH to the centrifuge tubes containing the soil (sieved only), and 5 ml of 10% TMAH to the agate ball milled soils. Centrifuge tubes, with lids loosened, were placed in a drying oven at 70^0 C for 3 h, with gentle shaking of the tubes after 1.5 h. After 3 h of heating, the samples were centrifuged at 3500 rpm for 30 min and filtered through 0.22 µm PTFE syringe filters. TMAH extracts were analysed by ICP-MS for I_{TMAH} and Se_{TMAH}. The ^{127}I concentrations were analysed in standard mode using ^{72}Ge, ^{185}Re and ^{103}Rh as internal standards to correct for drift. The ^{78}Se concentrations were determined

in hydrogen mode using ^{72}Ge, ^{103}Rh and ^{193}Ir as internal standards. A wash solution (1% freshly prepared TMAH) was used between samples. Data were captured using Qtegra software (Thermo-Scientific, Bremen, Germany).

General characteristics of the study soils are summarized in Table 4.10. The effect of the different soil-solution ratios (1:10, 2:10, 3:10, 4:10) is shown in Tables 4.11 and 4.12 for I_{TMAH} and Se_{TMAH} respectively, and Fig. 4.26. The TMAH-extractable iodine did not significantly differ ($P<0.05$) between the different soil-solution ratios. Similarly, Se_{TMAH} was not significantly different between the different soil-to-solution ratios, however, post hoc pairwise comparisons showed a significant difference ($P < 0.05$) between Se_{TMAH} at the extremes of the range (4:10 ratio and the 1:10 ratio). Surprisingly, the amount of extractable Se was 5–7% greater when a soil solution ratio of 4:10 was used suggesting that the difference was not due to the capacity of the system to extract Se.

Table A1. General characteristics of the experimental soils

Soil	pH (1:2.5)	LOI (%)	TIC (%)	TOC (%)	Total Se ($\mu g\ kg^{-1}$)	Se_{TMAH} ($\mu g\ kg^{-1}$)	I_{TMAH} ($mg\ kg^{-1}$)
BW-I	8.14	0.21	2.96	0.79	300	30	2.01
BD-R	8.13	1.00	0.48	1.64	520	190	7.21

Effect of ball milling

The effect of ball milling of the sieved soil before extraction with TMAH is shown in Tables A1 and A2, and Fig. 4.26, for I_{TMAH} and Se_{TMAH} respectively. Ball milling had no significant effect on the TMAH extraction of I_{TMAH} and Se_{TMAH}.

Table A2. Iodine concentration in TMAH extracts (I_{TMAH}; mg kg^{-1}) using different soil to TMAH solution ratios (agate ball milled soils and < 2 mm sieved)

Soil type	Sample code	Soil to solution ratios			
		1:10	2:10	3:10	4:10
< 2 mm sieved	BW-I	1.91	2.01	2.10	2.10
	BD-R	7.98	7.76	7.86	7.58
Agate ball milled	BW-I	1.92	2.04	2.03	2.07
	BD-R	8.27	8.12	7.90	8.14

Note: BW-I: Soil from Beletweyn (irrigated system); BD-R: Soil from Baidoa (rainfed system)

Table A3. Selenium concentration in TMAH extracts (Se_{TMAH}; µg kg^{-1}) using different soil to TMAH solution ratios (agate ball milled soils and < 2 mm sieved)

Soil type	Sample code	Soil to solution ratios			
		1:10	2:10	3:10	4:10
< 2 mm sieved	BW-I	32.6	36.6	37.5	38.0
	BD-R	224	222	232	231
Agate ball milled	BW-I	34.6	37.5	34.9	36.4
	BD-R	219	231	227	234

Note: BW-I: Soil from Beletweyn (irrigated system); BD-R: Soil from Baidoa (rainfed system)

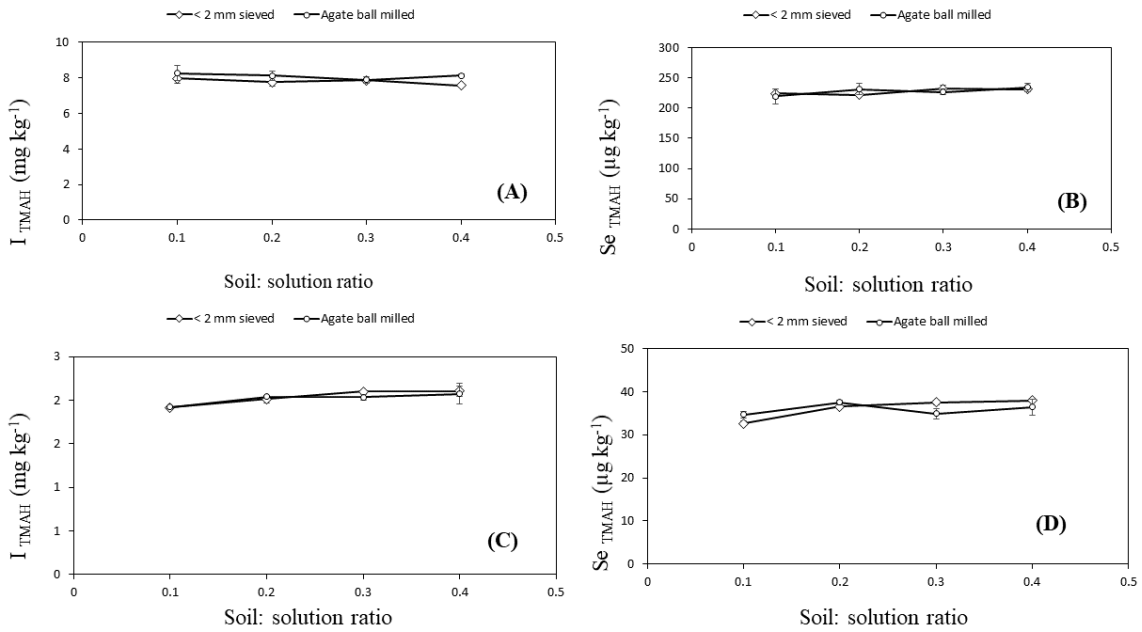


Figure A1. Selenium (Se_{TMAH}; µg kg^{-1}) and iodine (I_{TMAH}; mg kg^{-1}) concentration in TMAH extracts using different soil-to-solution ratios and comparing agate ball milled soils and with samples sieved to < 2 mm. A) and B) are high Se high I Baidoa soils; C) and D) are low Se low I Beletweyn soils.

5. Selenium and iodine in crop plants and their corresponding soils

5.1 Introduction

Selenium (Se) and iodine (I) are two essential micronutrients for animals and humans and are obtained through crops and water in the food chain. Currently, several indices are widely used to assess population nutrient status. These include:

(i) the Recommended Nutrient Intake (RNI), which is the dietary intake of a micronutrient likely to be sufficient for 97.5% of individuals in an age and sex-specific group (FAO & WHO, 2004).

(ii) the Estimated Average Requirement (EAR) which is the intake required that is likely to meet the needs of more than half of the healthy population in a particular age, sex and life stage.

(iii) the Recommended Dietary Allowance (RDA), which is the estimated amount of a nutrient per day considered necessary for the maintenance of good health.

The iodine RNI values for children, adults and pregnant women have been set at 120, 150 and 200 μg capita^{-1} d^{-1} respectively (World Health Organization, 2004; Watts et al., 2015) while the current EAR values for I have been set at 64, 107 and 143 μg capita^{-1} d^{-1} for children, adults and pregnant women, respectively. The Recommended Dietary Allowances (RDAs) for selenium are 55 μg day^{-1}, 60 μg day^{-1} and 70 μg day^{-1} for adults, pregnant women and for lactating women respectively (Monsen, 2000).

Concurrent Se and I deficiencies are widespread, in both developing and developed countries (Lyons, 2018). It is a problem that affects billions of people, worldwide: it is estimated that 30% are I deficient and 15% are Se deficient (White and Broadley, 2009). Micronutrient deficiencies are particularly widespread in the eastern African countries and approximately 75%, 52% and 26% of the population is currently living at risk of Zn, Se and I deficiencies respectively (Joy et al., 2014).

The selenium and iodine content of plant foods depends on their availability in the soil where they are cultivated. Selenium is taken up from the soil solution by plant roots principally in the form of inorganic Se (i.e. selenate (Se^{VI}) and selenite (Se^{IV}) or it can be in the form of organoselenium compounds such as selenocysteine (SeCys) and selenomethionine (SeMet) (White and Broadley

2009). Iodine can be taken up through the roots, primarily in the form of the inorganic species iodide and to a lesser extent as iodate (Burte et al., 1991; Whitehead, 1984). The plant uptake and hence the accumulation of Se and I in the edible parts of plants depends on soil factors such as the total Se and I content and the soil properties that affect their solubility, such as the pH and the redox potential (Eh) of the soil (De Temmerman et al., 2014; Shetaya et al., 2012).

Selenium in crops

According to the literature, Se concentration in plants can range from 0.005 mg kg^{-1} in deficient crops to 5500 mg kg^{-1} in selenium accumulators, but in most plants the Se contents are below 10 mg kg^{-1} (Fordyce, 2013). Selenium concentration varies between different food crops; for example the Se concentration of maize samples from Malawi (0.005–0.533 mg kg^{-1}) and wheat 0.1–1.9 mg kg^{-1} (Chilimba et al., 2011; Fordyce, 2013). The Se concentration in cereals may also vary from country to country depending on local soil conditions. For example, maize samples collected from Malawi, Africa (0.005–0.533 mg kg^{-1}) differ from maize grown in Se-adequate zones in China (0.021–2.324 mg kg^{-1}) (Chilimba et al., 2011; Fordyce, 2013). It also varies within the same country; for example, maize grown in Se-deficient areas of china (0.001–0.105 mg kg^{-1}) may be significantly different from equivalent crops grown in seleniferous areas in china (0.017–9.175 mg kg^{-1}) (Fordyce, 2013).

For humans and livestock to obtain sufficient Se a minimum dietary Se concentration of 50 to 100 μg kg^{-1} dry weight is required, and for an optimum level it is recommended that crops provide 150 to 200 μg Se kg^{-1} dry weight (Gardiner and Gorman, 1963; Gierus et al., 2002; Gissel-Nielsen et al., 1984).

Iodine in crops

The iodine contents of plant foods varies from 10 - 1000 μg kg^{-1} dry weight (Zimmermann, 2009). In many staple carbohydrate foods the iodine concentration is typically low, with median concentrations of 10 μg kg^{-1} in maize grain (Watts et al., 2015). Thus, generally, cereal crops such as rice and wheat cannot be relied on as an iodine source, however there is evidence that supports the feasibility of fortifying cereals with Se and I, as reported by Cakmak et al. (2017) and White and Broadley (2009). Biofortification of leafy vegetables may be a more efficient option than

cereal crops as greater iodine contents 155 µg kg^{-1} has been reported in leafy vegetables samples from Malawi (Watts et al., 2015).

In Somalia, soil nutrients deficiencies have been reported (SATG, 2019) and dietary micronutrient deficiencies, such as Se, could be exacerbated by relying on locally grown foods. However, according to a recent study iodine nutrition in Somalia is among the highest in the world and is possibly caused by drinking iodine-rich groundwater (Kassim et al., 2014; Zimmermann, 2013).

In this study maize, cowpea and mung bean were chosen as test crops as they are the main staple food crops and were, therefore, the only crop samples available from demonstration plots of the Somali Agricultural Technical Group (SATG). Currently, there are no existing data on the Se and iodine contents of the crops grown in Somali soils. The objectives of this study were to: (1) explore the Se and iodine status of the staple crops grown in Somali agricultural soils; (2) assess the contribution of a diet based on these crops to the supply of Se and iodine; (3) investigate soil parameters that may be used to predict plant Se and iodine concentrations.

5.2 Materials and methods

The details of the soil sampling, processing and analysis are given in Chapter 2.

Samples of maize, cowpea and mung bean grain collected from demonstration plots in Afgoi, Somalia were subjected to multi-elemental analysis using the sampling and analytical procedures described in Chapter 2 in Sections 2.3.3 and 2.4.5. Soils corresponding to these crops were collected, processed and analysed as described in Chapter 2 in sections 2.2, 2.3 and 2.4.

Crop samples were collected from the agricultural demonstration plots in Afgoi and nearby villages. Sampling sites included the 'Agri-Business Incubation Centre' (ABIC), Mire, Balbaley, Jambalol and Buhow; these sites are villages near Afgoi. The samples included maize cobs (*Zea mays* L.), Cowpea (*Vigna unguiculata* L.) and Mungbean (*Vigna radiata* L.). The varieties included: an improved local maize variety, two Cowpea varieties (local and Kenkunda); two mung bean varieties (local and Filsan). The demonstration plots were established by the Somali Technical Group (SATG) to establish and share knowledge, skills, and innovative technologies through agricultural field demonstration sites, and to establish network between farmers and stakeholders. Samples were collected from the plots during January and February (2016) and this was in series of trials to evaluate the yield and other agronomic characteristics of some varieties of maize, cowpeas and mung beans at ABIC in Afgoi and at demonstration sites in farmers' fields.

The chemical composition of these samples and the mean per-capita consumption of maize in Somalia was used to compute dietary intakes. Since there were no data for Somalia, the mean per-capita consumption of maize in east Africa (mean: 162 g cap^{-1} day^{-1}) were used to estimate the maize contribution to the intake of selected macronutrients and micronutrients including Se and I (Kornher, 2018). Therefore, only intake from maize is presented in this chapter because of its significance as a staple crop for the subsistence farming communities in Somalia.

5.3 Results and discussion

5.3.1 Soil characteristics

Soil characteristics are summarised in Table 5.1. The soils have a high pH and relatively low organic carbon contents (0.99 - 1.72 %). Exchangeable calcium (Ca), magnesium (Mg), potassium (K), and sodium (Na) accounted for 79%, 15%, 4%, and 2% of the cation exchange capacity (CEC) respectively. ICP-MS results for total soil I, Se and Zn are also presented in Table 5.1. TMAH-extractable I (I_{TMAH}) results show that the soils contain a high I content of 6.4 mg kg^{-1} which is significantly greater than the worldwide mean of 3.0 mg kg^{-1} (Johnson et al., 2003). Malawian and Pakistani soils with 2.1 mg kg^{-1} and 0.7 mg kg^{-1} respectively are substantially lower (Watts et al., 2015; Zia et al., 2015).

Total Se concentration in the soil sample (Se_{Tot}) ranged from 0.39 to 0.48 mg kg^{-1}. The sample with the highest Se concentration also had the highest organic matter content (0.34%) with a pH of 8.03. The average Se content of (0.42 mg kg^{-1} is comparable to the Se content of UK soils (<1 mg kg^{-1}) and the world average of 0.40 mg kg^{-1} but is slightly higher than that of Malawi (0.19 g kg^{-1}) or Finnish soils (0.01 mg kg^{-1}) (Broadley et al., 2006; Chilimba et al., 2011; Fordyce, 2013b)

The average Zn content of the soils was 61.1 mg kg^{-1} (range 56.7 to 67.8 mg kg^{-1}), comparable to the world average of 65 mg kg^{-1} and to the Zn content of USA soils (56.5 mg kg^{-1}) but lower than that of the UK soils (97 mg kg^{-1}) (Alloway, 2008).

5.3.2 Iodine, Se and Zn concentration in the grain samples

Results for total grain I, Se and Zn are presented in Table 5.2. TMAH-extractable iodine results show that these grains were generally low in their iodine content (range 0 to 0.04 mg kg^{-1}) with a mean concentration of 0.01 mg I kg^{-1}. Generally maize crops had similar I concentrations (0.01 mg kg^{-1}) and were significantly ($p<0.05$) different from the legume crops (0.02 mg kg^{-1}). Similar results have been reported for cereal crops in Malawi (0.01 mg kg^{-1}), Pakistan (0.01 mg kg^{-1}), and UK cereals (0.01 mg kg^{-1}) (Watts et al., 2015; Zia et al., 2015).

Selenium concentration in the grain sample ranged from 0.01 to 0.26 mg kg^{-1}. Cowpeas and mung beans had significantly ($p<0.05$) higher Se concentrations (89.1 µg Se kg^{-1}) than maize crops (17.0 µg kg^{-1}). The sample with the highest Se concentration was the indigenous cowpea crop (262 µg kg^{-1}). The average Se content in the cereal grain samples (17.0 µg kg^{-1}) was comparable to that of Malawi maize (19 µg kg^{-1}) but much lower than wheat in the USA (457 µg kg^{-1}) and Canada (760 µg kg^{-1}) (Adams et al., 2002). The Se content of the Somali samples was therefore far below the 50 -100 µg kg^{-1} level required for adequate human nutrition (Gissel-Nielsen et al., 1984).

The Zn concentration of both maize and legume crops ranged from 25.8 to 38.8 mg kg^{-1} with mean values of 30.8 mg kg^{-1}. The Zn content of the cowpeas and mung beans (34 mg kg^{-1}) was significantly ($p<0.05$) higher than maize crops (28 mg kg^{-1}). Overall, the Zn concentrations in the grain samples from Somalia were greater than those of maize grain from calcareous and non-calcareous soils in Malawi (median values 21.7 and 16.5 mg kg^{-1} respectively) (Joy et al., 2015).

Table 5.1. Physico-chemical characteristics of the experimental soils collected from demonstration plots in lower Shabelle, Somalia (mean ± SD, n = 9 plots).

Sample site	Plot	pH	LOI (%)	TIC (%)	TOC (%)	Exchangeable cations (cmolC kg^{-1})				I (mg kg^{-1})	Se (mg kg^{-1})	Zn (mg kg^{-1})
						K	Ca	Mg	Na			
ABIC	Plot 1	7.92	0.24±0.08	1.75±0.11	0.73±0.01	0.73±0.01	7.96±0.08	1.43±0.02	39.49±0.54	6.56	0.39	62.3
	Plot 2	7.91	0.27±0.05	1.68±0.04	0.84±0.00	0.84±0.00	7.85±0.06	1.44±0.00	40.19±0.25	6.41	0.40	67.8
	Plot 3	7.96	0.21±0.02	1.64±0.11	0.78±0.01	0.78±0.01	7.56±0.03	1.49±0.01	38.82±0.25	6.48	0.42	64.0
	Plot 4	7.92	0.31±0.09	1.56±0.08	0.65±0.01	0.65±0.01	8.01±0.12	1.44±0.02	40.58±0.63	6.42	0.42	62.8
MIRE	Plot 5	7.97	0.21±0.06	2.19±0.15	1.00±0.01	1.00±0.01	6.77±0.06	1.69±0.03	36.23±0.47	6.44	0.44	60.3
	Plot 6	7.97	0.28±0.09	1.67±0.15	1.60±0.01	1.60±0.01	6.84±0.08	1.73±0.00	35.99±0.27	6.24	0.42	56.7
BALBALEY	Plot 7	8.13	0.22±0.05	1.68±0.06	0.73±0.15	0.73±0.15	5.74±0.17	2.13±0.08	34.38±1.12	7.85	0.43	57.8
JAMBALUL	Plot 8	8.03	0.34±0.09	1.47±0.11	0.73±0.01	0.73±0.01	7.33±0.08	2.11±0.00	38.54±0.21	5.98	0.48	60.3
BUHOW	Plot 9	8.00	0.16±0.01	1.58±0.16	1.03±0.01	1.03±0.01	7.74±0.08	1.68±0.01	36.64±0.23	5.61	0.41	58.2

Note: K: Kenkunda; L: Local; F: Filsan; ABIC: Agribusiness Incubation Centre

Plot 1: Cowpea; Plot 2: Cowpea; Plot 3: Mung bean; Plot 4: Mung bean; Plot 5: Mung bean; Plot 6: Maize; Plot 7: Maize; Plot 8: Maize; Plot 9: Maize

Table 5.2. Grain total selenium (Se), Iodine (I) and Zinc (Zn) concentrations in maize, mung bean and cow pea grown in demonstration plots in lower Shabelle, Somalia (mean ± SD, n = 9 plots).

Site/plot		Crop	I	Se	Zn
			(µg kg^{-1})	(µg kg^{-1})	(mg kg^{-1})
ABIC	Plot 1	Cowpea	27.0	52.6	36.0
	Plot 2	Cowpea	13.0	262	38.3
	Plot 3	Mung bean	28.0	56.7	33.3
	Plot 4	Mung bean	15.0	34.2	28.8
MIRE	Plot 5	Mung bean	9.00	34.4	30.4
	Plot 6	Maize	10.0	21.1	25.8
BALBALEY	Plot 7	Maize	14.0	11.7	27.0
JAMBALUL	Plot 8	Maize	13.0	19.0	30.1
BUHOW	Plot 9	Maize	4.00	15.0	27.4

Note: K: Kenkunda; L: Local; F: Filsan; ABIC: Agribusiness Incubation Centre

5.3.3 Fractionation and speciation

Iodine fractionation

The concentration of iodine extracted in 0.01 M KNO_3 (I_{Sol}) from the Afgoi soil samples varied from 29.9 to 73.4 µg kg^{-1}. This was less than 1% (with a range of 0.5% to 1.2%) of the total soil iodine extracted by TMAH (I_{TMAH}). This is comparable (< 1%) to Malawi soils (27 µg kg^{-1}; 1% of the total I) and Pakistan soils (2% of total), but is significantly lower than soils from Morocco and UK (10% of total) (Johnson et al., 2002; Johnson, 1980; Watts et al., 2015; Zia et al., 2015) The concentration of iodine extracted with KH_2PO_4 (I_{Ads}) varied from 77.0 – 148 µg kg^{-1} which accounted for 1% (with a range of 1.2 – 2.4%) of I_{TMAH}. The total soil iodine concentrations (I_{TMAH}) ranged from 5.6 to 7.8 mg kg^{-1}, with an arithmetic mean concentration of 6.4 mg kg^{-1} which is greater than the worldwide geometric mean of 3 mg kg^{-1} (Johnson, 2003).

Iodine Speciation in I_{Sol} and I_{Ads}

Iodide (I^-) was the main *inorganic* species found in the nitrate extracts of soil samples, accounting for 89% of the detectable inorganic I of the soluble fraction (I_{Sol}); by contrast, iodate (IO_3^-) concentration was only 7.6% of I_{Sol}. In the adsorbed fraction (I_{Ads}) there was also a mix of species including (on average) iodate (30%) and iodide (69.7%) as shown in table 5.3.

Table 5.3. The chemical forms of iodine (I^- and IO_3^-) in the soils corresponding to the crop samples. Speciation is performed in both the operationally defined soluble and adsorbed fraction (mean ± SD, n = 9 plots).

Site	Plot	$IO_3^-{}_{Sol}$	$I^-{}_{Sol}$	Unknown I_{Sol}	$IO_3^-{}_{Ads}$	$I^-{}_{Ads}$	Unknown I_{Ads}
		(µg L^{-1})	(µg L^{-1})	(µg L^{-1})	(µg L^{-1})	(µg L^{-1})	(µg L^{-1})
ABIC	Plot 1	0.228	1.43	0.193	0.614	1.00	0.000
	Plot 2	0.297	2.09	0.274	0.827	0.734	0.000
	Plot 3	0.102	0.78	0.0790	0.344	1.11	0.000
	Plot 4	0.282	1.55	0.0000	0.947	1.31	0.000
MIRE	Plot 5	0.0963	2.04	0.00785	0.296	0.65	0.000
	Plot 6	0.121	2.96	0.000	0.249	1.12	0.000
BALBALEY	Plot 7	0.0477	1.73	0.000	0.210	1.30	0.000
JAMBALUL	Plot 8	0.0400	1.47	0.000	0.148	1.02	0.000
BUHOW	Plot 9	0.0764	1.06	0.000	0.197	0.577	0.000

Selenium fractionation

Concentrations of soluble Se (Se_{Sol}) accounted for less than 0.3% of Se_{Tot} in the soils and ranged from 0.39 to 1.78 µg kg^{-1}, with a mean of 0.80 µg kg^{-1}. This is less than the 'water soluble' Se reported for China, Indian 'Se-deficient soils' and Sri Lanka Se-deficient soils with 4 µg kg^{-1}, 19 – 66 µg kg^{-1} and 4.9 – 43.3 µg kg^{-1} respectively. Soluble Se is probably the most plant-available form (Fordyce, 2013). Adsorbed Se (Se_{Ads}) concentrations ranged between 6.06 and 11.09 µg kg^{-1}, with a mean of 7.59 µg kg^{-1} representing 1.8% (1.5 % - 2.3 %) of Se_{Tot}. Similar results were reported in a soil survey in Malawi (mean = 5.6 µg kg^{-1}; 3% of Se_{Tot}) (Chilimba et al., 2011).

Selenium Speciation in Se_{Sol} and Se_{Ads}

Speciation of these extracts showed that selenite was more abundant than selenate; nearly a third (31.7%) of the soluble Se was in the form of selenite, while 25.0% was selenate. The remaining Se_{Sol} (43.3%) was an unknown chemical species of Se (Table 5.4). Almost all the Se species detected in the KH_2PO_4 extracts was selenite (99%) possibly reflecting the greater strength of adsorption of selenite compared to selenate. Stroud et al. (2010) investigated the fate and speciation of Se following fertilization of wheat at 10 field sites in the UK, and the only inorganic Se species they detected at all depths in all trials was selenite.

Table 5.4. The chemical forms of selenium ($Se^{(vi)}$ and $Se^{(iv)}$) in the soils corresponding to the crop samples. Speciation was performed in both the operationally defined soluble and adsorbed fractions (mean ± SD, n = 9 plots).

Site	**Plot**	**$Se^{(IV)}_{Sol}$**	**$Se^{(VI)}_{Sol}$**	**Unknown Se_{Sol}**	**$Se^{(IV)}_{Ads}$**	**$Se^{(VI)}_{Ads}$**	**Unknown Se_{Ads}**
		(µg L^{-1})	(µg L^{-1})	(µg L^{-1})	(µg L^{-1})	(µg L^{-1})	(µg L^{-1})
ABIC	Plot 1	0.0735	0.0702	0.228	0.675	0.00000	0.000
	Plot 2	0.0782	0.0746	0.297	0.836	0.0126	0.000
	Plot 3	0.0800	0.0647	0.102	0.779	0.00359	0.002
	Plot 4	0.0859	0.0793	0.282	1.05	0.00967	0.000
MIRE	Plot 5	0.122	0.104	0.096	1.12	0.00504	0.000
	Plot 6	0.157	0.096	0.121	1.11	0.0125	0.003
BALBALEY	Plot 7	0.106	0.067	0.0477	0.919	0.00905	0.000
JAMBALUL	Plot 8	0.154	0.106	0.0400	1.28	0.0140	0.000
BUHOW	Plot 9	0.0885	0.0832	0.0764	0.707	0.0128	0.000

Table 5.5. Iodine and selenium concentration (µg kg^{-1}) of the soils from the demonstration plots in lower Shabelle, Somalia (mean ± SD, n = 9 plots) after a three-step sequential extraction. The operationally defined fractions are soluble I, exchangeable I, organic matter-bound I and the residual Se fraction.

Site/plot			I_{Tot}	I_{Sol}	I_{Ads}	Se_{Tot}	Se_{Sol}	Se_{Ads}
ABIC	Plot 1	Cowpea	6560	37.6	77.0	392	0.39	6.10
	Plot 2	Cowpea	6410	44.9	85.0	401	0.78	6.10
	Plot 3	Mung bean	6480	35.5	85.0	423	0.39	6.40
	Plot 4	Mung bean	6420	47.8	91.0	416	0.52	7.14
Mire	Plot 5	Mung bean	6440	54.0	130	443	0.97	8.40
	Plot 6	Maize	6240	73.4	148	420	1.78	9.60
Balbaley	Plot 7	Maize	7850	56.9	130	430	0.76	6.50
Jambalol	Plot 8	Maize	6000	48.5	117	480	1.15	11.1
Buhow	Plot 9	Maize	5610	29.9	85.0	410	0.56	7.20

Note: K: Kenkunda; L: Local; F: Filsan; ABIC: Agribusiness Incubation Centre

5.3.4 Correlations

Soil Iodine

There was an excellent agreement (positive correlation) between the I_{Ads} and I_{Sol} ($r=0.896$; $p< 0.001$) suggesting that the two fractions were in equilibrium with a similar K_d value (average 2.25) across the limited range of soils studied. However, the iodine fractions, I_{Sol}, I_{Ads} and I_{Tot} showed no correlation with the soil properties pH, LOI, TIC or TOC. The lack of correlation with soil characteristics that might be expected to affect adsorption of iodine may be due to the limited data set. By contrast, significant negative correlations were observed between the magnesium (Mg) content of the soil and I_{Tot} ($r=-0.672$; $p< 0.05$), I_{Sol} ($r=-0.672$; $p< 0.05$) and I_{Ads} ($r=-0.788$; $p< 0.05$). Similarly, there was a significant negative correlation between the Ca content of the soil and I_{Ads} ($r=-0702$; $p< 0.05$). Both Ca and Mg correlated with the total inorganic carbon but not the total organic carbon of the soil ($r=-0.741$; -0.783; $p< 0.05$) respectively. The soil carbonate minerals consist mainly of $CaCO_3$ (but possibly with variable degrees of Mg-substitution), and influence the pH and a range of other soil properties. Hence, a significant negative correlation was observed between the pH of the soil and I_{Sol} ($r=0.579$ at $p< 0.05$) and I_{Ads} ($r=0.535$ at $p< 0.05$). It appears therefore that soils with larger carbonate contents are generally associated with low iodine status.

Soil Se

Surprisingly, Se_{Tot}, Se_{Ads} and Se_{Sol} showed no correlation with pH, loss-on-ignition, total organic carbon or exchangeable cations. Again, the lack of correlation may be attributed to the limited dataset. The only significant correlations were between Se_{Tot} and Se_{Ads} ($r=-0.734$; $p< 0.05$) and between Se_{Sol} and I_{Ads} ($R^2=-0.704$; $p< 0.05$) possibly suggesting common factors affecting Se and I. A good correlation was observed between Se_{Ads} and selenite in the adsorbed fraction ($r= 0.986$, $p< 0.05$). Fig. 5.1, simply reflecting the predominance of Se^{IV} in the adsorbed fraction.

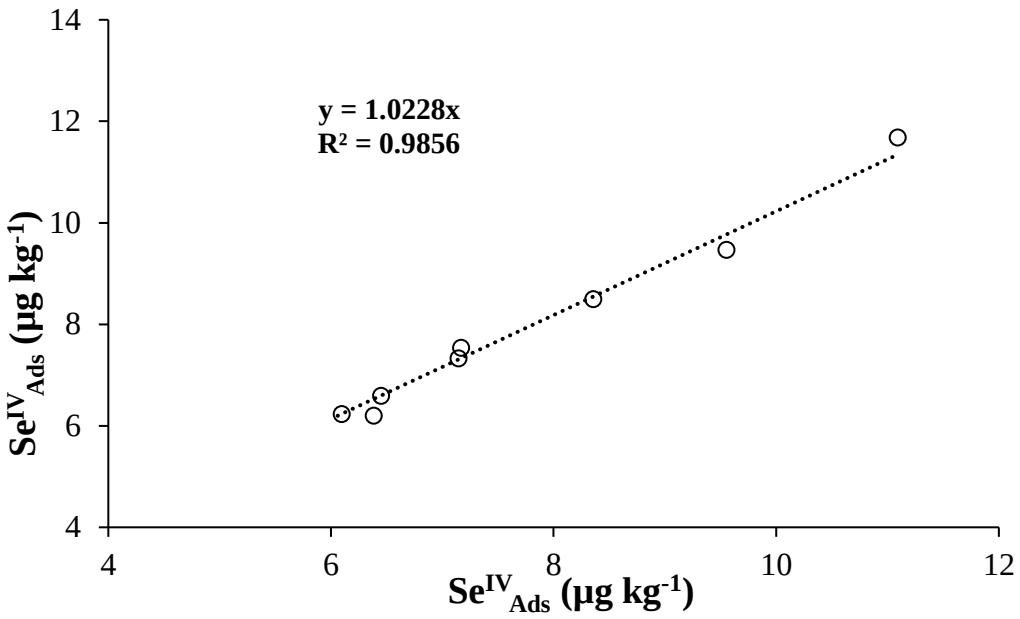


Figure 5.1. Phosphate-extractable selenite (Se^{IV}_{Ads}; µg kg^{-1}) as a function of the total phosphate extractable selenium (Se_{Ads}; µg kg^{-1}) for all soils collected from the demonstration plots in lower Shabelle, Somalia (n=9).

Grain Se

There was no correlation observed between the Se concentration in grains and soil pH, LOI, TIC and TOC, reflecting the lack of correlation with soil Se fractionation. However, there was an excellent correlation between the Se and iodine concentrations in the grains ($r=0.838$; $p<0.001$), and grain Se and Zn ($r=0.865$; $p<0.001$). There was a significant correlation between grain Se concentrations and the concentration of potassium (K) in soil ($r=-0.766$; $p<0.05$) and Zn ($r=0.851$; $p<0.001$) contents in the soil.

Soil Zinc

Almost no correlations were observed between the soil Zn content and soil characteristics. The exceptions were soil Ca and Zn concentrations ($r=0.819$; $p< 0.001$) and soil Zn concentration with I_{Ads} ($r=-0.687$; $p< 0.05$).

Grain Zn

The grain Zn concentration was positively and significantly correlated with Zn concentration in soils ($r=0.887$; $p< 0.001$). Similarly Kumar and Babel, (2011) reported that grain content of Zn increased with increased levels of zinc in soil. Grain Zn concentration significantly correlated with the soils Ca content ($r=0.683$; $P<0.05$).

5.3.5 Estimated dietary intakes

Macronutrients

Calcium concentration in grain ranged from 37.2 to 1600 mg kg^{-1}, with a mean of 660 mg kg^{-1}, median 868 mg kg^{-1}. The Ca concentrations (mg kg^{-1}) in grain samples were significantly different at the P-value 0.001 and followed the order: mung bean (1280; SD 233) > cowpea (919; SD 56.3) > maize (66.8; SD 18.6). Estimated dietary Ca intake from maize was therefore on average 10.8 mg d^{-1} which is much lower than the RDA of 1000-1200 mg d^{-1} reported in Table 5.6.

Potassium concentration in grain ranged from 3490 to 16200 mg kg^{-1}, with a median 13300 mg kg. The K concentration in grain samples were significantly different at the P-value 0.001 and followed the order mung bean (15400; SD 428) > Cow pea (13700, SD 507) > maize (4370; SD 554). Estimated potassium intake from a maize-based ration was on average 707 mg d^{-1} which is also much lower than RDA values of 1600-3500 mg d^{-1} reported in Table 5.6.

Magnesium concentration in grain ranged from 973 to 2420 mg kg^{-1}, with a mean of 1700 mg kg^{-1}, median 1920 mg kg. The mg concentration in grain samples were significantly different between crops at the P-value 0.001 and followed the order mung bean (2130; SD 203), Cow pea (1980, SD 60.1) > maize (1230; SD 171). Magnesium intake from maize was on average 200 mg d^{-1} which is also much lower than RDA values of 310-420 mg d^{-1} reported in Table 5.6.

Micronutrients

Zn

Zinc concentration in grain ranged from 23.0 to 38.9 mg kg^{-1}, with a mean of 30.8 mg kg^{-1}, median 30.3 mg kg. The Zn concentration in grain samples were significantly different between crops at the P-value 0.001 and followed the order Cow pea (37.2 mg kg^{-1}; SD 1.53) > mung bean (30.9 mg kg^{-1}; SD 2.10) > maize (27.6 mg kg^{-1}; SD 2.97). Intake of Zn is 4.47 mg d^{-1} and is therefore lower than the RDA of 8.0-11.0 mg d^{-1} reported in Table 5.6.

Fe

Iron concentration in grain ranged from 14.6 to 42.0 mg kg^{-1}, with a mean of 29.5 mg kg^{-1}, median 34.2 mg kg^{-1}. The Fe concentration in grain samples were significantly different between crops at the P-value 0.001 and followed the order Cow pea (38.3 mg kg^{-1}; SD 2.47),

mung bean (37.7 mg kg^{-1}; SD 3.19) > maize (19.1 mg kg^{-1}; SD 2.81). Estimated intake of Fe is 3.09 mg d^{-1} and is lower than the RDA of 8.00-11.0 mg d^{-1} as reported in Table 5.6.

Cu

Copper concentration in grain ranged from 1.46 to 15.7 mg kg^{-1}, with a mean of 6.29 mg kg^{-1}, median 4.71 mg kg^{-1}. The Cu concentration in grain samples were significantly different between crops at the P-value 0.001 and followed the order mung bean (12.9 mg kg^{-1}; SD 1.11) > Cow pea (5.27 mg kg^{-1}; SD 0.634) > maize (1.84 mg kg^{-1}; SD 0.202). Intake of Cu was 0.298 mg d^{-1} and which is lower than the RDA of 0.9 mg d^{-1} reported in Table 5.6.

Mn

Manganese concentration in grain ranged from 4.76 to 24.6 mg kg^{-1}, with a mean of 12.6 mg kg^{-1}, median 14.1 mg kg^{-1} (Fig. 6.1a). The Mn concentration in grain samples were significantly different between crops at the P-value 0.001 and followed the order Cow pea (21.5 mg kg^{-1}; SD 3.11) > mung bean (15.1 mg kg^{-1}; SD 0.967) > maize (6.27 mg kg^{-1}; SD 1.07). Intake of Mn is 1.02 mg d^{-1} which is slightly lower than the RDA values 1.8-2.3 mg d^{-1} in Table 5.6.

Mo

Molybdenum concentration in grain ranged from 401 to 20100 µg kg^{-1}, with a mean of 8610 µg kg^{-1}, median 10700 µg kg^{-1}. The Mo concentration in grain samples were significantly different between crops at the P-value 0.001 and followed the order mung bean (16300 µg kg^{-1}; SD 2670) > Cow pea (13300 µg kg^{-1}, SD 2770) > maize (503 µg kg^{-1}; SD 57.2). Intake of Mo is 81.5 µg d^{-1}, which is higher than the RDA of 45 µg d^{-1} recommended by the USA, reported in Table 5.7; the RNI by the UK is higher and is varying from 50-400 µg d^{-1}.

Cr

Chromium concentration in grain ranged from 0.00 to 160 µg kg^{-1}, with a mean of 46.6 µg kg^{-1}, median 32.1 µg kg^{-1}. The Cr concentration in grain samples were significantly different between crops at the P-value 0.002 and followed the order maize (76.6 µg kg^{-1}; SD 7.42) > mung bean (31.3 µg kg^{-1}; SD 13.2) and Cow pea (9.49 µg kg^{-1}, SD 7.42). Intake of Cr was also estimated and was 12.4 µg d^{-1} and was lower than the RDA of 25-35 µg d^{-1} in Table 5.7.

Ni

Nickel concentration in grain ranged from 259 to 5510 µg kg^{-1}, with a mean of 2420 µg kg^{-1}, median 3040 µg kg^{-1}. The Ni concentration in grain samples were significantly different

between crops at the P-value 0.001 and followed the order cowpea (4000 µg kg^{-1}, SD 605), mung bean (3690 µg kg^{-1}; SD 781) > maize (676 µg kg^{-1}; SD 196). Intake of Ni is 109 µg d^{-1} which is in the range of the RDA of 100-300 µg d^{-1} in Table 5.7.

Se

Selenium concentration in grain ranged from 11.0 to 266 µg kg^{-1}, with a mean of 56.3 µg kg^{-1}, median 32.4 µg kg^{-1}. The Se concentration in grain samples were significantly different between crops at the P-value 0.001 and followed the order Cow pea (158 µg kg^{-1}; SD 115) > mung bean (41.7 µg kg^{-1}; SD 11.3) and maize (16.7 µg kg^{-1}; SD 3.92). Intake of Se from a maize diet was estimated at 2.70 µg d^{-1}, which is therefore lower than the RDA of 70 µg d^{-1} in Table 5.7.

I

Iodine concentration in grain ranged from 0.361 to 41.2 µg kg^{-1}, with a mean of 14.6 µg kg^{-1}, median 13.0 µg kg^{-1} (Fig. 6.1a). The I concentration in grain samples were generally very low and did not different between crops significantly (P>0.05). The iodine content of maize was 10.0 µg kg^{-1}. Intake of I from a maize diet is very low and was estimated at 1.62 µg d^{-1} which is lower than the RDA of 150 µg d^{-1} reported in Table 5.7.

Table 5.6. Estimated dietary intakes for selected nutrient element; (Ca, K, Mg, Zn, Fe, Cu and Mn) from maize. Calculations are based on measured maize elemental compositions (ICP analysis; mg kg^{-1}) integrated with the mean per capita consumption of maize (kg $capita^{-1}$ $year^{-1}$) from two east African countries (Ethiopia and Kenya).

Nutrient Element	Measured Concentration	Dietary intake	RDA
	(mg/kg)	mg per capita per day	
Ca	67.0	10.8	1000-1200
K	4370	707	1600-3500
Mg	1230	200	310-420
Zn	27.6	4.47	8.0-11.0
Fe	19.1	3.09	8.0-18.0
Cu	1.84	0.298	0.9
Mn	6.27	1.02	1.8-2.3

Source: Required Daily Allowance, USA

Table 5.7. Estimated dietary intakes for selected nutrient element; (Mo, Cr, Ni, Se and I) from maize. Calculations are based on measured maize elemental compositions (ICP analysis; µg kg^{-1}) integrated with the mean per capita consumption of maize (kg $capita^{-1}$ $year^{-1}$) in two east African countries (Ethiopia and Kenya).

Nutrient Element	Measured Concentration	Dietary intake	RDA
	(µg/kg)	µg per capita per day	
Mo	503	81.5	45
Cr	77.0	12.4	25-35
Ni	676	109	100-300
Se	17.0	2.70	70
I	10.0	1.62	150

Source: Required Daily Allowance, USA

5.4 Conclusion and discussion

Selenium

The total Se content measured in the soil samples collected from the demonstration sites in Somalia ranged from 0.39 to 0.48 mg kg^{-1}, with an average of 0.42 mg kg^{-1}. According to the Se_{Tot} values measured in these soils, these soils are regarded as Se deficient soils. Soils containing selenium levels less than 0.6 mg kg are considered deficient for both animals and humans (Fordyce, 2005; Gupta and Gupta, 2002). In addition to the low Se_{Tot}, both the soluble Se (Se_{Sol}) and the adsorbed Se (Se_{Ads}) were also low, accounting for only a small portion of the *Se_{Tot}, with an* average of 0.80 µg kg^{-1} and 7.59 µg kg^{-1} respectively. The Se_{Sol} and the Se_{Ads} combined accounted on average for 2.1% of Se_{Tot}, this indicates the low bioavailability of Se in the Somali agricultural soils. Similar low bioavailable Se was reported for agricultural soils from Malawi (Chilimba et al., 2011). Speciation of the inorganic Se forms has revealed that it was mainly in the form of selenite, nearly a third (31.7%) of the soluble Se was in the form of selenite, while 25.0% was selenate. Almost all the Se species detected in the Se_{Ads} was selenite (99%), this is consistent with the strong selenite adsorption reported in the literature (Stroud et al., 2010). These results (although limited to demonstration plots) suggest that the organically bound and the recalcitrant soil Se may govern the bioavailability of Se in the Somali agricultural soils.

At these low Se levels in soils the Se concentration in the corresponding crops is expected to be low as well. Selenium concentration in grain was low and varied between the three crops: Cow pea (158 µg kg^{-1}; SD 115) had the highest Se content, followed by mung bean (41.7 µg kg^{-1}; SD 11.3) and maize (16.7 µg kg^{-1}; SD 3.92). The Se contents of maize (most staple crop in Somalia) and mung bean were below the level (50 -100 µg kg^{-1}) required for adequate human nutrition (Gissel-Nielsen et al., 1984). Interestingly, the Se content of Cow pea was relatively higher, and therefore is likely to satisfy the dietary Se requirement more than maize, i.e. if the appropriate amounts are taken up in the ration.

Since maize is the main staple food in Somalia, the dietary Se intakes from a maize based diet was estimated using a mean per capita consumption of 162 g d^{-1} (averaged from east African countries) and an average grain *Se* concentration of 16.7 µg kg^{-1} (measured in this study); the estimated Se intake from maize is therefore 2.70 µg *Se* $person^{-1}$ d^{-1}; which is lower than the values reported by Chilimba et al., (2011) from surveys in Malawi (6.7 µg *Se* $person^{-1}$ d^{-1}); this is may be due to the fact that the median maize grain Se concentration in Malawi was slightly higher 19.0 µg kg^{-1} than maize in Somalia.

Iodine

TMAH-extractable I (I_{TMAH}) results show that the soils contain a high I content of 6.4 mg kg^{-1} which is significantly greater than the worldwide mean of 3.0 mg kg^{-1} (Johnson et al., 2003). According to (Fordyce et al., 2000; Watts and Mitchell, 2009) soils containing iodine levels less than 3.1 mg kg^{-1} are considered as iodine deficient soils. Knowledge of total iodine concentration was further assisted with fractionation and speciation of the total iodine for predicting the bioavailability in these soils. Both soluble I and the adsorbed I were low accounting together for 2%; the I_{Sol} varied from 29.9 to 73.4 µg kg^{-1} accounting for less than 1% (with a range of 0.5% to 1.2%) of the total soil iodine extracted by TMAH (I_{TMAH}).

Similar low bioavailable I was reported for agricultural soils from Malawi (27 µg kg^{-1}; 1% of the total I), significantly higher bioavailability is reported in soils from Morocco and UK (10% of total) (Johnson et al., 2002; Watts et al., 2015). The concentration of iodine extracted with KH_2PO_4 (I_{Ads}) varied from 77.0 – 148 µg kg^{-1} which accounted for 1% (with a range of 1.2 – 2.4%) of I_{TMAH}. Speciation of the inorganic I forms has revealed that Iodide (I^-) was the main inorganic species found in the nitrate extracts representing 89% of the detectable inorganic I, while iodate (IO_3^-) concentration was only 7.6% of I_{Sol}. Similarly, in the adsorbed fraction (I_{Ads})

iodide was the dominant form representing (69.7%) while iodate accounted for (30%) of the inorganic I.

The I concentration in grain samples were generally very low, the iodine content of maize was 10.0 µg kg^{-1}, this is consistent with the fact that the native iodine content of most foods is low (Eastman and Zimmermann, 2018). Intake of I from a maize diet was estimated using a mean per capita consumption of 162 g d^{-1} (averaged from east African countries) and an average grain *Se* concentration of 10.0 µg kg^{-1} (measured in this study). It was found that maize can only supply 1.62 µg d^{-1} representing 1% of the RDA of 150 µg d^{-1}.

Dietary intakes of Ca from maize based diet was also low; the estimated dietary Ca intake from maize was on average 10.8 mg d^{-1} which cannot supply the RDA of 1000-1200 mg d^{-1}. Although it was expected that the Ca supply from these crops would be high due to the high Ca content of calcareous soils in arid and semi-arid regions, however low contribution of cereal crops for Ca supply to human intakes is reported in previous studies (Graham et al., 2001; White & Broadley, 2005). Results reported from cereals in Sweden show much higher concentrations of Ca (363–458 mg kg^{-1}), therefore providing higher dietary intake f 1110 mg d^{-1} as well.

Agricultural practices such as the introduction of Se fertilization, for example those reported in Malawi or in Finland can be used as an intervention tool that can strength the link between agriculture, nutrition, and health to tackle micronutrient malnutrition.

In order to address dietary nutrient deficiencies in Somalia, careful attention should be given to the nutrient content of maize. Maize which is the main staple crop is also regarded a carrier of essential nutrients to the Somali population. In addition, it is important to explore the exact amount of the per capita consumption. Further, it is important to explore the nutrient composition of sorghum grown in Somalia, as it is another staple crop in the country. Therefore, further work is recommended to extend this work into a wider range of Somali agricultural soils and their corresponding soils; a nationwide dietary survey is also required to confirm the generality of the conclusion above.

6. Selenium adsorption and fixation on calcareous and gypsiferous minerals

6.1 Introduction

Soil Se is primarily controlled by underlying geology, however its retention-release, speciation and uptake by plants are more important than its total concentration and are determined by numerous bio-physico-chemical parameters (Barker and Pilbeam, 2015; Broadley et al., 2006; Dhillon and Dhillon, 2003; Fordyce, 2013a; White et al., 2007). These include pH (Chilimba et al., 2011; Joy et al., 2015; Lakin, 1973), redox condition (Elrashidi et al., 1987; Krivovichev et al., 2011; Lakin, 1973), soil texture (Kabata-Pendias and Szteke, 2015), mineralogy (Myriam Duc et al., 2003; Goldberg and Glaubig, 1988; Hayes et al., 1987; Masscheleyn et al., 1990; Rajan, 1979; Su and Suarez, 2000), organic matter content (Johnsson, 1991) and competing ions (Stroud et al., 2010). Knowledge regarding Se interaction with soil phases is important. Selenium interaction with soil organic matter and iron oxides has been extensively studied (e.g. (Duc et al., 2006; Gissel-Nielsen et al., 1984; Peak and Sparks, 2002) and the adsorption of Se on calcareous minerals has been noted by numerous investigators (Dhillon and Dhillon, 1999; Goldberg and Glaubig, 1988), however these studies investigated whole soils and knowledge regarding specific interactions with calcite is more limited. In arid regions of the world where calcareous and gypsiferous soils cover large proportions of the available agricultural land added Se may be rapidly adsorbed onto carbonate (Goldberg and Glaubig, 1988); and calcium sulphate phases (Jones et al., 2017). Understanding this fixation of Se is important as subsequent plant uptake may be lower rendering biofortification treatments less effective.

Calcite ($CaCO_3$) is one of the most abundant minerals on the surface of the Earth, it is abundant in calcareous soils, groundwater aquifers and marine sediments (Aurelio et al., 2010). Calcite belongs to the carbonate mineral group which is divided into calcite and aragonite groups, and of which calcite is the most dominant and stable polymorph. The chemical compositions of calcite and aragonite are similar, but they differ in their crystal structure with calcite having a trigonal crystal system in contrast to aragonite where the crystal structure is orthorhombic.

Carbonate minerals play a significant role in controlling the geochemistry of other elements, through for example precipitation of siderite ($FeCO_3$), rhodochrosite ($MnCO_3$), strontianite ($SrCO_3$), smithsonite ($ZnCO_3$), witherite ($BaCO_3$), and cerussite ($PbCO_3$). Several studies have characterized how different anions incorporate and interact with calcite mineral surfaces cations (Alexandratos et al., 2007; Davis et al., 2000; Dove and Hochella, 1993; G. Montes-Hernandez et al., 2009; Paquette and Reeder, 1995; Rimstidt et al., 1998; Stipp et al., 2006)

Calcite interactions with trace elements are described as a surface-exchange process, where cations are exchanged with surface Ca ions and anions are substituted for surface CO_3 (Sø et al., 2008; Zachara et al., 1990, 1991). Batch adsorption isotherms can be used to confirm the validity of the surface-exchange reactions.

Calcite has varying affinities for adsorbing ions such as iron, nickel, strontium, cadmium, lead, copper, manganese, zinc, phosphate and arsenate (Andersson et al., 2014; Green-Pedersen et al., 1997; Reeder, 1996; Zachara et al., 1991), the degree of adsorption is dependent on the chemistry of the solution, pH, temperature and the ionic strength of the co-solutes (Cowan et al., 1990; Zachara et al., 1991). Sorption may vary depending on the species of the element for example Sø et al. (2008) found that arsenate is preferred over arsenite.

Although there is relatively small body of literature that is concerned with selenium sorption on calcite most, focusing on selenite, have shown that calcite is a sink for Se in carbonate rich soils and groundwater aquifers. For example, Cowan et al. (1990) investigated selenite adsorption in calcite suspensions over a pH range of 7.0 to 9.5, a range of selenite concentrations, and in the presence of competing co-existing anions such as sulphate and phosphate. They reported that selenite adsorption on $CaCO_3$ occurred in a manner consistent with its exchange at anionic specific surface sites saturated with CO_3^{2-}/HCO_3^-. They found that selenite sorption was decreased by the presence of competing anions and was limited to less than 5% of the total anionic specific surface sites. Aurelio et al. (2010) investigated whether selenite could be incorporated into calcite by substitution at CO_3 sites. They used a combination of macroscopic and nanoscopic studies including neutron diffraction, Extended X-ray Absorption Fine Structure (EXAFS) spectroscopy and theoretical modelling and found that calcite was able to accommodate up to 27.6 mmol Se kg^{-1} of solid within its structure by isomorphic substitution. Similarly, Montes-Hernandez et al. (2011) described how selenite incorporation into the calcite structure occur by employing synchrotron X-ray adsorption spectroscopy (XAS).

Although selenite substitution of CO_3 in calcite is preferred both Se species have been reported to substitute for carbonate in calcite as it grows (Aurelio et al., 2010; Heberling et al., 2014; Reeder et al., 1994; Staudt et al., 1994). Reeder et al. (1994) showed that selenate can reside in the CO_3 site in the calcite upon incorporation during growth. Their interpretation is similar to that reported by Lamble et al., (1995) and both studies are significant because they provide the first evidence that tetrahedral selenate substitution for CO_3 in calcite is possible. The work

done by Cheng et al., (1997) contradicts that of Reeder et al., (1994) and Lamble et al., (1995); they described the adsorption of selenite and selenate from water onto the surface of a single crystal of calcite using X-ray standing wave (XSW) spectroscopy. Their study suggested that calcite adsorbs selenite with a coverage of 0.02 monolayer equivalents but not selenate. A recent in-situ time-lapse atomic force microscopy (AFM) study (Renard et al., 2013) investigated organic and inorganic Se species incorporation into the calcite structure at room temperature (for Se concentrations in the range 1-400 mg L^{-1}) and found that selenite concentrations up to 70 mg L^{-1} could be incorporated but no evidence for selenate incorporation into calcite, only catalysis of the step progression rate.

It has also been shown that the presence of selenate and selenite in solution can increase the rate of calcite dissolution with the formation of Se-calcium surface precipitates due to the increased Ca concentration in the fluid closest to the mineral surface (Putnis et al., 2013). For selenite this precipitate is thought to be $CaSeO_3.H_2O$ based upon SEM observations and calcite has been suggested as an important reservoir of selenite in soils (Putnis et al. 2013). Selenite has also been reported to be incorporated in vaterite (μ-$CaCO_3$) (Aurelio et al., 2010).

The existing body of literature on Se incorporation onto the calcite structure, does not consider the isotopic exchangeability or lability of the Se, the effect of equilibration time on sorption or desorption. There is also little published data on Se sorption on gypsum, and therefore the nature of interaction between the different Se species and gypsum remains unclear. Jones et al. (2017) studied selenium and salt mobilization in wetland and arid upland soils, they found that soluble Se was most likely regulated by the solubility of a mixed sodium selenite-sulfate co-precipitate.

This study therefore aims to provide new insights to advance the understanding of selenite/selenate sorption on calcite, gypsum and on calcareous and gypsiferous soils, by employing time series batch experiments, desorption experiments, aging experiments and the use of ^{77}Se tracers to understand selenite lability and fixation. Incubation and co-precipitation experiments were also conducted under conditions similar to those of real environments. A series of EXAFS studies using greater Se concentrations were also undertaken to confirm the nature of the bonding of Se by the calcite.

The objectives of the study were to address the following questions:

1. To what extent do calcite/gypsum adsorb Se^{IV} and Se^{VI} and what are the differences in adsorption of the two species?

2. Do calcite/gypsum show time-dependent sorption of Se?

3. Is Se adsorption on calcite and gypsum 'reversible' (i.e. is there desorption hysteresis)?

4. Is the adsorption weak (labile) or strong?

5. Is Se sorption/fixation affected by changing the partial pressure of CO_2?

6. Is Se fixation in calcareous and gypsiferous soils a consequence of the presence of calcite and gypsum minerals?

6.2 Materials and methods

6.2.1 Materials, chemicals and standards

Analytical grade calcite and gypsum (calcium carbonate, $CaCO_3$; calcium sulphate, $CaSO_4.2H_2O$) was purchased from Thermo Fisher Scientific and used as received. Multi-isotopic selenite/selenate stocks of 1000 mg L^{-1} were prepared by dissolving sodium selenite/selenate salts in MilliQ water and was further diluted as appropriate.

6.2.2 Characterization of the calcite, gypsum and soils

Two soils, one predominantly calcareous and one containing gypsum were chosen and fully characterized, including determination of their carbonate and selenium contents as described in Chapter 2 Sections 2.3.2.4, 2.3.2.5, 2.4.4 and 2.4.5. The $CaCO_3$ content of the soil was determined by multiplying TIC by 8.3 (mass of $CaCO_3$/mass of C). The S content of the soils was determined after aqua regia digestion.

6.2.3 Sorption Experiments

Batch experiments were conducted at room temperature and at constant ionic strength using 0.01 M Ca $(NO_3)_2$ or 0.01 M $CaCl_2$ as the background electrolyte. Duplicate samples with a solid: solution ratio of 1:30 kg L^{-1} were prepared in 50 mL polyethylene centrifuge tubes and equilibrated for up to 7 days. Pre-equilibration results in calcite with a more uniform particle diameter through recrystallization, stabilising the calcite surface and enhancing the reproducibility of sorption (Ahmed et al., 2008; Elzinga et al., 2006). After pre-equilibration multi-isotopic Se was added and samples were shaken at room temperature for a pre-determined contact time (up to 21 days). The Se spike was prepared in Milli-Q water to ensure that there was no acidification and hence no pH change in the system.

The partial pressure of CO_2 was controlled, by employing three bubbling systems, (i) continuous bubbling of 4% CO_2, (ii) continuous bubbling of air, or (iii) swapping between bubbling of 4% CO_2 and air at three-day intervals. Attainment of equilibrium was monitored

by sampling daily and measuring pH and Ca and Se concentrations. Subsamples were collected at each contact time and centrifuged at 3500 rpm for 30 minutes before filtering through 0.22 µm PES membrane filters. Filtered samples were initially preserved by dilution in 0.05 M NH_4- EDTA (dilution factor of 1.2), however this was later amended to also include further dilution in 2% HNO_3 (dilution factor of 6) in order to reduce the calcium concentration and minimise the effect of the suppression during analysis. Samples were kept at 4^{o}C until analysis (Chapter 2 Section 2.4.8).

To assist in the design of the sorption experiments, a series of pilot experiments were carried out to establish the typical sorption capacities for Se species on calcite and gypsum. It is important to work in a realistic concentration range and this can be achieved by selecting a range encompassing typical Se concentrations in natural waters or concentrations in the soil solution. The highest Se concentration observed in Somali ground and surface water data (Chapter 3) was selected. The maximum target equilibrium concentration of the sorption experiment was one order of magnitude higher than the highest Se concentration recorded in groundwater, this was done by interpolation in Excel. Experimental conditions and parameters selected are given in Table 6.1.

Table 6.1. Summary of conditions for the batch experiments, the solid phase is either 1 g of calcite or gypsum

Trial	Volume (mL)	Electrolyte	Pre-equilibration	Concentration (mg L^{-1})	Species	Time (days)
1	30	0.01 M Ca $(NO_3)_2$	3 days	0, 1, 2, 3, 4 & 5	Se^{IV} & Se^{VI},	1-7
2	30	0.01 M Ca $(NO_3)_2$	1 week	0.025, 0.1, 0.3, 0.7 & 1	Se^{IV}	1-21
3	30	0.01 M Ca $(NO_3)_2$	1 week	0.005, 0.01, 0.015, 0.025 & 0.050	Se^{IV}	1-21
4	30	0.01 M Ca $(NO_3)_2$	1 week	0.005, 0.01, 0.015, 0.025 & 0.050	Se^{VI}	1-21

6.2.4 Determination of Isotopically Exchangeable Se

To determine isotopically exchangeable (E-value) Se, a spike of 0.4 mL of a 5 mg L^{-1} $^{77}Se^{IV}$ stock was added to the systems 24 hours before the designated contact time i.e. on days 6, 13 and 20, to allow enough time for the tracer to mix into the system.

6.2.5 Desorption Experiments

Desorption studies are important, in that they help to demonstrate that uptake is due to adsorption rather than precipitation or solid-state diffusion. Desorption experiments commenced after 21 days of equilibration using a process whereby half of the supernatant volume was replaced with an identical volume of a pre-equilibrated desorbing solution and shaken for 24 h. This process was repeated three times over three days. A solution pre-

equilibrated with the solid phases (calcite or gypsum) was used rather than using a freshly background electrolyte to ensure that the ionic strength of this solution was as close a match as possible to the solution being removed.

6.2.6 Speciation

Speciation analysis (see Chapter 2 Section 2.4.6) was performed on stock solutions and representative samples in order to monitor if there were changes occurring. After filtering the supernatants, the samples were split into two sets, one set was preserved for total selenium analysis. The other was kept in the cold storage without addition of a chelating agent until speciation analysis. Samples from all the contact times of 1, 3, 7, 14 and 21 days were included, and among the different treatment levels, the lowest concentration treatments i.e. the 25 $\mu g\ L^{-1}$ were systematically selected.

6.2.7 EXAFS Sample Preparation

Suspensions for the XAS work compromised 4 g of solid (i.e. calcite, gypsum, calcareous and gypsiferous soil that also contained calcite); 20 mL of solution (18 mL of MQ water + 2 mL of stock solution); selenium stock solution. The stock solution was Na –selenate prepared by dissolving 14.93 mg salt in 50 mL MQ water or Na-selenite 12.50 mg of the salt in 50 mL of MQ water. The calcareous soil was BW-R and the calcareous soil that had substantial gypsum selected was BB-I. The solid phases were weighed into centrifuge tubes, and treated with either selenite or selenate to give a final concentration of 30 mg L^{-1} and 25 mg L^{-1} respectively.

Aged samples were prepared on the 25th Jan 2018 and fresh samples on 16th July 2018. In order to allow the Se added to mix with the solid phases fresh samples were shaken overnight on the end over end shaker. Then all samples (i.e. both aged and fresh samples) were centrifuged (20 minutes at 4000 rpm) on the 17th of July 2018 and a portion of the supernatant was sampled and acidified for ICP analysis. Plug of soils was briefly washed with MQ water (5 mL), centrifuged and decanted leaving a wet paste for XAS analysis. In addition, supernatants were collected 10 ml for ICP-MS analysis (1:100 dilutions) and the remaining solution were kept for speciation analysis.

A co-precipitated calcite sample was prepared by bubbling first air, then CO_2, and then air again through the suspension over a period of 10 days.

The concentration of Se in the supernatant solutions was measured by ICP-MS to enable calculation of sorbed Se;

$$Se_{Ads} = C_i \left(\frac{V_i}{1000}\right) \times \left(\frac{V_r}{V_i}\right) \times \left(\frac{V_r}{V_w}\right)^n \quad \text{Equation 6.1}$$

Where Se_{Ads} is the mass of Se (µg) in the centrifuged sample plug and entrained solution, *Ci* is the concentration of Se (µg L^{-1}) in the supernatant solution following initial equilibration, *Vi* is the initial solution volume (mL) equilibrated with the solid material (mL), *Vr* is the volume (mL) of entrained liquid remaining after centrifugation, *Vw* is the total volume (mL) of the wash solution (mL), and *n* is the number of wash steps.

6.2.8 EXAFS Data Collection and Analysis

XAS spectra at the Se K-edge (12658 eV) were collected in fluorescence mode on the I20 scanning beamline at the Diamond Light Source (Oxfordshire, UK) using a Si (111) monochromator and calibration with a Bi-foil (90526 eV). All samples were analysed as pastes held in an Al holder with kapton windows and maintained at a temperature of -196 ˚C using a liquid nitrogen cryostat (Oxford instruments, Abingdon, UK) to minimise the effects of radiation damage. Data was collected using a 64-pixel solid-state Ge detector (Canberra, Oxfordshire, UK). For each sample a minimum of 6 scans were collected due to the dilute nature of the samples and the beam position was adjusted between each scan to minimise reduction of Se. For the soils the k-range of the spectra was limited to c. 10 Å due to the presence of a Pb L3 absorption edge at 13035 eV.

Multiple XAS scans were summed and averaged to reduce the signal to noise ratio using Athena v 0.9.25 (Ravel and Newville, 2005) before fitting using Artemis v 0.9.25 (Ravel and Newville, 2005). Goodness of fit was determined where R-values were <0.02 and Debye–Waller factors (σ^2) were ~0.02.

6.2.9 Modelling and calculations

The total adsorbed Se in mg kg^{-1} was calculated from Equation 6.2:

$$Se_{Ads} = (C_I - C_F) \times \frac{\mathrm{V}}{\mathrm{W}} \quad \text{Equation 6.2}$$

Where C_i is the initial concentration (µg L^{-1}), and C_f is the final concentration (µg L^{-1}). Adsorption isotherms where constructed by plotting the equilibrium solution concentration (x-axis) against the adsorbed concentration (y-axis). The Microsoft Excel Solver function was

used to predict the constants of the Freunlich and Langmuir isotherm models by minimising the sum of error squared.

The amount of Se desorbed was calculated by first considering the total amount adsorbed:

$$Se_{TA} = C_I \times V_{tot} \quad \text{Equation 6.3}$$

Where Se_{TA} is the total Se amounts at adsorption stage (µg), and V_{tot} is the total volume (mL), then the amount removed by a single desorption step was calculated:

$$Se_{rem} = Se_{TA} \times V_{rem} \quad \text{Equation 6.4}$$

The amount removed was then subtracted from the total amount to get the new concentration after the desorption step:

$$Se_{des\,1} = Se_{TA} - Se_{rem} \quad \text{Equation 6.5}$$

Where Se_{des1} is total Se concentration at the desorption stage one and this process repeated for the second and third desorption steps.

6.3 Results and Discussion

6.3.3 Characterization of the soils and mineral phases

The characteristics of the soils selected for the adsorption studies are shown in Table 6.2. They have low organic matter content and high total inorganic carbon. A high soil pH values ~8 confirms the alkalinity of these soils, which is primarily caused by weathering calcium carbonate-rich parent material in arid environments. The percentage of $CaCO_3$ in the calcareous and gypsiferous soils was 24.6% and 19.09% respectively. No S content was detectable in the calcareous soil, but in the gypsiferous soil an S concentration of 2240 mg kg^{-1} was measured.

Table 6.2. General characteristics of the experimental soils (n=2). Values are arithmetic mean of triplicate measurements ± the standard error.

Soil	pH	LOI (%)	TIC (%)	TOC (%)	Total Se (mg kg^{-1})	Se $_{TMAH}$ (mg kg^{-1})	S_A (mg kg^{-1})
C-S	8.14	0.21	2.96	0.79	0.300	0.030	n.d
G-S	7.87	0.26	2.30	0.65	0.332	0.040	2240

Note: C-S: Calcareous soil; G-S: Gypsiferrous soil

Measurements of Se_{tot} and Se_{TMAH}, differed by an order of magnitude possibly because Se is fixed in soil phases e.g. carbonates that are not accessed by TMAH extraction. If Se were

present in an organically bound form then a greater agreement in Se_{tot} and Se_{TMAH} would be expected. Chemical analysis of the solid phase starting materials demonstrated that they contained no detectable concentrations of Se.

6.3.4 Pre-Equilibration Time

Prior to the batch experiment, suspensions of the pure phases were characterized by equilibrating in 0.01 M Ca $(NO_3)_2$ for a week to mimic conditions of the subsequent batch experiments. The aim of this was to monitor pH changes and Ca content (Fig. 6.1) as a function of time to determine when equilibrium had been achieved and establish a suitable pre-equilibration time for subsequent experiments. The average pH (n =10) of the calcite suspensions after one week was 7.21±0.18, minimum and maximum pH were 6.6 and 7.6 respectively. Dissolved Ca were very constant with an average concentration of 382 ±3.6 mg L^{-1}. It is evident from both the pH and Ca curves that a one-week pre-equilibration period was enough to attain equilibrium before Se addition.

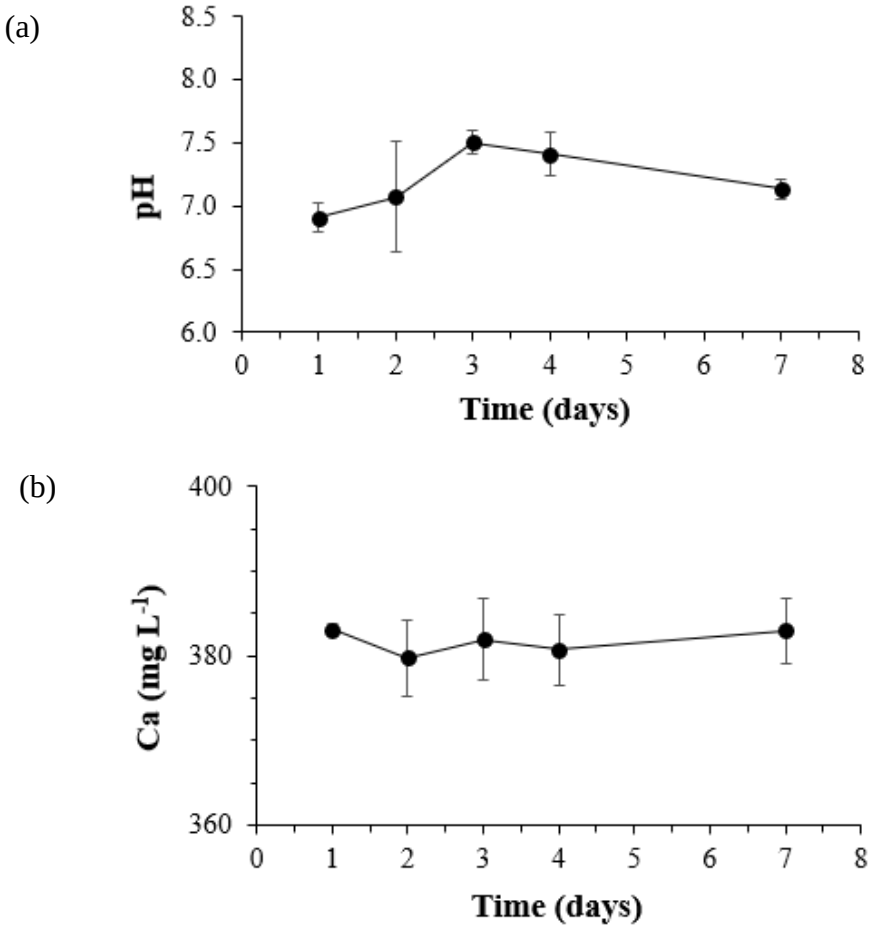


Figure 6.1. Changes in (a) pH and (b) dissolved Ca concentration in calcite suspensions; each measurement is an average of ten replicates. Systems were at ambient conditions with no pCO_2 control.

6.3.5 Selenium Sorption on Calcite

Selenium sorption behaviour onto calcite was initially investigated as a function of solid: solution ratio, Se concentration (0.005 mg L^{-1} – 5 mg L^{-1}), species (selenite, selenate), and contact time (1, 3, 7, 14 and 21 days).

6.3.5.1 Effect of the solid: solution ratio

The effect of solid: solution ratio on Se sorption to calcite was studied using a single initial Se concentration of 1 mg L^{-1} at three contact times (1, 7 and 14 days) at solid: liquid ratios of 0.01, 0.03, 0.05 and 0.1. The aim was to test the hypothesis that Se sorption on calcite is dependent on the solid: solution ratio. The ratio of solid-to-solution appears to influence Se sorption on calcite (Figure 6.2). As the amount of solid phase was increased the surface available for Se sorption was also increased. The data fitted best a power trendline (Figure 6.2). Regression

statistics were also obtained (R^2 = 0.799, p value = 0.003; R^2 = 0.797, p value = 0.003; R^2 = 0.804, p value = 0.003) for days 1, 7 and 14 respectively. A consistent trend for all the three contact times was observed.

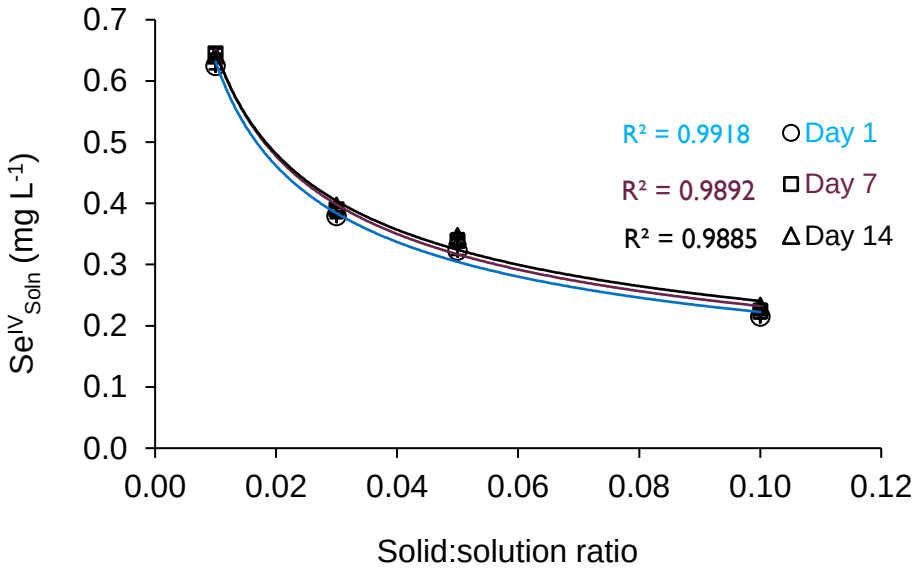


Figure 6.2. Selenite adsorption on calcite as a function of solid: solution ratio. Initial Se concentration was 1 mg L^{-1}.

6.3.5.2 Effect of Se concentration, Se species and contact time

The results of experiments using Se concentrations in the range 0.005 mg L^{-1} – 5 mg L^{-1} are shown in Figure 6.3. Strong adsorption of selenite was observed with a K_d value of ~130. Selenate adsorption was lower with a K_d value of ~5. Adsorption occurred rapidly with the majority (~80%) of the added Se adsorbed within 24 hours. The shape of the adsorption isotherms also suggests that there was no time-dependence. Similar observations were made by Sø et al. (2008), in a study of As sorption on calcite. Their data suggested very rapid sorption of arsenate on calcite, with equilibrium reached within 20 min by which time 76% of the arsenate was adsorbed. However, it is also possible that progressive sorption would have been observed if the experimental duration was longer, for example Ahmed et al. (2008) reported progressive Cd sorption on calcite in a long-term adsorption experiment of up to 210 days.

The pH of the selenite suspension was measured after collecting each subsample, although small pH variations were observed the Se addition did not have a significant effect on the pH of the suspension. The pH of the control (selenite free suspension) was on average 7.7 ± 0.05

while the pH of Se spiked suspensions averaged pH 7.8. Selenite adsorption did not appear limited by the capacity of the calcite to adsorb more Se below an initial concentration of c. 0.5 mg L^{-1}. This suggests that the selenite adsorption process typically involves a surface adsorption reaction rather than time-dependent precipitation or solid-phase diffusion into the calcite. The slight upward trend in the selenite isotherms at concentrations above 1 mg L^{-1} may however be a result of precipitation. For selenate (Figure 6.3b) the isotherms also appear to curve upwards at the highest initial concentrations, suggesting a precipitation reaction is occurring.

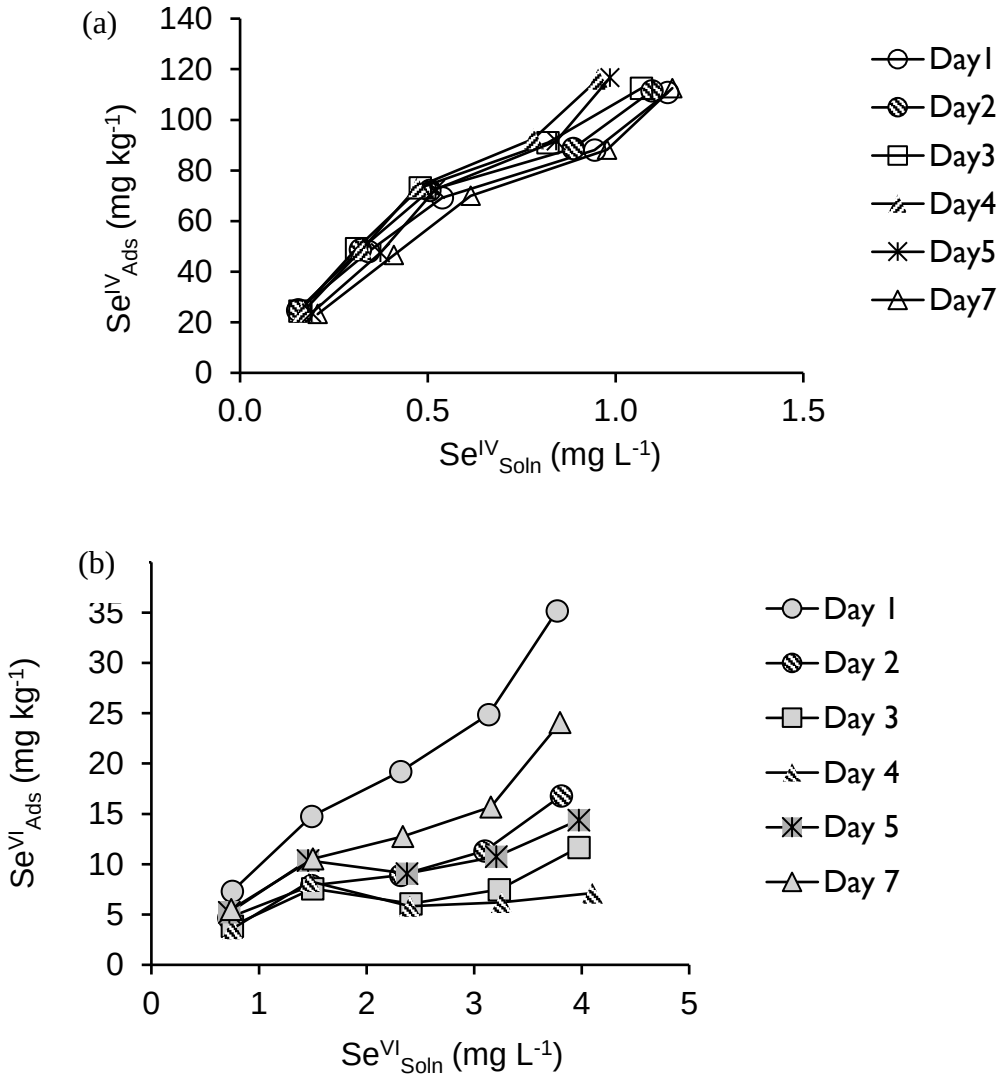


Figure 6.3. Selenite (a) and selenate (b) adsorption on calcite at initial concentrations in the range 1 to 5 mg L^{-1} using a 0.01 M Ca $(NO_3)_2$ background electrolyte.

The distribution coefficient, K_d (L kg^{-1}) can be used to better describe the total uptake capacity of the samples (Christensen et al., 1996). A plot of K_d for selenite as a function of time (Figure 6.4) shows a decreasing pattern with increasing contact time, this is confirmation that the

majority of the Se added is removed from the solution rapidly within 24 hours. It is apparent that the K_d is higher when the initial Se concentration is lower.

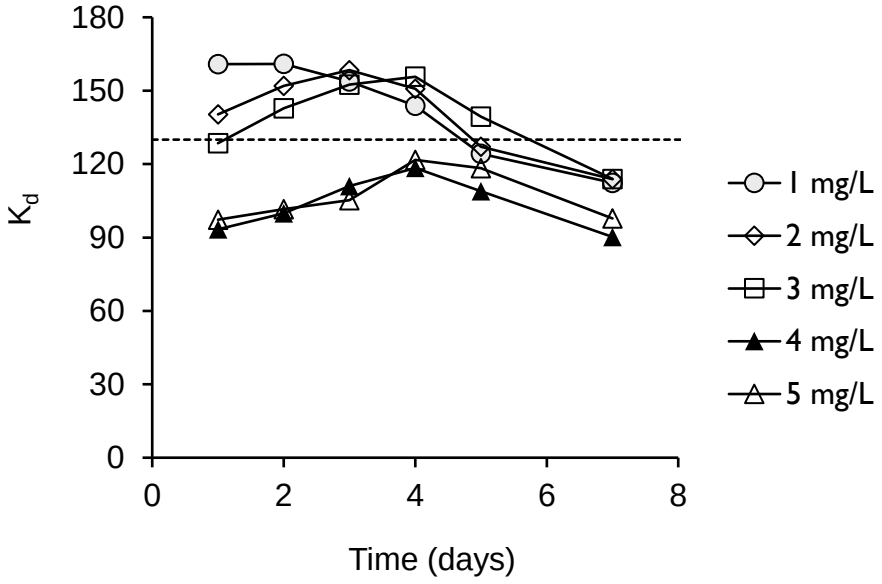


Figure 6.4. K_d values as a function of contact time for adsorption of selenite on calcite, a) 1 mg L^{-1}; b) 2 mg L^{-1}; c) 3 mg L^{-1}; d) 4 mg L^{-1} and e) 5 mg L^{-1}; dashed line is the average K_d value.

A second experiment was undertaken at lower selenite concentration 0.025, 0.1, 0.3, 0.7 and 1 mg L^{-1} to try and avoid problems with precipitation. Pre-equilibration time was also extended to a week and contact time after selenite addition to three weeks. Figure 6.5 shows selenite sorption at these lower initial Se concentrations. Little variation was observed between the different equilibrium contact times with the adsorbed selenite after 21 days (K_d=21) similar to the amount adsorbed at day 1 (K_d=22). The earliest times (days 1 and 3) show evidence of precipitation at the highest Se concentrations with an upward shifting of the selenite adsorption isotherm at day 1, coupled with a slight increase of the pH (0.1 pH units). However, at longer times (7, 14 and 21 days) no precipitation was observed. Therefore, it is possible that a local precipitate forms initially but then dissipates within the calcite and becomes more widely distributed across the calcite surface as adsorbed Se. The pH change for different initial selenite concentrations and contact times is shown in Figure 6.6.

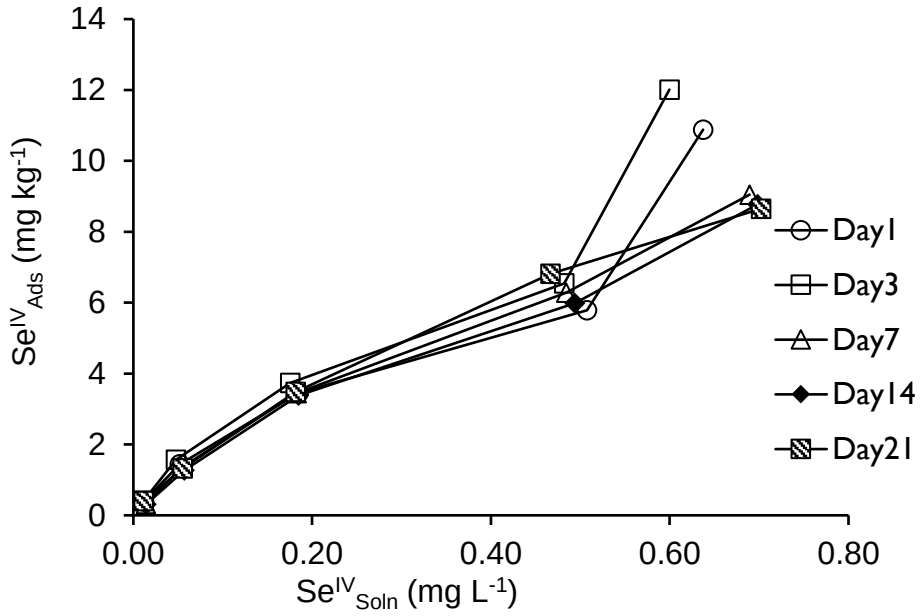


Figure 6.5. Selenite adsorption isotherm over a three-week period for initial concentrations in the range 0.025 – 1 mg L^{-1} and contact times of 1, 3, 7, 14 and 21 days. The background electrolyte was 0.01 M Ca $(NO_3)_2$.

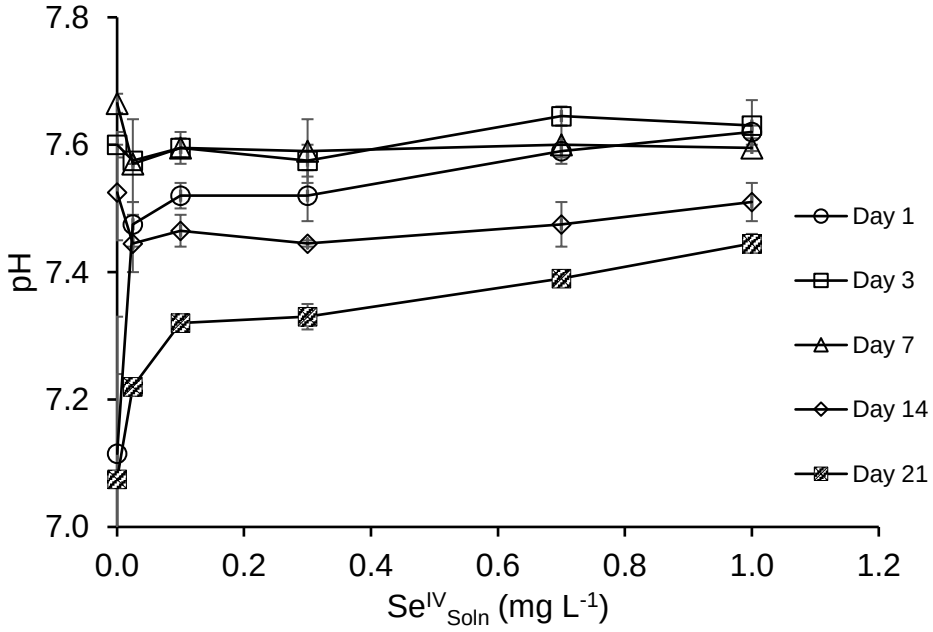


Figure 6.6. Change in the pH of the suspensions as a function of initial selenite concentration and contact time.

At these lower Se concentrations the K_d varied from 11 to 36, with an arithmetic mean of about 20. K_d was greater at the lower initial Se concentration (Figure 6.7). The proportion of adsorbed selenite was on average 40%, ranging between 28% and 54%. Greatest adsorption occurred at the lowest initial selenite concentrations, 0.025 mg L^{-1} and 0.1 mg L^{-1}.

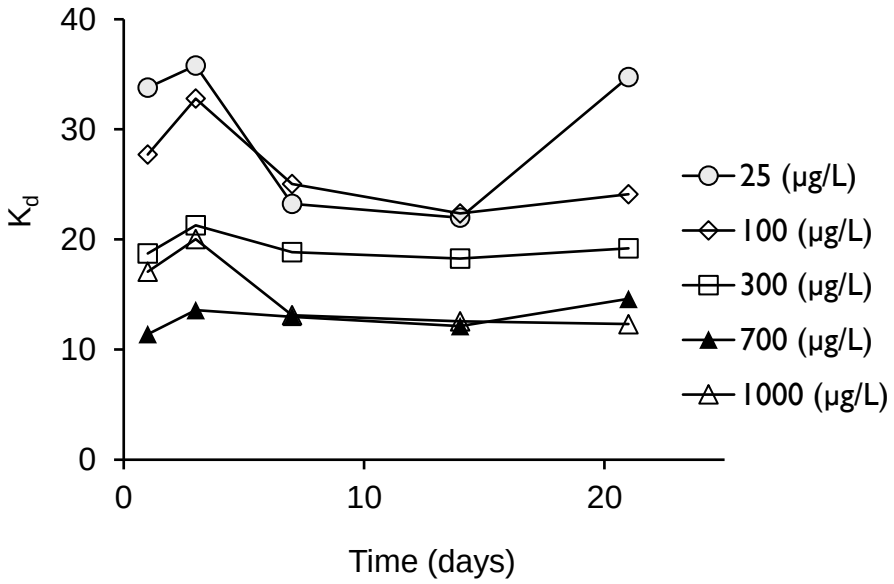


Figure 6.7. K_d values as a function of contact time; values are calculated from the experimental data presented in Figure 6; a) 0.025 mg L-1; b) 0.01 mg L^{-1}; c) 0.3 mg L^{-1}; d) 0.7 mg L^{-1} and e) 1 mg L^{-1}.

Desorption of selenite was commenced immediately after 21 days adsorption. Figure 6.8 demonstrates that some but not all of the selenite was desorbed over the three sequential desorption steps and that the percentage of selenite removal increased over time. The desorption process was fast but incomplete, indicating that some selenite had been incorporated into the calcite crystal lattice.

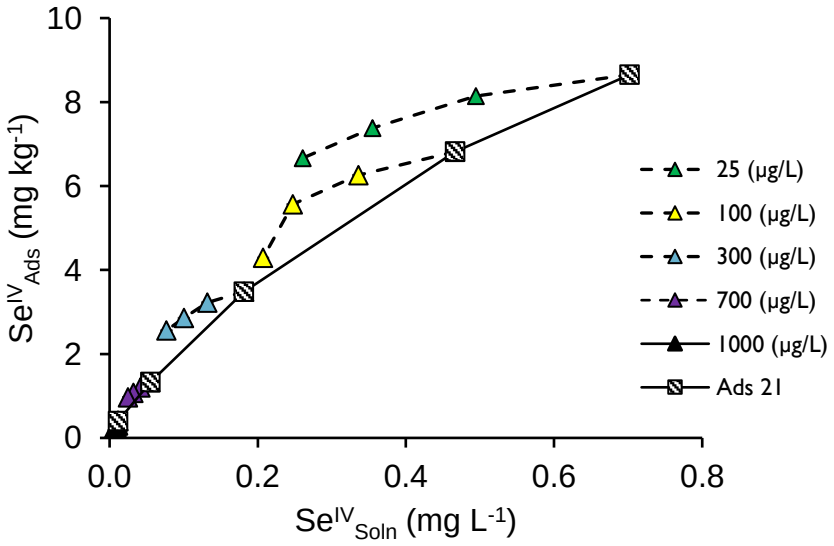


Figure 6.8. Selenite desorption isotherms following 21 days adsorption. Initial selenite concentrations were in the range 0.025 – 1 mg L^{-1}. The background electrolyte was 0.01 M Ca $(NO_3)_2$.

The experimental results were modelled satisfactorily using both individual Langmuir and Freundlich approaches or the combined Langmuir-Freundlich model. The data in Fig 6.9 seem to suggest that the Langmuir isotherm fits better than Freundlich isotherm which is in keeping with the concept of a definable adsorption maximum and reversible adsorption.

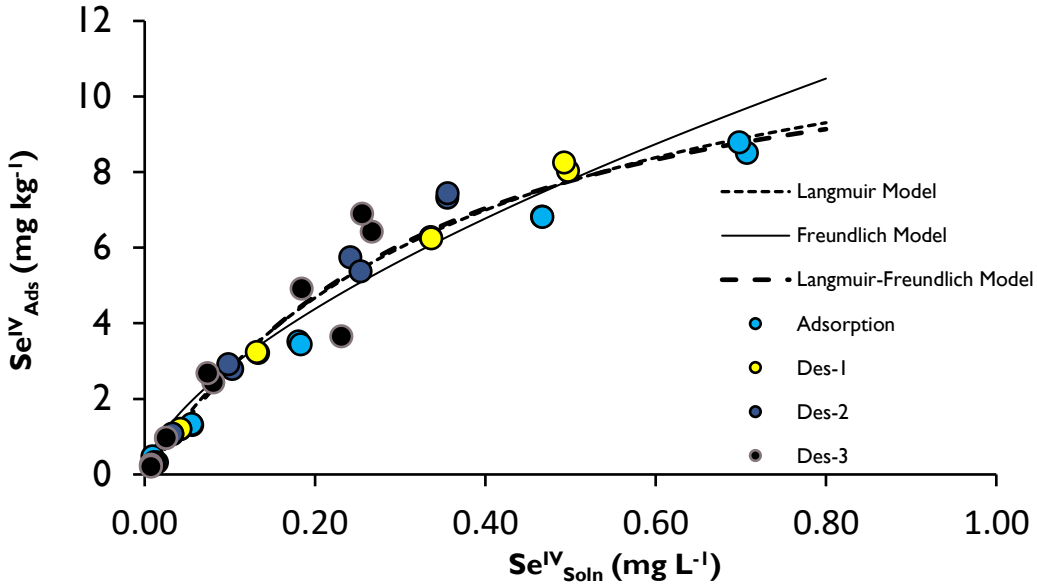


Figure 6.9. Langmuir and Freundlich modelling for the adsorption of selenite on calcite. Initial selenite concentrations were in the range 0.025 – 1.0 mg L^{-1}. The background electrolyte was 0.01 M Ca $(NO_3)_2$.

6.3.6 Selenium adsorption onto calcite under environmentally relevant conditions

To further minimize the risk of Se precipitation on the calcite surface and to consider likely Se sorption under realistic environmental conditions, further experiments were designed after considering the typical Se concentrations observed in the in calcareous ground and surface water samples collected in Somalia (see Chapter 3, Table 1 and 2). The greatest total Se concentration was 0.001 mg L^{-1}, therefore selenate and selenite concentrations in the range 0.005 – 0.05 mg L^{-1} were selected. Under these conditions a linear increase in adsorption is observed with increasing selenite and selenate concentration (Figure 6.10) with a K_d of ~30 for selenite. No precipitation was observed and adsorption was rapid and essentially complete within 24 hours with no time dependence.

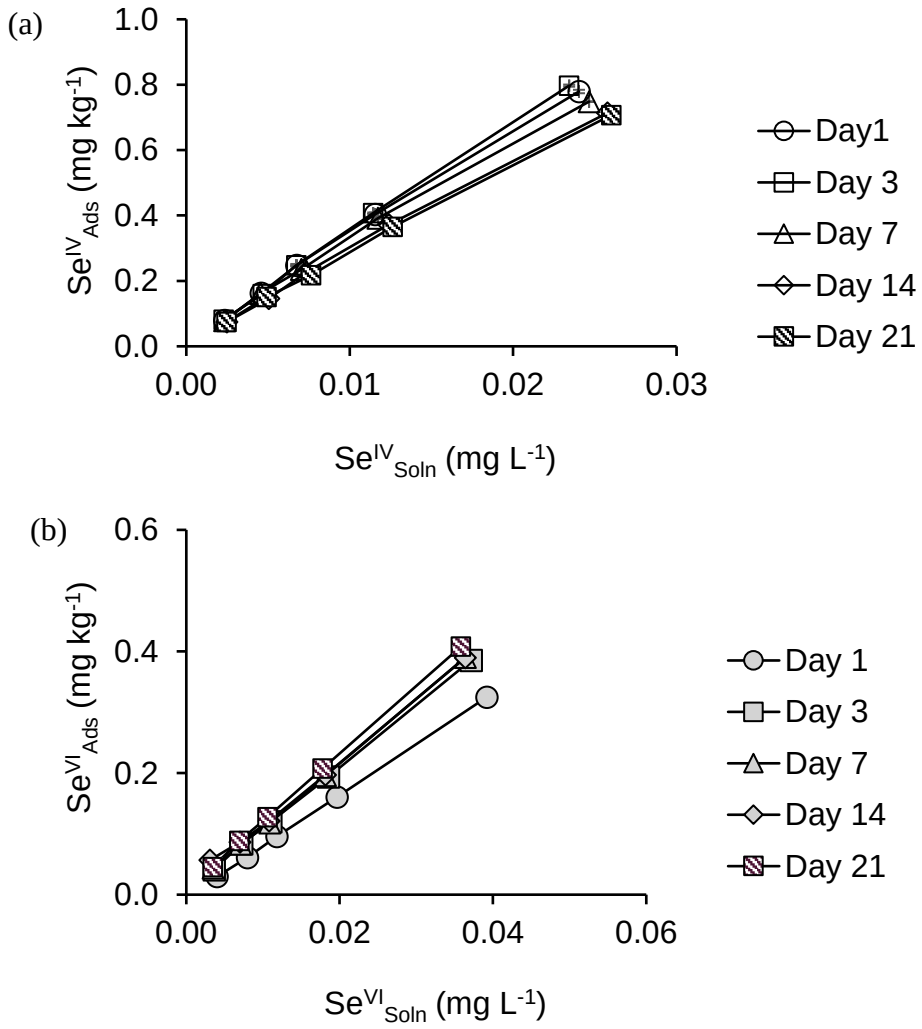


Figure 6.10. Selenite (a) and selenate (b) adsorption isotherms of environmentally realistic Se concentration 0.005 – 0.05 mg L^{-1} at contact times of 1, 3, 7, 14 and 21 days. The background electrolyte was 0.01 M Ca $(NO_3)_2$.

Comparison of selenite and selenate adsorption after three weeks of contact with the calcite (Figure 6.11) confirmed that calcite had a greater affinity for selenite (0.7 mg kg^{-1} at 21 days) than selenate (0.4 mg kg^{-1}) under the same experimental conditions at initial Se concentration of 0.05 mg L^{-1}.

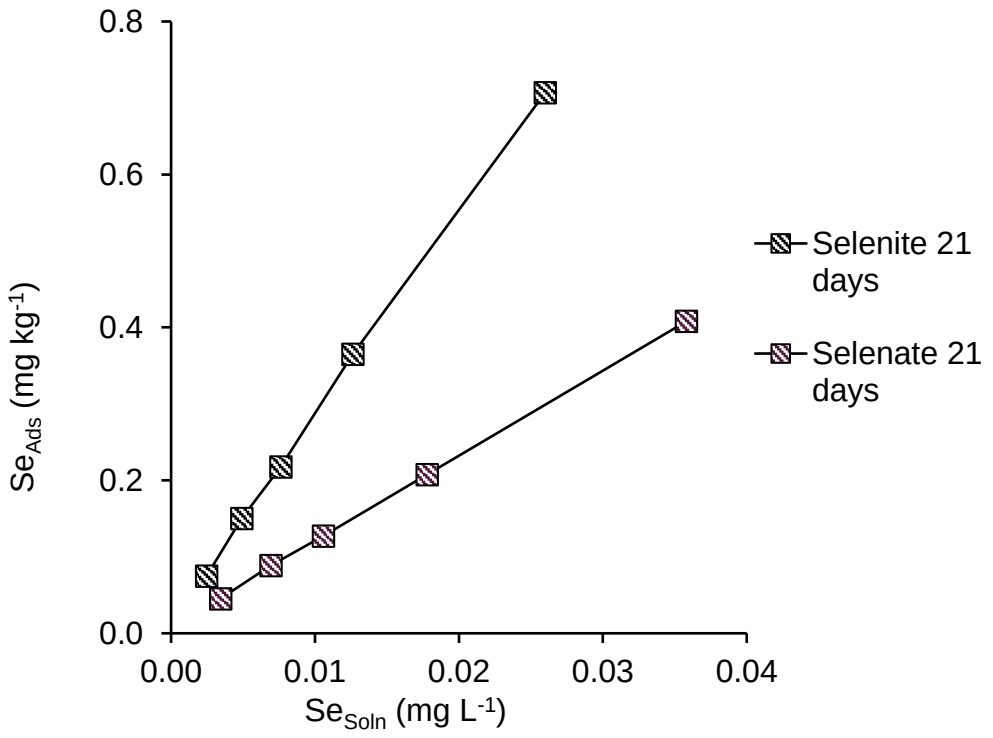


Figure 6.11. Comparison of selenite and selenate adsorption isotherms on calcite after 21 days contact time. Initial Se concentrations were 0.005 – 0.05 mg L^{-1}. The background electrolyte was 0.01 M Ca $(NO_3)_2$.

The process of anions adsorption on calcite was described by Zachara et al. (1990), who demonstrated that anion sorption parallels increasing positive charge on the calcite (Ca) surface and decreasing solution concentrations of the negative charge carbonate ions. These findings have agricultural significance, for example in the calcareous soils of Somalia with a high $CaCO_3$ equivalent to 242,600 mg kg^{-1}, the predicted Se fixation on $CaCO_3$ of these soils is potentially high.

Overall half of the added selenite is adsorbed on the calcite at initial Se concentrations of 5 – 50 µg L^{-1} with a slight decrease as a function of contact time, the average K_d value also decreased from c.35 to c.25 over 21 days (Figure 6.12, Table 6.3). To understand the extent to which calcite is a sink for Se in calcareous soils as has been shown for other trace elements (Ahmed et al., 2008; M. P. Andersson et al., 2014; Cowan et al., 1990; Green-Pedersen et al., 1997; Reeder, 1996; Zachara et al., 1991). It is important to investigate whether the adsorbed Se is permanently fixed, or is reversibly adsorbed.

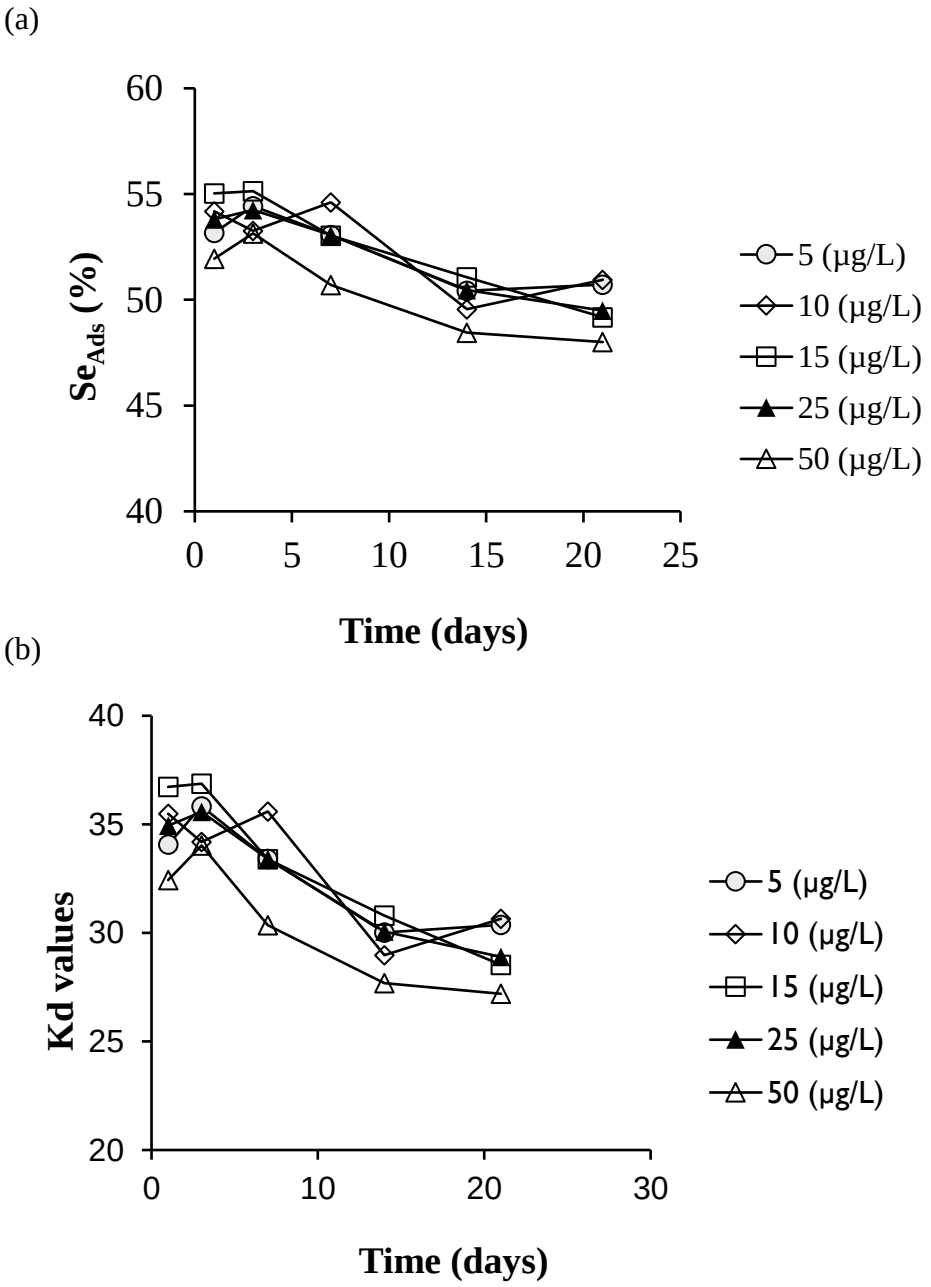


Figure 6.12. Change in (a) adsorbed Se (%) and (b) K_d as a function of contact time for Se concentrations of a) 5 µg L^{-1}, b) 10 µg L^{-1}, c) 15 µg L^{-1}, d) 25 µg L^{-1}, e) 50 µg L^{-1}.

Desorption started immediately after day 21 of adsorption and the results are shown in Figure 6.13. The K_d values for adsorption, and the three desorption steps for Se concentrations in both ranges investigated are summarized in Table 6.3. A hysteresis index (HI) was also calculated and after three successive desorption steps this averaged 0.3. This suggests that selenite desorption was not wholly reversible, and some Se remained strongly adsorbed or irreversibly bound to the calcite.

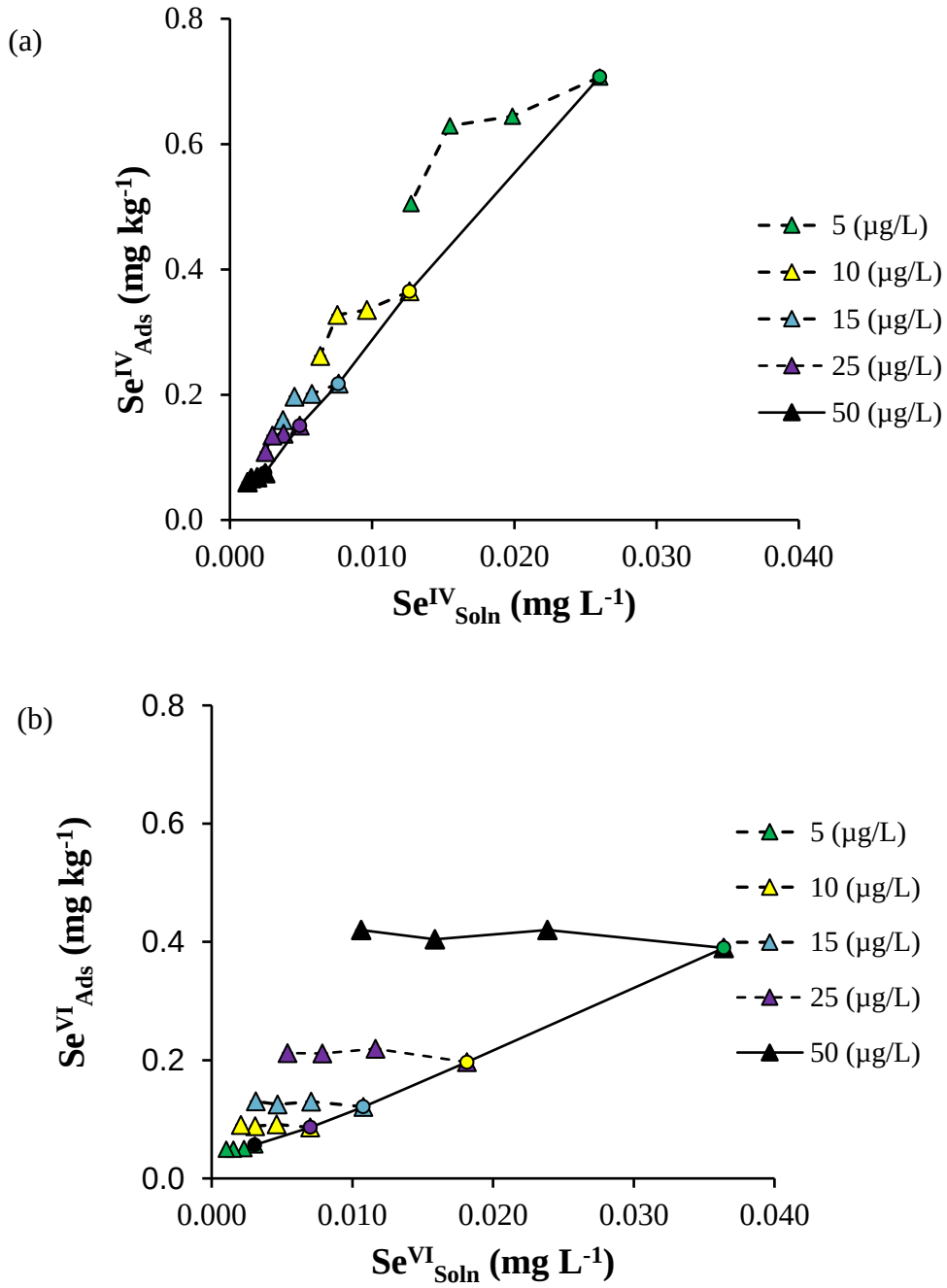


Figure 6.13. Selenite (a) and selenate (b) desorption isotherms following 21 days adsorption. Initial selenite concentrations were in the range 0.005 – 0.050 mg L^{-1}. The background electrolyte was 0.01 M Ca $(NO_3)_2$.

Table 6.3. The adsorption-desorption distribution coefficients (K_d) of $Se^{(IV)}$ into calcite. Values are arithmetic mean of duplicate measurements ± the standard error.

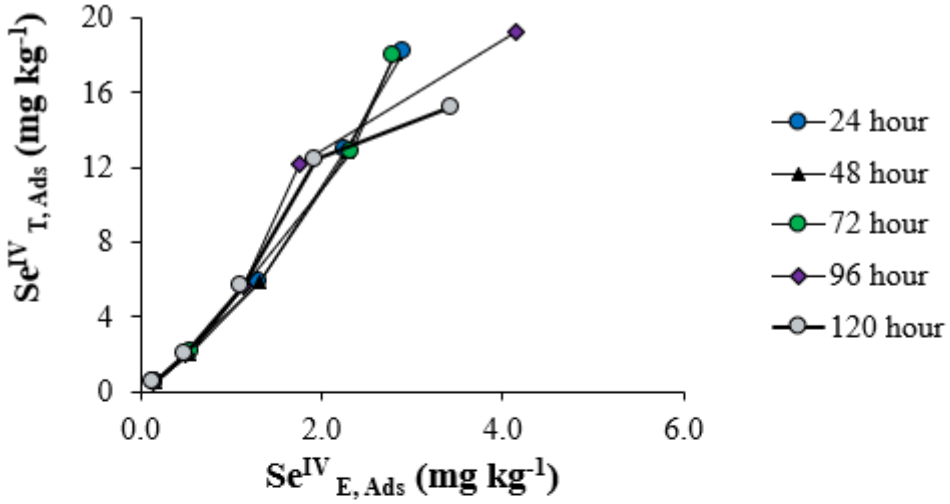
Added Se	Adsorption	Desorption 1	Desorption 2	Desorption 3
	K_d	K_d	K_d	K_d
$\mu g\ L^{-1}$	$L\ kg^{-1}$	$L\ kg^{-1}$	$L\ kg^{-1}$	$L\ kg^{-1}$
5	30	36	45	49
10	31	37	45	43
15	29	35	43	43
25	29	35	43	41
50	27	32	41	40
25	35	28	30	34
100	24	29	34	39
300	19	24	29	33
700	15	19	23	21
1000	12	16	21	26

6.3.7 Isotopic Exchangeability of Se adsorbed on calcite.

After finding strong Se adsorption on calcite and incomplete desorption, isotopic dilution was used to elucidate further the labile and fixed selenite/selenate fractions after first optimising the isotopic mixing time. Selenium fixation by calcite was studied by adding small quantities of ^{77}Se (selenite or selenite) to a calcite suspension that had first been equilibrated with the same species (selenite or selenite) multi-isotopic Se. The isotopically exchangeability ($Se_{E, Ads}$) was measured after a known equilibration time with multi-isotopic Se and equilibration of the ^{77}Se spike.

The validity and accuracy of the isotopic dilution technique was tested using five isotopic equilibration times, and at different initial background multi-isotopic Se concentrations. There are two distinct times that need to be differentiated: (i) multi-isotopic Se contact time (14 days was selected for this test experiment), and (ii) isotopic equilibration time that was tested over periods between 24 and 120 hrs. Results indicated that 24 hours was sufficient for time for equilibrium of the spiked isotope to be obtained with the Se present and even if the equilibration time was extended to 120 hours the labile pool remained equal to that at 24 hours (Figure 6.14). A spike equilibration time of 24 hrs was therefore selected.

(a)



(b)

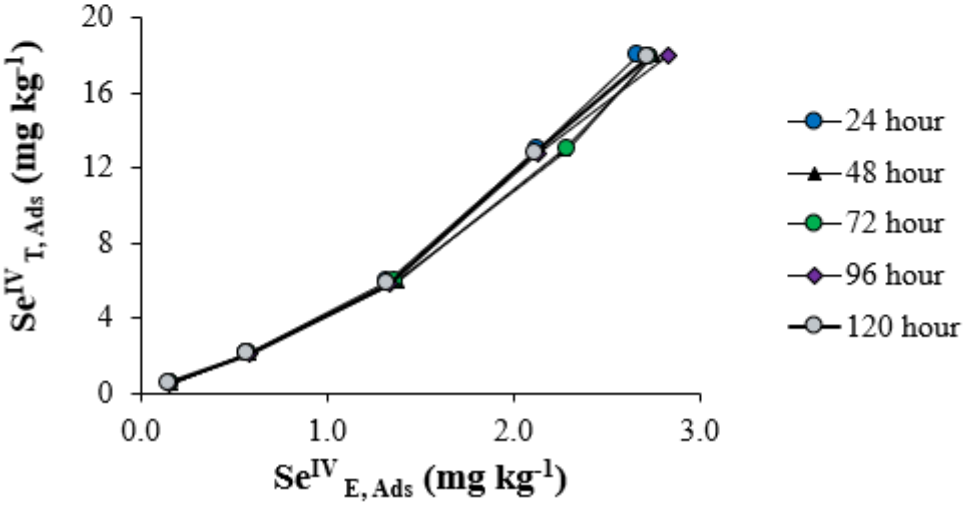


Figure 6.14. Test of the effect of ^{77}Se spike isotopic mixing time for a calcite suspension equilibrated with multi-isotopic Se for (a) 14 days and (b) 21 days.

Fixation of selenite is shown for both Se concentration ranges (i.e. 0.025 – 1 mg L^{-1} and 0.005 – 0.050 mg L^{-1}) in Figure 6.15, and the percentage of labile Se pools are shown in Figure 6.16. Most of the surface-bound multi-isotopic Se (background Se) was instantly exchanged with $^{77}Se^{IV}$. The isotopically exchangeable Se pool ($Se_{E,\ Ads}$) ranged from 60 to 95%, with an arithmetic mean of 72%, this suggests that approximately 30% of the selenite is fixed by the calcite. The variation in exchangeable Se pool due to the variations in the initial concentration (from the background Se) was clear, higher lability was found with lower initial Se

concentrations. Interestingly, the lability data for the 7, 14 and 21 days showed great consistent, this ensures the validity and reliability of the isotopic dilution experiment and therefore the labile adsorbed Se on calcite. It is worth noting that lability of the surface coated Se has paralleled the reversibility noted in the desorption experiment. This is the first study using advanced isotopic dilution to study the lability of Se species on calcite. The findings are consistent with other recent research, such as (Aurelio et al., 2010), who reported that calcite is potentially an important sink for Se during their Se^{IV} coprecipitation experiments at higher growth rates. This study has also environmental and agricultural significance as well.

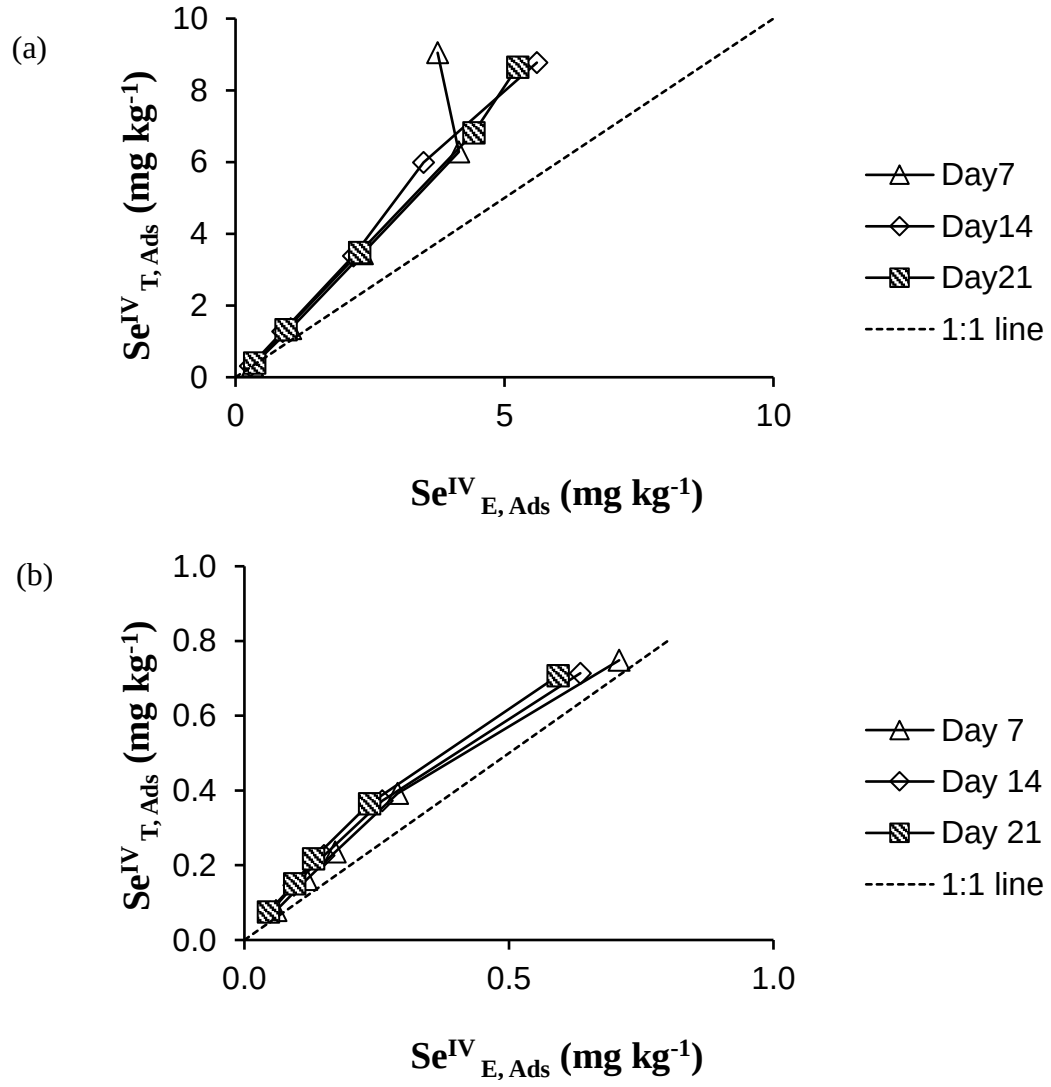
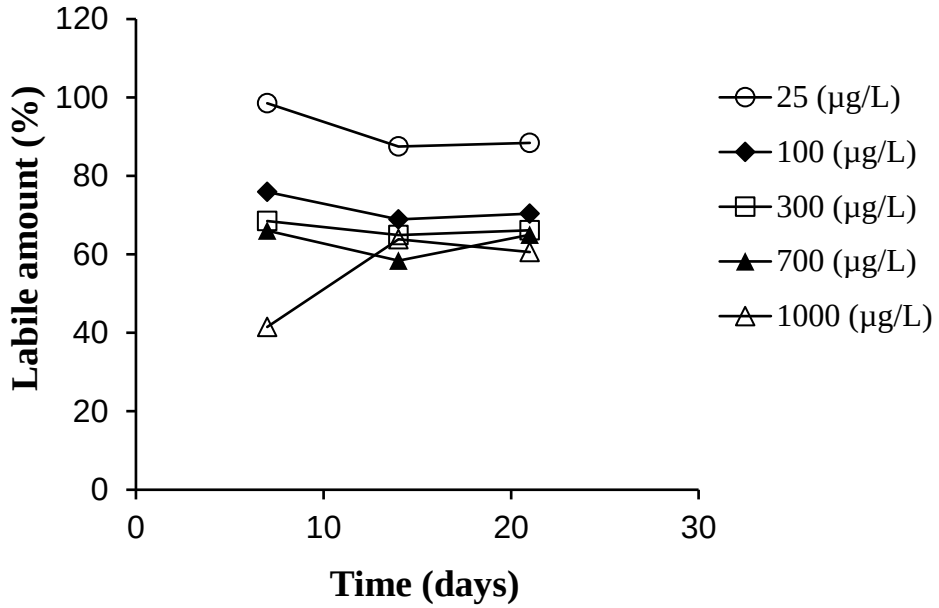


Figure 6.15. Labile adsorbed selenite plotted as a function of the total adsorbed for initial Se concentrations of (a) 0.025 – 1 mg L^{-1} and (b) 0.005 – 0.050 mg L^{-1}. Isotopic exchangeability was measured at three contact times after allowing 24-hour equilibration of the ^{77}Se spike. The dashed line is the 1:1 line.

(a)



(b)

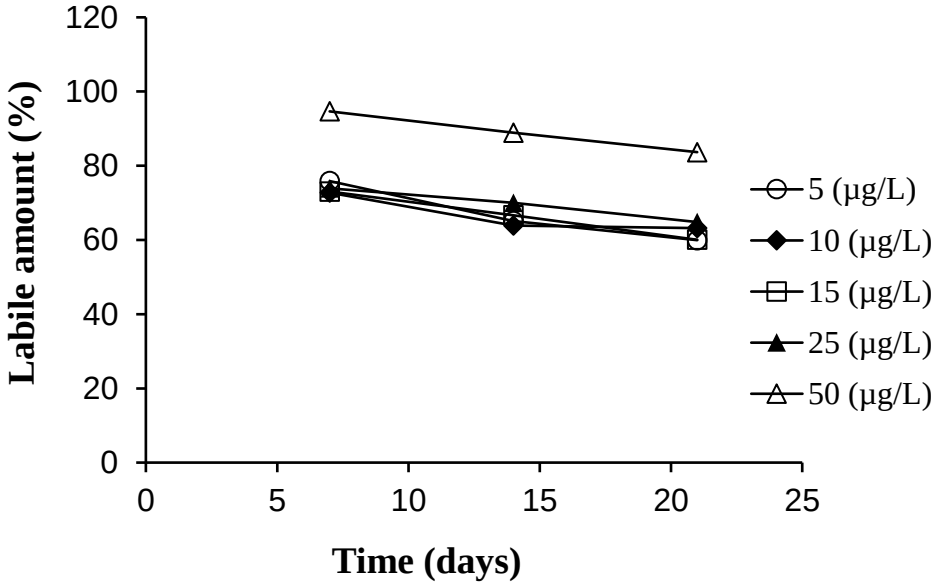


Figure 6.16. Labile amount of Se (%) plotted as a function of contact time (days) for initial Se concentrations of (a) 0.025 – 1 mg L^{-1} and (b) 0.005 – 0.050 mg L^{-1}.

Selenate adsorption on calcite was less than that of selenite and fixation was also lower (Figure 6.17). Isotopically exchangeable selenate was not detectable in the 7 and 14 days samples. After extending the isotopic equilibration time to 21 days labile Se was low but measurable with c. 10% of the selenite being labile. No isotopically exchangeable Se was measured in experiments for Se concentrations in the lower, more environmentally realistic range.

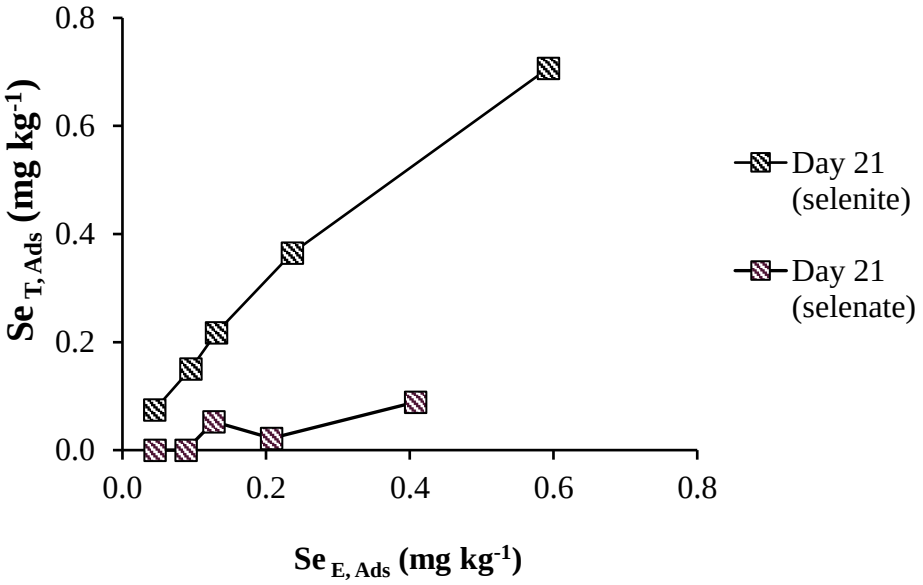


Figure 6.17. Comparison between labile adsorbed and total adsorbed selenite and selenate after 21 days reaction with calcite.

6.3.8 Effect of the CO_2/air bubbling on Se coprecipitation

Co-precipitation of Se^{IV} was studied by changing the partial pressure of CO_2 in calcite suspension systems. This was done to mimic the natural environment condition where calcite undergoes dissolution-precipitation reactions in response to fluctuations in the partial pressure of CO_2. Such fluctuations may result in occlusion of ions within the calcite structure. Although the experiment resulted in fluctuations of the pH of the system (see Fig 6.18 and Fig 6.19), no discernible difference in Se^{IV} sorption on calcite was observed (Figure 6.20).

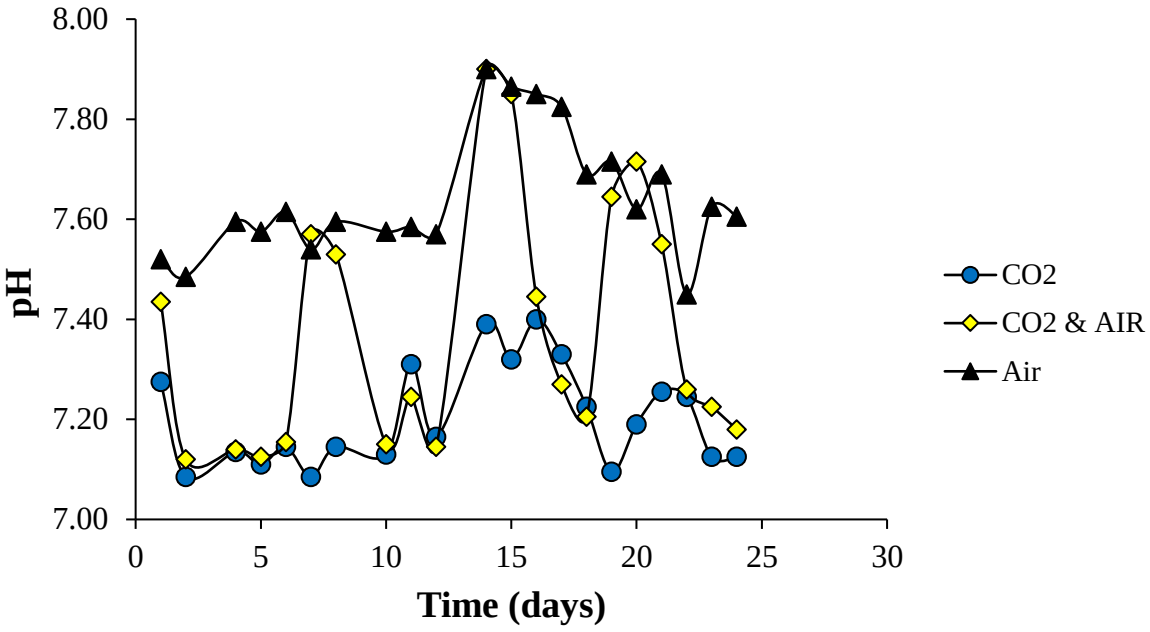


Figure 6.18. pH recorded under three experimental set ups; i) continuous CO_2 bubbling, ii) fluctuation between CO_2 & air, and iii) continuous air bubbling.

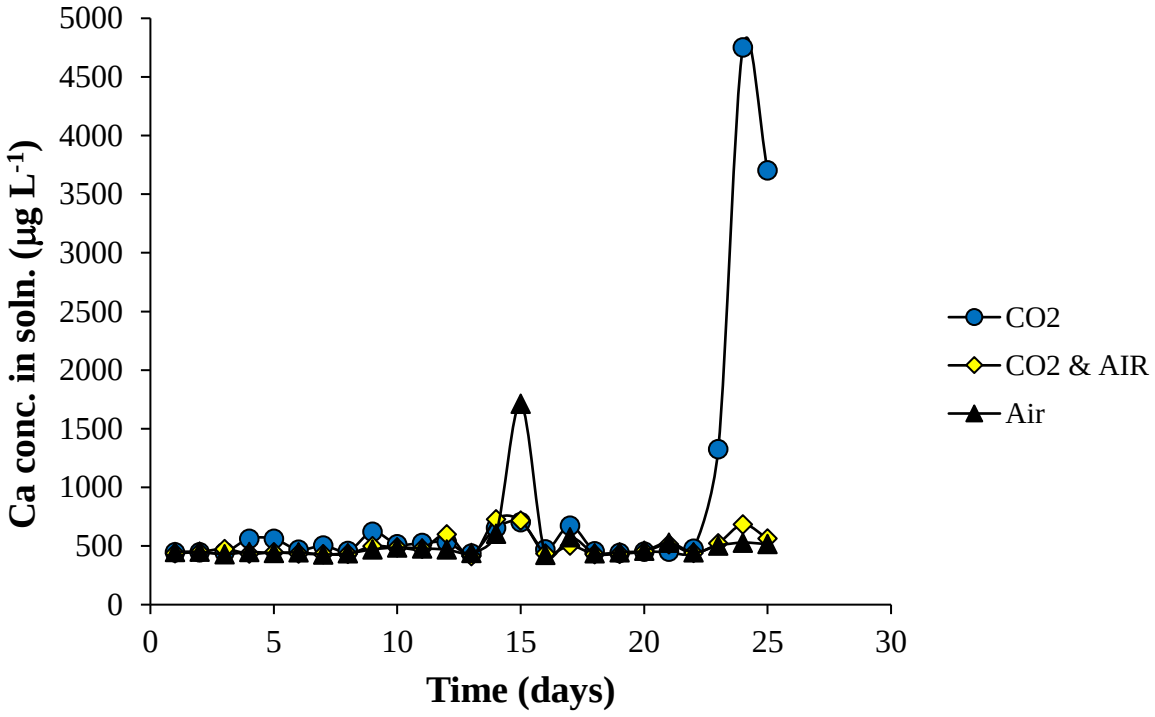


Figure 6.19. Dissolved Ca under three experimental set ups; i) continuous CO_2 bubbling, ii) fluctuation between CO_2 & air, and iii) continuous air bubbling.

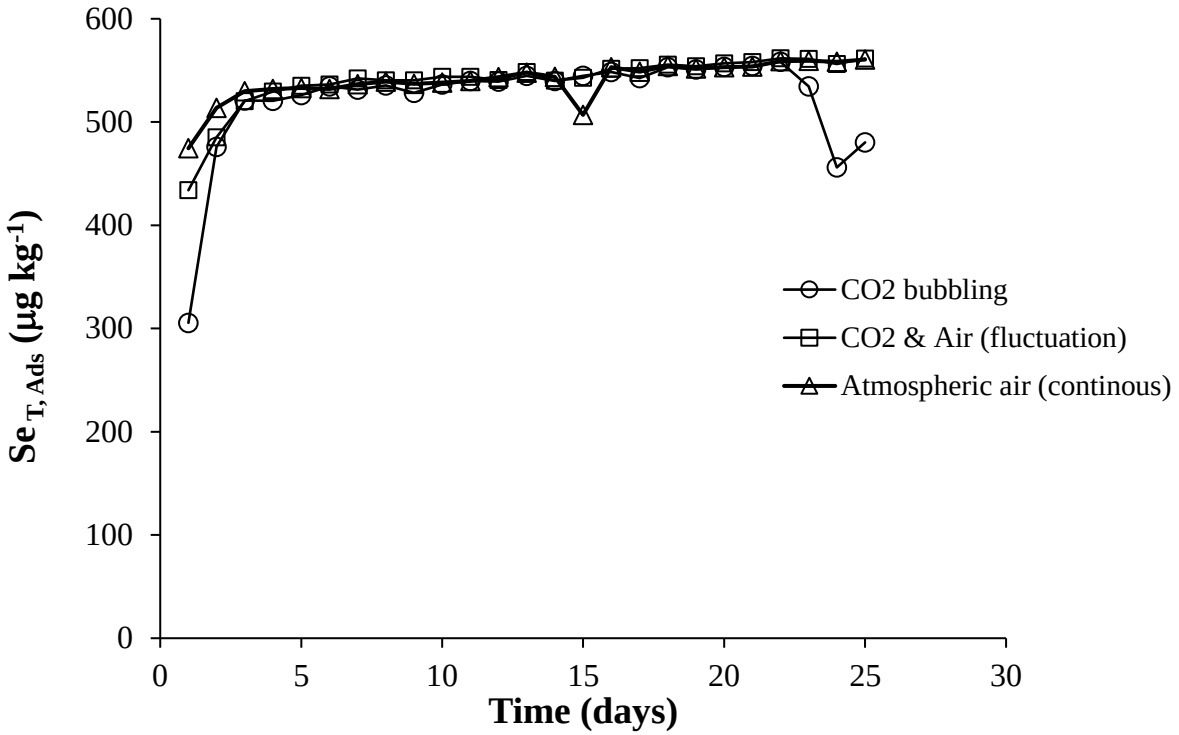


Figure 6.20. Comparison of Se adsorption in systems with i) continuous CO_2 bubbling, ii) fluctuation between CO_2 & air, and iii) continuous air bubbling, as a function of time (days).

6.3.9 Selenium Sorption on Gypsum

Batch adsorption experiment like those described for the Se sorption on calcite was conducted using both selenite and selenate species to give insight on the gypsum sorption capacity for the two species. Initial selenium solutions were 0.005 to 5 mg kg^{-1}. Gypsum sorbed variable amounts of selenite and selenate in the order: Se^{IV}-Day 7 > Se^{IV}-Day 1 > Se^{VI}-Day 7 > Se^{VI}-Day 1. Gypsum had greater affinity for Se^{IV} compared to Se^{VI}, and both Se species showed a time-dependency in this range finding experiment (Figure 6.21). The distribution coefficient (K_d) 3.20 and 0 for Se^{IV} and Se^{VI} respectively.

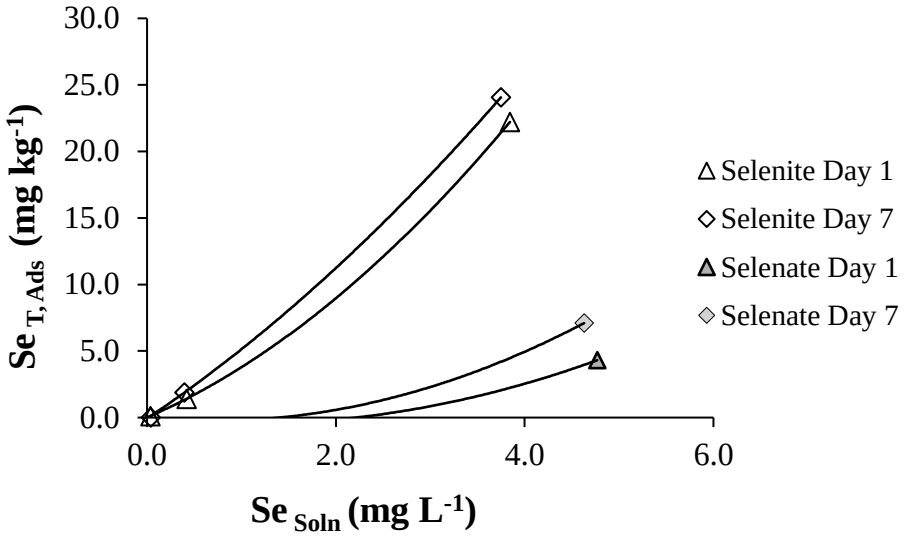


Figure 6.21. Comparison between the different Se species adsorbed on gypsum in range finding batch experiment; initial concentration 0.005 – 5 mg L^{-1}.

Selenite sorption on gypsum was further investigated at lower Se concentrations i.e. < 1 mg L^{-1} (Figure 6.22). Adsorption of Se^{IV} did not show a clear time-dependent pattern on gypsum. The K_d varied from 1.44 to 10.4, with an arithmetic mean of 4.60.

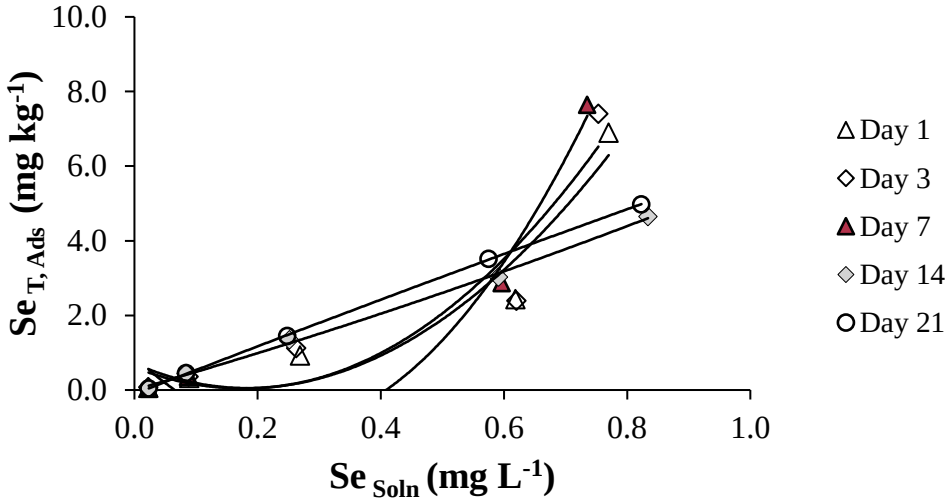


Figure 6.22. Selenite sorption on gypsum under lower Se concentration 25 μg L^{-1} – 1000 μg L^{-1}.

6.3.10 Isotopic Exchangeability of Se adsorbed on Gypsum

The lability of Se^{IV} adsorbed on gypsum was investigated using ^{77}Se-enriched isotopes (Figure 6.23) and suggested Se fixation onto the gypsum. Labile Se accounted on average for 25.8%, ranging from 0 to 40%, data not shown here.

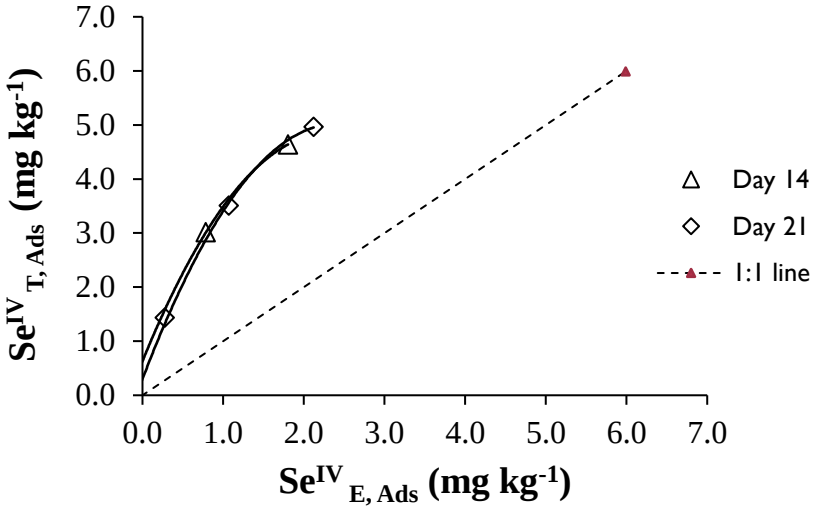


Figure 6.23. Labile adsorbed selenite plotted as a function of the total adsorbed for initial Se concentrations of (a) 0.025 – 1 mg L^{-1}. Isotopic exchangeability was measured after allowing 24-hour equilibration of the ^{77}Se spike. The dashed line is the 1:1 line.

6.3.11 EXAFS study of Adsorbed Selenium

EXAFS fitting parameters are given in Table 6.4 for samples where selenite and selenate were sorbed onto calcite, gypsum, and calcareous and gypsiferous soils. Figures 6.24 and 6.25 show the EXAFs and Fourier transform magnitude of the EXAFS for the samples.

Table 6.4. EXAFS fitting parameters derived for Se $^{(VI)}$ and Se $^{(IV)}$ sorption on calcite, gypsum, and calcareous and gypsiferous soils.

Sample	Se	Description	N	Type	R(Å)	DW	R-factor
4-H-C-A	$Se^{(IV)}$	Calcite, aged	3	O	1.693	0.00284	0.01284
			1.5	Ca	3.626	0.01293	
			1.5	Ca	3.482	0.00830	
			0.75	O	2.158	0.00255	
4-H-C-CoP-F	$Se^{(IV)}$	Calcite, co-precipitated, fresh	3	O	1.688	0.00164	0.02940
			2	Ca	3.498	0.00790	
			1.3	Ca	3.201	0.00115	
			2	O	2.884	0.00409	
4-H-SC-A	$Se^{(IV)}$	Calcareous soil, aged	2.5	O	1.702	0.00366	0.02885
			1.3	Ca	3.454	0.00715	
			1.0	Ca	3.209	0.01129	
			1.3	O	2.848	0.00516	
6-H-Sc-A	$Se^{(VI)}$	Calcite, aged	2.5	O	1.693	0.0534	0.02631
4-H-Gy-A	$Se^{(IV)}$	Gypsum, aged	2.5	O	1.665	0.00485	0.02196
			1.0	Ca	2.949	0.01375	
			2.0	Ca	3.787	0.01070	
4-H-SGy-A	$Se^{(IV)}$	Gypsiferous soil, aged	2.5	O	1.702	0.00217	0.00790
			1.0	Ca	3.509	0.01291	
			1.0	O	2.173	0.00975	
6-H-SGy-A	$Se^{(VI)}$	Gypsiferous soil, aged	1.2	O	1.606	0.00277	0.03869
			2	O	1.666	0.00277	

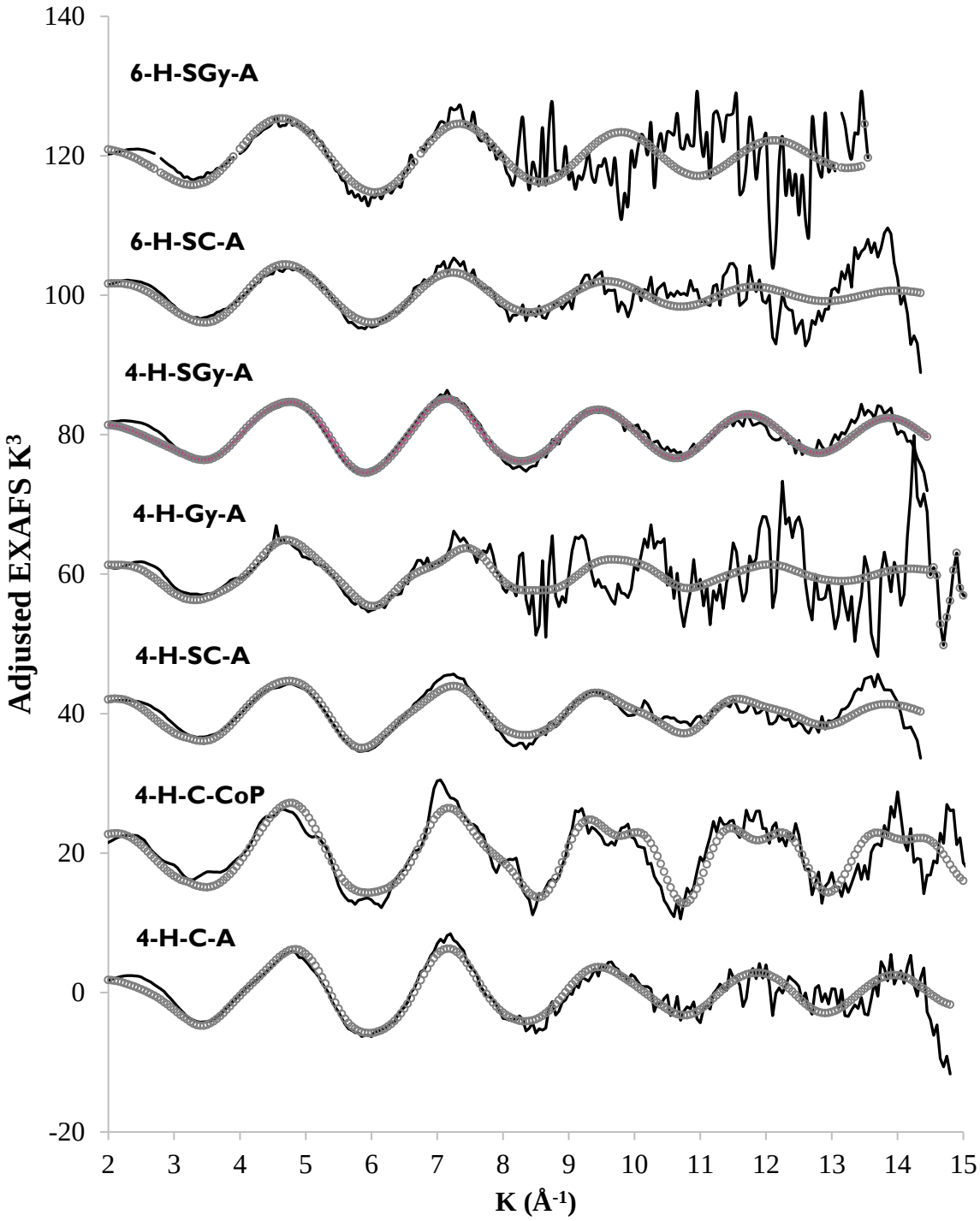


Figure 6.24. Adjusted k^3 weighted EXAFS spectra of raw data (solid lines) and model fit (circles).

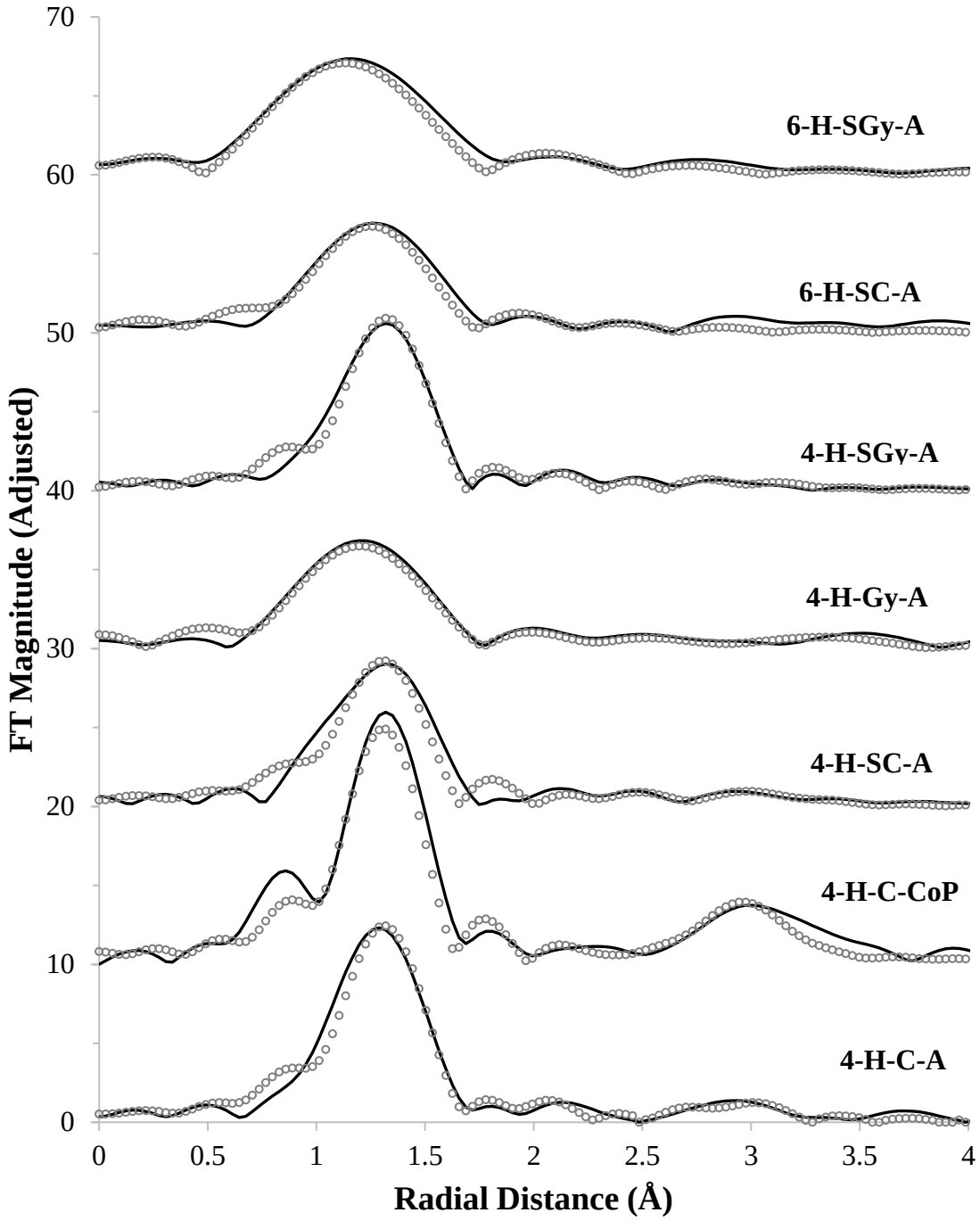


Figure 6.25. Fourier transform magnitude (k^2X (k)) of the EXAFS spectra for Se $^{(IV)}$ and Se $^{(VI)}$ incorporated into calcite, gypsum and soil samples. Solid lines correspond to raw data and circles to model fits. The FT magnitude is adjusted to stack the plots.

Aurelio et al. (2010) in an EXAFS study of calcite co-precipitated with selenite from supersaturated solutions observed that the central Se ion was surrounded by 2.8 O atoms at 1.67 Å, 1 O atom at 2.87 Å, 1.3 Ca atoms at 3.25 Å and 1.7 Ca atoms at a distance of 3.53 Å. These bond distances and co-ordination numbers are consistent with those observed in this study for the co-precipitated calcite and the calcareous soils (Table 6.4, Figures 6.24 & 6.25). Bond distances to Ca in the aged calcite samples are longer and may represent structural distortion of the calcite structure to incorporate the pyramidal selenite ion rather than the planar carbonate ion. Heberling et al. (2014) undertook a theoretical and EXAFS study of selenite incorporation into calcite. A mixed flow reactor was used to prepare a selenite doped calcite powder precipitated at a pH of 7.3-8.0 using $NaHCO_3$ as the source of carbonate and a Ca concentration of 0.006 mol L^{-1}. Single calcite crystals doped with selenite were also prepared. The EXAFS results of the doped calcite powder indicated 3 oxygen atoms (from the selenite ion) in the first shell at a distance of 1.68 Å, a second shell of c. 3 O atoms (from carbonate) at a distance of 2.88 Å and two shells of c. 3 Ca atoms as distances of 3.26 and 3.5 Å. These results are in good agreement with the results observed here for selenite in freshly co-precipitated calcite and calcareous soils although fewer Ca atoms were observed in the third and fourth shells. This may be a consequence of the low Debye-Waller factors as Heberling et al. (2014) demonstrated that if these are allowed to increase co-ordination numbers also increase and may more closely reflect expected values. Polly et al (2017) calculated local theoretical bond distances for the structural incorporation of selenite into the hydrated calcite 1014 surface and this predicted O atoms at distances of 1.72, 1.73 and 1.74 Å form the Se atom. Calcium atoms between the surface and second layer at a distance of 3.79 Å and Ca atoms within the surface plane at distances of 3.35, 3.46, 3.54 and 3.54 Å. These values are in good agreement with the values determined in this study for the adsorption of selenite on the aged hydrated calcite surface and the calcareous soil and suggest a mono-layer of adsorbed selenite on the calcite surface. Polly et al. (2017) also demonstrated that occlusion of selenite within the crystal structure is only feasible under conditions of calcite super-saturation. Growth of calcite at conditions close to equilibrium results in expulsion of selenite to enable growth. This is consistent with the observations here that freshly precipitate calcite has similar Ca-Se and Se-O bond distances to those observed for the aged and calcareous soil systems.

Reeder et al. (1994) in their EXAFS investigation of calcite grown from a selenate doped solution observed 4 O atoms at a distance of 1.63 Å, c. 2 Ca atoms at ~ 3.17 Å and c. 4 Ca atoms at ~ 3.49 Å noting that the large size of the selenate ion and its tetrahedral shape result

in substantial distortion of the calcite structure. Results for the aged calcite in this study (Table 6.4, Figure 6.24 & 6.25) suggest only very limited, if any, incorporation of selenate into the calcite structure with no model fitting a calcium shell probably a consequence of the substitution being energetically unfavourable.

There are no previously published studies on the adsorption or incorporation of selenium into gypsum. The EXAFS of selenite adsorbed onto gypsum and then aged for six months indicates c. 2.5 O atoms at a bond distance of c. 1.67 Å, consistent with what distances expected for adsorbed selenite ions and two Ca shells, one at 2.96 Å and two at 3.79 Å confirm selenite has sorbed to the gypsum surface. However, selenite sorption in the gypsiferous soil fits best to a model with c. 2.5 O atoms at a bond distance of ~ 1.70 Å and a Se-Ca bond of ~ 3.51 Å consistent with what would be anticipated for replacement of a carbonate ion in the calcite structure and significantly different from the fit for selenite sorbed onto gypsum. This indicates that although this soil has a significant gypsum content the selenite seems preferentially sorbed to the calcite phase rather than the gypsum. No evidence of selenate bonding to the gypsum structure was observed with > 3 O atoms fitting the model all with bond distances of 1.6-1.66 Å this is broadly consistent with bond distances for the dissolved selenate ion (1.657 Å) (Eklund and Persson, 2014) and may reflect a small amount of entrained soluble selenate in the samples despite washing of the samples.

6.4 Conclusions

Based on the Se sorption on calcareous and gypsiferrous minerals, strong selenium sorption on calcite was observed, results revealed that the degree of Se sorption is dependent on the Se species, selenite sorption was higher than selenate, the K_d value for selenite adsorption was about 30. Once selenite was added it was adsorbed onto the solid phase rapidly i.e. within 24 hours; in addition, there were no time-dependent sorption observed. Although, the majority of selenite was hold in a labile state there were also evidence of selenite fixation on calcite as suggested from the isotopic dilution experiments. Sorption on gypsum was much lower than that of calcite, the K_d was about 4.60. Selenite fixation on gypsum was also observed from the isotopic dilution experiment. EXAFS analysis has confirmed that selenite seems favourably sorbed to the calcite phase rather than the gypsum. This study indicated the importance of calcite in controlling the bioavailability of Se in calcareous soils. The results of this study confirm previous findings that had demonstrated selenite sorption on calcite in calcareous soils (Goldberg and Glaubig, 1988). The partition coefficients obtained in this study could be used to describe sorption to calcareous and gypsiferrous soils.

7. Iodine fixation on calcite and gypsum minerals

7.1. Introduction

Iodine is an essential micronutrient for both animals and humans; it plays a pivotal role in the synthesis of the thyroid hormones which controls various physiological processes in the body. It is important to understand the mechanisms that control the fate and transport of iodine in conditions of soil-water systems. The iodine content of plants is generally low because its transfer from soil to plants is also low (Johnson, 2003) and therefore, it is essential to gain knowledge regarding the iodine behaviour in the environment (Shetaya et al., 2012).

Although the geochemistry of iodine in the environment has been studied in detail (Fuge and Johnson, 2015; Fuge and Johnson, 1986; Johnson, 2003; Johnson, 2003), despite this there are many gaps in knowledge regarding the geochemistry of iodine due to constraints such as analytical detection of various iodine species (Humphrey et al., 2018).

Knowledge regarding the behaviour and distribution of iodine in the environment is used in a wide range of scientific disciplines. Research topics include the effect of iodine on the atmospheric ozone, the harmful health effects of the radioactive isotopes of iodine, the use of ^{129}I as a geochemical tracer, and, most notably, its essentiality in humans and other animals as a constituent of thyroid hormones (Fuge and Johnson, 2015).

In terrestrial environments, iodine exists either in the form of inorganic or organic form; its oxidation states include iodide (I^-), iodate (IO_3^-), elemental iodine (I_2) and organic iodine (Shetaya et al., 2012), the two inorganic forms of iodine (I^- and IO_3^-) can coexist in soils (Yuita, 1992). The distribution of these species varies according to the environmental condition for example, iodide was found to be the dominant inorganic iodine species in humid acidic soils, whereas iodate was found to be prevalent under aridic oxidizing conditions (Fuge and Johnson, 2015).

Understanding sorption of iodine by soils is essential as it controls the bioavailability for plant uptake (Shetaya et al., 2012). Awareness of iodine adsorption behaviour by soils is not recent, possibly one of the earliest studies that described iodide adsorption by several soils with varying properties is the study undertaken by (Whitehead, 1973). In the environment, the most important factor that influences iodine is the soil organic matter content due to its ability to incorporate large amounts of iodine. However, there are studies that show calcite can be a sink for iodine, for example iodate can be incorporated with precipitated calcite, whereas tiny

amounts (or no) iodide has been found to be incorporated onto carbonates, quartz, chlorite, montmorillonite, and muscovite (Neeway et al., 2019). Other inorganic soil components such as iron and aluminium oxides are also important (Dai et al., 2009; Dai et al., 2004) reported that adsorption of iodine was greater in soils rich in iron and aluminium oxides.

Shetaya et al. (2012) performed a time-dependent sorption study on soils of varying soil characteristics. Iodate, as $^{129}IO_3^-$ exhibited rapid sorption followed by time-dependant sorption, while for $^{129}I^-$ sorption reactions were more rapid with a less clear time-dependency trend. Initial iodate sorption depended mainly on the soil pH, while the time-dependent sorption was governed by the soil humus concentration (Shetaya et al., 2012).

Zhang et al. (2013) studied iodate incorporation into calcite in groundwater at the Hanford Site (USA); the minerology of these arid groundwater is characterized by calcite dominance. Analysis of Hanford Site groundwater demonstrated the incorporation of both stable and radioactive iodine into calcite particles. The mineral calcium carbonate has been reported for its ability to incorporate a wide range of metals and radionuclides (Kerisit et al., 2018).

Understanding the mechanism of iodine incorporation onto and into calcite and how the different iodine species behave is important. Precipitation of iodate and iodide onto calcite has been observed and reported in a study conducted by (Lu et al., 2010): in their laboratory experiment they demonstrated that iodate, rather than iodide, is the iodine species that is incorporated into marine carbonates. The greater affinity of calcite for iodate has also been reported by (Santschi et al., 2012), who have shown that the iodate K_d value was 89% greater than that of iodide in Hanford Site sediments. It has been suggested that iodate incorporation into carbonate occurs by the substitution of the carbonate ion in the calcite structure with iodate ion due the similarities of the distances between the Ca–O in Ca-$(IO_3)_2$ and that in calcite (Zhang et al., 2013).

Incorporation modes of iodate in calcite have also been observed and reported in a recent study (Kerisit et al., 2018). They used a combination of extended X-ray absorption fine structure spectroscopy (EXAFS) and Ab initio molecular dynamics (AIMD) simulations to determine local coordination environments in the iodate-calcite sorption system. They also described the associated charge compensation schemes (CCS) and any tendency for surface segregation. By contrast, there *is almost no* literature addressing iodine sorption on gypsum. (Söderlund et al., 2011) described the role of gypsum in the sorption of iodate, and reported very little sorption of I^- and IO_3^-.

Adsorption isotherms are often used to describe the sorption behaviour of a chemical species onto the soil solid phases. These graphical representations plot the adsorbed concentration as a function of the concentration in the soil solution at equilibrium. Several models have been developed to describe the adsorption mechanisms based on the shape of the adsorption isotherm. The most widely used adsorption models are the Freundlich and Langmuir equations (Sparks, 2003). The Freundlich model has been shown to be the best model to describe iodine sorption (Assemi and Erten, 1994; Dai et al., 2009; Dai et al., 2004; Sheppard et al., 1996; Shetaya et al., 2012).

The primary goal of this chapter was to study the sorption behaviour of ^{127}I in the form of iodate (IO_3^-) and iodide (I^-). Therefore, this chapter presents results showing sorption, desorption and the isotopic exchangeability of iodine in calcite and gypsum pure mineral suspensions. The data was obtained using both simple batch adsorption experiments and a system in which CO_2 partial pressure was controlled at an elevated level to simulate soil conditions. The isotopically exchangeable iodine, commonly called the 'labile pool' or 'E-value' was obtained using ^{129}I as an intrinsic tracer.

The objectives of the study were to answer the following questions.

1. To what extent does calcite/gypsum adsorb iodine?

2. Are there differences in behaviour between iodate and iodide species?

3. Do calcite and gypsum show time-dependent sorption of iodine?

4. Is iodine adsorption on calcite and gypsum 'reversible' (i.e. is there desorption hysteresis)?

5. Is the adsorption weak (labile) or strong as judged by determination of labile adsorbed species by isotopic dilution?

6. What is the effect of CO_2 or atmospheric air bubbling on iodine uptake on calcite and can fluctuating CO_2 partial pressure induce incorporation of iodine into the structure of Ca minerals by dissolution-precipitation cycling?

7.2. Materials and methods

7.2.1. Materials, chemicals and standards

The pure calcite and gypsum minerals used in this study are described in Chapter 6 (section 6.2.1.). Iodide and iodate stock solutions were prepared by diluting the 1000 mg L^{-1} stock that was prepared by dissolving the sodium iodide and sodium iodate salts respectively in MilliQ water, and were further diluted as appropriate. Samples were preserved in 0.05 M NH_4-EDTA prior to analysis.

7.2.2. Characterization of the calcite and gypsum

The characterization of the iodine-free pure mineral phases was done before commencing the sorption experiment, using a similar approach to the one described in Chapter 6 (section 6.2.2).

7.2.3. Sorption experiments

To study the interaction between iodine and calcite and gypsum, batch experiments of iodate and iodide adsorption were carried out. The approach used in this chapter follows that of the selenium study described in Chapter 6 (Section 6.2.3). The only variation was the use of both the natural stable isotope (^{127}I) and radioactive iodine (^{129}I). In addition, iodine samples were preserved in a chelating agent of 0.05 M NH_4- EDTA, and that the all iodine measurements were done by ICP-MS operating in standard mode. A couple of range finding experiments were conducted before the realistic low concentration experiments, the different experimental conditions and parameters are defined and tabulated (Table 7.1).

Table 7.1. Summary of the batch experimental conditions, the solid phase (*) is either calcite or gypsum

Trial	Weight (g)*	Volume (mL)	Background electrolyte	Pre-equilibration	Treatments (mg L^{-1})	Species	Time (days)
1	1.0	20	0.01 M $CaCl_2$	3 days	0.005, 0.05, 0.5 and 5	IO_3^-, I^-, Se^{IV} and Se^{VI},	1-7
2	1.0	30	0.01 M Ca $(NO_3)_2$	3 days	0, 1, 2, 3, 4 and 5	IO_3^-, I^-, Se^{IV} and Se^{VI},	1-7
3	1.0	30	0.01 M Ca $(NO_3)_2$	1 week	0.025, 0.1, 0.3, 0.7 and 1	IO_3^-	1-21
4	1.0	30	0.01 M Ca $(NO_3)_2$	1 week	0.005, 0.01, 0.015, 0.025 and 0.050	I^-	1-21

7.2.4. Background electrolyte

The details of the background solution (i.e. $Ca(NO_3)_2$ and $CaCl_2$) are further *discussed* in Chapter 6 (section 6.2.4)

7.2.5. Solid phase pre-equilibration

The solid phase, calcite or gypsum was pre-equilibrated for a week before the adsorption desorption experiments; this is further *discussed* in Chapter 6 (Section 6.2.5)

7.2.6. Desorption experiments

The approach used to describe the iodine desorption from calcite and gypsum is as described in Chapter 6 (Section 6.2.6).

7.2.7. Isotopically exchangeable iodine

In order to differentiate more clearly between two pools namely labile and non-labile iodine, isotopic dilution experiments were carried out using ^{129}I as a tracer. Iodine fixation by calcite was studied by adding small quantities (0.4 ml; conc. c. 5 mg L^{-1}) of ^{129}I to a calcite suspension that had been pre-equilibrated with a background stable isotope ^{127}I. The isotopically exchangeability or 'E-value' ($I_{E,\ Ads}$) was measured for three contact times i.e. after the equilibration of the ^{127}I for 7, 14 and 21 days. Thus, values of $I_{E,Ads,7}$, $I_{E,Ads,14}$, and $I_{E,Ads,21}$, were determined after 24-hour equilibration of the $^{129}IO_3^-$ to allow enough time for the tracer to mix into the system.

7.2.8. Effect of the CO_2 partial pressure fluctuation

The effects of alternating between 4% CO_2 and air (assumed to be 0.04% CO_2) were investigated and the details of this experimental approach are given in Chapter 6 (Section 6.2.3).

7.2.9. Speciation

The details of the speciation experiments are given in Chapter 6 in Section 6.2.9, the species studied were $^{127}I^-$, $^{127}IO_3^-$, $^{129}I^-$ and $^{129}IO_3^-$.

7.2.10. Modelling and calculations

The concentration data of ^{127}I in μg L^{-1} was exported from the ICP-MS lab book and was further processed using Excel. The amount of iodine adsorbed, initially in (μg L^{-1}), was calculated by subtracting the initial concentration from the final concentration. The initial concentration is calculated from the known added amount to the suspension; the final concentration is that measured by the ICP after each equilibration time. Then the total adsorbed ^{127}I in mg kg^{-1} was calculated using the following equation:

$$I_{Ads} = (C_{I-}C_F) \times \frac{V}{W} \qquad Equation\ 7.1$$

Where I_{Ads} is the I adsorbed (μg kg^{-1}), C_I is the initial concentration (μg L^{-1}), and C_F is the final concentration (μg L^{-1}). Then adsorption isotherms where created by plotting the equilibrium solution concentration (X-axis) against the adsorbed concentration (Y-axis).

Experimental data were further processed and subjected to Freundlich and Langmuir isotherm models. The Microsoft Excel Solver add-in was used to optimise the equation parameters of the Freundlich and Langmuir isotherm models by minimising the sum of error squared.

To calculate the desorbed iodine (amount), the total initial amount in solution was first determined using the equation below:

$$I_{TA} = C_I \times V_{tot} \qquad Equation\ 7.2$$

Where I_{TA} is the total amount present in solution at adsorption stage (µg), and V_{tot} is the total volume (mL), then the amounts removed by the desorption were calculated by considering the volume removed from the solution as follows:

$$I_{rem} = I_{TA} \times V_{rem} \qquad Equation\ 7.3$$

Then the amount removed were subtracted from the total amounts present in the suspension (solid and solution phases) to get the new concentrations after the desorption process, these steps were repeated for the desorption steps two and three.

$$I_{des\ 1} = I_{TA} - I_{rem} \qquad Equation\ 7.4$$

Where I_{des1} is total I concentration in solution at the desorption stage one.

7.3. Results and Discussion

7.3.1. Range finding sorption experiment

The first preliminary batch experiments were simply designed to investigate the sorption capacity of pure mineral phases i.e. calcite and gypsum for different iodine species. Thus, sorption of iodine was studied using initial concentrations that varied up to three orders of magnitude (0.005 – 5 mg L^{-1}). The fraction of adsorbed iodate (mg kg^{-1}) as a function of solution concentration (mg L^{-1}) is shown in Figure 7.1. There was strong iodate adsorption on calcite (K_d ~100). Figure 7.1 does not show any evidence of time-dependent sorption of iodate onto calcite, instead comparisons of the day 1 and day 7 isotherms show that the rate of iodate adsorption is fast and occurs within the first 24 hours. As can be observed from the shape of the isotherm, an approximately logarithmic trend line can describe the rate of iodate sorption, the values of R^2 for a logarithmic fit were 0.838 and 0.842 for days 1 and 7 respectively.

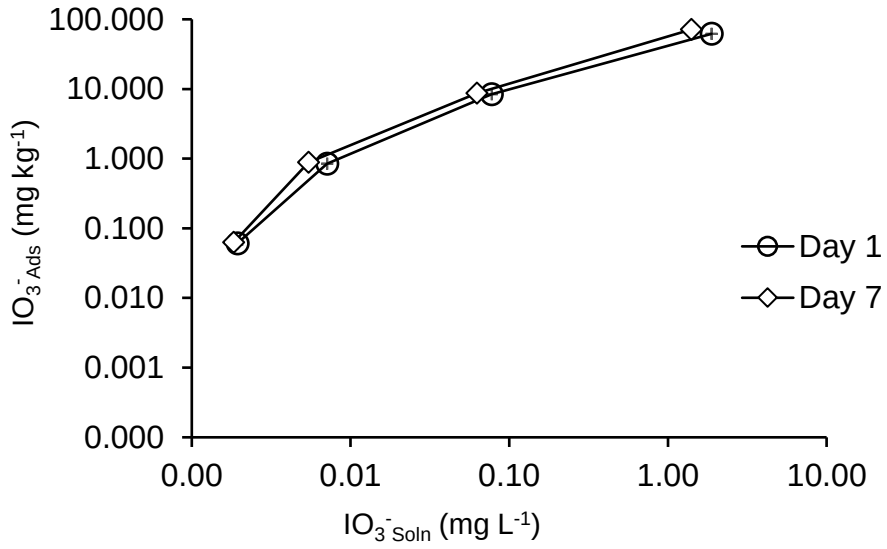


Figure 7.1. Pilot iodate sorption experiment (Pre-equilibration: 3 weeks; subsamples were collected for two contact times 1 and 7 days; initial concentrations (0.005 – 5 mg L^{-1}).

Iodide sorption on calcite on the other hand was much lower than that of iodate, the partition coefficient (K_d) was <5, presented in figure 7.2. The concentration of iodide in the aqueous phase remained nearly constant and there were no variations between the two contact times observed. Figure 7.3 allows the direct comparison of the two species on the same graph.

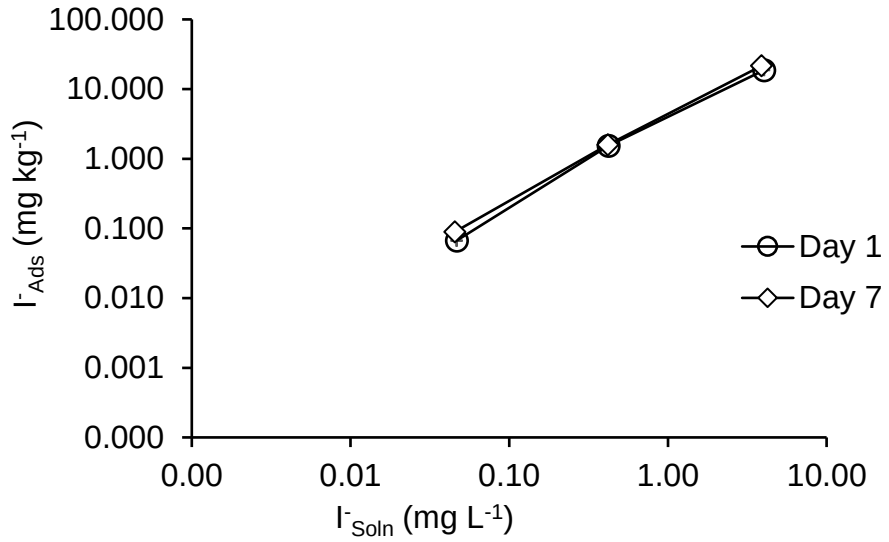


Figure 7.2. Pilot iodide sorption experiment (Pre-equilibration: 3 weeks; subsamples were collected for two contact times 1 and 7 days; initial concentrations (0.005 – 5 mg L^{-1}).

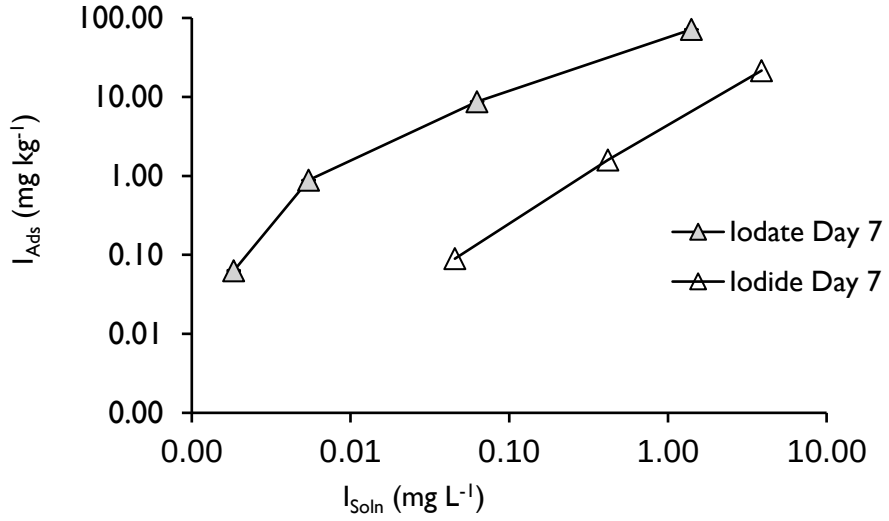


Figure 7.3. Comparison between iodate and iodide sorption experiment (Pre-equilibration: 3 weeks; subsamples were collected for two contact times 1 and 7 days; initial concentrations (0.005 – 5 mg L^{-1}).

Although the preliminary experiments showed that calcite strongly adsorbs iodine, with higher affinity for iodate, they were conducted using unrealistic high concentrations and only for two contact times. Therefore, since adsorption occurs rapidly, the sorption as a function of six contact times (1-7 days) was tested to obtain high resolution sorption isotherms. Figure 7.4 shows iodine adsorption on calcite as a function of contact time (up to 7 days). No significant differences were observed between all these contact times, rather 80% of the iodate was adsorbed within the first 24 hours, after this period of time, the adsorption rate was slower. The

strongest sorption of IO_3^- on calcite occurred at low concentrations (< 1 mg L^{-1}) for all contact times.

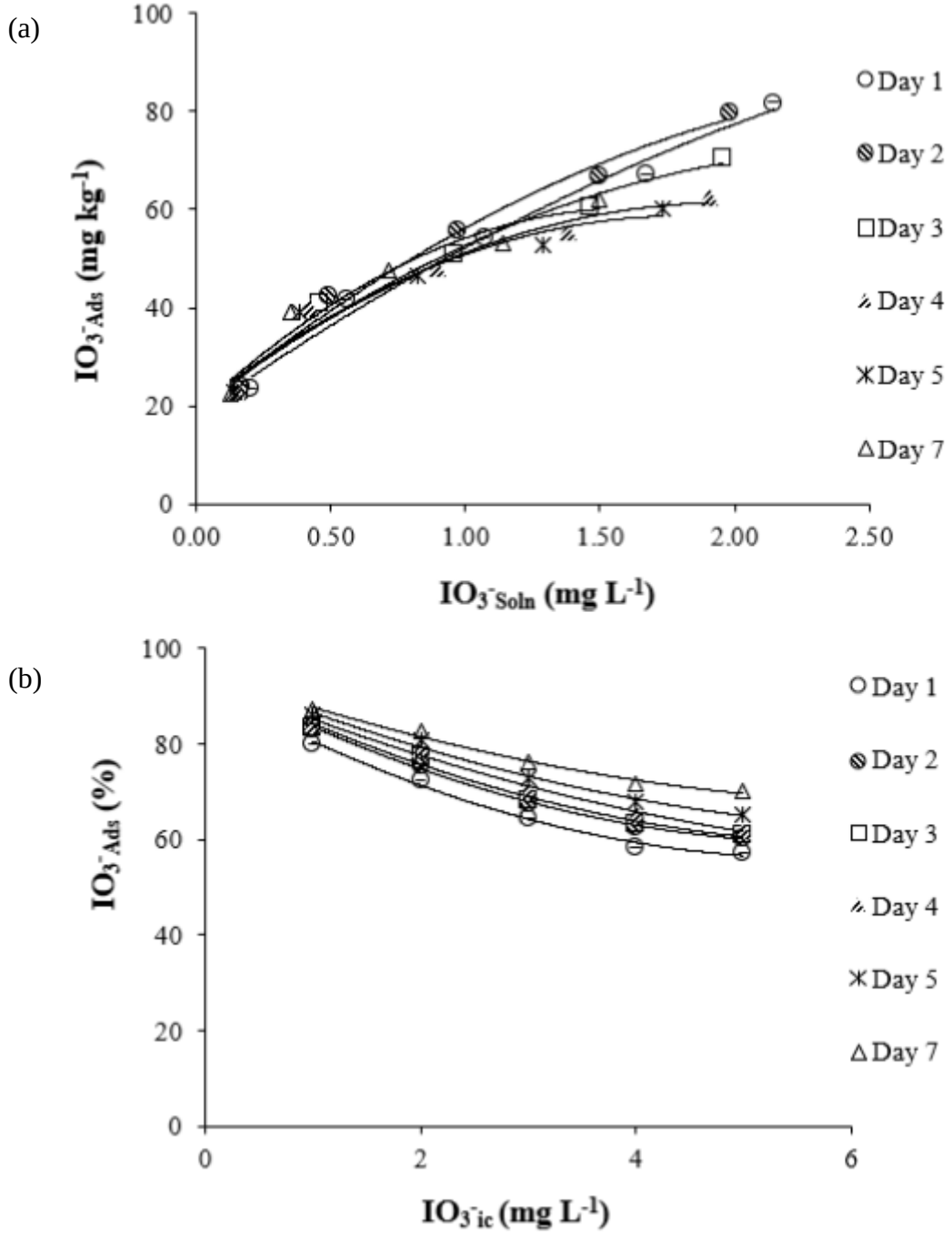


Figure 7.4. Iodate sorption as a function of six contact times; initial concentrations (5 g L^{-1} – 5 mg L^{-1}). (a) Adsorbed amounts (mg kg^{-1}); (b) Adsorbed amounts (%).

7.3.2. Sorption under realistic environmental conditions

Sorption of iodine onto soil minerals such as calcite, under realistic environmental conditions, occurs at a low concentration range (less than 1 mg L^{-1}). In the current study the iodine behaviour in calcareous groundwater from Somalia which has high iodine content of ~ 2 mg L^{-1} (Chapter 4), was investigated. To this aim, iodate adsorption isotherms from the preliminary experiment were used to estimate the amount of iodine required to achieve an equilibrium concentration that was broadly similar to the average concentrations in groundwater from Somalia. Initial concentrations in the range up to 1 mg L^{-1} were used, and the contact times were extended for 21 days. Figure 7.5 shows iodate sorption on calcite at concentrations that are intended to simulate calcareous groundwater from Somalia. There was evidence of moderately strong iodate adsorption; the Freundlich K_d was 25. Adsorption also occurred quite rapidly but apparently decreased as with greater contact time; there appeared to be lower adsorption at 14 and 21 days, compared to contact times of 1, 3 and 7 days.

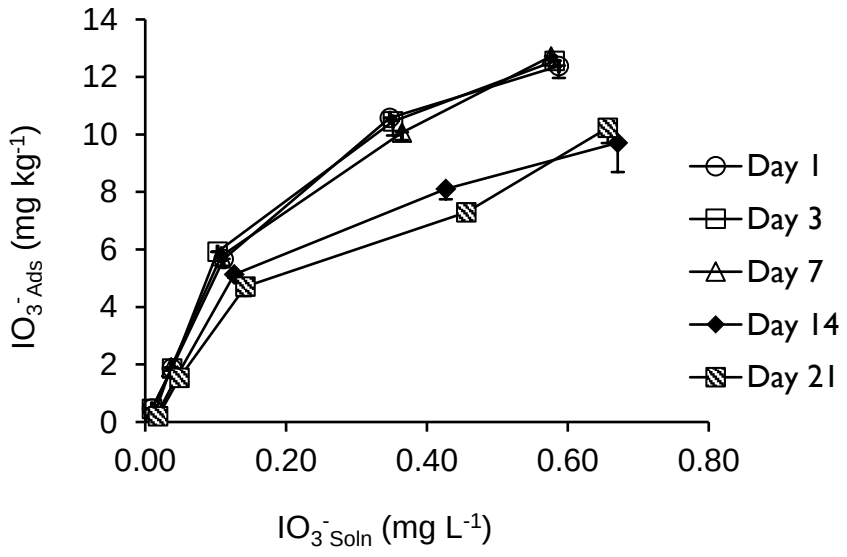


Figure 7.5. Iodate adsorption isotherm over a three-week equilibration period. The initial concentration was 0.025 – 1 mg L^{-1}; contact times were 1, 3, 7, 14 and 21 days; the background electrolyte was 0.01 M Ca $(NO_3)_2$.

The model-fitting results showed that the Freundlich adsorption isotherm provided a good fit to the iodate adsorption data on calcite (Fig 7.6). This is consistent with previous studies (e.g. Shetaya et al., 2012). In iodine dynamics study, Shetaya et al. (2012) modelled sorption on different soils with contrasting properties (pH, Fe/Mn oxides, organic carbon and iodine contents) using Freundlich model. The Freundlich K_d values ranged from 16 to 99 L kg^{-1}. At higher iodine concentrations there appeared to be evidence of adsorption hysteresis as the desorption trends fell above the adsorption isotherm model line. However, at lower

concentrations (< 0.2 mg L^{-1}) the desorption fell much more closely to the adsorption trend. Overall, there was therefore only limited evidence of a fixation reaction transferring adsorbed iodine to a non-reactive state, especially at concentrations expected in soil pore waters.

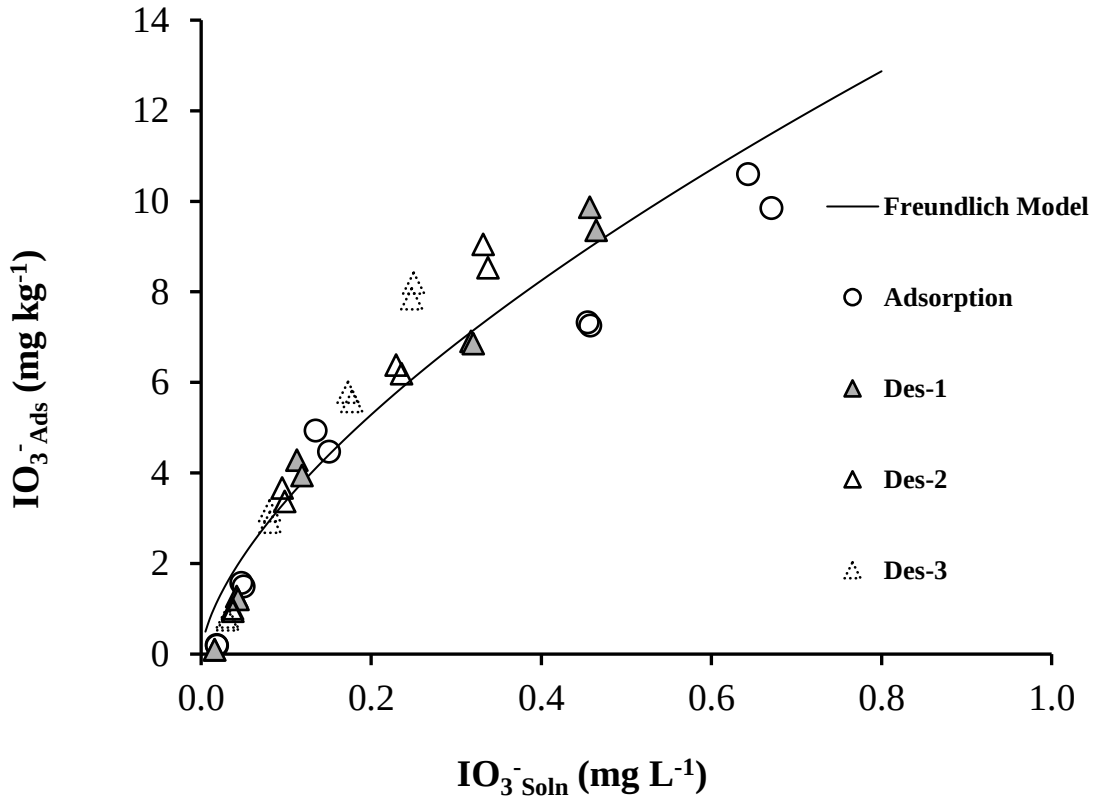


Figure 7.6. Iodate adsorption isotherm on calcite described by the Freundlich adsorption model (K_d = 25; n = 0.64). Adsorption was for a period of 21 days, followed by three desorption events at 24-hour intervals.

7.3.3. Comparison between ^{127}I and ^{129}I adsorption

Results showed that the adsorption of both iodine isotopes was similar. Mean Freundlich K_d values for ^{127}I-iodate and ^{129}I-iodate were 25 and 30 respectively (Fig. 7.7). The adsorption was slightly higher with the ^{129}I, this could be due the higher ^{129}I concentrations that were used. Initially ^{129}I was added at higher levels to measure the isotopically exchangeable fraction.

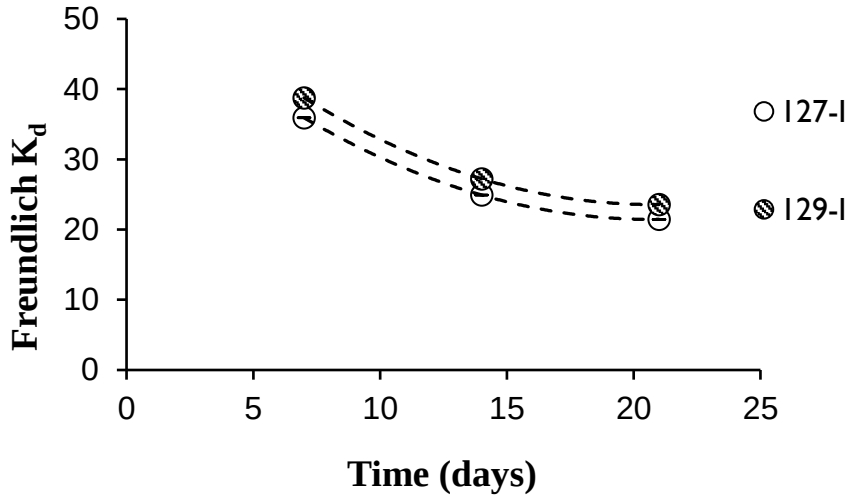


Figure 7.7. Comparison of the adsorption strength (Freundlich K_d) on calcite of ^{127}I and ^{129}I isotopes, added as iodate, as a function of time (21 days).

7.3.4. $^{127}IO_3^-$ desorption

Although iodate was strongly adsorbed on calcite, the adsorption appears to be reversible (Fig. 7.8). Desorption experiments started immediately after the adsorption experiment i.e. after 21 days of equilibration. Desorption hysteresis was observed at high concentrations, but at low concentration the desorption was completely reversible. The predominance of reversible binding of iodate to calcite is important because this means that $CaCO_3$ in soil could act as a reservoir to capture iodine in irrigation and rainfall, and prevent it from leaching, but then release it for future uptake by plants in response to depletion of the soil solution iodate. This process is different from binding of iodine to soil organic matter (OM); humus sorbs iodine, from added iodate and iodide, in largely irreversible forms which are probably not available for plant uptake (Shetaya et al., 2012).

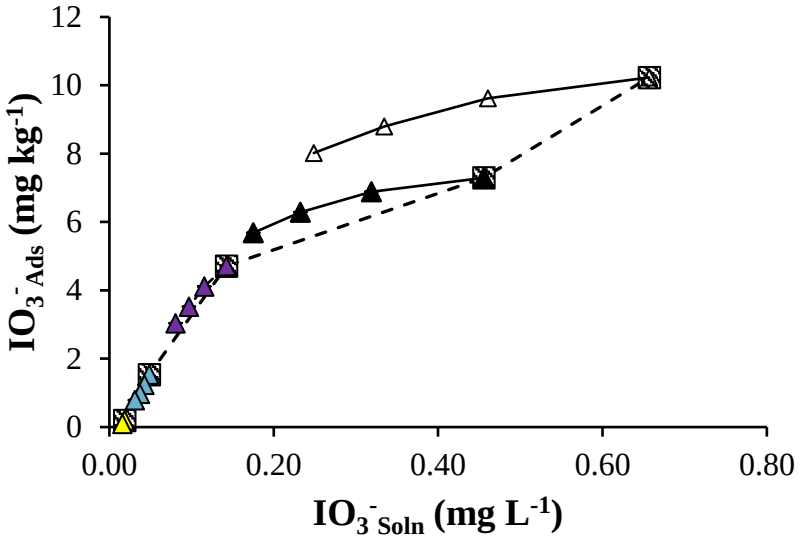


Figure 7.8. Iodate desorption isotherm following a three-week initial adsorption equilibration period; the initial concentrations were relatively low (0.025 – 1 mg L^{-1}); desorption commenced after 21 days adsorption; the background solution was 0.01 M Ca $(NO_3)_2$.

7.3.5. Iodate fixation into pure calcium carbonate minerals

The desorption experiments suggested only limited evidence for iodate fixation in calcite. The isotopically exchangeable iodate data are shown as a comparison with total iodate adsorption and as a percentage of total iodate adsorbed in Figures 7.9 & 7.10 respectively. Almost all the surface bound $^{127}IO_3^-$ was exchangeable with the tracer ^{127}I. The average labile pool was close to 100% of the adsorbed iodine. Furthermore, the labile pool remained unchanged for up to 21 days. This has implications in terms of availability to plant, and could indicate that liming is potentially a useful way to ensure iodine remains available for long terms.

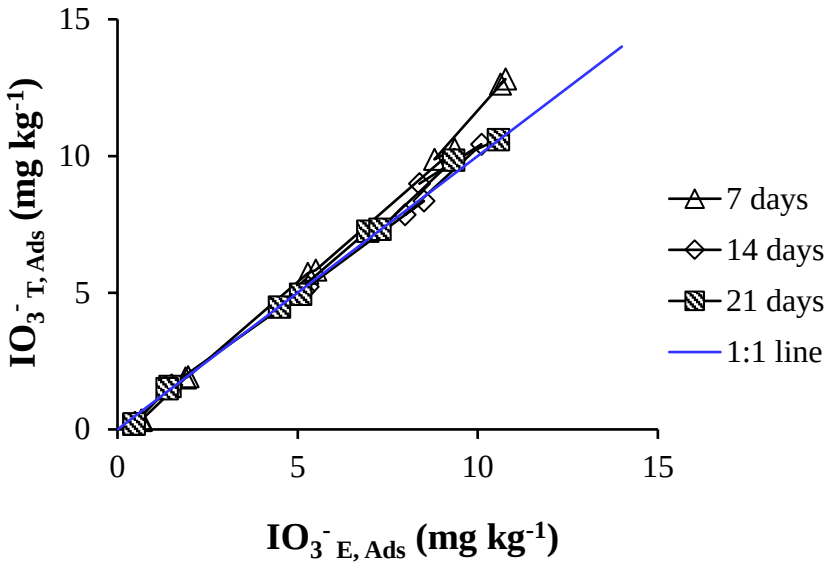


Figure 7.9. Labile adsorbed iodate-I ($IO_3^-{}_{E,\ Ads}$) on calcite plotted as a function of the total adsorbed iodate-I. Equilibration was for 7, 14 and 21 days.

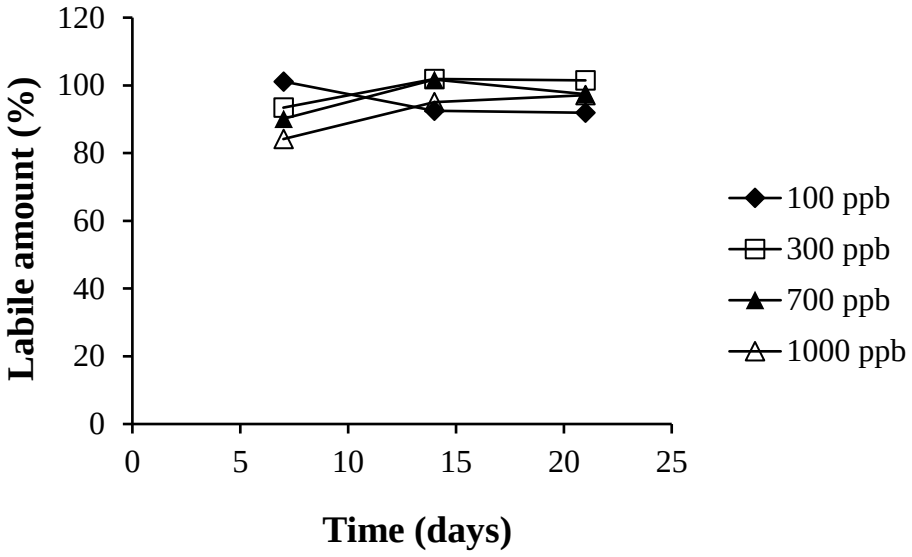


Figure 7.10. Labile iodate as a percentage of the total adsorbed iodate (%) plotted as a function of the contact time (days); 4 initial IO_3^- concentrations were used (100, 300, 700 and 1000 µg L^{-1}).

7.3.6. Speciation of iodine in iodate-calcite adsorption experiments

Interpretation of iodate adsorption and isotopic exchangeability may be compromised by any change in iodine speciation during adsorption or desorption. To check the speciation of iodine in solution HPLC-ICP-MS was used, as described in section 2.4.6. Fortunately, results showed no evidence of reduction to iodide, or the presence of any other iodine species. It can therefore be assumed that all the iodate remained unchanged after a 3-week experimental time (Table 7.2). It should be stressed that this is how iodate is expected to behave in a pure $CaCO_3$ suspension with no organic materials or possible reductants present. This is expected to differ from iodine behaviour in soil, where iodate is liable to be reduced to iodide and combine with soil humic materials (Shetaya et al., 2012). The speciation experiments also confirmed the finding that iodate is more strongly adsorbed on calcite compared with gypsum. The initial iodate concentration was 25 µg L^{-1}; this was lower in the calcite suspension but remained close to the initial value in the gypsum suspension (Table 7.2).

Table 7.2. Iodate ($^{127}IO_3^-$) speciation during the batch adsorption experiment. Each value is the mean of duplicate experiments.

S phase	Initial concentration	Contact time	$^{127}IO_3^-$	$^{127}I^-$
	(µg L^{-1})	(days)	(µg L^{-1})	(µg L^{-1})
Calcite	25	1	6.32	0.00
Calcite	25	3	6.42	0.00
Calcite	25	7	10.6	0.00
Calcite	25	14	11.4	0.00
Calcite	25	21	17.8	0.00
Gypsum	25	1	25.1	0.00
Gypsum	25	3	25.9	0.00
Gypsum	25	7	31.7	0.00
Gypsum	25	14	31.1	0.00
Gypsum	25	21	31.3	0.00

7.3.7. Effect of the CO_2/air bubbling on iodate co-precipitation

The environmental factors affecting the carbonate minerals in arid and semi-arid environmental conditions were investigated. A fluctuating 4% CO_2-air bubbling regime was imposed, in an attempt to induce calcite dissolution and precipitation, thereby mimicking the effect of respiration of plant roots, the rhizosphere and also microbes. The experiment as described in the selenium chapter (Chapter 6), was successful in term of causing the pH fluctuation to the system, however it did not show any evidence of incorporation of iodate into the calcite structure over the time period of the trial (Fig. 7.11).

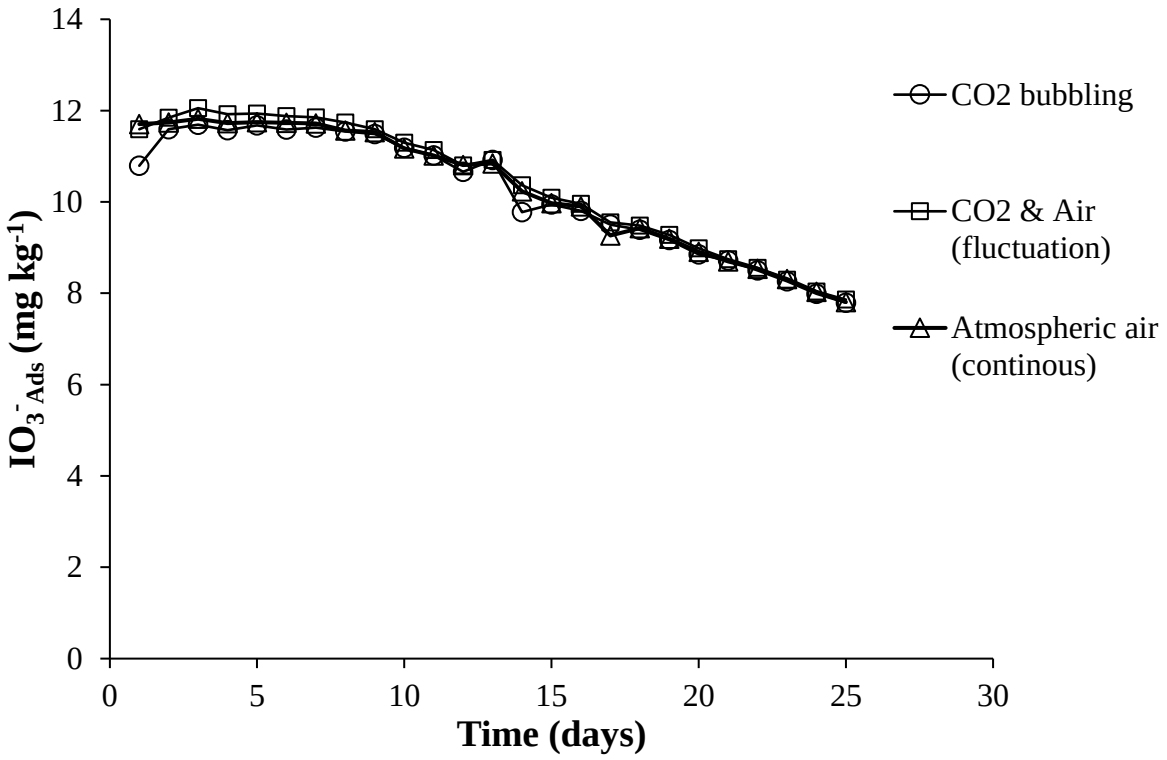


Figure 7.11. Comparison of iodate adsorption under continuous suspension aeration with CO_2 (4%) and air and under a fluctuating (CO_2-air) regime as a function of time (days).

7.3.8. Adsorption and fixation of iodate on gypsum

At initial concentration of 0.025 – 1 mg L^{-1}, iodate adsorption ranged between 0 and 3.10 mg kg^{-1}, with an arithmetic mean of 0.780 mg kg^{-1} (Fig. 7.12). The Freundlich K_d values ranged from 0 to 5.23, with an arithmetic mean of 2.08; this indicates that sorption on gypsum was much lower compared to iodate adsorption on calcite (Freundlich K_d of 25) under similar initial concentrations (0.025 – 1 mg L^{-1}). As seen for calcite, the longer-term equilibration (14 and 21 days) appeared to produce lower adsorption strength which, again, was unexpected. There was also evidence, from the desorption trends, of adsorption hysteresis at higher concentrations. However, the isotopically exchangeable iodine (E-values; Fig. 7.13) seemed to indicate that there was no IO_3^- fixation into the gypsum structure.

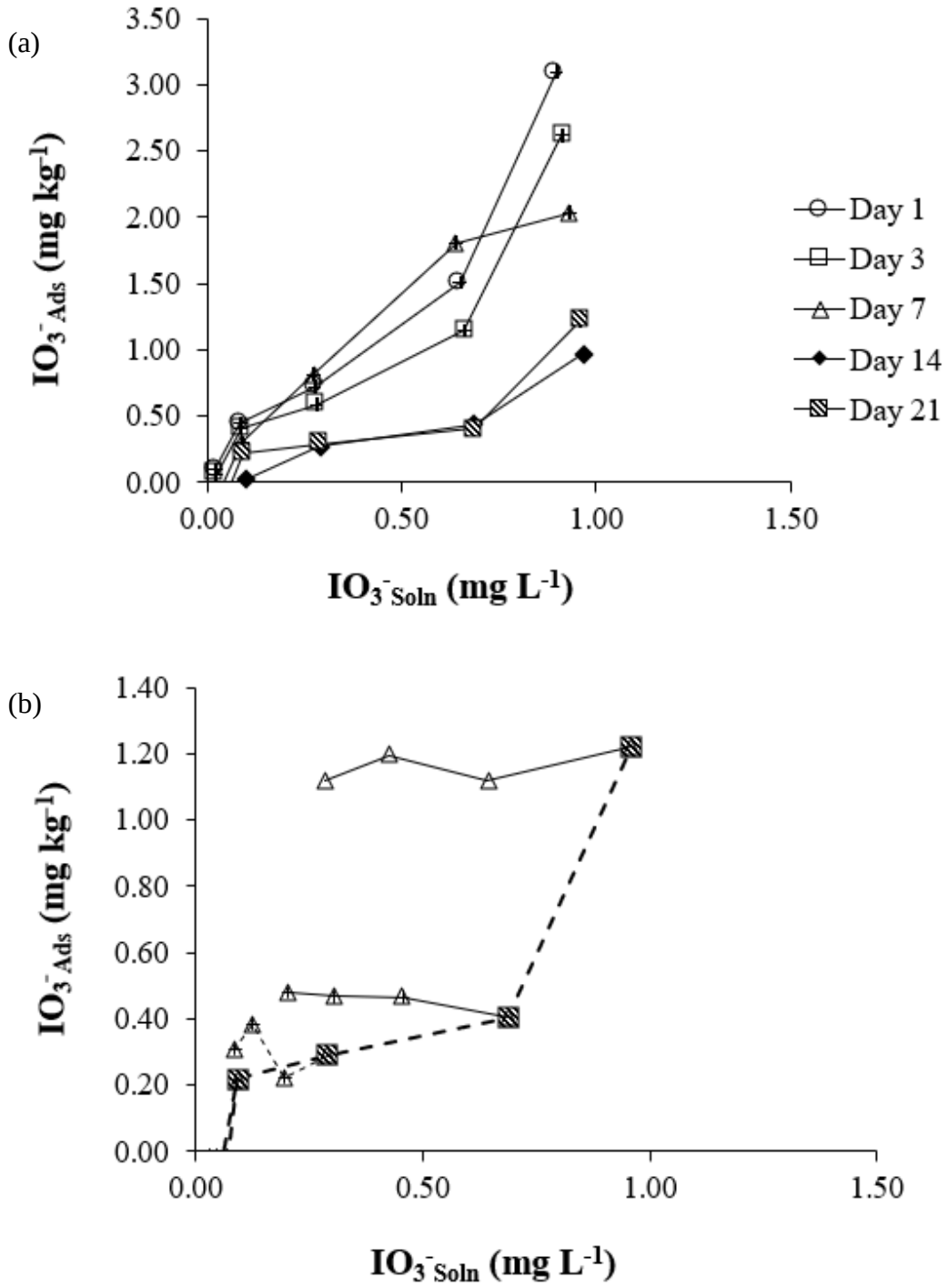


Figure 7.12. Adsorption–desorption of iodine (in the iodate form) by gypsum; a) adsorption; b) desorption.

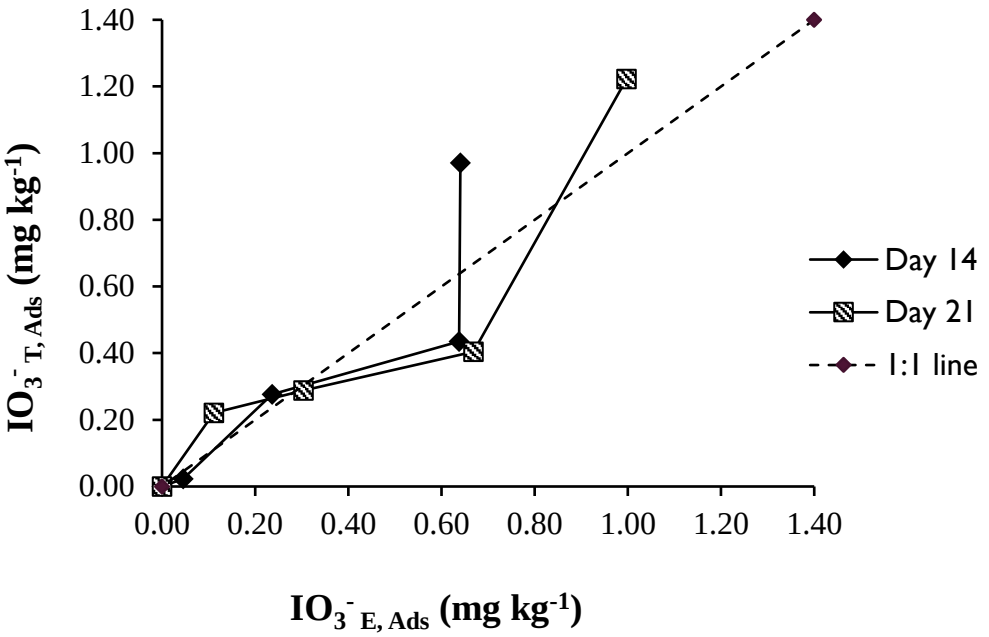


Figure 7.13. Labile adsorbed iodate plotted as a function of the total adsorbed; the initial I concentrations of 0.025 – 1 mg L^{-1}.

7.4. Conclusions

Calcite is an important part of the soil geocolloidal complex for iodine adsorption in soils. Adsorption of freshly added I (e.g. in irrigation water or rainfall) on calcite occurs rapidly (< 24 hours) and there was no evidence of a consistent time-dependence to the adsorption of iodate. There was clear desorption hysteresis for iodate, but only at higher concentrations. This suggests there is only limited evidence of fixation into the calcite structure at iodine concentrations typically occurring in the soil solution. Furthermore, isotopic dilution experiments show that almost all the added iodate remained completely isotopically exchangeable. Again, this suggests that added iodate remains labile and there is no evidence of fixation over the timescale studied, either by deeper incorporation into the calcite structure or even through strong surface adsorption. Finally, an experiment in which a fluctuating 4% CO_2-air bubbling regime was imposed, in an attempt to induce calcite dissolution and precipitation, failed to show any evidence of incorporation of iodate into the calcite structure over the time period of the trial.

Iodate adsorption on gypsum was comparatively small compared to retention on calcite. However, although the data for gypsum was rather poor compared to that for calcite, the trends for time-dependent adsorption and desorption showed some commonality. Nevertheless, for both calcite and gypsum the isotopic exchangeability of the added iodate suggested the absence of a fixation reaction.

Thus, the fate of iodate added in irrigation water or precipitation to calcareous soils is likely to include adsorption on calcite alongside the expected sorption into soil humus. However, such adsorption appears to hold iodate in a labile state and so is likely to retain iodine in a plant available form rather than rapidly fix it into non-available organic fractions within humus. Adsorption on gypsum in gypsiferous soils may be significant where the gypsum content is high but the adsorption capacity of the calcite is far greater and $CaCO_3$ is likely to be the main site of labile iodate sorption in Somali soils.

8. General Discussion and Conclusions

Overview

Selenium (Se) and iodine (I) content and bioavailability in the soil-water systems are the main factors determining their level in the food chain (plant – animal – human). In Somalia, extensive research on native Se and iodine in soil-water-plant systems has not yet been undertaken (Fig. 8.1). Understanding the mechanisms and factors influencing Se and I bioavailability in soil for plant uptake is essential for designing proper agricultural management practices that can tackle human micronutrient deficiencies. In this thesis, research on Se and I total concentration, speciation, bioavailability in agricultural soils in Somalia was performed, the study covered the three media in soil-water-plant systems. In addition, the chemical behaviour of Se and I were further investigated using EXAFS and batch adsorption experiments in order to understand the role of the prevailing pure soil mineral phases (i.e. calcite and gypsum) in typical arid-zone soils, as in Somalia, on the availability of Se and iodine. In Chapter 3, the total concentrations and speciation of Se and I in samples of surface water (from the Shabelle river) and groundwater sources were studied. The concentration and speciation of Se and iodine in Somali water samples can be used as indicators to predict uptake by plants (via irrigation) and also can give insight into direct human intake from this source. In Chapter 4, the concentration, extractability and speciation of Se and iodine in soils were studied using a combination of a single step extraction or sequential extractions, aqua regia digestions and HF digestions. From this study, a better understanding regarding the level, distribution, fractionation and speciation of Se in different Somali agricultural soils was achieved. In Chapter 5, a pilot study was conducted to determine the multi-elemental composition (including Se and I) of staple crops grown in several demonstration plots in Somalia managed by the Somali Agricultural Technical Group (SATG). In Chapter 6, Se sorption on calcite and gypsum was carried out using batch adsorption experiments, utilizing isotopic dilution techniques and EXAFS studies. From this study, a better understanding on the sorption and fixation capacities of pure calcite and gypsum for the different Se species (Se^{IV} and Se^{VI}) was achieved. In Chapter 7, a batch sorption study similar to that in Chapter 6 was conducted, but the experiments were carried out using different iodine species (I^- and IO_3^-). From this study, a better understanding of K_d values, which indicate the strength of sorption of the different iodine species on calcite and gypsum was achieved. In the current chapter (Chapter 8), the main findings from all previous chapters will be discussed in a general context, and the implications of the findings for utilization and future research will be presented.

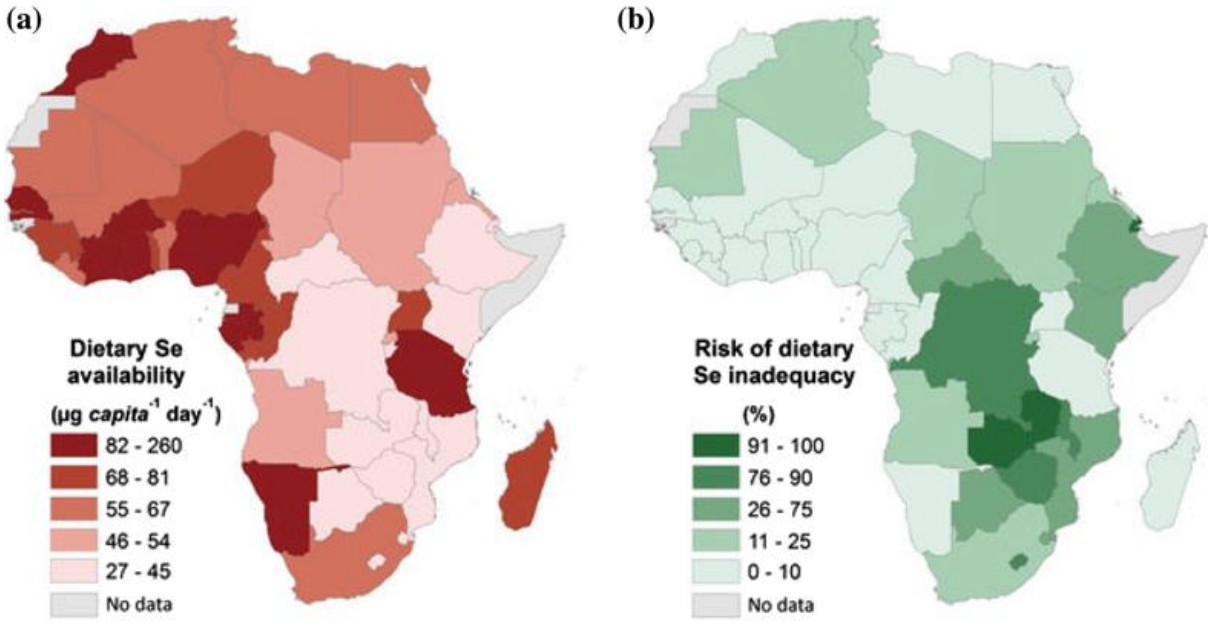


Figure 8.1. Dietary selenium availability (a) and risk of inadequacy (b) in Africa

Source: Hurst et al., 2013 (Soil-type influences human selenium status and underlies widespread selenium deficiency risks in Malawi).

8.1. Water survey

Selenium

Chapter 3 of this thesis showed that the total Se concentration in Somali surface water and groundwater ranged over two orders of magnitude, from 0.09 µg L^{-1} to 9.25 µg L^{-1}, for groundwater and 0.40 µg L^{-1} to 1.60 µg L^{-1} for surface water samples. The mean total Se concentration was 3.63 µg L^{-1} and 0.595 µg L^{-1} for the groundwater and surface water respectively. This finding is in line with the levels of selenium in groundwater and surface water (0.06 to about 400 µg L^{-1}) reported by the (World Health Organization, 2011), and also agrees well with the values reported by (Fordyce, 2007) who suggested that the total Se contents of most natural waters rarely exceeds 10 µg L^{-1}. The Se concentration in other east Africa country was also low, the Se content in Ethiopia for example was generally low, the median values being lower for spring and surface water sources. However, elevated Se concentrations (15–7600 µg L^{-1}) was reported for ground waters of the rift valley region (Gebreeyessus and Zewge, 2019).

Selenium speciation in the groundwater and surface water samples from Somalia also showed that Se is mainly present as selenate, accounting for 50 - 80% of the total Se, the remaining Se is in the form of organically bound Se 20 -50%. The Se that is mainly associated with the organic matter was highest in river water and tube well samples. The predominant Se species is influenced principally by the Eh and pH of the waters; under oxidizing conditions, Se^{VI} will predominate at pH values less than 8.15. In addition, speciation is strongly influenced by relative adsorption strength in soils. (Zhang and Sparks, 1990b) also indicated the predominance of selenate species in water compared to selenite because of strong adsorption of selenite onto soil and sand particles, therefore lowering its chance of ending up in waterways.

The predominance of inorganic Se species in water samples was also found in the studies of (Chandrasekaran et al., 2009) for Indian groundwater samples, in which their speciation analysis of the groundwater used for irrigation and drinking showed selenate to be the predominant species. The total Se contents of the Indian tube well water samples ranged from 12 to 93 μg L^{-1}, higher than the Somali water samples, but still unlikely to cause Se toxicity at normal rates of water consumption (Chandrasekaran et al., 2009).

Selenium input via irrigation with Somali groundwater and surface water was also estimated; the Se input from irrigation of maize with groundwater or surface water can be estimated to be in the ranges 8.50 – 13.6 g ha^{-1} $season^{-1}$ or 3.00 to 4.80 g ha^{-1} $season^{-1}$ respectively. A study by Ros et al. (2014) estimated low supply of Se from irrigation or sprinkling water in Dutch i.e. maximally 0.36 g Se ha^{-1}. Although there is evident of Se addition via irrigation, high sulphate in groundwater in Somalia may lead to competition between sulphate from the irrigation water and Se (Zhao et al., 2007).

Iodine

The iodine concentrations of the Somali groundwater and surface water samples were presented in Chapter 3. The iodine concentration in groundwater samples collected from four districts in Somalia varied between 404 and 5160 μg L^{-1}, with an arithmetic mean of 1690 μg L^{-1}, a median of 990 μg L^{-1}. The iodine concentration in Somali surface water samples (i.e. the Shabelle river, Somalia) varied between 133 and 388 μg L^{-1}, with an arithmetic mean of 218 μg L^{-1}, a median of 187 μg L^{-1}. The difference between the Somali groundwater and surface water is supported by (Fuge and Johnson, 2015), who suggested that generally groundwaters are more enriched than surface water. Within Somalia, ground water samples showed a geographical variation, with a significant difference ($P<0.001$) between the study regions. The

iodine concentration was highest in samples from Afgoi (2940 μg L^{-1}), followed by Bal'ad (1480 μg L^{-1}), Baidoa (471 μg L^{-1}) and Beletweyn (441 μg L^{-1}). Geographical variation in the iodine content of ground water is common and where reported elsewhere, for example, in Denmark iodine concentration in ground water varied largely between regions (Pedersen et al., 1999). The iodine contents of the Somali groundwater is relatively high and is possibly the main cause of the excessive iodine intakes reported in Somali populations, according to urinary iodine biomarker surveys (Kassim et al., 2014). In Somalia, approximately 95% of the population rely on their drinking water from groundwater, which is the only water resource in most of the country, excluding villages of the valleys of the two perennial rivers Juba and Shabelle (BGS, 2020). According to Kassim et al., (2014), the median UICs for Somali population was >300 μg L indicating excessive iodine intake. Visible goitre was also reported < 4%; the excessive iodine intakes was associated with the drinking water source with populations drinking borehole water having a higher UIC (569 vs. 385 μg L^{-1}; $P < 0.001$). By contrast, a study of iodine status among Somali immigrants in Norway have shown variations from Somalis living in Somalia. The urinary iodine concentration (UIC) in Somali immigrants in Norway varied from 13 to 263 μg L^{-1} with a median value of 62.5 μg L^{-1} indicating that these populations would have mild iodine deficiency (Madar et al., 2018).

Similar excessive iodine intakes was also reported for populations relying on high iodine groundwater in China and were associated with greater incidence of goitre and hypothyroidism (Andersen et al., 2009). The studies of Andersen et al. (2009) reported the iodine contents in iodine rich groundwater in China to vary from 135 to 880 μg L^{-1}. In the literature, iodine-rich groundwaters have been reported reaching up to 2800 μg L^{-1} in Jiangsu and up to 4100 μg L^{-1} in Shanxi Province (Fuge and Johnson, 2015). Globally, low dietary iodine content is the problem and is reported across all continents. Compared to Somali water samples the iodine concentration in tap water was low in Denmark (1 to 139 μg L^{-1}), Malawi (1 to 54 μg L^{-1}) and in Israel (5 – 10 μg L^{-1}) (Pedersen et al., 1999a; Rosenthal and Mates, 1986; Watts et al., 2015a). According to Johnson et al. (2003), around 2.2 billion people (38% of the world's population) live in regions with iodine deficiency. There are only a few countries where populations rely on the iodine rich groundwater such as in China and (Johnson et al., 2003; Kassim et al., 2014).

Further study on I speciation in groundwater and surface water samples from Somalia showed that I in these samples is mainly present associated with (dissolved) organic matter (88 - 94 %), the rest of the iodine was present in the inorganic form. The dominant inorganic iodine species

was usually iodide, ranging between 1.4% and 8% of the total iodine content. On average, iodate accounted for 3.5% of the total iodine, whereas iodide content was 5.6%. The distribution of these inorganic iodine species may have been determined principally by variation in the Eh and pH of the water sources; iodide is the predominant form across a wide range of pH levels and an Eh under 0.6 mV while iodate is the favoured species under very oxidizing conditions.

The predominance of organic I in water samples was also found by Andersen et al. (2002) who suggested that iodine was coexisting with humic substances of marine origin. Soluble organically bound iodine was also the major fraction in rain samples as resolved from iodine speciation in rain, snow and aerosols (Andersen et al., 2002). The significance of the interactions between iodine and organic matter has been emphasized and reviewed in many studies (Ashworth and Shaw, 2006a; Bors et al., 1988; Hu et al., 2007; Li et al., 2017; Maillant et al., 2007; Muramatsu et al., 1990; Neal and Truesdale, 1976; Qian et al., 2017; Santschi et al., 2017; Yeager et al., 2017); (Neeway et al., 2019). As yet there has been no research into the bioaccessibility of organic-iodine complexes in drinking water.

8.2. Soil survey

Soil Characterisation

Soil pH is known to influence the concentration and speciation of bioavailable Se and I in the soil solution. The pH values of the soil samples from the study region were all above 7, ranging from 7.9 to 8.4, with an arithmetic mean of 8.1±0.1. The amount and speciation of the bioavailable Se and I in soil solution is also influenced by the organic matter content of the soil; both soil organic matter (SOM; LOI) and total organic carbon (TOC) content were measured. Estimated soil organic matter content (% loss-on-ignition) ranged from 0.17% to 1.07%, with an arithmetic mean of 0.4%±0.2. The highest LOI was noted in samples from Baidoa, Bay region (1%±0.2). The mean values of TIC and TOC were 2.0% ±1.0 and 1.1%±0.4 respectively; the TIC content was approximately 60% of the total soil carbon. The four major exchangeable cations were calcium (Ca), magnesium (Mg), potassium (K), and sodium (Na) accounting for 82%, 12%, 5%, and 1% of the cation exchange capacity (CEC) respectively. The mean total exchangeable cation (Ca, Mg, K and Na) concentration was (53 cmolc kg^{-1}). Multi-elemental analysis of the Somali Agricultural soils has revealed the distribution of the cations to follow the order: Ca_{Tot} (mean: 67,500 mg kg^{-1}) > Al_{Tot} (mean: 45,800 mg kg^{-1}) > Fe_{Tot} (mean: 39,800 mg kg^{-1}) > K_{Tot} (mean: 11,900 mg kg^{-1}) > Mg_{Tot} (mean: 10,700 mg kg^{-1})

> Na_{Tot} (mean: 1,820 mg kg^{-1}) > Ti_{Tot} (mean: 1,600 mg kg^{-1}) > Mn_{Tot} (mean: 790 mg kg^{-1}) > P_{Tot} (mean: 546 mg kg^{-1}) > Ba_{Tot} (mean: 267 mg kg^{-1}) > Sr_{Tot} (mean: 243 mg kg^{-1}).

Selenium

Chapter 4 of this thesis have shown that the total Se concentration (Se_{Tot}) in the Somali agricultural soil samples varied from 300 to 520 µg kg^{-1}, with an arithmetic mean of 400 µg kg^{-1}.

The mean Se_{Tot} of 400 µg kg^{-1} is coincidentally identical to the world mean of 400 µg kg^{-1}, but is higher than that of Malawi (190 µg kg^{-1}) or Finnish soils (10 µg kg^{-1}) (Chilimba et al., 2011; Fordyce, 2005; Fordyce, 2013). Within the Somali agricultural soils, regional variations were found between sampling locations, the highest Se concentration was found in soils from Baidoa, Bay region. The Se_{Tot} in samples from Beletweyn and Buloburte were 25% below the world average. According to Fordyce (2005), soils that have concentrations of Se < 600 µg kg^{-1} are considered Se deficient. Similarly, Gupta and Gupta (2000) reported that in general, a soil with less than 600 µg kg^{-1} of Se is considered Se-deficient. All the soil samples from the 12 agricultural sites contained less than 600 µg kg^{-1} Se; more than 50% of the measured soils contained less than 400 µg Se kg^{-1}. This indicates that agricultural soils in southern Somalia may be prone to problems related to Se deficiency in agricultural produce.

The speciation of Se in the Somali agricultural soils (both rainfed and irrigated land) was also studied (Chapter 4). A 0.01 M KNO_3 extraction, which has been proposed to estimate total soluble elements in soil solution and to evaluate bioavailability of the elements in soils, was used to determine solubility of Se in the soils. The Se solubility in 0.01 M KNO_3 soil extraction (Se_{Sol}) was low, varying from 2.00 to 5.00 µg kg^{-1} in the rainfed soils and 2.00 to 4.00 µg kg^{-1} in the irrigated soils (Table 4.4), with an arithmetic mean of 3.67 and 3.17 µg kg^{-1} for the rainfed and irrigated fields respectively. In general, the concentrations of Se_{Sol} accounted for less than 1% of Se_{Tot}, ranging from 0.5 to 1.4 %. Speciation analysis of the Se_{Sol} fraction was performed using HPLC-ICP-MS to provide a more detailed picture of the different Se forms. The speciation analysis showed that the inorganic soluble Se ($Se_{Sol\text{-}Inorg}$) varied from 31.2% to 66.9% of the total Se_{Sol} with an arithmetic mean of 50.7%, while the soluble organic Se ($Se_{Sol\text{-}Org}$) varied from 33.1% to 68.8, with an arithmetic mean of 49.3%. The $Se_{Sol\text{-}Inorg}$ contained both inorganic Se oxyanions i.e. 26% selenate (Se^{VI}) and 24% selenite (Se^{IV}).

Selenium in the 'adsorbed' fraction was also measured by extraction with 0.016 M KH_2PO_4. and the speciation of Se_{Ads} in the soils was also evaluated. This fraction can be regarded as 'readily bioavailable' Se (or 'exchangeable') and possible originates from Se bound to Fe/Al oxides. The concentrations of the Se_{Ads} accounted on average for 3% of the Se_{Tot}, ranging from 1.3 to 5.3%. Concentrations of the Se_{Ads} fraction were 3-fold higher than those of Se_{Sol}. Similar concentrations of extractable Se in UK agricultural soils were reported by Stroud et al. (2010), who found low extractable soil Se concentrations (2.4 –12.4 µg kg^{-1}). The speciation analysis of the Se_{Ads} fraction provided a more detailed picture of the different Se forms in this fraction and indicated that 71% of the Se_{Ads} was inorganic, while 29% was organic. The majority of the inorganic exchangeable Se was selenite; in fact, in most of the samples Se^{VI} was not present in the $Se_{Ads.}$ This finding confirms experimentally the literature view that Se^{VI} is more mobile that Se^{VI}; Se^{IV} tends to bond more strongly than Se^{VI} with amorphous Fe and Al oxides. Other similar studies that reported the magnitude of Se^{IV} sorption include that of (Supriatin et al., 2015). Further study on Se extractability in soils also showed that Se in Somali agricultural soils is mainly associated with soil organic matter (Chapter 4). The majority (mean 40%) of total Se in soils was present as organic Se extractable with 10% TMAH; it was 10-fold greater than the Se_{Sol} and Se_{Ads} combined. Moreover, the extractability of Se in different reagents used in this study follows in general the order $Se_{Sol} < Se_{Ads} < Se_{TMAH} < Se_{Tot}$; this is in good agreement with the conclusion that Se in soil is predominantly present in organic form. However, the Se_{TMAH} in these soils varied; for example, Se_{TMAH} in soils from Baidoa (Bay region) were significantly ($p<0.05$) greater than in other regions, accounting for 70% of the Se_{Tot}, while Se_{TMAH} accounted for only 15% and 17% of the Se_{Tot} in samples from Beletweyn and Buloburte respectively; the soils with low Se_{TMAH} are characterised with high carbonate minerals. The Se pool in the low-Se_{TMAH} soils was regarded as residual Se due to its resistance to the 10% TMAH extraction. The residual Se ($Se_{Residue}$) was calculated by subtracting the Se_{Sol}, Se_{Ads} and Se_{TMAH} from the Se_{Tot} and was found to vary from 30 – 70% of the Se_{Tot} in the Somali agricultural soils.

The soil properties that are correlated with the soil Se were discussed in Chapter 4.

Correlation analysis in Chapter 4 also showed evidence of association between Se and soil organic matter in the Somali agricultural soils. These associations can be summarized as follows.

- Soil organic matter showed a strong correlation with Se_{Tot} whether expressed as LOI (R^2= 0.628; p < 0.001) or as TOC (R^2= 0.400; p < 0.001).
- The association between the Se_{TMAH} with the soil organic matter content (LOI) was also strong (r=0.844);
- The association with the LOI is supported by a positive correlation between the TOC and the Se_{TMAH} (r=0.529);
- The presence of Se mainly in organically bound forms was also suggested by a very strong correlation between Se_{Tot} (HF digest) and Se_{TMAH} (r=0.901);
- Understanding the mechanisms responsible for these associations is important in the context of the Somali soils.

Further, other soil parameters that effect the Se have been identified. The observation of the strong correlation between the Fe_{Tot} and Al_{Tot} with Se_{Tot}, (R^2= 0.742; p < 0.001 and R^2= 0.751; p < 0.001 respectively), suggest that some Se is possibly associated with oxides of Fe and Al. By contrast, negative correlations were found between Se_{Tot} and TIC (r = -0.761), soil pH (r = -0.137) and Ca_{Tot} (r = -0.793) suggesting carbonate-rich soils accumulate less Se than organic-rich soils.

The soil parameters that appear to influence Se_{Sol} were further investigated; a correlation analysis was performed and can be summarized as follows.

- There was a weak negative correlation with pH (r = -0.355; P-value < 0.05)
- The soil organic matter content was negatively correlated with the Se_{Sol} (r = -0.330), this was consistent with the negative correlation seen between DOC and the Se concentration in groundwater and surface water samples (reported in Chapter 3). A positive correlation between organic matter and Se_{Tot} is expected if the Se was being accumulated in humus but it might also be expected that the solubility of Se would be low in soils with a high organic matter content due to strong adsorption.
- A positive and weak correlation between the Se_{Sol} and the TIC (r=0.177), Mg r=0.348) and Ca (r=0.262) was also noted.

The role of soil inorganic carbon in determining the amount, solubility and speciation of Se in soils:

The findings from Chapter 4 of this thesis indicated that the solubility of soil Se in Somali calcareous soils may be associated with the presence of carbonate minerals; evidence for this association can be summarized as follows.

- A negative correlation was found between Se_{Tot} and TIC (r = -0.761), soil pH (r = -0.137) and Ca_{Tot} (r = -0.793);
- The amount of TMAH extractable Se decreased with the increase in pH, Ca_{Tot} and Mg_{Tot}., (Fig. 8.2a, b and c respectively);
- Similarly, the TMAH extractable Se decreased with increasing $CaCO_3$ content, (Fig. 8.3);
- The residual fraction, which comprised a large fraction of the Se_{Tot} correlated with the soil $CaCO_3$ (r = 0.842) suggesting an association between Se_{Resid} and calcite (Fig. 8.4).

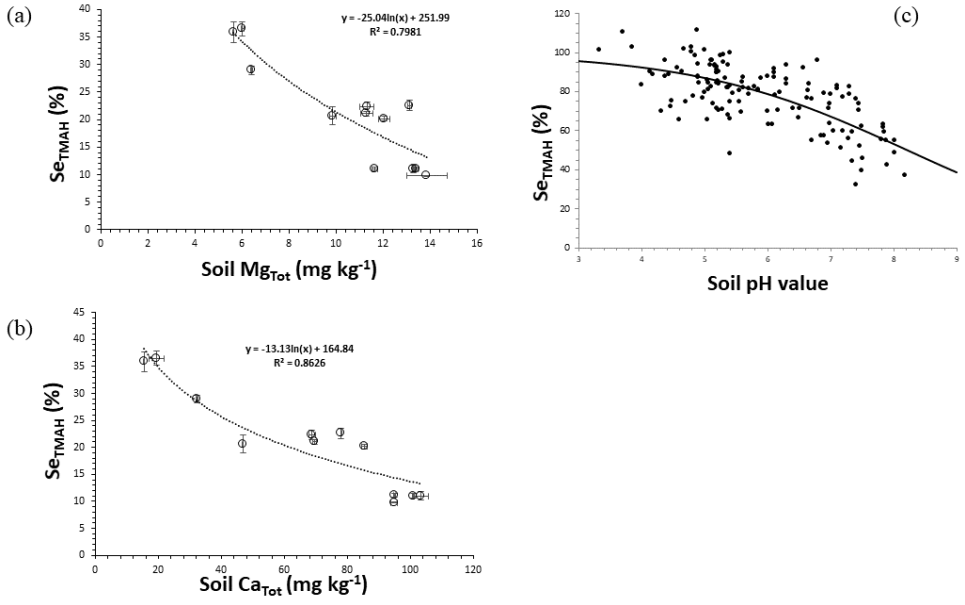


Figure 8.2. Correlations between Se_{TMAH} and soil properties: (a) Mg_{Tot}, (b) Ca_{Tot} and (c) soil pH; Note that Fig 8.2 c is compiled from several datasets.

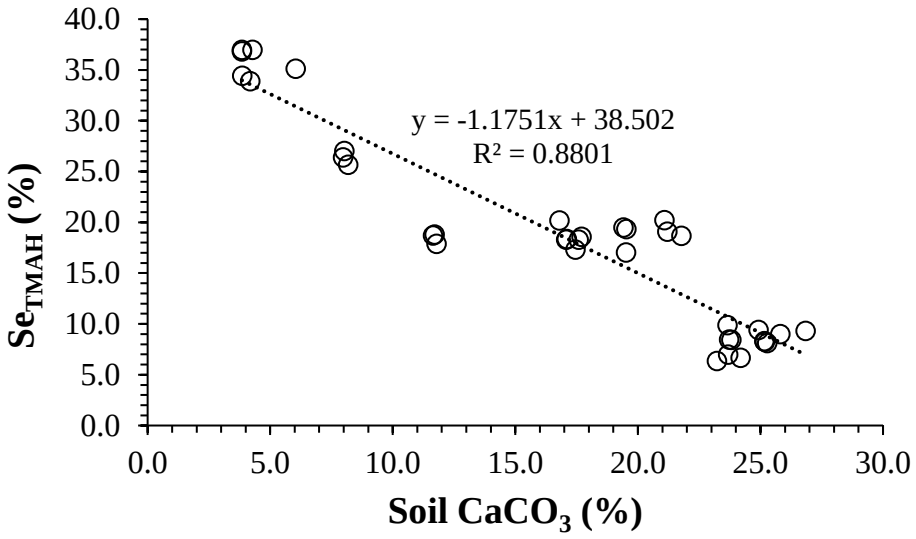


Figure 8.3. The percentage of Se_{TMAH} as a function of soil $CaCO_3$ content (%)

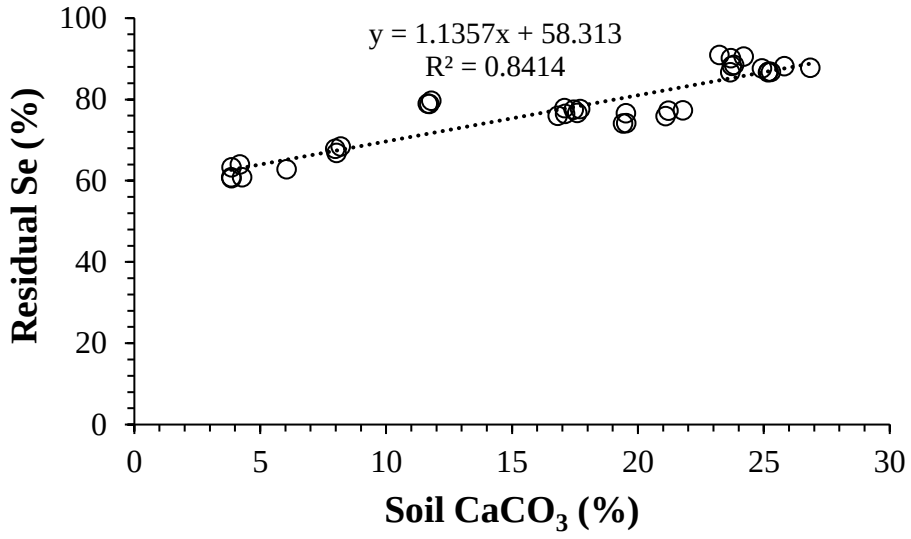


Figure 8.4. Relationship between residual soil Se (%) and the corresponding soil $CaCO_3$ content (%) in the soils of the study area (n=12).

Iodine

In addition to Se, Chapter 4 of this thesis have also shown that the total I concentration (I_{Tot}) in the Somali agricultural soil samples varied from 1.81 to 7.81 mg kg^{-1}, with an arithmetic mean of 4.75 mg kg^{-1}. The mean I_{Tot} of 4.75 mg kg^{-1} is similar to the world mean of 5.00 mg kg^{-1}, but is slightly greater than the worldwide geometric mean of 3.00 mg kg^{-1} (Johnson et al., 2003), and is also higher than that of Malawi and Pakistani soils (Watts et al., 2015; Zia et al., 2015). Within the Somali agricultural soils, regional variations were found between sampling locations, the highest I concentration was found in soils from Baidoa, Bay region; these soils are also characterized with relatively higher soil organic matter compared with other soils. This indicates that while some Somali Agricultural soils contain low *iodine* levels (1.81 mg kg^{-1}) there are *iodine* rich *soils* present as well. This variation may then be reflected in the crops grown in these soils, animals and humans consuming these foods may be susceptible to either iodine deficiency or iodine sufficiency. But such conclusion cannot be drawn relying only on the I_{Tot}, therefore it is further important to understand the bioavailability of element in the soil and the influencing factors.

As described for the investigation of Se fractionation and speciation, a 0.01 M KNO_3 extraction, which has been proposed to estimate total soluble I in soil solution, was adopted to evaluate bioavailability of the I in soils. The I solubility in 0.01 M KNO_3 soil extraction (I_{Sol}) was low, varying from 2 to 11 % of $I_{Tot,}$ with an arithmetic mean of 4%. Speciation analysis of the I_{Sol} showed that the dissolved soil organic matter plays a significant role in determining the solubility and speciation of I in Somali Agricultural soils. On average about 93% of the I_{Sol} was organic, and only 7% was inorganic existing as iodide (6%) and iodate (1%).

A 0.016 M KH_2PO_4 extraction, which has been proposed to estimate total adsorbed I (I_{Ads}) was also used, sequentially following extraction with 0.01 M KNO_3, to evaluate the speciation of the I_{Ads} fraction in the soils. This fraction is important as it is the 'readily bioavailable' I (or 'exchangeable') and possible originates from the fraction bound to Fe/Al oxides. The concentrations of I_{Ads} accounted, on average, for 6% of the I_{Tot}, ranging from 3 to 8%; concentrations of I_{Ads} were, on average, 74% higher than those of the soluble fraction. As also found for I_{Sol}, 95% of I_{Ads} was organic, and only 5% was in inorganic forms including both iodate and iodide species. On average, the sum of the soluble and adsorbed iodine accounted for 10% of the total soil iodine, suggesting that 10% of the soil I_{Tot} may be bioavailable. Similar results were reported for cold water extractable fraction of total iodine in UK soils (<10%) and

in Morocco (2 – 10%). The species distribution is likely to have been influenced by the pH and Eh of soils, iodide is the dominant iodine form in acidic soils, whereas iodate is the favoured iodine form in arid alkaline environments.

8.3. Crops survey: Demonstration plots

The link between crops nutritional composition (including Se and I) and their corresponding soils was investigated and reported for the first time for Somali soils. The Se concentrations of the demonstration crops grown in Somalia were low, resulting in a very low estimated dietary intakes. In fact, the Se concentrations in maize were lower than recorded for Malawi. Iodine contents were also generally very low. It is evident from this study that neither Se nor I dietary requirements can be satisfied from relying on unfortified maize as the staple carbohydrate crop. This suggests that communities that rely on maize cultivated within subsistence farming systems are likely to be prone to nutritional deficiencies, including Se and I. Iodine intake is possibly adequate or excessive according to the groundwater survey (reported in Chapter 3). The data obtained from this study, although limited to the SATG demonstration plots, suggests the need to biofortify to increase the Se content of Somali stable crops, in order to provide adequate dietary Se intake, and offset potential health consequences. Successful biofortification attempts can be adopted such the Se fertilization of crops in Finland, when the Finnish government decided to increase the Se content of cereals by 10-fold (Eurola, 2005). But before any intervention with biofortification is attempted, it would be important to conduct a well-structured nationwide survey covering all agricultural soil types and all crop types as well.

8.4. Batch adsorption experiments

The mechanism controlling the solubility and lability of Se (Se^{IV} and Se^{VI}) and I (IO_3^- and I^-) in calcareous and gypsiferous minerals were monitoring over a period of 21 days using both whole soils and pure mineral phases. Batch sorption experiments confirmed that there was greater/stronger Se sorption on calcite compared with gypsum. This emphasizes the importance of calcite in controlling Se sorption and subsequent bioavailability in soils of arid and semi-arid environments. The magnitude of the sorption was significantly affected by the Se species, both calcite and gypsum had greater affinities for Se^{IV}. Sorption occurred rapidly (i.e. 24 hours) and the sorption isotherm did not show a time-dependent pattern and was largely reversible. Furthermore, there was little evidence of fixation within this time period from isotopic exchange studies, notwithstanding the association between inert (residual) forms of Se and the $CaCO_3$ content of the Somali soils. This suggests either that (i) gradual fixation of Se into the

structure of the $CaCO_3$ must occur over much longer timescales than covered by the batch adsorption experiments or (ii) the Se was already contained within native $CaCO_3$ from the original soil parent material.

Iodate sorption experiments have revealed that in calcareous soils such as those of Somalia adsorption on calcite is significant and must operate alongside the expected sorption into soil humus. The isotopically exchangeability of iodate revealed that such adsorption appears to hold iodate in a labile state and so is likely to retain iodine in a plant-available form rather than rapidly fix it into non-available organic fractions within humus. There is evidence of sorption on gypsum in gypsiferous soils, but the sorption was more important in calcareous Somali soils.

8.5. Future work

- The findings from this study suggest the need for further investigation of the dietary intakes of selenium and iodine, this could be done by conducting a detailed dietary survey to understand the status of these nutrients of people.
- There is an urgent need for a better understanding on the high iodine content and it is link with the excess dietary iodine intakes reported in the literature.
- Future studies using both pot experiments and field trials to investigate the feasibility of the agronomic Se biofortification, focusing on maize, sorghum and vegetables.
- Future extended surveys to cover a wider soil types, crops and water resources.
- In this study a large fraction of the soil Se resisted the TMAH extraction, therefore a detailed investigation on the characterization of the recalcitrant soil Se and mechanisms of solubilisations is recommended.

References

Abdel-Moati, M. A. R. (1999). Iodine speciation in the Nile River estuary. *Marine Chemistry*, *65*(3–4), 211–225.

Abernathy, C., Cole, D., Cassidy, M., Morris, M., Gomez, G., & Lacker, L. (2003). Drinking Water Advisory : Consumer Acceptability Advice and Health Effects Analysis. *EPA*.

Adams, M. L., Lombi, E., Zhao, F. J., & McGrath, S. P. (2002). Evidence of low selenium concentrations in UK bread-making wheat grain. *Journal of the Science of Food and Agriculture*. https://doi.org/10.1002/jsfa.1167

Adelana, S., & MacDonald, A. (2008). *Applied groundwater studies in Africa: IAH selected papers on hydrogeology* (Vol. 13). CRC Press.

Ahmed, I. A. M., Crout, N. M. J., & Young, S. D. (2008). Kinetics of Cd sorption, desorption and fixation by calcite: A long-term radiotracer study. *Geochimica et Cosmochimica Acta*. https://doi.org/10.1016/j.gca.2008.01.014

Alexandratos, V. G., Elzinga, E. J., & Reeder, R. J. (2007). Arsenate uptake by calcite: Macroscopic and spectroscopic characterization of adsorption and incorporation mechanisms. *Geochimica et Cosmochimica Acta*. https://doi.org/10.1016/j.gca.2007.06.055

Alloway, B. J. (2008). Zinc in soils and crop nutrition. International Zinc Association, Brussels. In *International Fertilizer Industry Association, Paris*.

Andersen, S., Guan, H., Teng, W., & Laurberg, P. (2009). Speciation of iodine in high iodine groundwater in China associated with goitre and hypothyroidism. *Biological Trace Element Research*, *128*(2), 95.

Andersen, S., Petersen, S. B., & Laurberg, P. (2002). Iodine in drinking water in Denmark is bound in humic substances. *European Journal of Endocrinology*, *147*(5), 663–670.

Andersson, M., Karumbunathan, V., & Zimmermann, M. B. (2012). Global Iodine Status in 2011 and Trends over the Past Decade. *The Journal of Nutrition*. https://doi.org/10.3945/jn.111.149393

Andersson, M. P., Sakuma, H., & Stipp, S. L. S. (2014). Strontium, nickel, cadmium, and lead substitution into calcite, studied by density functional theory. *Langmuir*. https://doi.org/10.1021/la500832u

Ashworth, D. J., & Shaw, G. (2006a). Effects of moisture content and redox potential on in situ Kd values for radioiodine in soil. *Science of the Total Environment*, *359*(1–3), 244–254.

Ashworth, D. J., & Shaw, G. (2006b). Soil migration, plant uptake and volatilisation of radio-selenium from a contaminated water table. *Science of the Total Environment*, *370*(2–3), 506–514.

Assemi, S., & Erten, H. (1994). Sorption of radioiodine on organic rich soil, clay minerals and alumina. *Journal of Radioanalytical and Nuclear Chemistry*, *178*(1), 193–204.

Aurelio, G., Fernández-Martínez, A., Cuello, G. J., Román-Ross, G., Alliot, I., & Charlet, L. (2010). Structural study of selenium(IV) substitutions in calcite. *Chemical Geology*. https://doi.org/10.1016/j.chemgeo.2009.12.004

Bajaj, M., Eiche, E., Neumann, T., Winter, J., & Gallert, C. (2011). Hazardous concentrations of selenium in soil and groundwater in North-West India. *Journal of Hazardous Materials*, *189*(3), 640–646.

Balistrieri, L. S., & Chao, T. T. (1990). Adsorption of selenium by amorphous iron oxyhydroxide and manganese dioxide. *Geochimica et Cosmochimica Acta*, *54*(3), 739–751.

Bar-Yosef, B., & Meek, D. (1987). Selenium sorption by kaolinite and montmorillonite. *Soil Science*, *144*(1), 11–19.

Barker, A. V, & Pilbeam, D. J. (2015). *Handbook of plant nutrition*. CRC press.

BARROW, N. J., & WHELAN, B. R. (1989). Testing a mechanistic model. VIII. The effects of time and temperature of incubation on the sorption and subsequent desorption of selenite and selenate by a soil. *Journal of Soil Science*. https://doi.org/10.1111/j.1365-2389.1989.tb01251.x

Beals, D. M., Chastagner, P., & Turner, P. (1992). *Analysis of iodine-129 in aqueous samples by inductively coupled plasma-mass spectrometry*. Westinghouse Savannah River Co., Aiken, SC (United States).

Bergaya, F., & Lagaly, G. (2013). *Handbook of clay science* (Vol. 5). Newnes.

BGS. (2020). *Hydrogeology of Somalia*. http://earthwise.bgs.ac.uk/index.php/Hydrogeology_of_Somalia

Bolan, N. S., Loganathan, P., & Saggar, S. (2005). *Calcium and magnesium in soils*.

Boldrin, P. F., Faquin, V., Ramos, S. J., Boldrin, K. V. F., Ávila, F. W., & Guilherme, L. R. G. (2013). Soil and foliar application of selenium in rice biofortification. *Journal of Food Composition and Analysis*, *31*(2), 238–244.

Borge, A. (1997). A comparison of buffered and unbuffered ammonium salts to determine exchangeable base cations in acid soils. *Communications in Soil Science and Plant Analysis*, *28*(15–16), 1421–1428.

Bors, J., Martens, R., & Kühn, W. (1988). Studies on the role of natural and anthropogenic organic substances in the mobility of radioiodine in soils. *Radiochimica Acta*, *44*(1), 201–206.

Bowles, J. F. W. (1997). R.M. Cornell and U. Schwertmann The Iron Oxides: Structure, Properties Reactions Occurrence and Uses. Weinheim and New York (VCH Verlagsgeseiischaft mbH). 1996, xxxi + 573 pp. Price DM 328.00. ISBN 3-527-28576-8. *Mineralogical Magazine*. https://doi.org/10.1180/minmag.1997.061.408.20

Bowley, H. E. (2013). *Iodine dynamics in the terrestrial environment*. University of Nottingham.

Broadley, M. R., White, P. J., Bryson, R. J., Meacham, M. C., Bowen, H. C., Johnson, S. E., Hawkesford, M. J., McGrath, S. P., Zhao, F.-J., Breward, N., Harriman, M., & Tucker, M. (2006). Biofortification of UK food crops with selenium. *Proceedings of the Nutrition Society*. https://doi.org/10.1079/pns2006490

Brouwer, C., & Heibloem, M. (1986). Irrigation Water Management: Irrigation Water Needs Part I Principles of irrigation water needs Part II Determination of irrigation water needs

a manual prepared jointly. *FAO*.

Brown, C. F., Geiszler, K. N., & Lindberg, M. J. (2007). Analysis of 129I in groundwater samples: Direct and quantitative results below the drinking water standard. *Applied Geochemistry*, *22*(3), 648–655.

Burte, P. P., Nair, A. G. C., Manohar, S. B., & Prakash, S. (1991). Iodide and iodine uptake in plants. *Journal of Radioanalytical and Nuclear Chemistry Letters*. https://doi.org/10.1007/BF02163633

Cakmak, I., Prom-u-thai, C., Guilherme, L. R. G., Rashid, A., Hora, K. H., Yazici, A., Savasli, E., Kalayci, M., Tutus, Y., Phuphong, P., Rizwan, M., Martins, F. A. D., Dinali, G. S., & Ozturk, L. (2017). Iodine biofortification of wheat, rice and maize through fertilizer strategy. *Plant and Soil*. https://doi.org/10.1007/s11104-017-3295-9

Cao, X.-Y., Jiang, X.-M., Dou, Z. H., Rakeman, M. A., Kareem, A., Zang, M. L., Ma, T., O'Donnell, K., DeLong, N., & DeLong, G. R. (1994). Iodination of irrigation water as a method of supplying iodine to a severely iodine-deficient population in Xinjiang, China. *The Lancet*, *344*(8915), 107–110.

Cardoso, B. R., Apolinário, D., da Silva Bandeira, V., Busse, A. L., Magaldi, R. M., Jacob-Filho, W., & Cozzolino, S. M. F. (2016). Effects of Brazil nut consumption on selenium status and cognitive performance in older adults with mild cognitive impairment: a randomized controlled pilot trial. *European Journal of Nutrition*, *55*(1), 107–116.

Carmignani, L., Conti, P., & Fantozzi, P. L. (2002). Geology of the Mesozoic-Tertiary sedimentary basins in southwestern Somalia. *Journal of African Earth Sciences*, *34*(1–2), 3–20.

Chandrasekaran, K., Ranjit, M., & Arunachalam, J. (2009). Determination of inorganic selenium species [Se (IV) and Se (VI)] in tube well water samples in Punjab, India. *Chemical Speciation & Bioavailability*, *21*(1), 15–22.

Chao, T. T., & Sanzolone, R. F. (1989). Fractionation of soil selenium by sequential partial dissolution. *Soil Science Society of America Journal*. https://doi.org/10.2136/sssaj1989.03615995005300020012x

Chapman, H. D. (1965). Cation-exchange capacity 1. *Methods of Soil Analysis. Part 2. Chemical and Microbiological Properties*, *methodsofsoilanb*, 891–901.

Chasteen, T. G., & Bentley, R. (2003). Biomethylation of selenium and tellurium: microorganisms and plants. *Chemical Reviews*, *103*(1), 1–26.

Cheng, L., Lyman, P. F., Sturchio, N. C., & Bedzyk, M. J. (1997). X-ray standing wave investigation of the surface structure of selenite anions adsorbed on calcite. *Surface Science*. https://doi.org/10.1016/S0039-6028(97)00167-2

Chilimba, A. D. C., Young, S. D., Black, C. R., Meacham, M. C., Lammel, J., & Broadley, M. R. (2012). Agronomic biofortification of maize with selenium (Se) in Malawi. *Field Crops Research*, *125*, 118–128.

Chilimba, A. D. C., Young, S. D., Black, C. R., Rogerson, K. B., Louise Ander, E., Watts, M. J., Lammel, J., & Broadley, M. R. (2011). Maize grain and soil surveys reveal suboptimal dietary selenium intake is widespread in Malawi. *Scientific Reports*. https://doi.org/10.1038/srep00072

Christensen, T. H., Lehmann, N., Jackson, T., & Holm, P. E. (1996). Cadmium and nickel distribution coefficients for sandy aquifer materials. *Journal of Contaminant Hydrology*. https://doi.org/10.1016/0169-7722(96)00012-5

Clark, L. C., Combs, G. F., Turnbull, B. W., Slate, E. H., Chalker, D. K., Chow, J., Davis, L. S., Glover, R. A., Graham, G. F., Gross, E. G., Krongrad, A., Lesher, J. L., Park, H. K., Sanders, B. B., Smith, C. L., & Taylor, J. R. (1996). Effects of selenium supplementation for cancer prevention in patients with carcinoma of the skin: A randomized controlled trial. *Journal of the American Medical Association*. https://doi.org/10.1001/jama.276.24.1957

Coleman, N. T., Weed, S. B., & McCracken, R. J. (1959). Cation-Exchange Capacity and Exchangeable Cations in Piedmont Soils of North Carolina 1. *Soil Science Society of America Journal*, *23*(2), 146–149.

Comandini, P., Cerretani, L., Rinaldi, M., Cichelli, A., & Chiavaro, E. (2013). Stability of iodine during cooking: investigation on biofortified and not fortified vegetables. *International Journal of Food Sciences and Nutrition*, *64*(7), 857–861.

Combs, G. F. (2001). Selenium in global food systems. *British Journal of Nutrition*, *85*(5), 517–547.

Combs Jr, G. F., & Combs, S. B. (1986). *The role of selenium in nutrition.* Academic Press, Inc.

Coppin, F., Chabroullet, C., & Martin-Garin, A. (2009). Selenite interactions with some particulate organic and mineral fractions isolated from a natural grassland soil. *European Journal of Soil Science*, *60*(3), 369–376.

Courtman, C., Van Ryssen, J., & Oelofse, A. (2012). Selenium concentration of maize grain in South Africa and possible factors influencing the concentration. *South African Journal of Animal Science*. https://doi.org/10.4314/sajas.v42i5.2

Cowan, C. E., Zachara, J. M., & Resch, C. T. (1990). Solution ion effects on the surface exchange of selenite on calcite. *Geochimica et Cosmochimica Acta*, *54*(8), 2223–2234.

Critchley, W., Siegert, K., & Chapman, C. (1991). A Manual for the Design and Construction of Water Harvesting Schemes for Plant Production. In *FOOD AND AGRICULTURE ORGANIZATION OF THE UNITED NATIONS - Rome*.

Curtin, D., Hanson, R., Lindley, T. N., & Butler, R. C. (2006). Selenium concentration in wheat (Triticum aestivum) grain as influenced by method, rate, and timing of sodium selenate application. *New Zealand Journal of Crop and Horticultural Science*, *34*(4), 329–339.

Dai, J. L., Zhang, M., Hu, Q. H., Huang, Y. Z., Wang, R. Q., & Zhu, Y. G. (2009). Adsorption and desorption of iodine by various Chinese soils: II. Iodide and iodate. *Geoderma*. https://doi.org/10.1016/j.geoderma.2009.07.020

Dai, J L, Zhu, Y. G., Huang, Y. Z., Zhang, M., & Song, J. L. (2006). Availability of iodide and iodate to spinach (Spinacia oleracea L.) in relation to total iodine in soil solution. *Plant and Soil*, *289*(1–2), 301–308.

Dai, Jiu Lan, Zhang, M., & Zhu, Y. G. (2004). Adsorption and desorption of iodine by various Chinese soils I. Iodate. *Environment International*. https://doi.org/10.1016/j.envint.2003.10.007

Dávila, M., Acosta, N., Betancourt, C., & Negrón, J. (1999). Chitinolytic capacity of fungi isolated from agricultural soils infested with the root-knot nematode (Meloidogyne spp.) in Puerto Rico. *The Journal of Agriculture of the University of Puerto Rico*, *83*(3–4), 189–199.

Davis, K. J., Dove, P. M., & De Yoreo, J. J. (2000). The role of Mg2+ as an impurity in calcite growth. *Science*. https://doi.org/10.1126/science.290.5494.1134

De Temmerman, L., Waegeneers, N., Thiry, C., Du Laing, G., Tack, F., & Ruttens, A. (2014). Selenium content of Belgian cultivated soils and its uptake by field crops and vegetables. *Science of the Total Environment*. https://doi.org/10.1016/j.scitotenv.2013.08.016

Delange, Francois. (2000). The role of iodine in brain development. *Proceedings of the Nutrition Society*, *59*(1), 75–79.

Delange, François, de Benoist, B., Pretell, E., & Dunn, J. T. (2001). Iodine deficiency in the world: where do we stand at the turn of the century? *Thyroid*, *11*(5), 437–447.

DeLaune, R. D., & Reddy, K. R. (2005). *Redox potential*.

Dhillon, K. S., & Dhillon, S. K. (1999). Adsorption-desorption reactions of selenium in some soils of India. *Geoderma*. https://doi.org/10.1016/S0016-7061(99)00040-3

Dhillon, K. S., & Dhillon, S. K. (2003). Quality of underground water and its contribution towards selenium enrichment of the soil-plant system for a seleniferous region of northwest India. *Journal of Hydrology*. https://doi.org/10.1016/S0022-1694(02)00259-7

Dhillon, K S, & Dhillon, S. K. (2003). Distribution and management of seleniferous soils. *Advances in Agronomy*, *79*(1), 119–184.

Dhillon, Karaj S, & Dhillon, S. K. (2014). Development and mapping of seleniferous soils in northwestern India. *Chemosphere*, *99*, 56–63.

Dove, P. M., & Hochella, M. F. (1993). Calcite precipitation mechanisms and inhibition by orthophosphate: In situ observations by Scanning Force Microscopy. *Geochimica et Cosmochimica Acta*. https://doi.org/10.1016/0016-7037(93)90381-6

Duan, L., Wang, W., Sun, Y., & Zhang, C. (2016). Iodine in groundwater of the Guanzhong Basin, China: sources and hydrogeochemical controls on its distribution. *Environmental Earth Sciences*. https://doi.org/10.1007/s12665-016-5781-4

Duc, M., Lefèvre, G., & Fédoroff, M. (2006). Sorption of selenite ions on hematite. *Journal of Colloid and Interface Science*. https://doi.org/10.1016/j.jcis.2006.01.029

Duc, Myriam, Lefevre, G., Fedoroff, M., Jeanjean, J., Rouchaud, J. C., Monteil-Rivera, F., Dumonceau, J., & Milonjic, S. (2003). Sorption of selenium anionic species on apatites and iron oxides from aqueous solutions. *Journal of Environmental Radioactivity*, *70*(1–2), 61–72.

Eastman, C. J., & Zimmermann, M. B. (2018). The iodine deficiency disorders. In *Endotext [Internet]*. MDText. com, Inc.

Eiche, E., Nothstein, A. K., Göttlicher, J., Steininger, R., Dhillon, K. S., & Neumann, T. (2019). The behaviour of irrigation induced Se in the groundwater-soil-plant system in Punjab, India. *Environmental Science: Processes & Impacts*.

Eklund, L., & Persson, I. (2014). Structure and hydrogen bonding of the hydrated selenite and

selenate ions in aqueous solution. *Dalton Transactions*. https://doi.org/10.1039/c3dt53468e

Elmi, A. A. (1991). Livestock production in Somalia with special emphasis on camels. *Nomadic Peoples*, 87–103.

Elrashidi, M A, Adriano, D. C., Workman, S. M., & Lindsay, W. L. (1987). Chemical equilibria of selenium in soils: a theoretical development1. *Soil Science*, *144*(2), 141–152.

Elrashidi, Moustafa A. (2018). Selenium Distribution for Soils Derived from Mancos Shale in Gunnison and Uncompahgre River Basins, West-Central Colorado. *Communications in Soil Science and Plant Analysis*, *49*(9), 1083–1091.

Elzinga, E. J., Rouff, A. A., & Reeder, R. J. (2006). The long-term fate of Cu2+, Zn2+, and Pb2+ adsorption complexes at the calcite surface: An X-ray absorption spectroscopy study. *Geochimica et Cosmochimica Acta*. https://doi.org/10.1016/j.gca.2006.02.026

Encyclopedia Britanica. (2020). *Encyclopedia Britanica*. https://www.britannica.com/place/Somalia/Economy

Etteieb, S., Magdouli, S., Zolfaghari, M., & Brar, S. (2019). Monitoring and analysis of selenium as an emerging contaminant in mining industry: A critical review. *Science of the Total Environment*, 134339.

Eurola, M. (2005). Twenty years of selenium fertilization. *Conference Proceedings, AgriFood Research Report*, *69*, 108.

Fairweather-Tait, S. J., Bao, Y., Broadley, M. R., Collings, R., Ford, D., Hesketh, J. E., & Hurst, R. (2011). Selenium in human health and disease. In *Antioxidants and Redox Signaling*. https://doi.org/10.1089/ars.2010.3275

FAO. (1990). *Management of gypsiferous soils* (Issue 62). Food & Agriculture Org.

FAO. (2003). *The State of Food Insecurity in the World*. http://www.fao.org/3/j0083e/j0083e00.pdf

FAO. (2018). *Rebuilding Resilient and Sustainable Agriculture in Somalia*. http://www.fao.org/3/I8841EN/i8841en.pdf

FAO SWALIM. (2020). *FAOSTAT*. FAO. http://www.faoswalim.org/water/water-resources/ground-water

FAO, & WHO. (2004). Vitamin and mineral requirements in human nutrition. Second edition. *World Health Organization and Food and Agriculture Organization of the United Nations*. https://doi.org/92 4 154612 3

Feist, L. J., & Parker, D. R. (2001). Ecotypic variation in selenium accumulation among populations of Stanleya pinnata. *New Phytologist*, *149*(1), 61–69.

Feng, X., & Redfern, S. A. T. (2018). Iodate in calcite, aragonite and vaterite CaCO3: Insights from first-principles calculations and implications for the I/Ca geochemical proxy. *Geochimica et Cosmochimica Acta*, *236*, 351–360.

Fernández-Martínez, A., & Charlet, L. (2009). Selenium environmental cycling and bioavailability: A structural chemist point of view. In *Reviews in Environmental Science and Biotechnology*. https://doi.org/10.1007/s11157-009-9145-3

Field, C. W. (1972). Sulfur: element and geochemistry. *Encyclopedia of Geochemistry and Environmental Sciences: New York, Van Nostrand Reinhold Co*, 1142–1148.

Fitzgerald, N. J. (2002). *Somalia: issues, history, and bibliography*. Nova Publishers.

Fleming, G. A. (1980). Essential micronutrients. II. Iodine and selenium. *Applied Soil Trace Elements. Edited by Brian E. Davies*.

Food, F. A. O. (1973). Agriculture Organization of the United Nations (FAO): Calcareous soils: Report of the FAO/UNDP regional seminar on reclamation and management of calcareous soils (FAO Soils Bulletin 21). *Cairo, Egypt*.

Fordyce, F. (2005). *Selenium deficiency and toxicity in the environment. In 'Essentials of medical geology–Impacts of the natural environment on public health'(Eds O Selinus, B Alloway, JA Centeno, RB Finkelman, R Fuge, U Lindh, P Smedley) pp. 373-415*. Elsevier-Academic Press, London.

Fordyce, F M, Brereton, N., Hughes, J., Luo, W., & Lewis, J. (2010). An initial study to assess the use of geological parent materials to predict the Se concentration in overlying soils and in five staple foodstuffs produced on them in Scotland. *Science of the Total Environment*, *408*(22), 5295–5305.

Fordyce, Fiona. (2007). Selenium geochemistry and health. *AMBIO: A Journal of the Human Environment*, *36*(1), 94–98.

Fordyce, Fiona M. (2013). Selenium deficiency and toxicity in the environment. In *Essentials of Medical Geology: Revised Edition*. https://doi.org/10.1007/978-94-007-4375-5_16

Fordyce, Fiona M., Johnson, C. C., Navaratna, U. R. B. B., Appleton, J. D., & Dissanayake, C. B. (2000). Selenium and iodine in soil, rice and drinking water in relation to endemic goitre in Sri Lanka. *Science of the Total Environment*, *263*(1–3), 127–141. https://doi.org/10.1016/S0048-9697(00)00684-7

Foundation, B. N. (2001). *Selenium and health*. British Nutrition Foundation.

Frost, R. R., & Griffin, R. A. (1977). EFFECT OF pH ON ADSORPTION OF ARSENIC AND SELENIUM FROM LANDFILL LEACHATE BY CLAY MINERALS. *Soil Science Society of America Journal*. https://doi.org/10.2136/sssaj1977.03615995004100010019x

Fuge, R, Ander, E. L., & Nicholson, K. (1998). Geochemical barriers and the distribution of iodine in the secondary environment: implications for radio-iodine. *Energy and the Environment: Geochemistry of Fossil, Nuclear and Renewable Resources, MacGregor Science, Aberdeen*, 163–170.

Fuge, R, Johnson, C. C., & Phillips, W. J. (1978). Iodine in granitic and associated rocks. *Chemical Geology*, *22*, 347–352.

Fuge, Ron. (1996). Geochemistry of iodine in relation to iodine deficiency diseases. *Geological Society, London, Special Publications*, *113*(1), 201–211.

Fuge, Ron. (2013). Soils and iodine deficiency. In *Essentials of Medical Geology: Revised Edition*. https://doi.org/10.1007/978-94-007-4375-5_17

Fuge, Ron, & Johnson, C. C. (2015). Iodine and human health, the role of environmental geochemistry and diet, a review. In *Applied Geochemistry*. https://doi.org/10.1016/j.apgeochem.2015.09.013

Fuge, Ronald, & Johnson, C. C. (1986). The geochemistry of iodine—a review. *Environmental Geochemistry and Health*, *8*(2), 31–54.

Gabos, M. B., Goldberg, S., & Alleoni, L. R. F. (2014). Modeling selenium (IV and VI) adsorption envelopes in selected tropical soils using the constant capacitance model. *Environmental Toxicology and Chemistry*, *33*(10), 2197–2207.

Gardiner, M. R., & Gorman, R. C. (1963). Further observations on plant selenium levels in Western Australia. *Australian Journal of Experimental Agriculture*. https://doi.org/10.1071/EA9630284

Gavin, R., Haji, H., & Porter, P. (2019). The relative contributions of cereal production, imports, and aid to Somali food security. *African Journal of Food Agriculture Nutrition and Development*, *19*(03), 14587–14601. https://doi.org/10.18697/ajfand.86.18025

Gebreeyessus, G. D., & Zewge, F. (2019). A review on environmental selenium issues. *SN Applied Sciences*. https://doi.org/10.1007/s42452-018-0032-9

Gierus, M., Schwarz, F. J., & Kirchgessner, M. (2002). Selenium supplementation and selenium status of dairy cows fed diets based on grass, grass silage or maize silage. *Journal of Animal Physiology and Animal Nutrition*. https://doi.org/10.1046/j.1439-0396.2002.00359.x

Gilfedder, B. S., Petri, M., & Biester, H. (2007). Iodine speciation in rain and snow: Implications for the atmospheric iodine sink. *Journal of Geophysical Research: Atmospheres*, *112*(D7).

Gissel-Nielsen, G. (1998). Effects of selenium supplementation of field crops. In *Environmental chemistry of selenium* (pp. 121–134). CRC Press.

Gissel-Nielsen, G., Gupta, U. C., Lamand, M., & Westermarck, T. (1984). Selenium in Soils and Plants and its Importance in Livestock and Human Nutrition. *Advances in Agronomy*. https://doi.org/10.1016/S0065-2113(08)60459-9

Goldberg, S., & Glaubig, R. A. (1988). Anion sorption on a calcareous, montmorillonitic soil - selenium. *Soil Science Society of America Journal*. https://doi.org/10.2136/sssaj1988.03615995005200040010x

Goldberg, Sabine. (2013). Modeling selenite adsorption envelopes on oxides, clay minerals, and soils using the triple layer model. *Soil Science Society of America Journal*, *77*(1), 64–71.

Gonzali, S., Kiferle, C., & Perata, P. (2017). Iodine biofortification of crops: agronomic biofortification, metabolic engineering and iodine bioavailability. *Current Opinion in Biotechnology*, *44*, 16–26.

Graham, R. D., Welch, R. M., & Bouis, H. E. (2001). *Addressing micronutrient malnutrition through enhancing the nutritional quality of staple foods: principles, perspectives and knowledge gaps*.

Green-Pedersen, H., Jensen, B. T., & Pind, N. (1997). Nickel adsorption on mno2, fe(oh)3, montmorillonite, humic acid and calcite: A comparative study. *Environmental Technology (United Kingdom)*. https://doi.org/10.1080/09593331808616599

Gunnarsdottir, I., Gustavsdottir, A. G., & Thorsdottir, I. (2009). Iodine intake and status in Iceland through a period of 60 years. *Food and Nutrition Research*.

Gupta, U. C., & Gupta, S. C. (2000). Selenium in soils and crops, its deficiencies in livestock and humans: implications for management. *Communications in Soil Science and Plant Analysis*, *31*(11–14), 1791–1807.

Gupta, U. C., & Gupta, S. C. (2002). Quality of animal and human life as affected by selenium management of soils and crops. *Communications in Soil Science and Plant Analysis*, *33*(15–18), 2537–2555.

Gustafsson, J. P., & Johnsson, L. (1994). The association between selenium and humic substances in forested ecosystems—laboratory evidence. *Applied Organometallic Chemistry*. https://doi.org/10.1002/aoc.590080209

Hadden, R. L. (2007). The Geology of Somalia : a Selected Bibliography of Somalian Geology , Geography and Earth Science. *US Army Corps of Engineers*.

Haldimann, M., Eastgate, A., & Zimmerli, B. (2000). Improved measurement of iodine in food samples using inductively coupled plasma isotope dilution mass spectrometry. *Analyst*, *125*(11), 1977–1982.

Hamdy, A. A., & Gissel-Nielsen, G. (1977). Fixation of selenium by clay minerals and iron oxides. *Zeitschrift Für Pflanzenernährung Und Bodenkunde*, *140*(1), 63–70.

Hartikainen, H. (2005). Biogeochemistry of selenium and its impact on food chain quality and human health. *Journal of Trace Elements in Medicine and Biology*. https://doi.org/10.1016/j.jtemb.2005.02.009

Hayes, K. F., Roe, A. L., Brown, G. E., Hodgson, K. O., Leckie, J. O., & Parks, G. A. (1987). In situ X-ray absorption study of surface complexes: Selenium oxyanions on α-FeOOH. *Science*, *238*(4828), 783–786.

Heberling, F., Vinograd, V. L., Polly, R., Gale, J. D., Heck, S., Rothe, J., Bosbach, D., Geckeis, H., & Winkler, B. (2014). A thermodynamic adsorption/entrapment model for selenium(IV) coprecipitation with calcite. *Geochimica et Cosmochimica Acta*. https://doi.org/10.1016/j.gca.2014.02.044

Hetzel, B. S., & Pandav, C. S. (1994). *SOS for a billion: the conquest of iodine deficiency disorders*. Oxford University Press.

Hillel, D., & Hatfield, J. L. (2005). *Encyclopedia of Soils in the Environment* (Vol. 3). Elsevier Amsterdam.

Hooda, P. (2010). *Trace elements in soils*. John Wiley & Sons.

Horel, A., Lichner, Ľ., Alaoui, A., Czachor, H., Nagy, V., & Tóth, E. (2014). Transport of iodide in structured clay-loam soil under maize during irrigation experiments analyzed using HYDRUS model. *Biologia*, *69*(11), 1531–1538.

Hou, X., Chai, C., Qian, Q., Liu, G., Zhang, Y., & Wang, K. (1997). The study of iodine in Chinese total diets. *Science of the Total Environment*, *193*(3), 161–167.

Houghton-Carr, H. A., Print, C. R., Fry, M. J., Gadain, H., & Muchiri, P. (2011). An assessment of the surface water resources of the Juba-Shabelle basin in southern Somalia. *Hydrological Sciences Journal*. https://doi.org/10.1080/02626667.2011.585470

Hu, Q., Moran, J. E., & Blackwood, V. (2007). *Geochemical cycling of iodine species in soils*. Lawrence Livermore National Lab.(LLNL), Livermore, CA (United States).

Humphrey, O. S., Young, S. D., Bailey, E. H., Crout, N. M. J., Ander, E. L., & Watts, M. J. (2018). Iodine soil dynamics and methods of measurement: a review. *Environmental Science: Processes & Impacts*, *20*(2), 288–310.

Hurst, R., Armah, C. N., Dainty, J. R., Hart, D. J., Teucher, B., Goldson, A. J., Broadley, M. R., Motley, A. K., & Fairweather-Tait, S. J. (2010). Establishing optimal selenium status: Results of a randomized, double-blind, placebo-controlled trial. *American Journal of Clinical Nutrition*. https://doi.org/10.3945/ajcn.2009.28169

Hurst, R., Siyame, E. W. P., Young, S. D., Chilimba, A. D. C., Joy, E. J. M., Black, C. R., Ander, E. L., Watts, M. J., Chilima, B., Gondwe, J., Kang'Ombe, D., Stein, A. J., Fairweather-Tait, S. J., Gibson, R. S., Kalimbira, A. A., & Broadley, M. R. (2013). Soil-type influences human selenium status and underlies widespread selenium deficiency risks in Malawi. *Scientific Reports*. https://doi.org/10.1038/srep01425

Hurtevent, P., Thiry, Y., Levchuk, S., Yoschenko, V., Henner, P., Madoz-Escande, C., Leclerc, E., Colle, C., & Kashparov, V. (2013). Translocation of 125I, 75Se and 36Cl to wheat edible parts following wet foliar contamination under field conditions. *Journal of Environmental Radioactivity*, *121*, 43–54.

Inspectorate, D. W. (2010). What are the drinking water standards. *Drinking Water Inspectorate, London*.

Jacobs, L. W. (1989). Selenium in agriculture and the Environment, soil Science Society of America Special Publication 23. *SSSA, Madison, WI, USA*.

Jezek, P., Skarpa, P., Losak, T., Hlusek, J., Juzl, M., & Elzner, P. (2012). Selenium – An Important Antioxidant in Crops Biofortification. In *Antioxidant Enzyme*. https://doi.org/10.5772/50356

Jo, I. S., & Koh, M. H. (2004). Chemical changes in agricultural soils of Korea: data review and suggested countermeasures. *Environmental Geochemistry and Health*, *26*(2), 105–117.

Johnson, C. C. (2003). The geochemistry of iodine and its application to environmental strategies for reducing the risk from iodine deficiency disorders (IDD). *British Geological Survey Commissioned Report*.

Johnson, C.C. (2003). Database of the iodine content of soils populated with data from published literature. *British Geological Survey Commissioned Report*.

Johnson, C C, Fordyce, F. M., & Stewart, A. G. (2003). *Iodine geochemistry and environmental controls on iodine deficiency disorders: a new approach to a classic geochemistry and health problem*.

Johnson, C C, Strutt, M. H., Hmeurras, M., & Mounir, M. (2002). Iodine in the Environment of the High Atlas Mountain area of Morocco. *British Geological Survey, Keyworth, Nottingham, UK*.

Johnson, Christopher Charles. (1980). *The geochemistry of iodine and a preliminary investigation into its potential use as a pathfinder element in geochemical exploration.* University College of Wales.

Johnsson, L. (1991). Selenium uptake by plants as a function of soil type, organic matter content and pH. *Plant and Soil*. https://doi.org/10.1007/BF00011899

Jones, C. P., Grossl, P. R., Amacher, M. C., Boettinger, J. L., Jacobson, A. R., & Lawley, J. R. (2017). Selenium and salt mobilization in wetland and arid upland soils of Pariette Draw, Utah (USA). *Geoderma*. https://doi.org/10.1016/j.geoderma.2017.06.028

Joy, E. J. M., Ander, E. L., Young, S. D., Black, C. R., Watts, M. J., Chilimba, A. D. C., Chilima, B., Siyame, E. W. P., Kalimbira, A. A., Hurst, R., Fairweather-Tait, S. J., Stein, A. J., Gibson, R. S., White, P. J., & Broadley, M. R. (2014). Dietary mineral supplies in Africa. *Physiologia Plantarum*. https://doi.org/10.1111/ppl.12144

Joy, E. J. M., Broadley, M. R., Young, S. D., Black, C. R., Chilimba, A. D. C., Ander, E. L., Barlow, T. S., & Watts, M. J. (2015). Soil type influences crop mineral composition in Malawi. *Science of the Total Environment*. https://doi.org/10.1016/j.scitotenv.2014.10.038

Kabata-Pendias, A., & Szteke, B. (2015). *Trace elements in abiotic and biotic environments*. CRC Press.

Kang, Y., Nozato, N., Kyuma, K., & Yamada, H. (1991). Distribution and forms of selenium in paddy soil. *Soil Science and Plant Nutrition*, *37*(3), 477–485.

Kassim, I A R, Seal, A. J., & Moloney, G. (2010). *National micronutrient and anthropometric survey, Somalia 2009*.

Kassim, Ismail A. R., Moloney, G., Busili, A., Nur, A. Y., Paron, P., Jooste, P., Gadain, H., & Seal, A. J. (2014). Iodine Intake in Somalia Is Excessive and Associated with the Source of Household Drinking Water. *The Journal of Nutrition*, *144*(3), 375–381. https://doi.org/10.3945/jn.113.176693

Kerisit, S. N., Smith, F. N., Saslow, S. A., Hoover, M. E., Lawter, A. R., & Qafoku, N. P. (2018). Incorporation Modes of Iodate in Calcite. *Environmental Science & Technology*, *52*(10), 5902–5910.

Keskinen, R., Ekholm, P., Yli-Halla, M., & Hartikainen, H. (2009). Efficiency of different methods in extracting selenium from agricultural soils of Finland. *Geoderma*. https://doi.org/10.1016/j.geoderma.2009.07.014

Khatri, N., & Tyagi, S. (2015). Influences of natural and anthropogenic factors on surface and groundwater quality in rural and urban areas. *Frontiers in Life Science*, *8*(1), 23–39.

Kiferle, C., Gonzali, S., Holwerda, H. T., Real Ibaceta, R., & Perata, P. (2013). Tomato fruits: a good target for iodine biofortification. *Frontiers in Plant Science*, *4*, 205.

Kikkert, J., & Berkelaar, E. (2013). Plant uptake and translocation of inorganic and organic forms of selenium. *Archives of Environmental Contamination and Toxicology*, *65*(3), 458–465.

Kodama, S., Takahashi, Y., Okumura, K., & Uruga, T. (2006). Speciation of iodine in solid environmental samples by iodine K-edge XANES: Application to soils and ferromanganese oxides. *Science of the Total Environment*, *363*(1–3), 275–284.

Kornher, L. (2018). Maize markets in Eastern and Southern Africa (ESA) in the Context of Climate Change. *The State of Agricultural Commodity Markets (SOCO) Background Paper*, 58.

Krivovichev, V. G., Charykova, M. V, Yakovenko, O. S., & Depmeier, W. (2011). Thermodynamics of arsenates, selenites, and sulfates in the oxidation zone of sulfide ores:

IV. Eh-pH diagrams of the Me-Se-H 2 O systems (Me= Co, Ni, Fe, Cu, Zn, Pb) at 25° C. *Geology of Ore Deposits*, *53*(7), 514–527.

Kumar, M., & Babel, A. L. (2011). Available Micronutrient Status and Their Relationship with Soil Properties of Jhunjhunu Tehsil, District Jhunjhunu, Rajasthan, India. *Journal of Agricultural Science*. https://doi.org/10.5539/jas.v3n2p97

Kumssa, D. B., Joy, E. J. M., Ander, E. L., Watts, M. J., Young, S. D., Walker, S., & Broadley, M. R. (2015). Dietary calcium and zinc deficiency risks are decreasing but remain prevalent. *Scientific Reports*, *5*, 10974.

Lakin, H. W. (1973). Selenium in our environment. *Advances in Chemistry Series*, *123*, 96–111.

Lamble, G. M., Lee, J. F., Staudt, W. J., & Reeder, R. J. (1995). Structural studies of selenate incorporation into calcite crystals. *Physica B: Physics of Condensed Matter*. https://doi.org/10.1016/0921-4526(94)00763-L

Lawson, P. G., Daum, D., Czauderna, R., Meuser, H., & Härtling, J. W. (2015). Soil versus foliar iodine fertilization as a biofortification strategy for field-grown vegetables. *Frontiers in Plant Science*, *6*, 450.

Leung, A. M., & Braverman, L. E. (2014). Consequences of excess iodine. In *Nature Reviews Endocrinology*. https://doi.org/10.1038/nrendo.2013.251

LÉVESQUE, M. (1974). SELENIUM DISTRIBUTION IN CANADIAN SOIL PROFILES. *Canadian Journal of Soil Science*. https://doi.org/10.4141/cjss74-008

Li, H., McGrath, S. P., & Zhao, F. (2008). Selenium uptake, translocation and speciation in wheat supplied with selenate or selenite. *New Phytologist*, *178*(1), 92–102.

Li, J., Zhou, H., Wang, Y., Xie, X., & Qian, K. (2017). Sorption and speciation of iodine in groundwater system: The roles of organic matter and organic-mineral complexes. *Journal of Contaminant Hydrology*, *201*, 39–47.

Li, R., Li, D.-W., Liu, H.-P., Hong, C.-L., Song, M.-Y., Dai, Z.-X., Liu, J.-W., Zhou, J., & Weng, H.-X. (2017). Enhancing iodine content and fruit quality of pepper (Capsicum annuum L.) through biofortification. *Scientia Horticulturae*, *214*, 165–173.

Li, X., Wu, Y., Li, B., Yang, Y., & Yang, Y. (2018). Selenium accumulation characteristics and biofortification potentiality in turnip (Brassica rapa var. rapa) supplied with selenite or selenate. *Frontiers in Plant Science*, *8*, 2207.

Longombe, A. O., & Geelhoed, G. W. (1997). Iodine deficiency disorders and infertility in northeast Zaire. *Nutrition*, *4*(13), 342–343.

Losi, M. E., & Frankenberger Jr, W. T. (1997). Bioremediation of selenium in soil and water. *Soil Science*, *162*(10), 692–702.

Lounsbury, A. W., Yamani, J. S., Johnston, C. P., Larese-Casanova, P., & Zimmerman, J. B. (2016). The role of counter ions in nano-hematite synthesis: Implications for surface area and selenium adsorption capacity. *Journal of Hazardous Materials*. https://doi.org/10.1016/j.jhazmat.2016.01.078

Lu, Z., Jenkyns, H. C., & Rickaby, R. E. M. (2010). Iodine to calcium ratios in marine carbonate as a paleo-redox proxy during oceanic anoxic events. *Geology*.

https://doi.org/10.1130/G31145.1

Lyons, G. (2018). Biofortification of cereals with foliar selenium and iodine could reduce hypothyroidism. In *Frontiers in Plant Science*. https://doi.org/10.3389/fpls.2018.00730

Mackowiak, C. L., & Grossl, P. R. (1999). Iodate and iodide effects on iodine uptake and partitioning in rice (Oryza sativa L.) grown in solution culture. *Plant and Soil*, *212*(2), 133–141.

Madar, A. A., Meltzer, H. M., Heen, E., & Meyer, H. E. (2018). Iodine status among somali immigrants in Norway. *Nutrients*. https://doi.org/10.3390/nu10030305

Maillant, S., Sheppard, M. I., Echevarria, G., Denys, S., Villemin, G., Tekely, P., Leclerc-Cessac, E., & Morel, J. L. (2007). Aged anthropogenic iodine in a boreal peat bog. *Applied Geochemistry*, *22*(5), 873–887.

Manceau, A., & Charlet, L. (1994). The mechanism of selenate adsorption on goethite and hydrous ferric oxide. *Journal of Colloid and Interface Science*, *168*(1), 87–93.

Mannar, M. G. V., & Hurrell, R. F. (2018). *Food fortification in a globalized world*. Academic Press.

Mao, H., Wang, J., Wang, Z., Zan, Y., Lyons, G., & Zou, C. (2014). Using agronomic biofortification to boost zinc, selenium, and iodine concentrations of food crops grown on the loess plateau in China. *Journal of Soil Science and Plant Nutrition*, *14*(2), 459–470.

Marschner, H. (2011). *Marschner's mineral nutrition of higher plants*. Academic press.

Martens, D. A. (2003). *United States Department of Agriculture (USDA)*.

Masscheleyn, P. H., Delaune, R. D., & Patrick Jr, W. H. (1990). Transformations of selenium as affected by sediment oxidation-reduction potential and pH. *Environmental Science & Technology*, *24*(1), 91–96.

Materechera, S. A. (1999). Neubauer seedling technique to determine availability of nutrient elements for wheat from selected South African soils. *Communications in Soil Science and Plant Analysis*, *30*(19–20), 2755–2767.

Mathers, A. W., Young, S. D., McGrath, S. P., Zhao, F.-J., Crout, N. M. J., & Bailey, E. H. (2017). Determining the fate of selenium in wheat biofortification: an isotopically labelled field trial study. *Plant and Soil*, *420*(1–2), 61–77.

Mayland, H. F., Gough, L. P., & Stewart, K. C. (1991). *Chapter E: Selenium mobility in soils and its absorption, translocation, and metabolism in plants*.

Mayland, H. F., James, L. F., Panter, K. E., & Sonderegger, J. L. (1989). Selenium in seleniferous environments. *Selenium in Agriculture and the Environment*, *seleniuminagric*, 15–50.

Mc Kenzie, R. M. (1989). Manganese oxides and hydroxides. *Minerals in Soil Environments*, 439–465.

Medrano-Macías, J., Leija-Martínez, P., González-Morales, S., Juárez-Maldonado, A., & Benavides-Mendoza, A. (2016). Use of iodine to biofortify and promote growth and stress tolerance in crops. *Frontiers in Plant Science*, *7*, 1146.

Mikkelsen, R. L., Page, A. L., & Bingham, F. T. (1989). Factors affecting selenium

accumulation by agricultural crops 1. *Selenium in Agriculture and the Environment, seleniuminagric*, 65–94.

Missana, T., Alonso, U., & García-Gutiérrez, M. (2009). Experimental study and modelling of selenite sorption onto illite and smectite clays. *Journal of Colloid and Interface Science*, *334*(2), 132–138.

Monsen, E. R. (2000). Dietary reference intakes for the antioxidant nutrients: vitamin C, vitamin E, selenium, and carotenoids. *Journal of the American Dietetic Association*. https://doi.org/10.1016/S0002-8223(00)00189-9

Montes-Hernandez, G., Concha-Lozano, N., Renard, F., & Quirico, E. (2009). Removal of oxyanions from synthetic wastewater via carbonation process of calcium hydroxide: Applied and fundamental aspects. *Journal of Hazardous Materials*. https://doi.org/10.1016/j.jhazmat.2008.11.120

Montes-Hernandez, German, Sarret, G., Hellmann, R., Menguy, N., Testemale, D., Charlet, L., & Renard, F. (2011). Nanostructured calcite precipitated under hydrothermal conditions in the presence of organic and inorganic selenium. *Chemical Geology*, *290*(3–4), 109–120.

Muchiri, P. W. (2007). *Climate of Somalia*.

Muramatsu, Y, Uchida, S., & Ohmomo, Y. (1990). Determination of I-129 and I-127 in soil and tracer experiments on the adsorption of iodine on soil. *Journal of Radioanalytical and Nuclear Chemistry*, *138*(2), 377–384.

Muramatsu, Yasuyuki, & Wedepohl, K. H. (1998). The distribution of iodine in the earth's crust. *Chemical Geology*, *147*(3–4), 201–216.

Muthusi, F. M. (2007). Rural water supply assessment. *SWALIM Technical Reports*.

Neal, C., & Truesdale, V. W. (1976). The sorption of iodate and iodide by riverine sediments: its implications to dilution gauging and hydrochemistry of iodine. *Journal of Hydrology*, *31*(3–4), 281–291.

Neeway, J. J., Kaplan, D. I., Bagwell, C. E., Rockhold, M. L., Szecsody, J. E., Truex, M. J., & Qafoku, N. P. (2019). A review of the behavior of radioiodine in the subsurface at two DOE sites. *Science of the Total Environment*. https://doi.org/10.1016/j.scitotenv.2019.07.146

Øgaard, A. F., Sogn, T. A., & Eich-Greatorex, S. (2006). Effect of cattle manure on selenate and selenite retention in soil. *Nutrient Cycling in Agroecosystems*, *76*(1), 39–48.

Paquette, J., & Reeder, R. J. (1995). Relationship between surface structure, growth mechanism, and trace element incorporation in calcite. *Geochimica et Cosmochimica Acta*. https://doi.org/10.1016/0016-7037(95)00004-J

Peak, D. (2006). Adsorption mechanisms of selenium oxyanions at the aluminum oxide/water interface. *Journal of Colloid and Interface Science*, *303*(2), 337–345.

Peak, D., Saha, U. K., & Huang, P. M. (2006). Selenite adsorption mechanisms on pure and coated montmorillonite: an EXAFS and XANES spectroscopic study. *Soil Science Society of America Journal*, *70*(1), 192–203.

Peak, D., & Sparks, D. L. (2002). Mechanisms of selenate adsorption on iron oxides and

hydroxides. *Environmental Science & Technology*, *36*(7), 1460–1466.

Pedersen, K. M., Laurberg, P., Nøhr, S., Jørgensen, A., & Andersen, S. (1999). Iodine in drinking water varies by more than 100-fold in Denmark. Importance for iodine content of infant formulas. *European Journal of Endocrinology*. https://doi.org/10.1530/eje.0.1400400

Peitzsch, M., Kremer, D., & Kersten, M. (2009). Microfungal alkylation and volatilization of selenium adsorbed by goethite. *Environmental Science & Technology*, *44*(1), 129–135.

Pinstrup-Andersen, P. (2009). Food security: definition and measurement. *Food Security*, *1*(1), 5–7.

Polemio, M., & Rhoades, J. D. (1977). Determining Cation Exchange Capacity: A New Procedure for Calcareous and Gypsiferous Soils 1. *Soil Science Society of America Journal*, *41*(3), 524–528.

Polly, R., Heberling, F., Schimmelpfennig, B., & Geckeis, H. (2017). Quantum Chemical Investigation of the Selenite Incorporation into the Calcite (1014) Surface. *Journal of Physical Chemistry C*. https://doi.org/10.1021/acs.jpcc.7b03499

Pombo, L. C. A. (1995). APPLICATION OF A TANNERY RESIDUE IN 2 BRAZILIAN RED-YELLOW PODZOLIC SOILS. *Journal of the American Leather Chemists Association*, *90*(10), 299–307.

Porter, P. M., Porter, H. L., & Rafle, A. D. (1988). Land-use systems for Vertisols in the Bay Region of Somalia. *MANAGEMENT OF VERTISOLS IN SUB-SAHARAN AFRICA*, 308.

Preedy, V., Burrow, G., & Watson, R. (2009). Comprehensive Handbook of Iodine. In *Comprehensive Handbook of Iodine*. https://doi.org/10.1016/B978-0-12-374135-6.X0001-5

Putnis, C. V., Renard, F., King, H. E., Montes-Hernandez, G., & Ruiz-Agudo, E. (2013). Sequestration of selenium on calcite surfaces revealed by nanoscale imaging. *Environmental Science and Technology*. https://doi.org/10.1021/es403637u

Qian, K., Li, J., Xie, X., & Wang, Y. (2017). Organic and inorganic colloids impacting total iodine behavior in groundwater from the Datong Basin, China. *Science of the Total Environment*, *601*, 380–390.

Qin, H. B., Zhu, J. M., & Su, H. (2012). Selenium fractions in organic matter from Se-rich soils and weathered stone coal in selenosis areas of China. *Chemosphere*. https://doi.org/10.1016/j.chemosphere.2011.10.055

RAJAN, S. S. S. (1979). ADSORPTION OF SELENITE, PHOSPHATE AND SULPHATE ON HYDROUS ALUMINA. *Journal of Soil Science*. https://doi.org/10.1111/j.1365-2389.1979.tb01020.x

Ramkissoon, C., Degryse, F., da Silva, R. C., Baird, R., Young, S. D., Bailey, E. H., & McLaughlin, M. J. (2019). Improving the efficacy of selenium fertilizers for wheat biofortification. *Scientific Reports*, *9*(1), 1–9.

Ravel, B., & Newville, M. (2005). ATHENA, ARTEMIS, HEPHAESTUS: data analysis for X-ray absorption spectroscopy using IFEFFIT. *Journal of Synchrotron Radiation*, *12*(4), 537–541.

Rayman, M. P. (2000). The importance of selenium to human health. *The Lancet*, *356*(9225), 233–241.

Rayman, M. P. (2002). The argument for increasing selenium intake. *Proceedings of the Nutrition Society*, *61*(2), 203–215.

Rayman, M. P. (2004). The use of high-selenium yeast to raise selenium status: how does it measure up? *British Journal of Nutrition*. https://doi.org/10.1079/bjn20041251

Rayman, M. P. (2005). Selenium in cancer prevention: a review of the evidence and mechanism of action. *Proceedings of the Nutrition Society*. https://doi.org/10.1079/pns2005467

Rayman, M. P. (2008). Food-chain selenium and human health: Emphasis on intake. In *British Journal of Nutrition*. https://doi.org/10.1017/S0007114508939830

Rayman, M. P. (2012). Selenium and human health. In *The Lancet*. https://doi.org/10.1016/S0140-6736(11)61452-9

Reeder, R. J. (1996). Interaction of divalent cobalt, zinc, cadmium, and barium with the calcite surface during layer growth. *Geochimica et Cosmochimica Acta*. https://doi.org/10.1016/0016-7037(96)00034-8

Reeder, R. J., Lamble, G. M., Lee, J.-F., & Staudt, W. J. (1994). Mechanism of SeO42− substitution in calcite: An XAFS study. *Geochimica et Cosmochimica Acta*, *58*(24), 5639–5646.

Reifenhäuser, C., & Heumann, K. G. (1990). Development of a definitive method for iodine speciation in aquatic systems. *Fresenius' Journal of Analytical Chemistry*, *336*(7), 559–563.

Reilly, C. (2006). Selenium in food and health. In *Selenium in Food and Health*. https://doi.org/10.1007/978-0-387-33244-4

Reimann, C., Bjorvatn, K., Frengstad, B., Melaku, Z., Tekle-Haimanot, R., & Siewers, U. (2003). Drinking water quality in the Ethiopian section of the East African Rift Valley I - Data and health aspects. *Science of the Total Environment*. https://doi.org/10.1016/S0048-9697(03)00137-2

Renard, F., Montes-Hernandez, G., Ruiz-Agudo, E., & Putnis, C. V. (2013). Selenium incorporation into calcite and its effect on crystal growth: An atomic force microscopy study. *Chemical Geology*. https://doi.org/10.1016/j.chemgeo.2012.12.017

Rhoades, J. D. (1982). Cation Exchange Capacity 1. *Methods of Soil Analysis. Part 2. Chemical and Microbiological Properties, methodsofsoilan2*, 149–157.

Rimstidt, J. D., Balog, A., & Webb, J. (1998). Distribution of trace elements between carbonate minerals and aqueous solutions. *Geochimica et Cosmochimica Acta*. https://doi.org/10.1016/S0016-7037(98)00125-2

Risher, J. (2011). *Toxicological profile for selenium (Update)*. DIANE Publishing.

Rodriguez, M. J. M., Rivero, V. C., & Ballesta, R. J. (2005). Selenium distribution in topsoils and plants of a semi-arid Mediterranean environment. *Environmental Geochemistry and Health*, *27*(5–6), 513–519.

Rodriguez, M. J. M., Rivero, V. C., Ballesta, R. J., Moreno Rodriguez, M. J., Cala Rivero, V., & Jiménez Ballesta, R. (2005). Selenium distribution in topsoils and plants of a semi-arid

Mediterranean environment. *Environmental Geochemistry and Health*, *27*(5–6), 513–519. https://doi.org/10.1007/s10653-005-8625-9

Ros, G. H., Van Rotterdam, A. M. D., Bussink, D. W., & Bindraban, P. S. (2016). Selenium fertilization strategies for bio-fortification of food: an agro-ecosystem approach. *Plant and Soil*, *404*(1–2), 99–112.

Ros, G. H., Van Rotterdam, A. M. D., Doppenberg, G. D., Bussink, D. W., & Bindraban, P. S. (2014). Se fertilization: an agro-ecosystem approach. *VFRC Report*, *3*, 62.

Rosenthal, E., & Mates, A. (1986). Iodine concentrations in groundwater of northern Israel and their relation to the occurrence of goiter. *Applied Geochemistry*, *1*(5), 591–600.

Saha, U., Fayiga, A., & Sonon, L. (2017). Selenium in the soil-plant environment: a review. *International Journal of Applied Agricultural Sciences*, *3*(1), 1–18.

Santschi, P. H., Xu, C., Zhang, S., Ho, Y., Li, H., Schwehr, K., & Kaplan, D. I. (2012). *Laboratory report on iodine (129I and 127I) speciation, transformation and mobility in Handford groundwater, suspended particles and sediments*. Savannah River Site (SRS), Aiken, SC (United States).

Santschi, P. H., Xu, C., Zhang, S., Schwehr, K. A., Grandbois, R., Kaplan, D. I., & Yeager, C. M. (2017). Iodine and plutonium association with natural organic matter: A review of recent advances. *Applied Geochemistry*, *85*, 121–127.

Scheuner, E. T., Makeschin, F., Wells, E. D., & Carter, P. Q. (2004). Short-term impacts of harvesting and burning disturbances on physical and chemical characteristics of forest soils in western Newfoundland, Canada. *European Journal of Forest Research*, *123*(4), 321–330.

Schwarz, K., & Foltz, C. M. (1957). Selenium as an Integral Part of Factor 3 Against Dietary Necrotic Liver Degeneration. *Journal of the American Chemical Society*. https://doi.org/10.1021/ja01569a087

Sebhat, M. Y. (2015). Assessments of water demands for the Juba and Shabelle Rivers in Somalia. *Journal of Agriculture and Environment for International Development (JAEID)*, *109*(2), 165–177.

Séby, F., Gautier, M. P., Lespes, G., & Astruc, M. (1997). Selenium speciation in soils after alkaline extraction. *Science of the Total Environment*, *207*(2–3), 81–90.

Shallari, S., Schwartz, C., Hasko, A., & Morel, J. L. (1998). Heavy metals in soils and plants of serpentine and industrial sites of Albania. *Science of the Total Environment*, *209*(2–3), 133–142.

Shand, P., & Frengstad, B. (2001). *Baseline groundwater quality: A comparison of selected British and Norwegian aquifers*.

Shen, H., Liu, S., Sun, D., Zhang, S., Su, X., Shen, Y., & Han, H. (2011). Geographical distribution of drinking-water with high iodine level and association between high iodine level in drinking-water and goitre: a Chinese national investigation. *British Journal of Nutrition*, *106*(2), 243–247.

Sheppard, M. I., Hawkins, J. L., & Smith, P. A. (1996). Linearity of iodine sorption and sorption capacities for seven soils. *Journal of Environmental Quality*, *25*(6), 1261–1267.

Sheppard, M. I., & Thibault, D. H. (1992). Chemical behaviour of iodine in organic and mineral soils. *Applied Geochemistry*, *7*(3), 265–272.

Shetaya, W. H., Young, S. D., Watts, M. J., Ander, E. L., & Bailey, E. H. (2012). Iodine dynamics in soils. *Geochimica et Cosmochimica Acta*. https://doi.org/10.1016/j.gca.2011.10.034

Sigurdsson, G., & Franzson, L. (1988). Urinary iodine excretion in Icelandic men and women. *Iceland Med J (in Icelandic)*, *74*, 183–187.

Smedley, P. (2000). *Water quality fact sheet: Iodine*.

Smoleń, S., Ledwożyw-Smoleń, I., & Sady, W. (2016). The role of exogenous humic and fulvic acids in iodine biofortification in spinach (Spinacia oleracea L.). *Plant and Soil*, *402*(1–2), 129–143.

Smoleń, S., Sady, W., Ledwożyw-Smoleń, I., Strzetelski, P., Liszka-Skoczylas, M., & Rożek, S. (2014). Quality of fresh and stored carrots depending on iodine and nitrogen fertilization. *Food Chemistry*, *159*, 316–322.

Sø, H. U., Postma, D., Jakobsen, R., & Larsen, F. (2008). Sorption and desorption of arsenate and arsenite on calcite. *Geochimica et Cosmochimica Acta*. https://doi.org/10.1016/j.gca.2008.09.023

Söderlund, M., Lusa, M., Lehto, J., Hakanen, M., Vaaramaa, K., & Lahdenperä, A.-M. (2011). *Sorption of iodine, chlorine, technetium and cesium in soil*. Posiva Oy.

Sparks, D. L. (2003). *Environmental soil chemistry*. Elsevier.

Sparks, D. L. (2012). *Advances in agronomy* (Vol. 118). Academic Press.

Statwick, J., & Sher, A. A. (2017). Selenium in soils of western Colorado. *Journal of Arid Environments*, *137*, 1–6.

Staudt, W. J., Reeder, R. J., & Schoonen, M. A. A. (1994). Surface structural controls on compositional zoning of SO2-4 and SeO2-4 in synthetic calcite single crystals. *Geochimica et Cosmochimica Acta*. https://doi.org/10.1016/0016-7037(94)90287-9

Stipp, S. L. S., Christensen, J. T., Lakshtanov, L. Z., Baker, J. A., & Waight, T. E. (2006). Rare Earth element (REE) incorporation in natural calcite: Upper limits for actinide uptake in a secondary phase. *Radiochimica Acta*. https://doi.org/10.1524/ract.2006.94.9-11.523

Stroud, J. L., Broadley, M. R., Foot, I., Fairweather-Tait, S. J., Hart, D. J., Hurst, R., Knott, P., Mowat, H., Norman, K., Scott, P., Tucker, M., White, P. J., McGrath, S. P., & Zhao, F. J. (2010). Soil factors affecting selenium concentration in wheat grain and the fate and speciation of Se fertilisers applied to soil. *Plant and Soil*. https://doi.org/10.1007/s11104-009-0229-1

Stroud, Jacqueline L., McGrath, S. P., & Zhao, F. J. (2012). Selenium speciation in soil extracts using LC-ICP-MS. *International Journal of Environmental Analytical Chemistry*. https://doi.org/10.1080/03067310903111661

Stuanes, A. O., Ogner, G., & Opem, M. (1984). Ammonium Nitrate as Extractant for Soil Exchangeable Cations, Exchangeable Acidity and Aluminum. *Communications in Soil Science and Plant Analysis*. https://doi.org/10.1080/00103628409367516

Su, C., & Suarez, D. L. (2000). Selenate and selenite sorption on iron oxides: An infrared and

electrophoretic study. *Soil Science Society of America Journal*. https://doi.org/10.2136/sssaj2000.641101x

Sun, G.-X., Meharg, A. A., Li, G., Chen, Z., Yang, L., Chen, S.-C., & Zhu, Y.-G. (2016). Distribution of soil selenium in China is potentially controlled by deposition and volatilization? *Scientific Reports*, *6*, 20953.

Supriatin, S. (2016). Selenium speciation and bioavailability in Dutch agricultural soils: the role of soil organic matter. In *Selenium speciation and bioavailability in Dutch agricultural soils: the role of soil organic matter*.

Supriatin, Supriatin, Weng, L., & Comans, R. N. J. (2015). Selenium speciation and extractability in Dutch agricultural soils. *Science of the Total Environment*. https://doi.org/10.1016/j.scitotenv.2015.06.005

Suzuki, H., Higuchi, T., Sawa, K., Ohtaki, S., & Horiuchi, Y. (1965). "Endemic coast goitre" in Hokkaido, Japan. *Acta Endocrinologica*.

Tagami, K., Uchida, S., Takeda, A., & Yamasaki, S. (2010). Estimation of plant-unavailable iodine concentrations in agricultural fields. *Soil Science Society of America Journal*, *74*(5), 1562–1567.

Tan, J., Zhu, W., Wang, W., Li, R., Hou, S., Wang, D., & Yang, L. (2002). Selenium in soil and endemic diseases in China. *Science of the Total Environment*. https://doi.org/10.1016/S0048-9697(01)00889-0

Terry, N., Zayed, A. M., De Souza, M. P., & Tarun, A. S. (2000). Selenium in higher plants. *Annual Review of Plant Biology*, *51*(1), 401–432.

Truesdalea, V. W., & Jones, S. D. (1996). The variation of iodate and total iodine in some UK rainwaters during 1980–1981. *Journal of Hydrology*, *179*(1–4), 67–86.

UNICEF. (2015). *The situation of Women and Children in Somalia*. The Situation of Women and Children in Somalia. https://www.unicef.org/somalia/children.html

United Nations Population Division, D. of E. and S. A. (2019). *World Population Prospects 2019: Highlights*.

Ure, A. M., & Berrow, M. L. (1982). The elemental constituents of soils. *Environmental Chemistry. Volume 2. A Review of the Literature Published up to Mid-1980*. https://doi.org/10.1039/9781847555991-00094

US EPA, M. (2009). *National primary drinking water regulations*. EPA-816-F-09–004 Search PubMed.

Van den Bossche, J. P., & Bernacsek, G. M. (1991). Source book for the inland fishery resources of Africa. Vol. 3. In *CIFA technical paper. 1991*.

Vargas, R. R., Omuto, C., & Alim, M. S. (2007). *Soil survey of the Juba and Shabelle riverine areas in Southern Somalia*.

Venema, J. H., & Vargas, R. (2007). *Land suitability assessment of the Juba and Shabelle riverine areas in Southern Somalia*.

Voutchkova, D. D., Ernstsen, V., Kristiansen, S. M., & Hansen, B. (2017). Iodine in major Danish aquifers. *Environmental Earth Sciences*, *76*(13), 447.

Vuori, E., Vääriskoski, J., Hartikainen, H., Vakkilainen, P., Kumpulainen, J., & Niinivaara, K. (1989). Sorption of selenate by Finnish agricultural soils. *Agriculture, Ecosystems & Environment*, *25*(2–3), 111–118.

Wang, J., Bailey, E. H., Sanders, H. K., Izquierdo, M., Crout, N. M. J., Shaw, G., Yang, L., Li, H., Wei, B., & Young, S. D. (2020). Using chemical fractionation and speciation to describe uptake of technetium, iodine and selenium by Agrostis capillaris and Lolium perenne. *Journal of Environmental Radioactivity*, *212*, 106131.

Wang, M. C., & Chen, H. M. (2003). Forms and distribution of selenium at different depths and among particle size fractions of three Taiwan soils. *Chemosphere*, *52*(3), 585–593.

Wang, S., Liang, D., Wang, D., Wei, W., Fu, D., & Lin, Z. (2012). Selenium fractionation and speciation in agriculture soils and accumulation in corn (Zea mays L.) under field conditions in Shaanxi Province, China. *Science of the Total Environment*, *427*, 159–164.

Wang, Z., & Gao, Y. (2001). Biogeochemical cycling of selenium in Chinese environments. *Applied Geochemistry*, *16*(11–12), 1345–1351.

Watts, M. J., Joy, E. J. M., Young, S. D., Broadley, M. R., Chilimba, A. D. C., Gibson, R. S., Siyame, E. W. P., Kalimbira, A. A., Chilima, B., & Ander, E. L. (2015). Iodine source apportionment in the Malawian diet. *Scientific Reports*. https://doi.org/10.1038/srep15251

Watts, M. J., & Mitchell, C. J. (2009). A pilot study on iodine in soils of Greater Kabul and Nangarhar provinces of Afghanistan. *Environmental Geochemistry and Health*, *31*(4), 503.

Watts, M. J., O'reilly, J., Maricelli, A., Coleman, A., Ander, E. L., & Ward, N. I. (2010). A snapshot of environmental iodine and selenium in La Pampa and San Juan provinces of Argentina. *Journal of Geochemical Exploration*, *107*(2), 87–93.

Wells, N. (1967). *Selenium in horizons of soil profiles*.

White, J. G., & Zasoski, R. J. (1999). Mapping soil micronutrients. *Field Crops Research*. https://doi.org/10.1016/S0378-4290(98)00130-0

White, P. J., & Broadley, M. R. (2005). Biofortifying crops with essential mineral elements. *Trends in Plant Science*, *10*(12), 586–593.

White, P. J., & Broadley, M. R. (2009). Biofortification of crops with seven mineral elements often lacking in human diets - Iron, zinc, copper, calcium, magnesium, selenium and iodine. In *New Phytologist*. https://doi.org/10.1111/j.1469-8137.2008.02738.x

White, P. J., Broadley, M. R., Bowen, H. C., & Johnson, S. E. (2007). Selenium and its relationship with sulfur. In *Sulfur in plants an ecological perspective* (pp. 225–252). Springer.

Whitehead, D. C. (1973). Studies on iodine in British soils. *Journal of Soil Science*, *24*(2), 260–270.

Whitehead, D. C. (1974). The influence of organic matter, chalk, and sesquioxides on the solubility of iodide, elemental iodine, and iodate incubated with soil. *Journal of Soil Science*, *25*(4), 461–470.

Whitehead, D. C. (1979). Iodine in the UK environment with particular reference to agriculture. *Journal of Applied Ecology*, 269–279.

Whitehead, D. C. (1984). The distribution and transformations of iodine in the environment. *Environment International*. https://doi.org/10.1016/0160-4120(84)90139-9

WHO. (1996). Trace elements in human nutrition and health World Health Organization. *World Health Organization*.

WHO. (2006). *Guidelines on food fortification with micronutrients*.

WHO, S. (1987). Environmental Health Criteria 58, IPLS International Program on Chemical Safety. *World Health Organization, Geneva, Switzerland*.

Wijnja, H., & Schulthess, C. P. (2000). Vibrational spectroscopy study of selenate and sulfate adsorption mechanisms on Fe and Al (hydr) oxide surfaces. *Journal of Colloid and Interface Science*, *229*(1), 286–297.

Wilde, F. D., Radtke, D. B., Gibs, J., & Iwatsubo, R. T. (1998). National field manual for the collection of water-quality data: US Geological Survey Techniques of Water-Resources Investigations, book 9, chap. *A-6, Variously Paged*.

Wisser, D., Frolking, S., Douglas, E. M., Fekete, B. M., Vörösmarty, C. J., & Schumann, A. H. (2008). Global irrigation water demand: Variability and uncertainties arising from agricultural and climate data sets. *Geophysical Research Letters*, *35*(24).

World Health Organization. (2001). Assessment of iodine deficiency disorders and monitoring their elimination: a guide for programme managers. In *WHO, Geneva*. Geneva: World Health Organization.

World Health Organization. (2004). Iodine status worldwide: WHO Global Database on Iodine Deficiency. In *Geneva: World Health Organization*.

World Health Organization. (2011). Selenium in Drinking-water. *WHO Press*. https://doi.org/WHO/HSE/WSH/10.01/14

Wu, X., & Låg, J. (1988). Selenium in Norwegian farmland soils. *Acta Agriculturae Scandinavica*, *38*(3), 271–276.

Xin-Min, J., Xue-Yi, C., Ji-Yong, J., Tai, M., James, D. W., Rakeman, M. A., Zhi-Hong, D., Mamette, M., Amette, K., & Ming-Li, Z. (1997). Dynamics of environmental supplementation of iodine: four years' experience of iodination of irrigation water in Hotien, Xinjiang, China. *Archives of Environmental Health: An International Journal*, *52*(6), 399–408.

Yamada, H., Kiriyama, T., Onagawa, Y., Hisamori, I., Miyazaki, C., & Yonebayashi, K. (1999). Speciation of iodine in soils. *Soil Science and Plant Nutrition*, *45*(3), 563–568.

Yamada, H., Kiriyama, T., & Yonebayashi, K. (1996). Determination of total iodine in soils by inductively coupled plasma mass spectrometry. *Soil Science and Plant Nutrition*. https://doi.org/10.1080/00380768.1996.10416633

Yanai, R. D., Phillips, R. P., Arthur, M. A., Siccama, T. G., & Hane, E. N. (2005). Spatial and temporal variation in calcium and aluminum in northern hardwood forest floors. *Water, Air, and Soil Pollution*, *160*(1–4), 109–118.

Yeager, C. M., Amachi, S., Grandbois, R., Kaplan, D. I., Xu, C., Schwehr, K. A., & Santschi, P. H. (2017). Microbial transformation of iodine: From radioisotopes to iodine deficiency. In *Advances in applied microbiology* (Vol. 101, pp. 83–136). Elsevier.

Yläranta, T. (1983). Selenium in Finnish agricultural soils. *Annales Agriculturae Fenniae*, *22*, 122–136.

Yläranta, T. (1982). Volatilization and leaching of selenium added to soils. *Annales Agriculturae Fenniae*, *21*, 103–114.

Young, J. R., Ellis, E. C., & Hidy, G. M. (1988). Deposition of Air-borne Acidifiers in the Western Environment. *Journal of Environment Quality*. https://doi.org/10.2134/jeq1988.00472425001700020031x

Yuita, K. (1992). Dynamics of iodine, bromine, and chlorine in soil. *Soil Science and Plant Nutrition*. https://doi.org/10.1080/00380768.1992.10416491

Zachara, J. M., Cowan, C. E., & Resch, C. T. (1990). *Metal cation/anion adsorption on calcium carbonate: Implications to metal ion concentrations in groundwater*. Pacific Northwest Lab., Richland, WA (USA).

Zachara, J. M., Cowan, C. E., & Resch, C. T. (1991). Sorption of divalent metals on calcite. *Geochimica et Cosmochimica Acta*. https://doi.org/10.1016/0016-7037(91)90127-Q

Zayed, A., Lytle, C. M., & Terry, N. (1998). Accumulation and volatilization of different chemical species of selenium by plants. *Planta*, *206*(2), 284–292.

Zhang, P., & Sparks, D. L. (1990). Kinetics of selenate and selenite adsorption/desorption at the goethite/water interface. *Environmental Science & Technology*, *24*(12), 1848–1856. https://doi.org/10.1021/es00082a010

Zhang, S., Xu, C., Creeley, D., Ho, Y. F., Li, H. P., Grandbois, R., Schwehr, K. A., Kaplan, D. I., Yeager, C. M., Wellman, D., & Santschi, P. H. (2013). Iodine-129 and iodine-127 speciation in groundwater at the Hanford site, U.S.: Iodate incorporation into calcite. *Environmental Science and Technology*. https://doi.org/10.1021/es401816e

Zhang, Y., Pan, G., Chen, J., & Hu, Q. (2003). Uptake and transport of selenite and selenate by soybean seedlings of two genotypes. *Plant and Soil*, *253*(2), 437–443.

Zhang, Y. Q., & Moore, J. N. (1997). Changes in selenium speciation in wetland sediments induced by laboratory testing. *Communications in Soil Science and Plant Analysis*, *28*(3–5), 341–350.

Zhao, F. J., Lopez-Bellido, F. J., Gray, C. W., Whalley, W. R., Clark, L. J., & McGrath, S. P. (2007). Effects of soil compaction and irrigation on the concentrations of selenium and arsenic in wheat grains. *Science of the Total Environment*. https://doi.org/10.1016/j.scitotenv.2006.09.028

Zhao, J., Chen, Z., & Maberly, G. (1998). Iodine-rich drinking water of natural origin in China [10]. In *Lancet*. https://doi.org/10.1016/S0140-6736(05)61375-X

Zia, M. H., Watts, M. J., Gardner, A., & Chenery, S. R. (2015). Iodine status of soils, grain crops, and irrigation waters in Pakistan. *Environmental Earth Sciences*. https://doi.org/10.1007/s12665-014-3952-8

Zimmermann, M. B. (2009). Iodine deficiency. In *Endocrine Reviews*. https://doi.org/10.1210/er.2009-0011

Zimmermann, M. B. (2013). Iodine deficiency and excess in children: Worldwide status in 2013. *Endocrine Practice*. https://doi.org/10.4158/EP13180.RA

Zimmermann, M. B., Jooste, P. L., & Pandav, C. S. (2008). Iodine-deficiency disorders. *The Lancet*, *372*(9645), 1251–1262.

Zimmermann, M. B., & Köhrle, J. (2002). The impact of iron and selenium deficiencies on iodine and thyroid metabolism: Biochemistry and relevance to public health. *Thyroid*. https://doi.org/10.1089/105072502761016494

Appendices

Appendix B: Aqua regia data

Table B1: Aqua regia data of the study soils

S Site	B	Na	Mg	P	S	K	Ca	Ti	Li	Be	Al	V	Cr	Mn	Fe	Co
	(mg/kg)	(mg/kg)	(mg/kg)	(mg/kg)	(mg/kg)	(mg/kg)	(mg/kg)	(mg/kg)	(mg/kg)	(mg/kg)	(mg/kg)	(mg/kg)	(mg/kg)	(mg/kg)	(mg/kg)	(mg/kg)
BW-R	0.310	21.1	999	44.7	0.00	515	8330	28.5	1.27	0.0960	2230	6.85	3.88	54.8	2840	1.25
BW-I	0.296	23.1	856	72.5	0.00	417	9880	40.5	0.83	0.0715	1600	5.77	2.75	60.4	2360	1.09
BB-R	0.395	8.47	920	33.3	0.00	646	9850	24.4	1.32	0.0914	2160	7.34	3.35	89.3	2520	1.21
BB-I	0.651	20.3	949	35.6	2240	562	9860	27.0	1.44	0.0930	2020	6.04	3.15	62.6	2440	1.11
JH-R	0.689	15.7	934	55.8	0.00	663	6980	32.7	1.34	0.0860	1980	6.09	3.29	51.2	2620	1.17
JH-I	0.506	10.9	883	43.6	0.00	546	7200	25.9	1.40	0.0866	2040	6.07	3.43	58.5	2570	1.22
BA-R	0.076	4.33	446	24.6	0.00	311	2980	20.5	0.74	0.0657	1280	4.20	2.48	29.9	1870	0.81
BA-I	0.023	26.4	558	56.5	0.00	472	3490	11.5	1.09	0.119	1680	4.24	2.91	51.0	2200	0.97
AF-R	0.136	4.51	745	26.6	0.00	502	5310	15.9	1.38	0.117	2260	5.83	4.17	53.5	2740	1.24
AF-I	0.136	12.1	745	29.7	0.00	472	5330	16.9	1.41	0.118	2080	6.00	3.99	53.8	2660	1.22
BD-R	0.000	15.8	252	10.9	0.00	52.8	969	1.09	0.85	0.154	1700	7.19	6.62	68.8	3050	1.40
BD-I	0.000	0.00	219	4.58	0.00	39.3	809	1.30	0.90	0.159	1700	7.14	6.69	65.8	3080	1.40

Table B2: Continue aqua regia data

S Site	Ni	Cu	Zn	As	Se	Rb	Sr	Mo	Ag	Cd	Cs	Ba	Tl	Pb	U
	(mg/kg)	(mg/kg)	(mg/kg)	(mg/kg)	(mg/kg)	(mg/kg)	(mg/kg)	(mg/kg)	(mg/kg)	(mg/kg)	(mg/kg)	(mg/kg)	(mg/kg)	(mg/kg)	(mg/kg)
BW-R	3.25	2.13	3.91	0.288	0.0167	3.00	33.0	0.0598	0.00221	0.0297	0.222	28.9	0.0236	1.16	0.253
BW-I	2.36	2.02	3.68	0.214	0.0206	2.55	26.6	0.0500	0.00372	0.0246	0.114	19.5	0.0146	0.72	0.097
BB-R	2.86	2.04	3.07	0.277	0.0176	3.04	34.2	0.0969	0.00560	0.0290	0.183	36.6	0.0200	1.00	0.197
BB-I	2.61	1.96	3.29	0.262	0.0252	2.70	114	0.102	0.00312	0.0213	0.161	8.84	0.0172	0.74	0.180
JH-R	2.63	1.99	3.93	0.212	0.0292	3.10	19.3	0.0593	0.00873	0.0284	0.158	22.5	0.0197	0.98	0.103
JH-I	2.83	1.99	3.49	0.254	0.0229	3.07	22.5	0.0735	0.00838	0.0278	0.168	25.5	0.0206	1.08	0.121
BA-R	1.99	1.28	2.61	0.189	0.0257	1.83	7.66	0.0342	0.00305	0.0144	0.091	12.7	0.0112	0.71	0.050
BA-I	2.52	1.59	4.70	0.272	0.0254	2.70	13.9	0.0608	0.00956	0.0302	0.124	20.5	0.0206	1.40	0.109
AF-R	3.46	1.94	3.71	0.295	0.0212	3.39	18.4	0.0662	0.00733	0.0313	0.211	28.5	0.0258	1.52	0.130
AF-I	3.35	1.89	3.62	0.337	0.0234	3.14	19.8	0.0986	0.00729	0.0299	0.198	27.4	0.0245	1.41	0.128
BD-R	3.84	1.43	0.98	0.467	0.0188	0.690	2.93	0.0366	0.0131	0.0207	0.203	42.3	0.0218	4.50	0.100
BD-I	3.78	1.42	0.73	0.405	0.0179	0.631	2.27	0.0274	0.0131	0.0208	0.219	39.5	0.0211	4.78	0.106

Appendix C : Pearson correlation coefficients (chapter 4, soils).

Table C1: Pearson correlations to investigate the effect of the pH, LOI, TOC, TIC and exchangeable cations on the Se and iodine fractionation.

	pH	LOI	TIC	TOC	CEC	Na exch.	Mg exch.	K exch.	Ca exch.	Soluble Se	Adsorbed Se	Se TMAH	Residual Se	Total Se	Soluble I	Adsorbed I	I TMAH
LOI	-0.120																
TIC	-0.146	-0.663															
TOC	-0.190	0.471	-0.445														
CEC	-0.652	0.197	-0.096	-0.143													
Na_exch.	-0.174	0.717	-0.432	0.528	0.244												
Mg_exch.	-0.188	0.719	-0.197	0.558	-0.106	0.522											
K_exch.	-0.185	-0.304	0.111	0.358	-0.211	0.133	-0.134										
Ca_exch.	-0.619	0.140	-0.076	-0.204	0.996	0.177	-0.180	-0.240									
Soluble Se	-0.355	-0.330	0.177	-0.041	0.061	-0.279	-0.019	-0.043	0.070								
Adsorbed Se	0.047	-0.266	-0.157	0.136	-0.043	-0.324	-0.155	0.168	-0.030	0.430							
Se TMAH	0.105	0.844	-0.877	0.529	-0.008	0.481	0.551	-0.212	-0.048	-0.238	0.093						
Residual Se	-0.399	-0.608	0.766	-0.232	0.074	-0.225	-0.206	0.498	0.073	0.249	-0.044	-0.819					
Total Se	-0.137	0.792	-0.761	0.633	0.039	0.526	0.661	0.060	-0.020	-0.125	0.191	0.901	-0.493				
Soluble I	-0.617	0.193	-0.006	-0.165	0.879	0.081	-0.137	-0.255	0.884	-0.055	-0.127	-0.025	0.062	-0.003			
Adsorbed I	-0.201	0.800	-0.512	0.280	0.391	0.344	0.476	-0.390	0.360	-0.428	-0.124	0.705	-0.533	0.649	0.560		
I TMAH	-0.176	0.765	-0.470	0.517	0.171	0.519	0.621	0.089	0.111	-0.585	-0.149	0.683	-0.332	0.759	0.236	0.809	
Total I	-0.191	0.772	-0.472	0.505	0.199	0.515	0.613	0.065	0.140	-0.581	-0.151	0.684	-0.339	0.755	0.271	0.830	0.999

Small Medium Large

Table C2: Pearson correlations to investigate the effect of the major cations on the fractionation of Se and iodine.

	B	Na	Mg	P	S	K	Ca	Ti	Soluble Se	Adsorbed Se	Se TMAH	Residual Se	Total Se	Soluble I	Adsorbed I	I TMAH
Na	0.223															
Mg	0.533	0.220														
P	0.294	0.848	0.573													
S	0.034	-0.010	0.349	-0.072												
K	0.159	0.599	0.605	0.728	0.063											
Ca	0.621	0.162	0.949	0.477	0.394	0.522										
Ti	-0.317	-0.458	-0.328	-0.302	-0.368	-0.656	-0.443									
Soluble Se	0.311	0.026	0.348	0.212	0.184	0.208	0.262	-0.011								
Adsorbed Se	-0.456	-0.128	0.014	-0.002	0.083	0.369	-0.086	-0.082	0.430							
Se TMAH	-0.683	-0.397	-0.864	-0.559	-0.369	-0.685	-0.920	0.689	-0.238	0.093						
Residual Se	0.492	0.446	0.893	0.688	0.274	0.669	0.801	-0.315	0.249	-0.044	-0.819					
Total Se	-0.693	-0.277	-0.632	-0.329	-0.342	-0.504	-0.793	0.795	-0.125	0.191	0.901	-0.493				
Soluble I	-0.055	-0.323	0.176	-0.345	0.78	-0.364	0.198	0.082	-0.055	-0.127	-0.025	0.062	-0.003			
Adsorbed I	-0.489	-0.661	-0.468	-0.697	0.025	-0.784	-0.477	0.673	-0.428	-0.124	0.705	-0.533	0.649	0.560		
I TMAH	-0.632	-0.355	-0.409	-0.350	-0.215	-0.459	-0.513	0.683	-0.585	-0.149	0.683	-0.332	0.759	0.236	0.809	
Total I	-0.629	-0.375	-0.407	-0.372	-0.188	-0.481	-0.508	0.686	-0.581	-0.151	0.684	-0.339	0.755	0.271	0.830	0.999

Small Medium Large

Table C3: Pearson correlations to investigate the effect of trace elements on the fractionation of Se and iodine.

	Li	Be	Al	V	Cr	Mn	Fe	Co	Ni	Cu	As	Rb	Sr	Ag	Ba	Se TMAH	Residual Se	Total Se	Soluble I	Adsorbed I	I TMAH
Be	0.956																				
Al	0.935	0.895																			
V	0.933	0.833	0.900																		
Cr	0.944	0.893	0.871	0.952																	
Mn	0.872	0.843	0.735	0.872	0.854																
Fe	0.976	0.927	0.925	0.971	0.984	0.873															
Co	0.948	0.872	0.880	0.985	0.985	0.881	0.989														
Ni	0.959	0.897	0.900	0.971	0.994	0.864	0.991	0.991													
Cu	0.828	0.717	0.834	0.932	0.809	0.798	0.870	0.892	0.849												
As	0.954	0.912	0.869	0.942	0.994	0.882	0.979	0.975	0.991	0.793											
Rb	-0.684	-0.573	-0.512	-0.787	-0.839	-0.708	-0.770	-0.838	-0.818	-0.666	-0.823										
Sr	-0.381	-0.463	-0.491	-0.421	-0.469	-0.289	-0.452	-0.424	-0.447	-0.281	-0.441	0.202									
Ag	0.598	0.751	0.604	0.353	0.412	0.466	0.498	0.386	0.417	0.296	0.44	0.047	-0.455								
Ba	-0.795	-0.765	-0.660	-0.758	-0.746	-0.826	-0.796	-0.793	-0.762	-0.792	-0.758	0.667	-0.047	-0.390							
Se TMAH	0.818	0.818	0.732	0.737	0.873	0.644	0.831	0.808	0.838	0.504	0.862	-0.677	-0.615	0.536	-0.468						
Residual Se	-0.453	-0.458	-0.311	-0.425	-0.622	-0.399	-0.500	-0.522	-0.559	-0.142	-0.615	0.642	0.498	-0.151	0.149	-0.819					
Total Se	0.873	0.862	0.854	0.771	0.830	0.63	0.856	0.806	0.823	0.626	0.815	-0.524	-0.552	0.679	-0.554	0.901	-0.493				
Soluble I	0.261	0.143	0.023	0.219	0.186	0.412	0.194	0.231	0.199	0.234	0.225	-0.370	0.704	-0.133	-0.562	-0.025	0.062	-0.003			
Adsorbed I	0.840	0.734	0.681	0.844	0.846	0.893	0.830	0.854	0.847	0.705	0.866	-0.773	-0.150	0.287	-0.715	0.705	-0.533	0.649	0.560		
I TMAH	0.892	0.858	0.853	0.810	0.77	0.839	0.829	0.794	0.799	0.746	0.795	-0.444	-0.355	0.689	-0.661	0.683	-0.332	0.759	0.236	0.809	
Total I	0.897	0.858	0.848	0.817	0.778	0.851	0.834	0.803	0.807	0.751	0.804	-0.465	-0.332	0.671	-0.676	0.684	-0.339	0.755	0.271	0.83	0.999

Small | Medium | Large

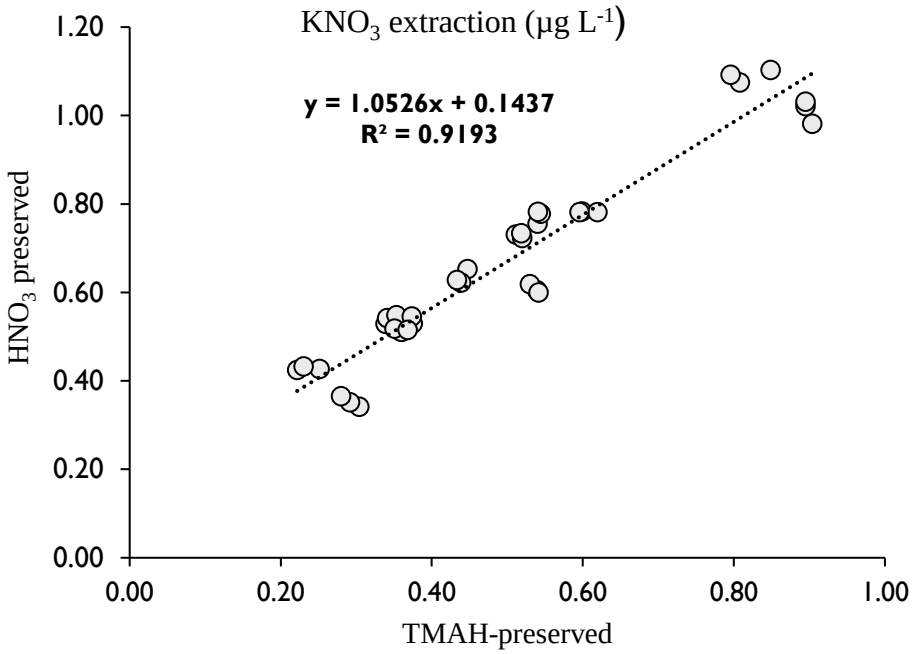
Table C4: Pearson correlations between Se and iodine species and the general properties of the soil

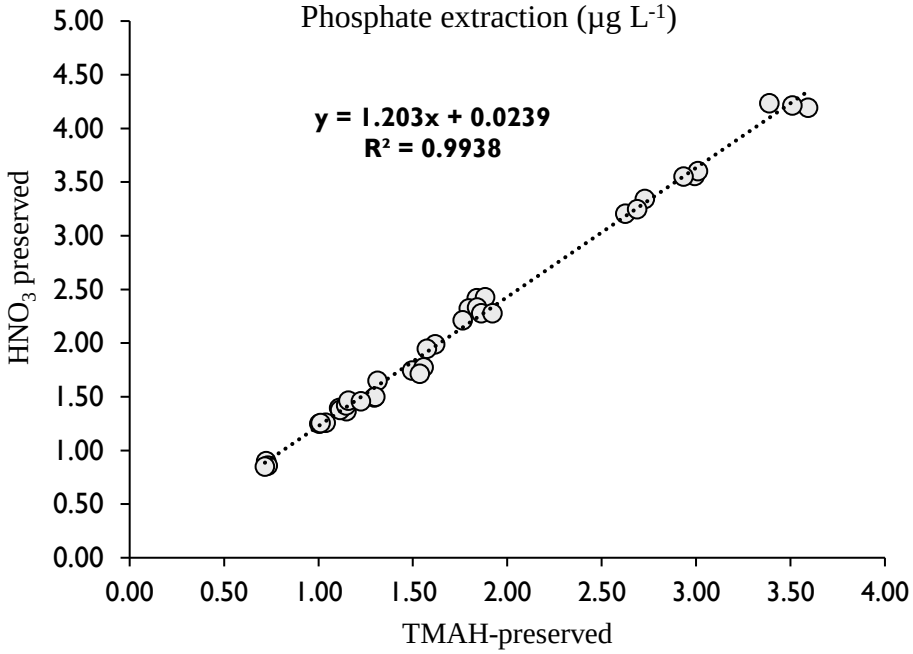
	pH	LOI	TIC	TOC	CEC	B	Na	Ca	Ca_exch.	Se (IV)-Soluble	Se (IV)-Adsorbed	Se (VI)-Soluble	Se (VI)-Adsorbed	IO3_Soluble	IO3_adsorbed	I-_soluble
LOI	-0.120															
TIC	-0.146	-0.663														
TOC	-0.190	0.471	-0.445													
CEC	-0.652	0.197	-0.096	-0.143												
B	-0.023	-0.466	0.636	-0.486	-0.161											
Na	-0.066	-0.441	0.146	0.034	-0.218	0.223										
Ca	-0.304	-0.702	0.947	-0.400	0.116	0.621	0.162									
Ca exch.	-0.619	0.140	-0.076	-0.204	0.996	-0.129	-0.214	0.142								
Se (IV)-Soluble	0.222	-0.419	-0.139	0.041	-0.248	-0.220	0.104	-0.081	-0.217							
Se (IV)-Adsorbed	0.077	-0.279	-0.142	0.125	-0.091	-0.449	-0.131	-0.085	-0.077	0.871						
Se (VI)-Soluble	-0.357	-0.149	0.406	-0.156	0.002	0.618	-0.081	0.379	-0.005	-0.209	-0.265					
Se (VI)-Adsorbed	-0.509	0.028	0.225	-0.241	0.438	0.464	-0.136	0.278	0.435	-0.462	-0.485	0.820				
IO3_Soluble	-0.316	-0.013	0.170	-0.305	0.715	0.061	-0.325	0.342	0.736	-0.178	-0.145	-0.119	0.183			
IO3_adsorbed	0.002	-0.218	0.418	-0.342	0.261	0.187	-0.288	0.484	0.288	-0.168	-0.143	-0.181	-0.055	0.820		
I-_soluble	-0.530	0.273	-0.059	-0.168	0.809	-0.079	-0.443	0.113	0.811	-0.240	-0.091	0.030	0.297	0.819	0.454	
I-_adsorbed	-0.538	0.305	-0.067	-0.142	0.919	-0.195	-0.482	0.109	0.915	-0.343	-0.105	-0.081	0.334	0.792	0.453	0.875

Small Medium Large

Appendix D: Comparison between HNO_3 and TMAH preservation

Selenium, KNO_3, KH_2PO_4 extraction (HNO_3 vs TMAH preserved)





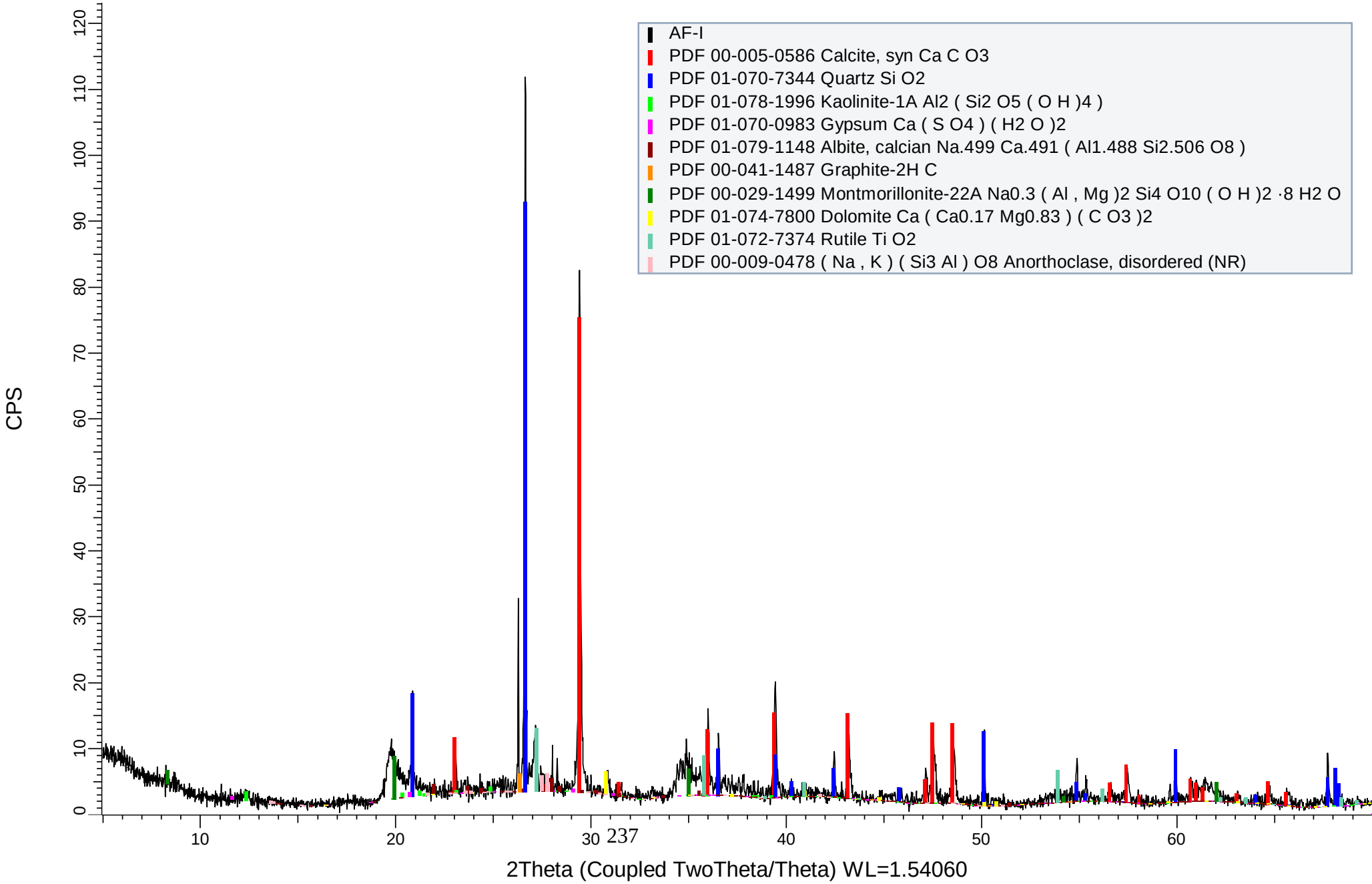
Appendix E: Notes on XRD phase identification

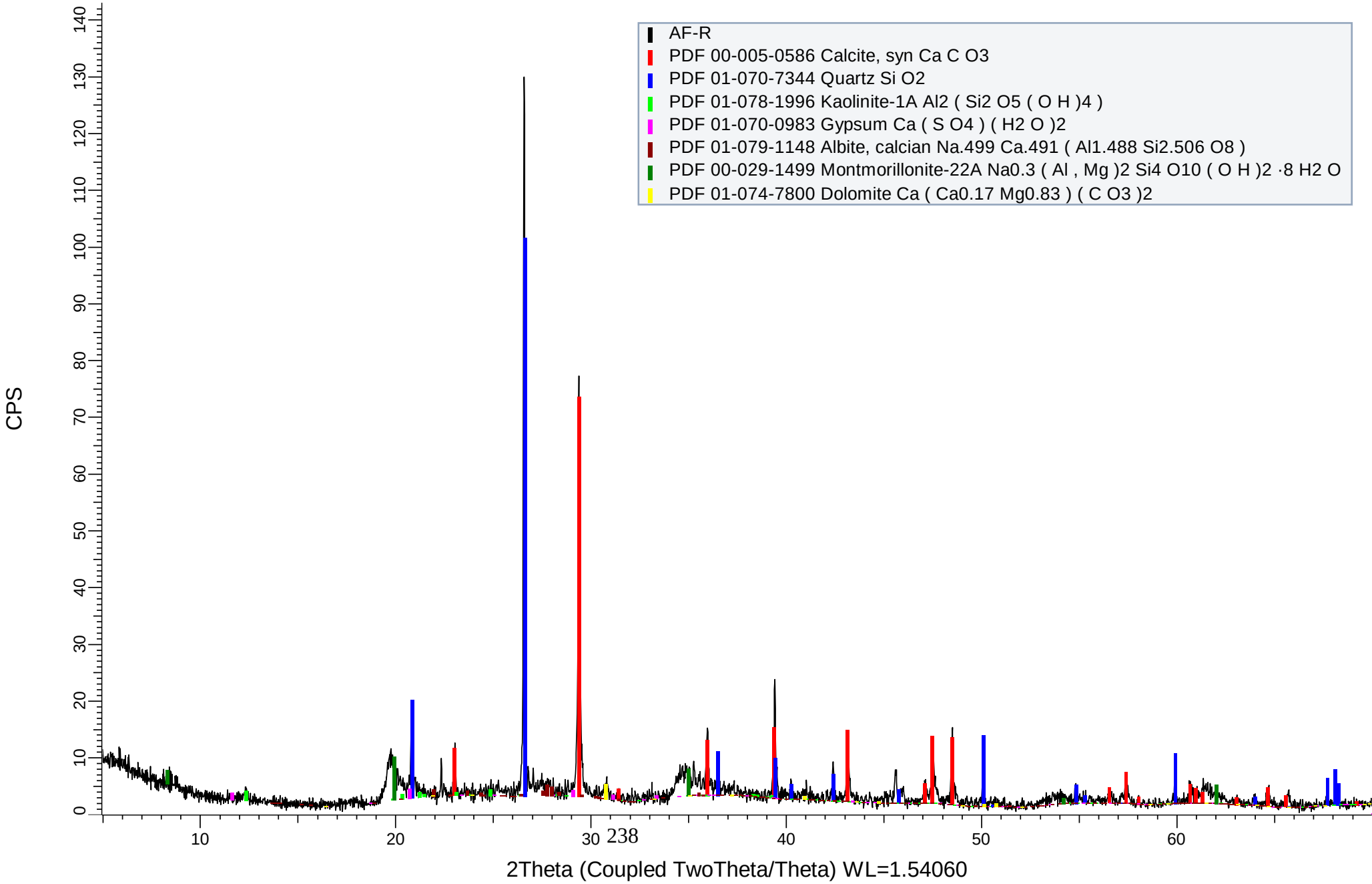
Not all peaks have been satisfactorily matched so some other phases may be present.

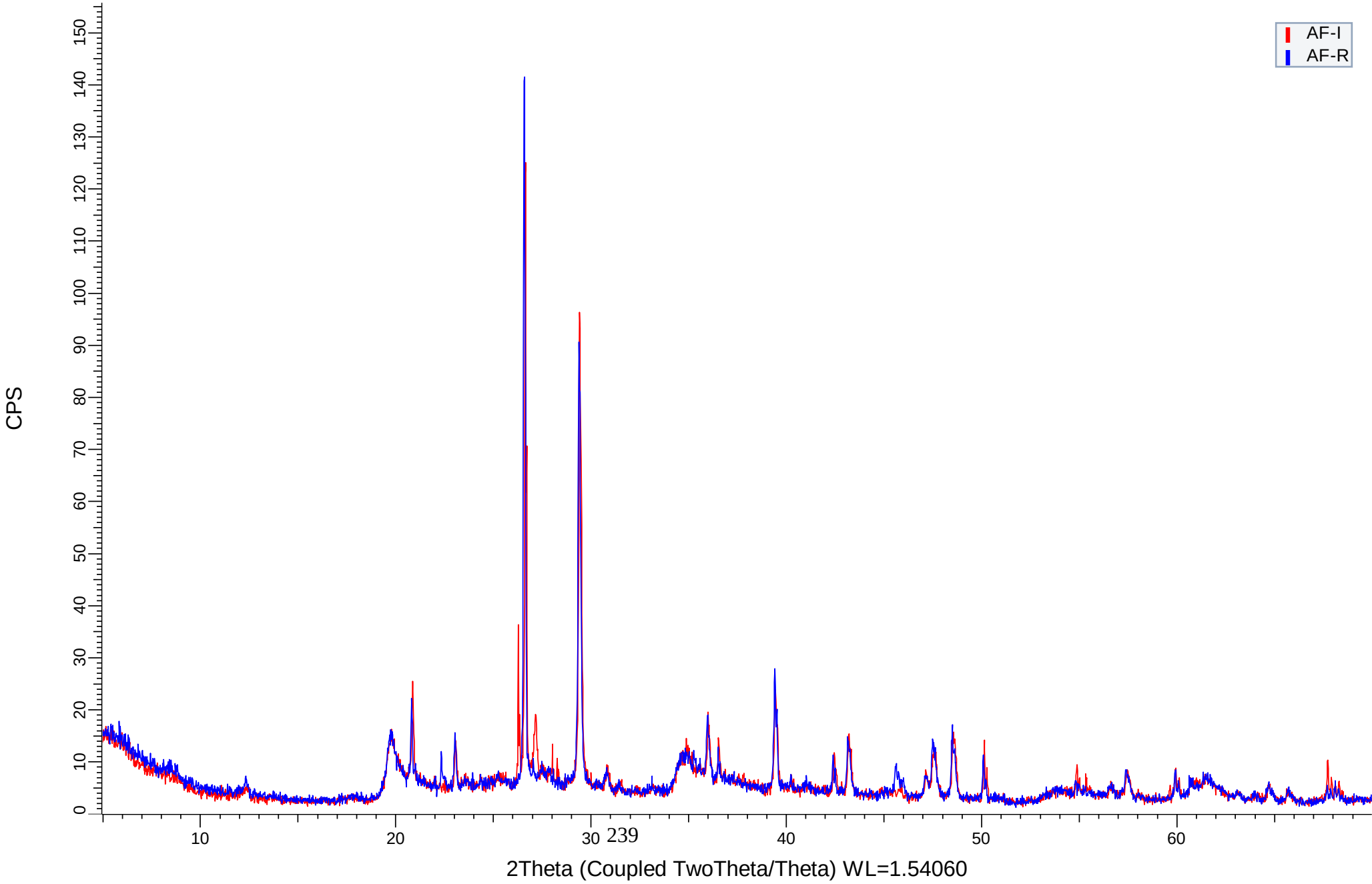
The identification is less certain where fewer clear peaks are matching, and could be improved with a knowledge of the context of the source and chemical analysis of the sample.

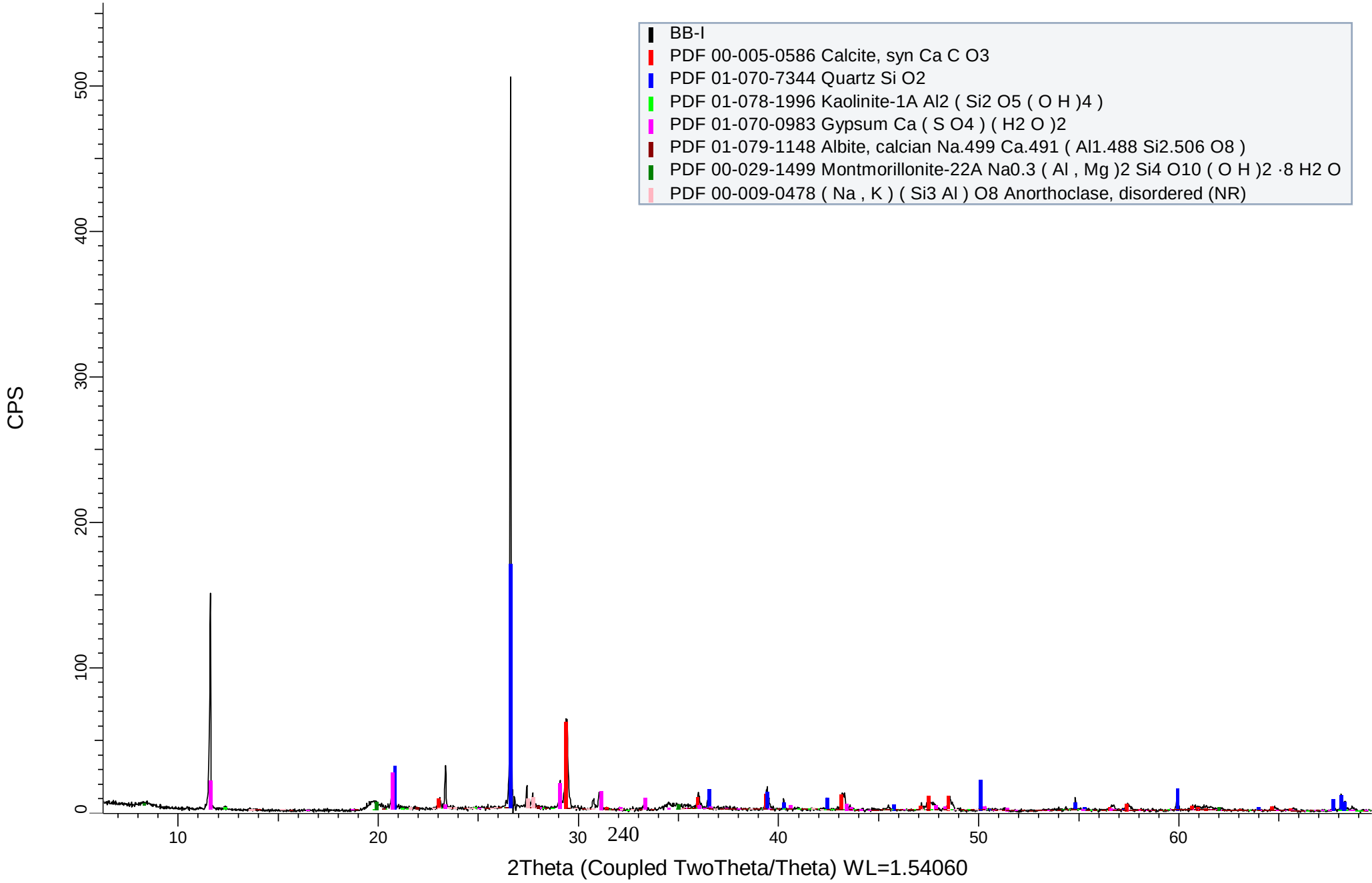
Some minerals are difficult to distinguish by XRD from others that are closely related, e.g. members of the plagioclase series; dolomite and ankerite.

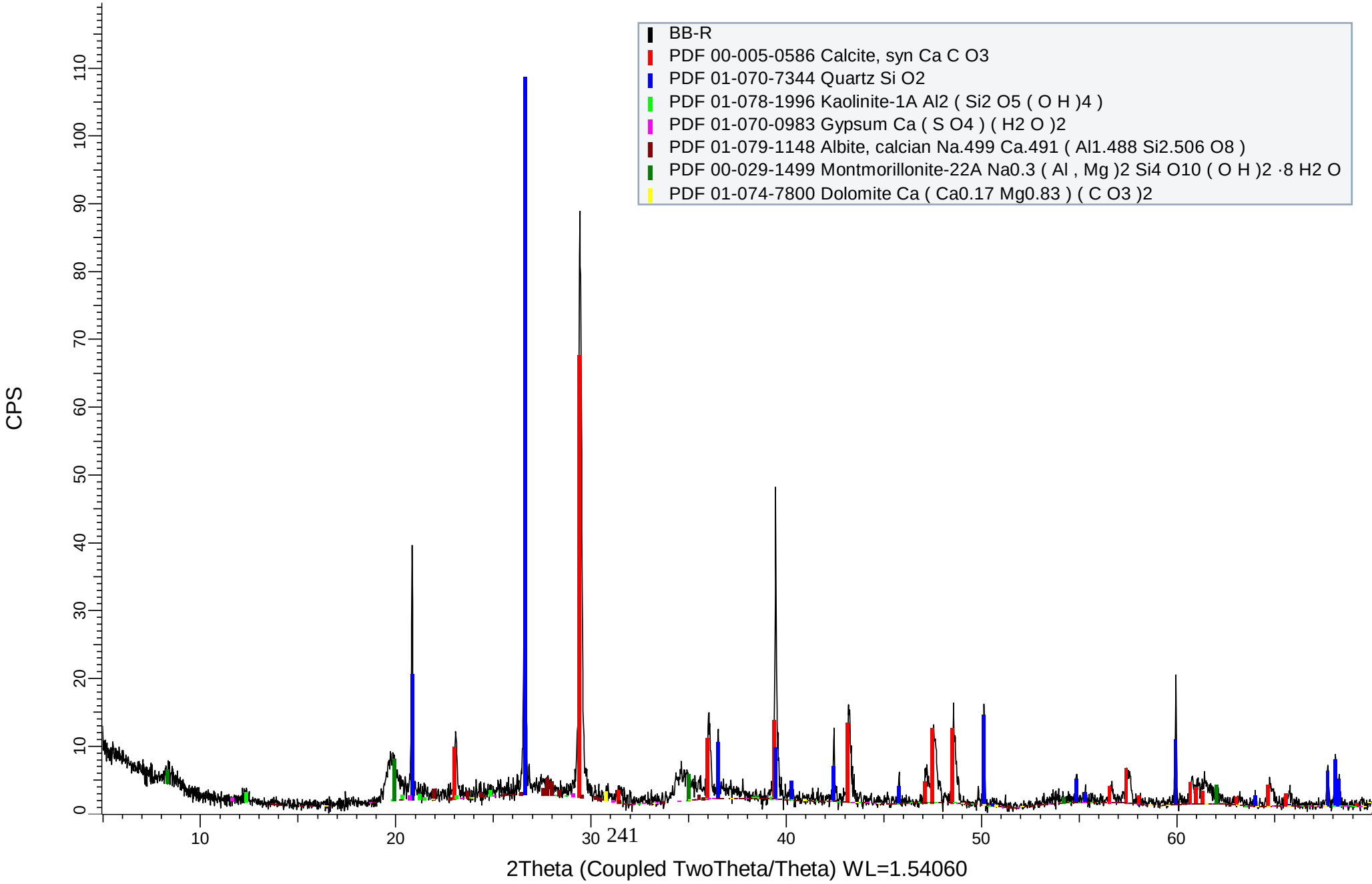
The patterns for calcite and gypsum have been included with all samples for reference, even when no matching peaks are observed. BB-I is the only sample with a clear match for gypsum.

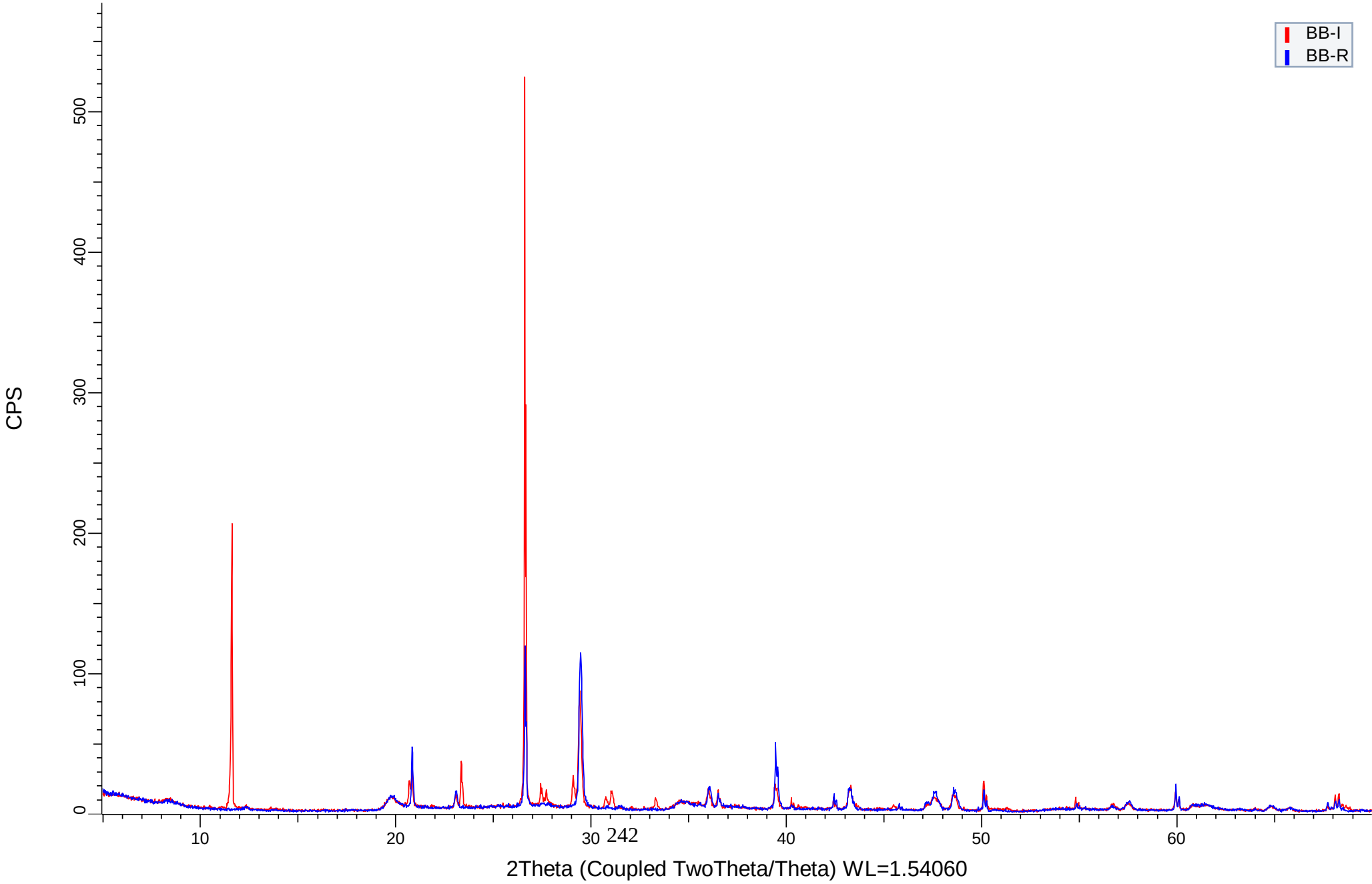

AF-I
PDF 00-005-0586 Calcite, syn Ca C O3
PDF 01-070-7344 Quartz Si O2
PDF 01-078-1996 Kaolinite-1A Al2 (Si2 O5 (O H)4)
PDF 01-070-0983 Gypsum Ca (S O4) (H2 O)2
PDF 01-079-1148 Albite, calcian Na.499 Ca.491 (Al1.488 Si2.506 O8)
PDF 00-041-1487 Graphite-2H C
PDF 00-029-1499 Montmorillonite-22A Na0.3 (Al , Mg)2 Si4 O10 (O H)2 ·8 H2 O
PDF 01-074-7800 Dolomite Ca (Ca0.17 Mg0.83) (C O3)2
PDF 01-072-7374 Rutile Ti O2
PDF 00-009-0478 (Na , K) (Si3 Al) O8 Anorthoclase, disordered (NR)
CPS
0
10
20
30
40
50
60
70
80
90
100
110
120
10
20
30
40
50
60
2Theta (Coupled TwoTheta/Theta) WL=1.54060

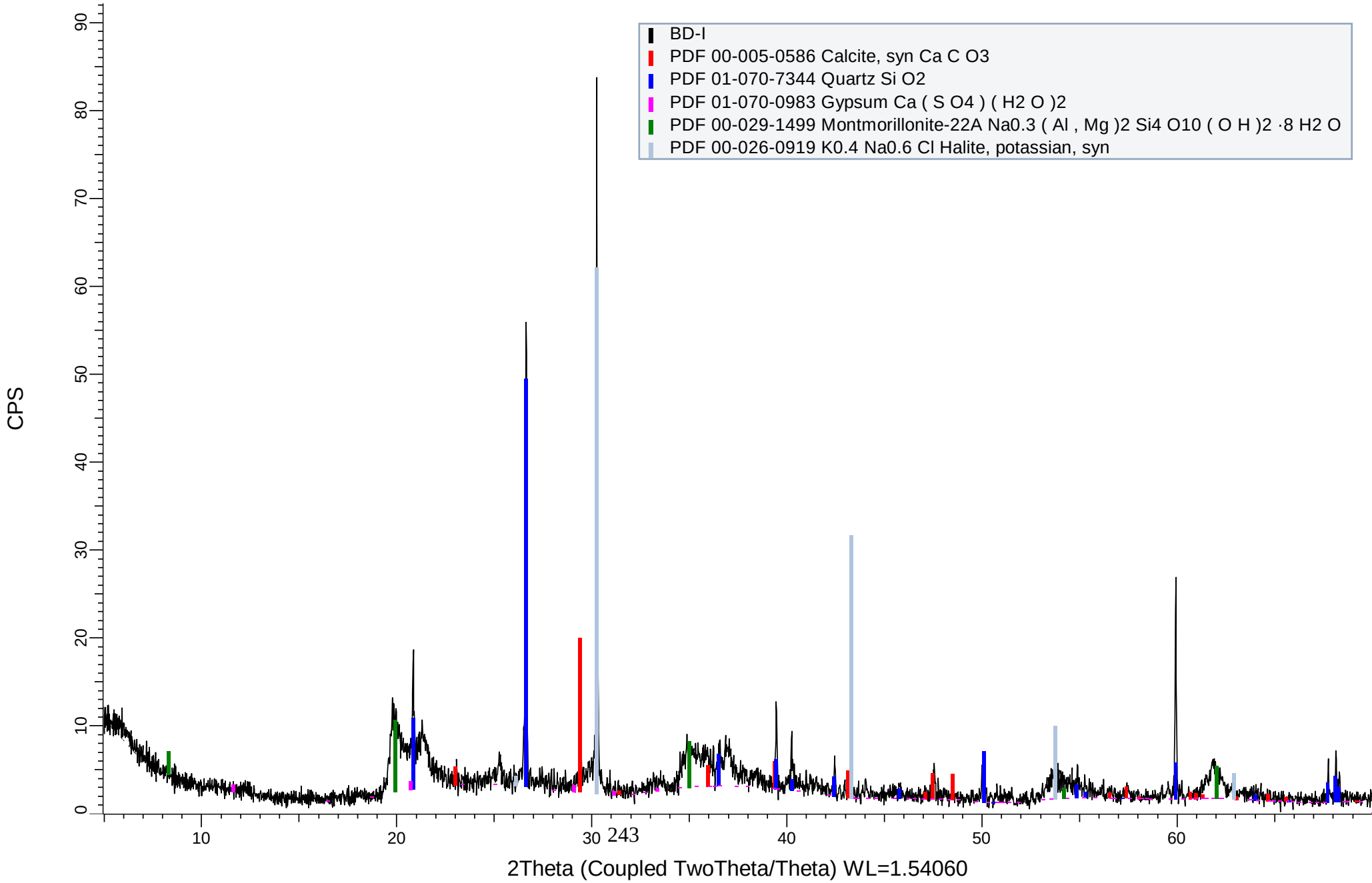

AF-R
PDF 00-005-0586 Calcite, syn Ca C O3
PDF 01-070-7344 Quartz Si O2
PDF 01-078-1996 Kaolinite-1A Al2 (Si2 O5 (O H)4)
PDF 01-070-0983 Gypsum Ca (S O4) (H2 O)2
PDF 01-079-1148 Albite, calcian Na.499 Ca.491 (Al1.488 Si2.506 O8)
PDF 00-029-1499 Montmorillonite-22A Na0.3 (Al , Mg)2 Si4 O10 (O H)2 ·8 H2 O
PDF 01-074-7800 Dolomite Ca (Ca0.17 Mg0.83) (C O3)2
CPS
0
10
20
30
40
50
60
70
80
90
100
110
120
130
140
10
20
30
40
50
60
2Theta (Coupled TwoTheta/Theta) WL=1.54060

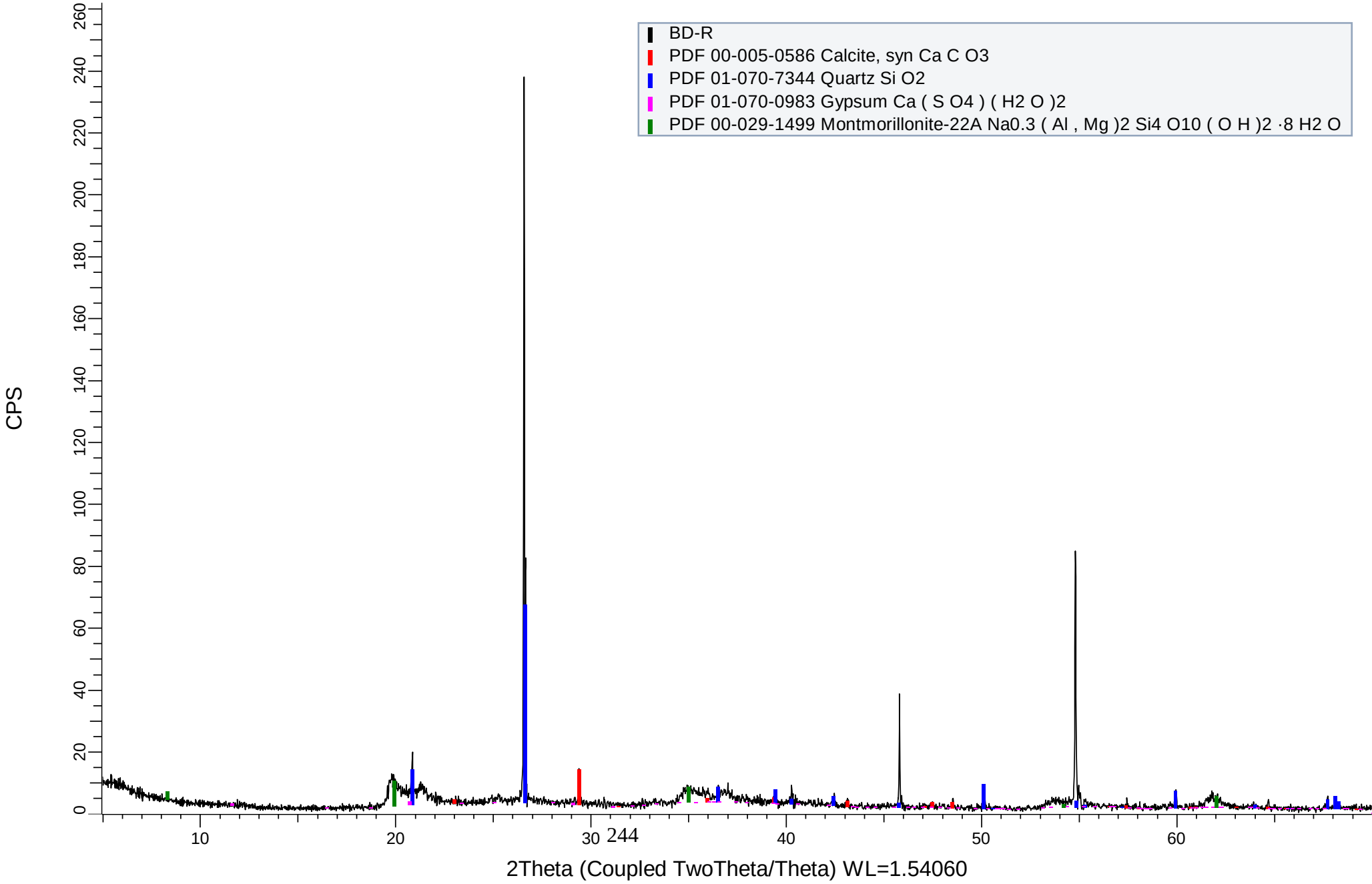

AF-I
AF-R
CPS
0
10
20
30
40
50
60
70
80
90
100
110
120
130
140
150
10
20
30
40
50
60
2Theta (Coupled TwoTheta/Theta) WL=1.54060

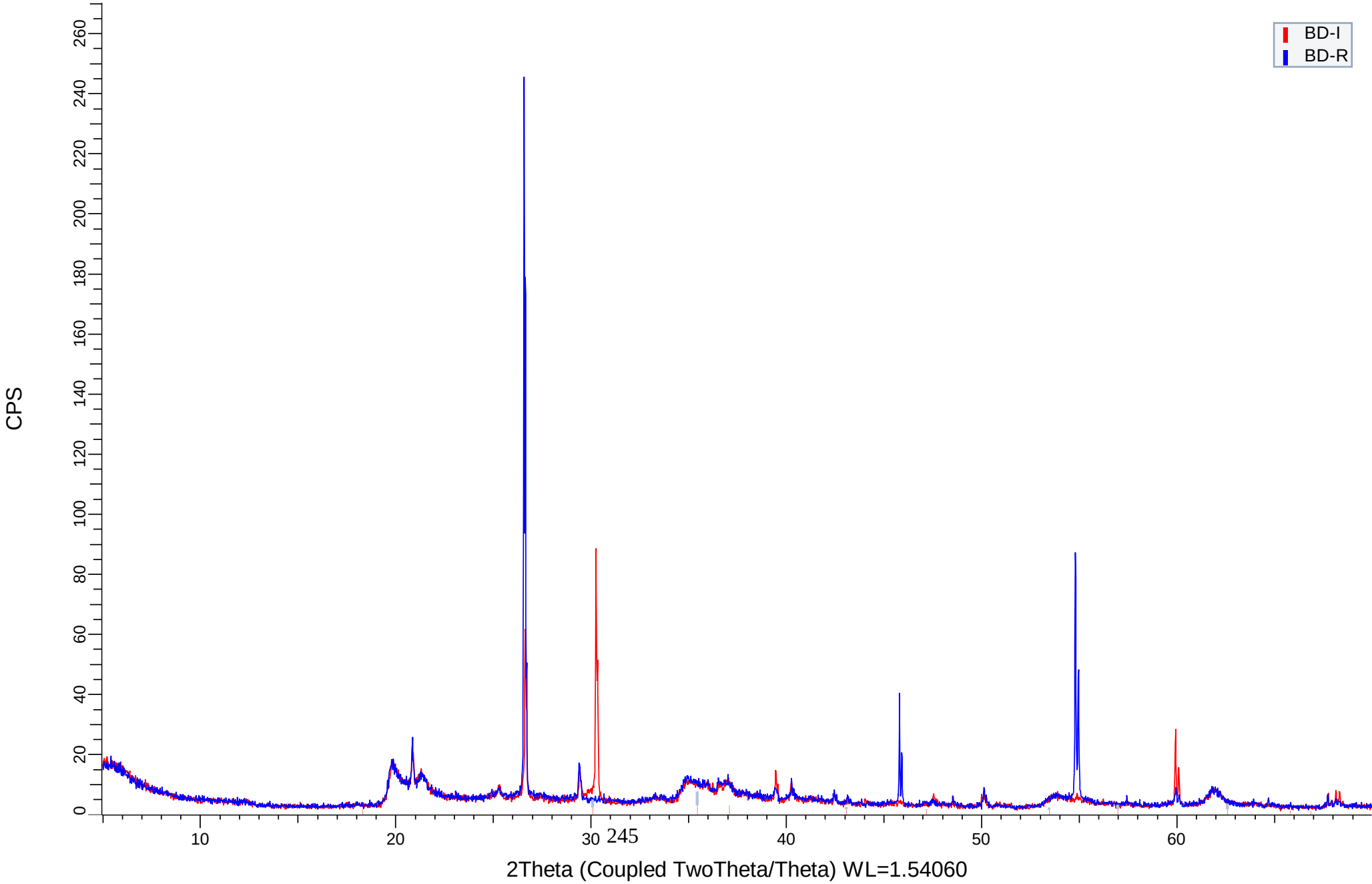

BB-I
PDF 00-005-0586 Calcite, syn Ca C O3
PDF 01-070-7344 Quartz Si O2
PDF 01-078-1996 Kaolinite-1A Al2 (Si2 O5 (O H)4)
PDF 01-070-0983 Gypsum Ca (S O4) (H2 O)2
PDF 01-079-1148 Albite, calcian Na.499 Ca.491 (Al1.488 Si2.506 O8)
PDF 00-029-1499 Montmorillonite-22A Na0.3 (Al , Mg)2 Si4 O10 (O H)2 ·8 H2 O
PDF 00-009-0478 (Na , K) (Si3 Al) O8 Anorthoclase, disordered (NR)
CPS
0
100
200
300
400
500
10
20
30
40
50
60
240
2Theta (Coupled TwoTheta/Theta) WL=1.54060

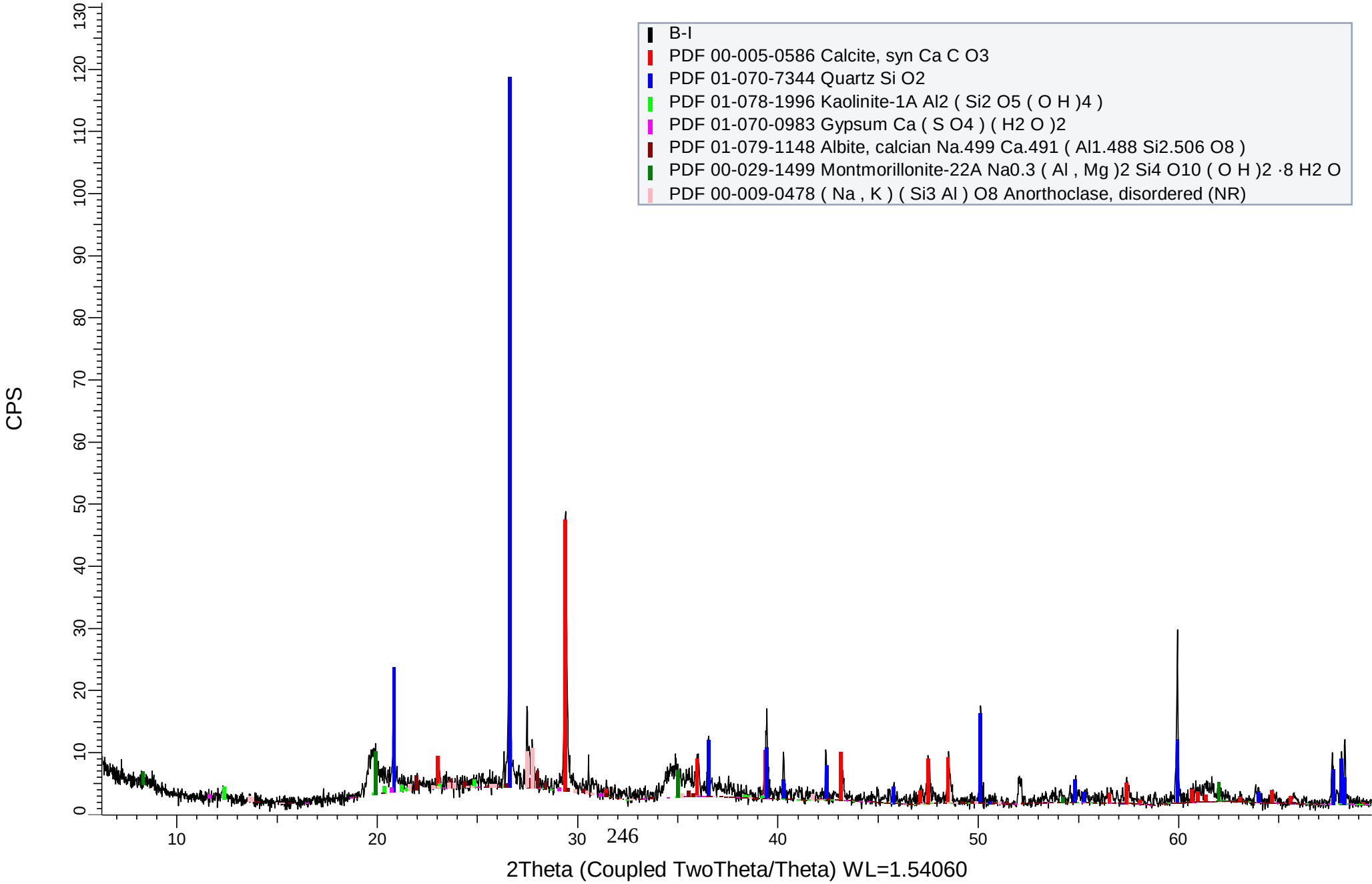

BB-R
PDF 00-005-0586 Calcite, syn Ca C O3
PDF 01-070-7344 Quartz Si O2
PDF 01-078-1996 Kaolinite-1A Al2 (Si2 O5 (O H)4)
PDF 01-070-0983 Gypsum Ca (S O4) (H2 O)2
PDF 01-079-1148 Albite, calcian Na.499 Ca.491 (Al1.488 Si2.506 O8)
PDF 00-029-1499 Montmorillonite-22A Na0.3 (Al , Mg)2 Si4 O10 (O H)2 ·8 H2 O
PDF 01-074-7800 Dolomite Ca (Ca0.17 Mg0.83) (C O3)2
CPS
0
10
20
30
40
50
60
70
80
90
100
110
10
20
30
40
50
60
2Theta (Coupled TwoTheta/Theta) WL=1.54060

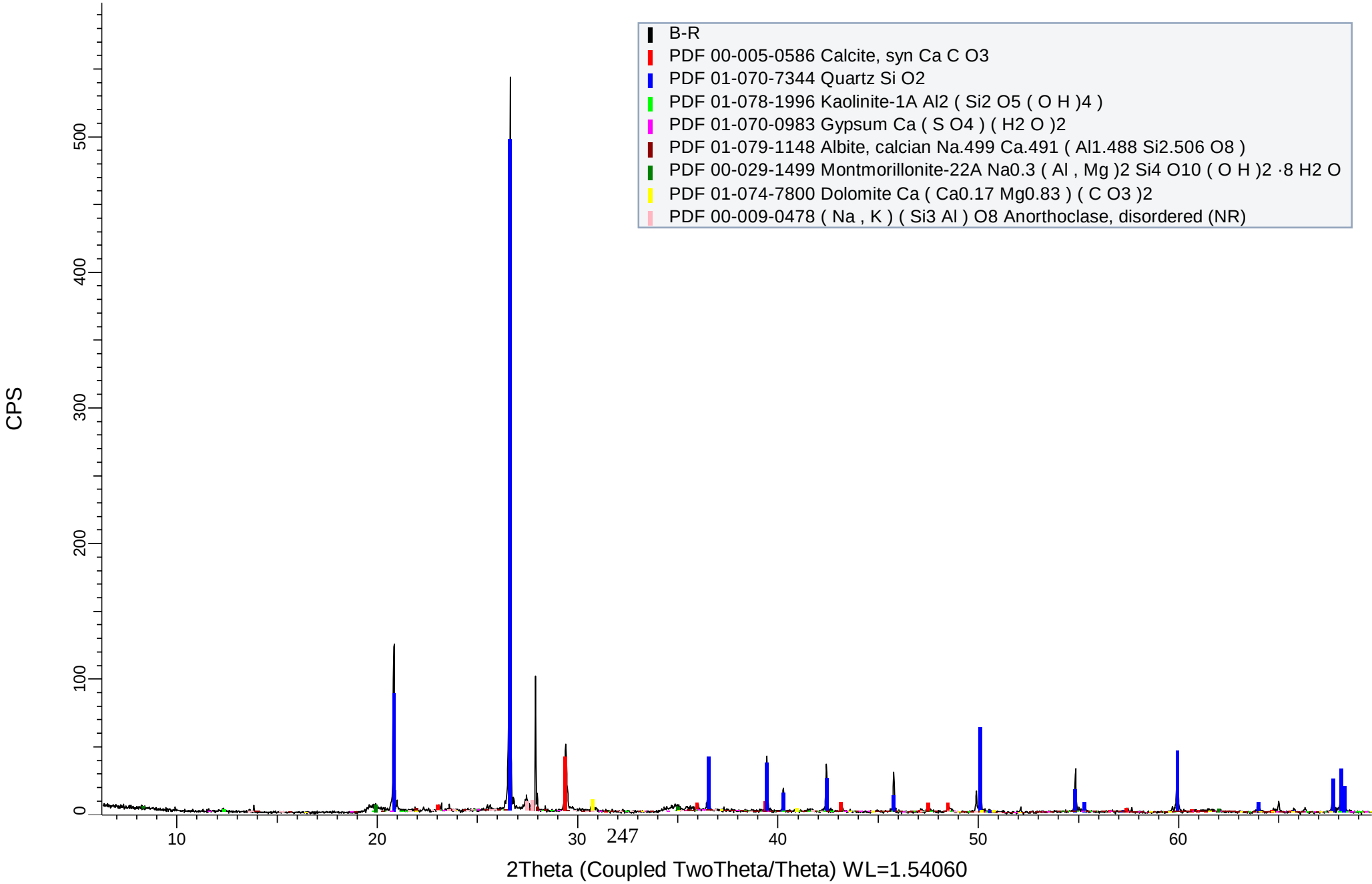

BB-I
BB-R
CPS
0
100
200
300
400
500
10
20
30
40
50
60
2Theta (Coupled TwoTheta/Theta) WL=1.54060

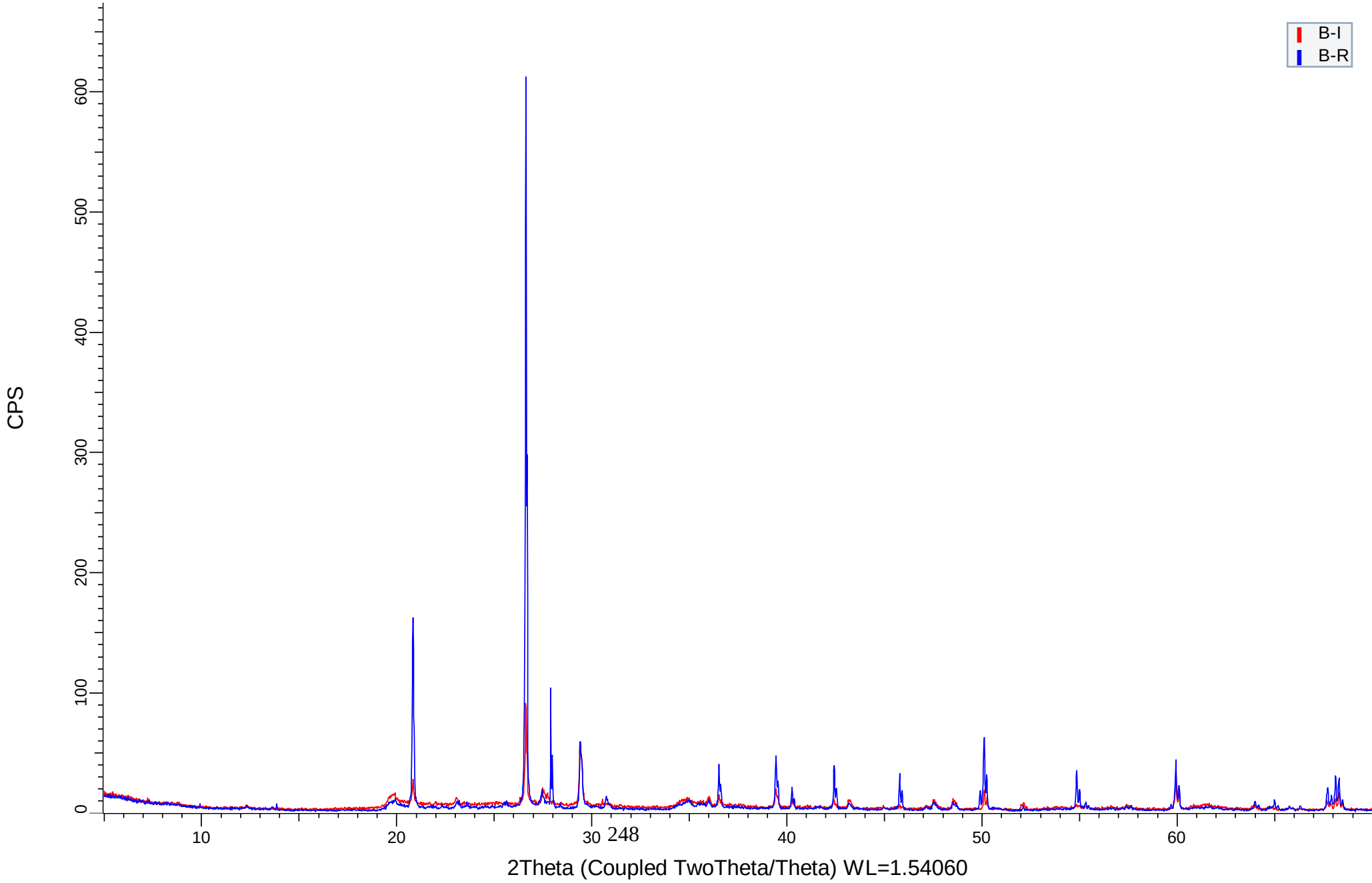

BD-I
PDF 00-005-0586 Calcite, syn Ca C O3
PDF 01-070-7344 Quartz Si O2
PDF 01-070-0983 Gypsum Ca (S O4) (H2 O)2
PDF 00-029-1499 Montmorillonite-22A Na0.3 (Al , Mg)2 Si4 O10 (O H)2 ·8 H2 O
PDF 00-026-0919 K0.4 Na0.6 Cl Halite, potassian, syn
CPS
0
10
20
30
40
50
60
70
80
90
10
20
30
40
50
60
2Theta (Coupled TwoTheta/Theta) WL=1.54060

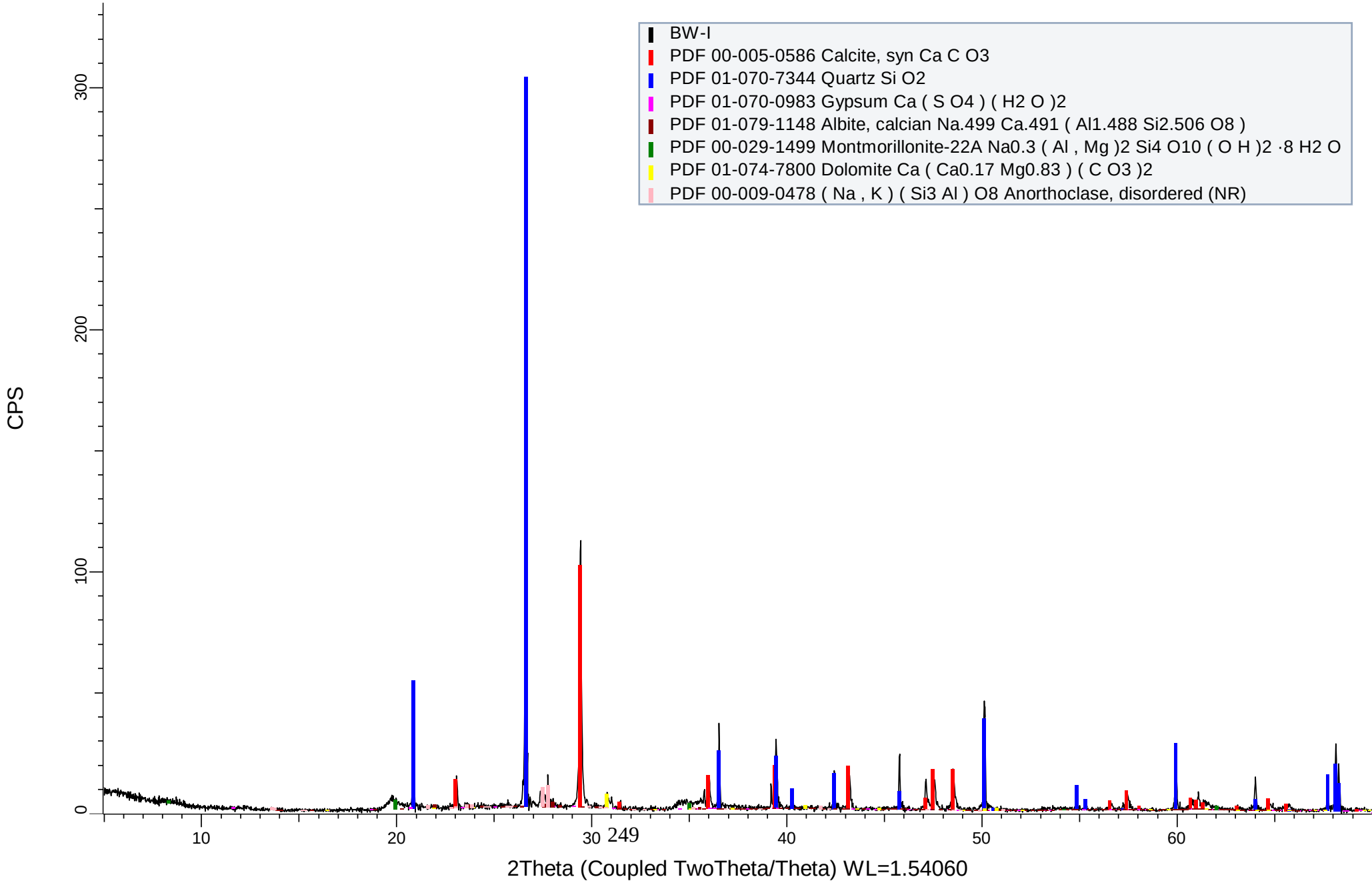

BD-R
PDF 00-005-0586 Calcite, syn Ca C O3
PDF 01-070-7344 Quartz Si O2
PDF 01-070-0983 Gypsum Ca (S O4) (H2 O)2
PDF 00-029-1499 Montmorillonite-22A Na0.3 (Al , Mg)2 Si4 O10 (O H)2 ·8 H2 O
CPS
0
20
40
60
80
100
120
140
160
180
200
220
240
260
10
20
30
40
50
60
2Theta (Coupled TwoTheta/Theta) WL=1.54060

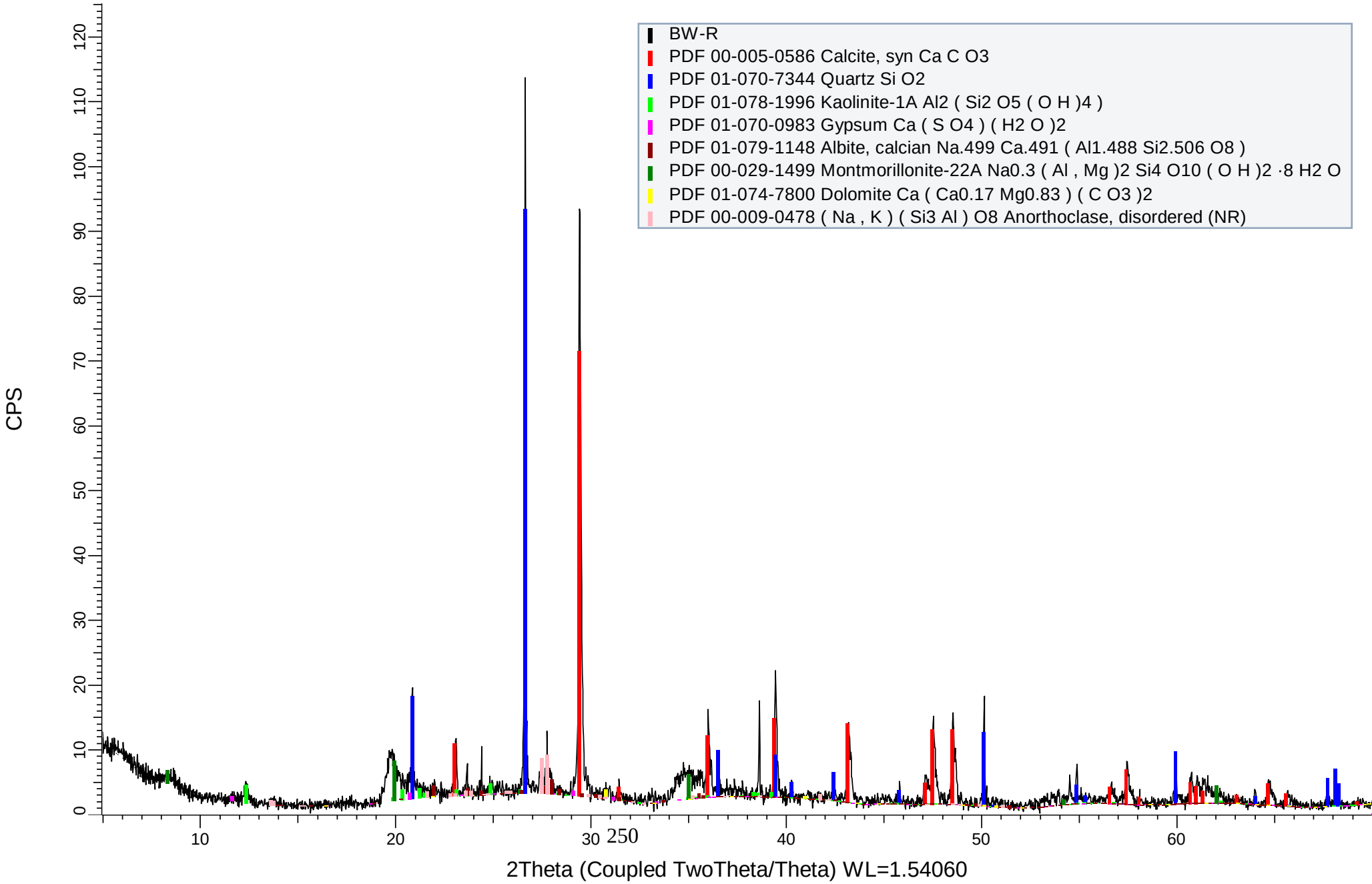

BD-I
BD-R
CPS
0
20
40
60
80
100
120
140
160
180
200
220
240
260
10
20
30
40
50
60
2Theta (Coupled TwoTheta/Theta) WL=1.54060

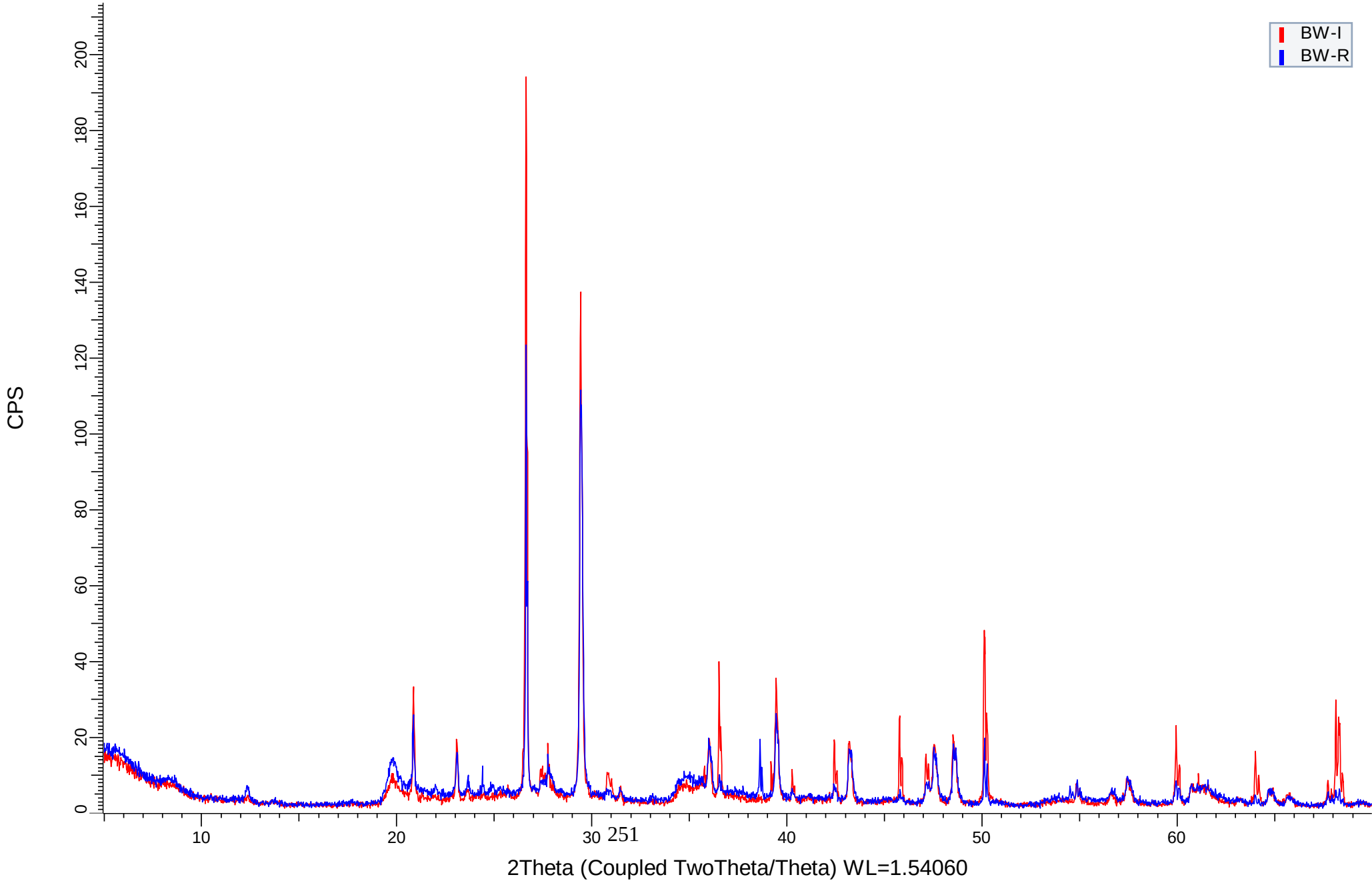

B-I
PDF 00-005-0586 Calcite, syn Ca C O3
PDF 01-070-7344 Quartz Si O2
PDF 01-078-1996 Kaolinite-1A Al2 (Si2 O5 (O H)4)
PDF 01-070-0983 Gypsum Ca (S O4) (H2 O)2
PDF 01-079-1148 Albite, calcian Na.499 Ca.491 (Al1.488 Si2.506 O8)
PDF 00-029-1499 Montmorillonite-22A Na0.3 (Al , Mg)2 Si4 O10 (O H)2 ·8 H2 O
PDF 00-009-0478 (Na , K) (Si3 Al) O8 Anorthoclase, disordered (NR)
CPS
0
10
20
30
40
50
60
70
80
90
100
110
120
130
10
20
30
40
50
60
2Theta (Coupled TwoTheta/Theta) WL=1.54060

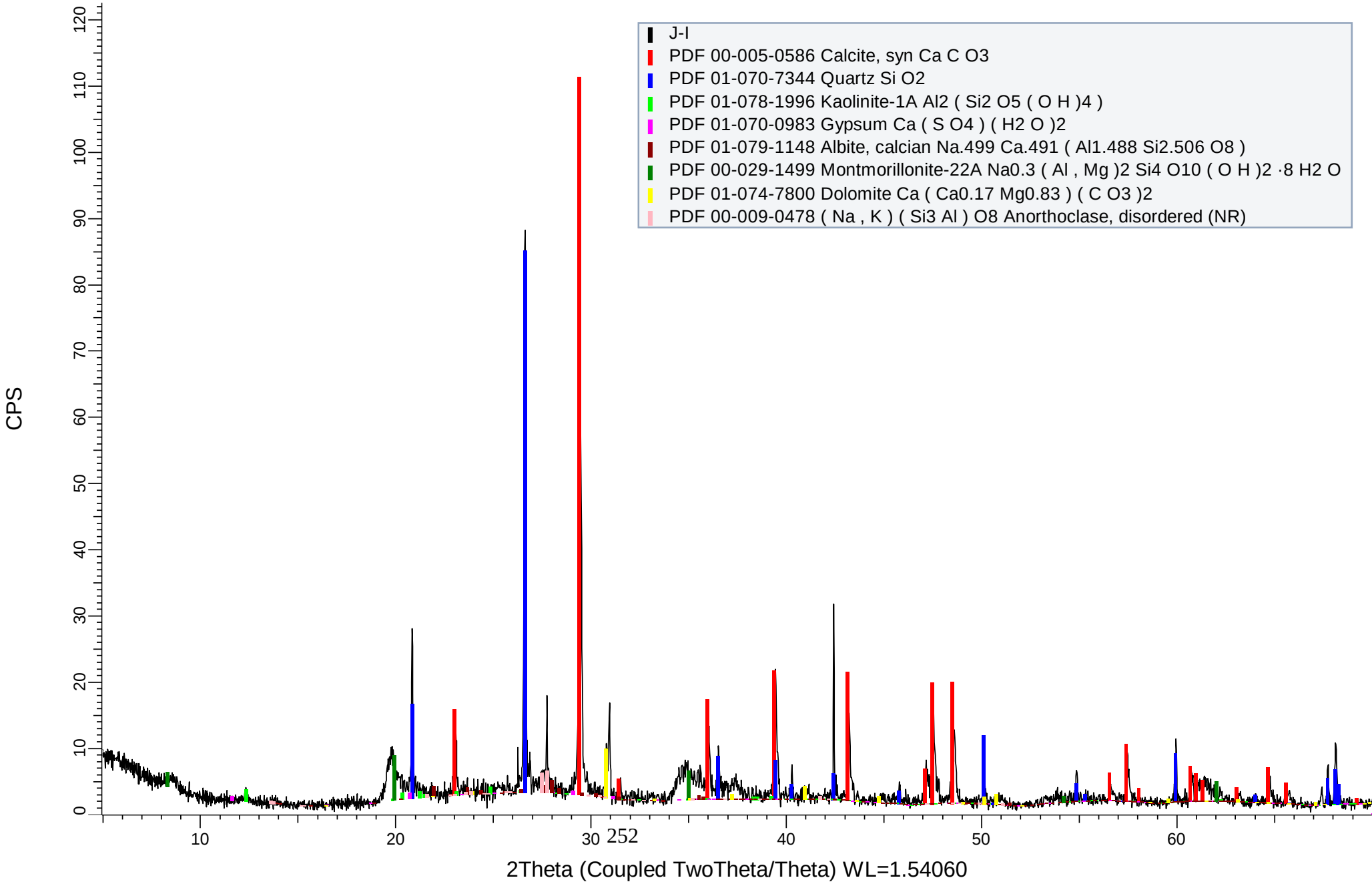

B-R
PDF 00-005-0586 Calcite, syn Ca C O3
PDF 01-070-7344 Quartz Si O2
PDF 01-078-1996 Kaolinite-1A Al2 (Si2 O5 (O H)4)
PDF 01-070-0983 Gypsum Ca (S O4) (H2 O)2
PDF 01-079-1148 Albite, calcian Na.499 Ca.491 (Al1.488 Si2.506 O8)
PDF 00-029-1499 Montmorillonite-22A Na0.3 (Al , Mg)2 Si4 O10 (O H)2 ·8 H2 O
PDF 01-074-7800 Dolomite Ca (Ca0.17 Mg0.83) (C O3)2
PDF 00-009-0478 (Na , K) (Si3 Al) O8 Anorthoclase, disordered (NR)
CPS
0
100
200
300
400
500
10
20
30
40
50
60
2Theta (Coupled TwoTheta/Theta) WL=1.54060

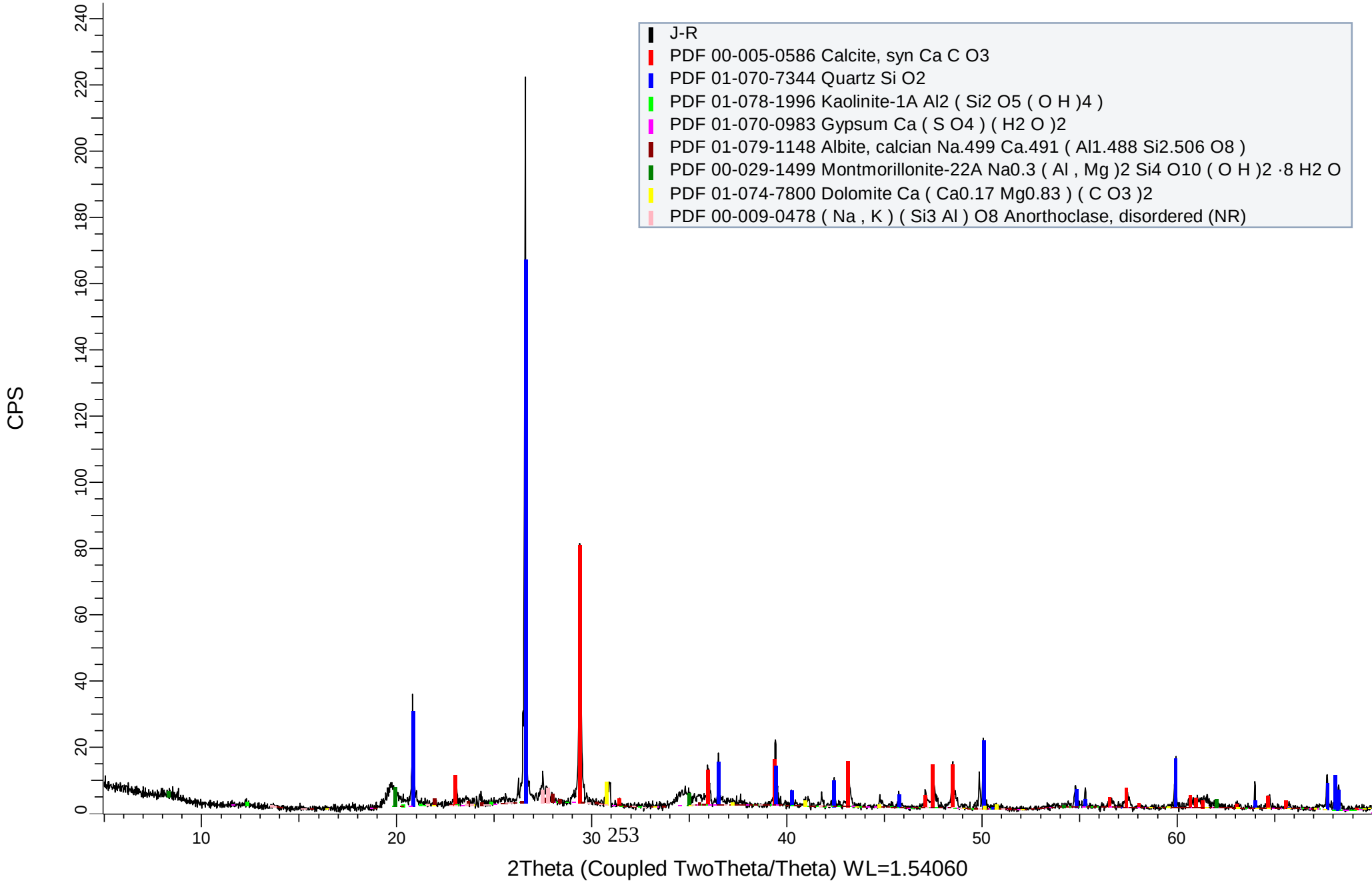

B-I
B-R
CPS
0
100
200
300
400
500
600
10
20
30
40
50
60
2Theta (Coupled TwoTheta/Theta) WL=1.54060

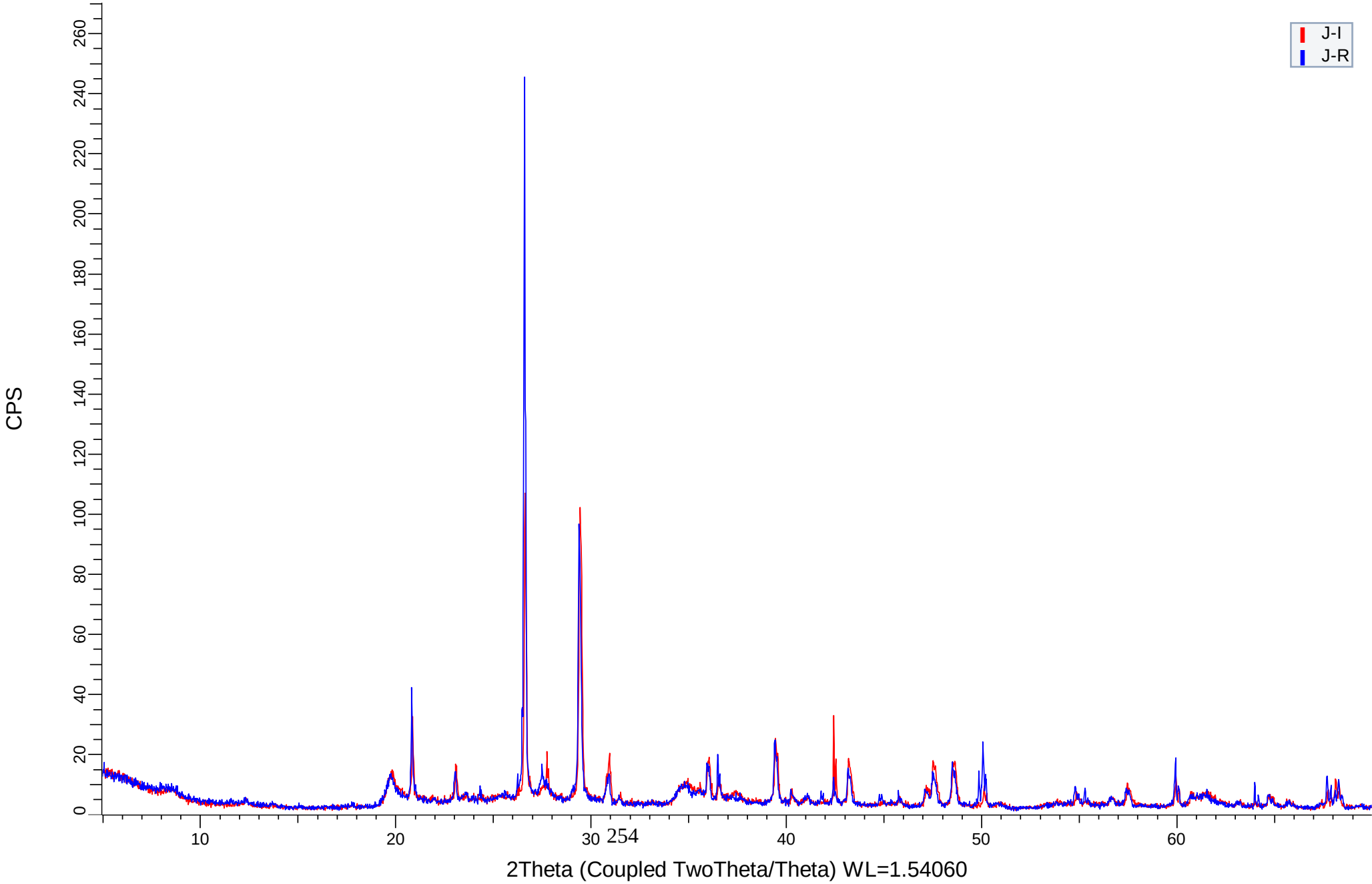

BW-I
PDF 00-005-0586 Calcite, syn Ca C O3
PDF 01-070-7344 Quartz Si O2
PDF 01-070-0983 Gypsum Ca (S O4) (H2 O)2
PDF 01-079-1148 Albite, calcian Na.499 Ca.491 (Al1.488 Si2.506 O8)
PDF 00-029-1499 Montmorillonite-22A Na0.3 (Al , Mg)2 Si4 O10 (O H)2 ·8 H2 O
PDF 01-074-7800 Dolomite Ca (Ca0.17 Mg0.83) (C O3)2
PDF 00-009-0478 (Na , K) (Si3 Al) O8 Anorthoclase, disordered (NR)
CPS
0
100
200
300
10
20
30
40
50
60
2Theta (Coupled TwoTheta/Theta) WL=1.54060


BW-R
PDF 00-005-0586 Calcite, syn Ca C O3
PDF 01-070-7344 Quartz Si O2
PDF 01-078-1996 Kaolinite-1A Al2 (Si2 O5 (O H)4)
PDF 01-070-0983 Gypsum Ca (S O4) (H2 O)2
PDF 01-079-1148 Albite, calcian Na.499 Ca.491 (Al1.488 Si2.506 O8)
PDF 00-029-1499 Montmorillonite-22A Na0.3 (Al , Mg)2 Si4 O10 (O H)2 ·8 H2 O
PDF 01-074-7800 Dolomite Ca (Ca0.17 Mg0.83) (C O3)2
PDF 00-009-0478 (Na , K) (Si3 Al) O8 Anorthoclase, disordered (NR)
CPS
0
10
20
30
40
50
60
70
80
90
100
110
120
10
20
30
250
40
50
60
2Theta (Coupled TwoTheta/Theta) WL=1.54060


BW-I
BW-R
CPS
0
20
40
60
80
100
120
140
160
180
200
10
20
30
40
50
60
2Theta (Coupled TwoTheta/Theta) WL=1.54060


J-I
PDF 00-005-0586 Calcite, syn Ca C O3
PDF 01-070-7344 Quartz Si O2
PDF 01-078-1996 Kaolinite-1A Al2 (Si2 O5 (O H)4)
PDF 01-070-0983 Gypsum Ca (S O4) (H2 O)2
PDF 01-079-1148 Albite, calcian Na.499 Ca.491 (Al1.488 Si2.506 O8)
PDF 00-029-1499 Montmorillonite-22A Na0.3 (Al , Mg)2 Si4 O10 (O H)2 ·8 H2 O
PDF 01-074-7800 Dolomite Ca (Ca0.17 Mg0.83) (C O3)2
PDF 00-009-0478 (Na , K) (Si3 Al) O8 Anorthoclase, disordered (NR)
CPS
0
10
20
30
40
50
60
70
80
90
100
110
120
10
20
30
40
50
60
2Theta (Coupled TwoTheta/Theta) WL=1.54060


J-R
PDF 00-005-0586 Calcite, syn Ca C O3
PDF 01-070-7344 Quartz Si O2
PDF 01-078-1996 Kaolinite-1A Al2 (Si2 O5 (O H)4)
PDF 01-070-0983 Gypsum Ca (S O4) (H2 O)2
PDF 01-079-1148 Albite, calcian Na.499 Ca.491 (Al1.488 Si2.506 O8)
PDF 00-029-1499 Montmorillonite-22A Na0.3 (Al , Mg)2 Si4 O10 (O H)2 ·8 H2 O
PDF 01-074-7800 Dolomite Ca (Ca0.17 Mg0.83) (C O3)2
PDF 00-009-0478 (Na , K) (Si3 Al) O8 Anorthoclase, disordered (NR)
CPS
0
20
40
60
80
100
120
140
160
180
200
220
240
10
20
30
40
50
60
2Theta (Coupled TwoTheta/Theta) WL=1.54060


J-I
J-R
CPS
0
20
40
60
80
100
120
140
160
180
200
220
240
260
10
20
30
40
50
60
2Theta (Coupled TwoTheta/Theta) WL=1.54060

Appendix F: Photographs from the field survey and laboratory experiments:



Figure F1: Soil sampling from agricultural fields in South Somalia to assess the Se and I availabilities. Samples were collected from both rainfed and irrigated sites.



Figure F2: Soil sample processing in local lab prior to delivery to Nottingham University.



Figure F3: Surface water sampling sites (Shabelle river, Somalia).



Figure F4: Onsite filtering of the water samples for chemical analysis.



Figure F5: Representative maize cobs were sampled from Somali Agricultural Technical Group (SATG) demonstration plots.

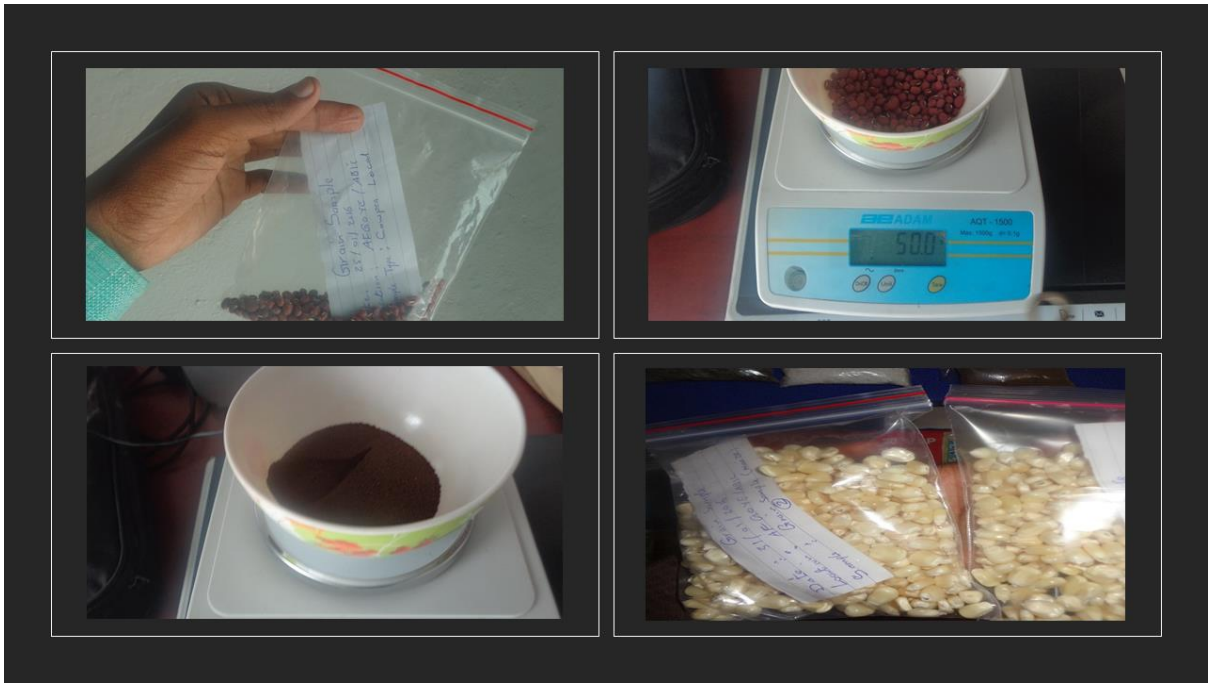


Figure F6: Maize (*Zea mays* L.), cowpea (*Vigna unguiculata* L.) and mung bean (*Vigna radiata* L.), and samples of their corresponding soils were collected from several farms (n=9).



Figure F7: Representative sample of maize cobs and their corresponding soils. Maize cobs were shelled, weighed, and stored in sealed and labelled plastic bags.

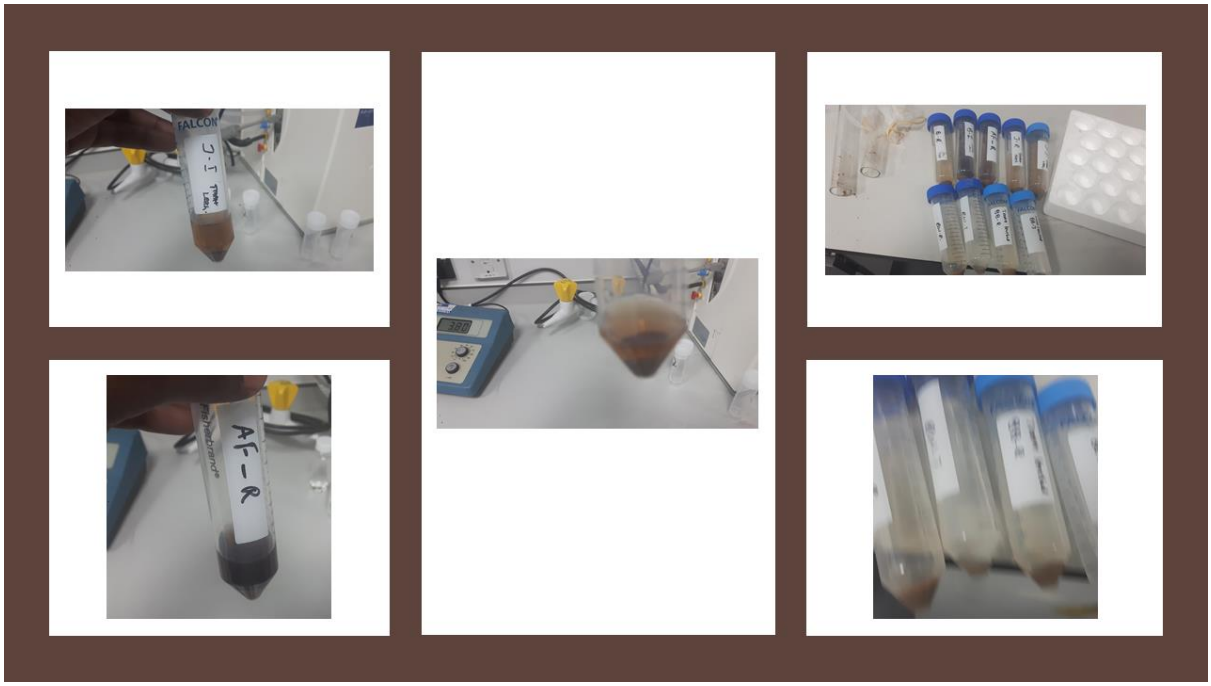
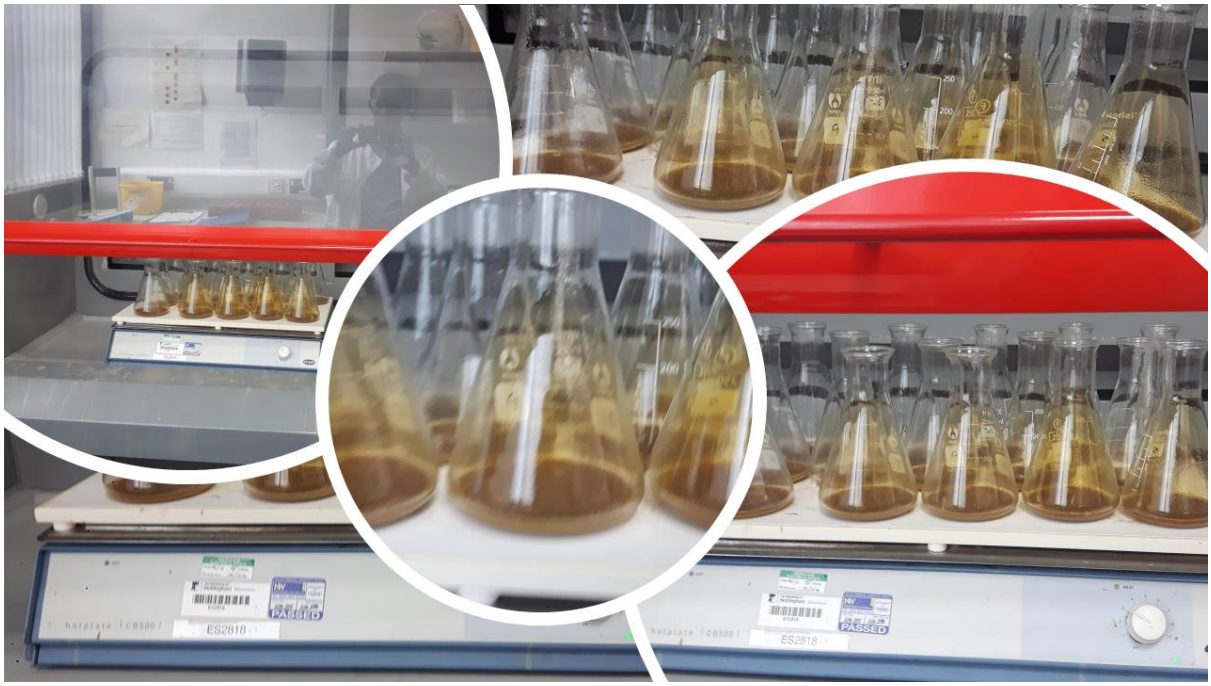


Figure F8: Laboratory characterization of the soil samples (e.g. pH, single and sequential extractions).



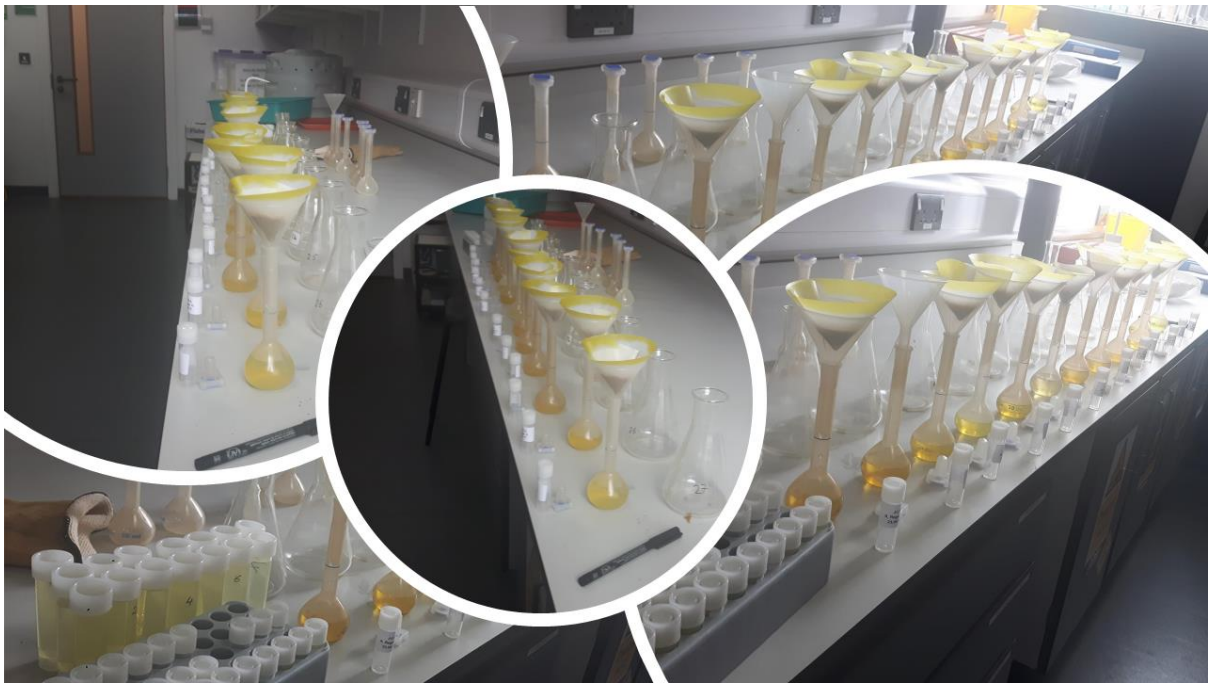


Figure F9: The aqua regia digestion of the soil samples.

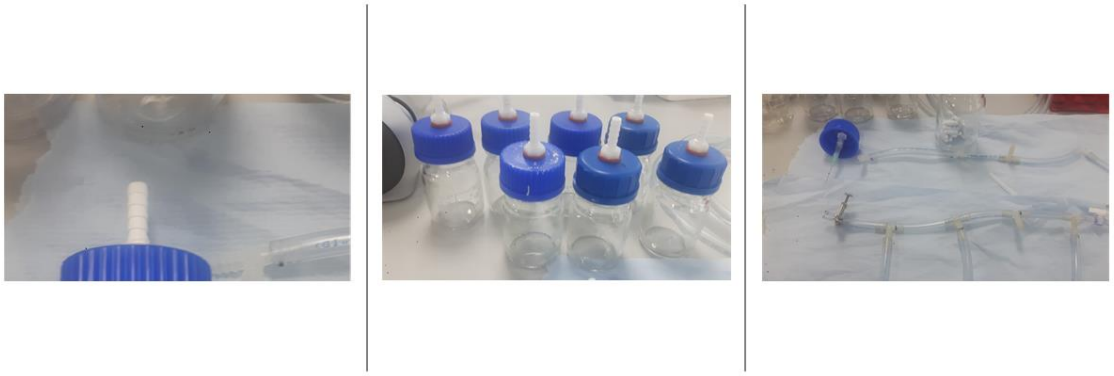




Figure F10: Experimental set up of the Se and I coprecipitation with calcite using three experimental set ups; i) continuous CO_2 bubbling, ii) fluctuation between CO_2 & air, and iii) continuous air bubbling.



Figure F11: Batch adsorption-desorption experiments were conducted to understand Se and I sorption/fixation on calcareous minerals. Samples were collected at various time intervals to understand the influence of contact time.